Loop Quantum Gravity Effects on Spherical Black Holes

A Covariant Approach to Singularity Resolution

Asier Alonso Bardaji

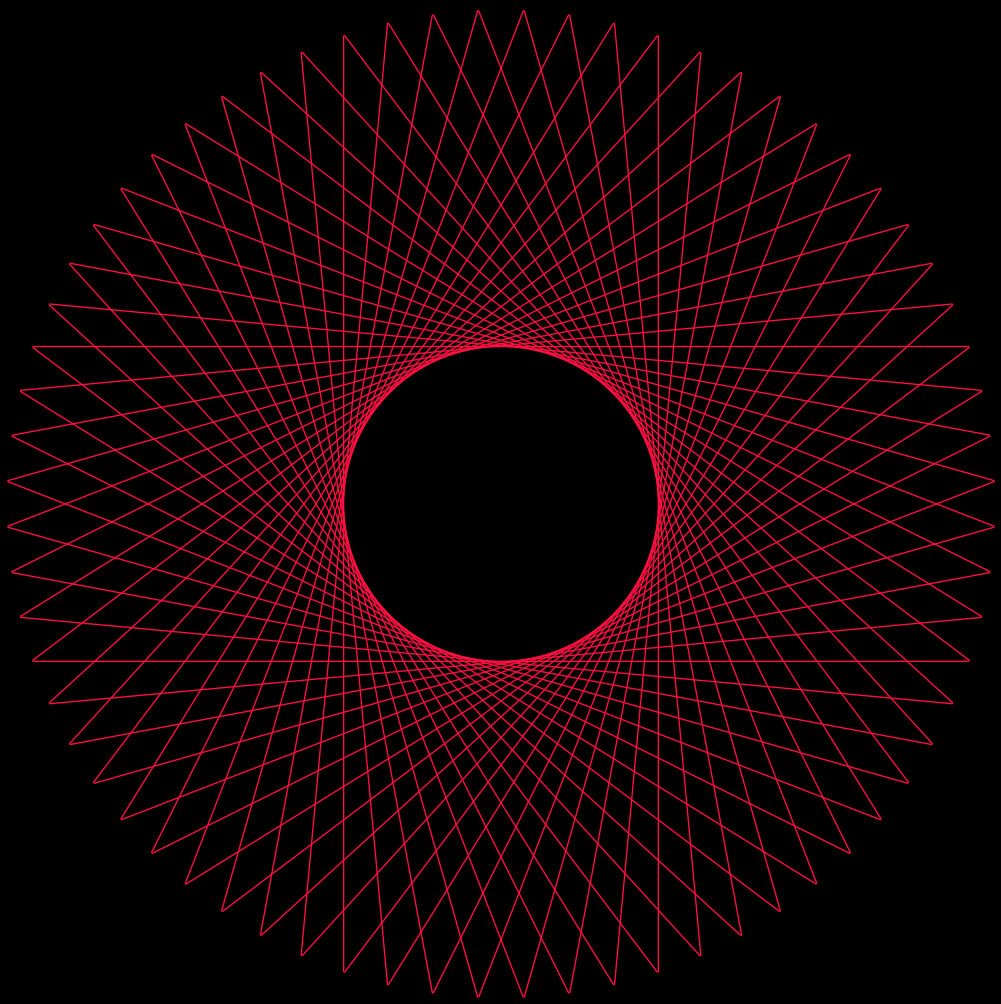

eman ta zabal zazu

Universidad del País Vasco

Euskal Herriko Unibertsitatea

2023

eman ta zabal zazu

Universidad del País Vasco

Euskal Herriko Unibertsitatea

A thesis submitted in partial fulfilment of the requirements for the Degree of Doctor of Philosophy

Loop Quantum Gravity Effects on Spherical Black Holes

A Covariant Approach to Singularity Resolution

Asier Alonso Bardaji

Supervisor

David Brizuela

March 2023

This PhD thesis was completed under the FPI fellowship PRE2018-086516 funded by MCIN/AEI/10.13039/501100011033 and by "ESF Investing in your future".

The author also acknowledges financial support from Grants FIS2017-85076-P and PID2021-123226NB-I00 funded by MCIN/AEI/10.13039/501100011033 and by "ERDF A way of making Europe" as well as Basque Government Grants IT956-16 and IT1628-22.

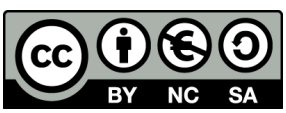

*A mi **Aita** y **Ama***

To know and not to know, to be conscious of complete truthfulness while telling carefully constructed lies, to hold simultaneously two opinions which canceled out, knowing them to be contradictory and believing in both of them, to use logic against logic... to forget whatever it was necessary to forget, then to draw it back into memory at the moment when it was needed, and then promptly to forget it again...

Nineteen Eighty-Four
by George Orwell.

Acknowledgements
Agradecimientos/Esker Onak

Life escapes all barriers. Life breaks free. Life expands to new territories. Painfully, perhaps even dangerously. But life finds a way.

Jurassic Park
by Michael Crichton.

Knowing beforehand that it is impossible to express all my gratitude in the following lines, I yet want to mention all of you who helped me through these long years. First of all, I must recognise my supervisor David Brizuela for his patience and dedication, even during the most awkward times of the pandemic. I honestly thank Raül Vera for our enjoyable discussions. I must thank the professors in the Department for their kindness, and especially Iñaki Garay, after introducing me to the magical world of quantum gravity. I am grateful to professors Iván Agulló and Edward Wilson-Ewing for welcoming me to both LSU and UNB, and equally to professors Alejandro Pérez and Parampreet Singh for the first reading of this manuscript. Exceptional thanks to Adrià Delhom and also to all my coffee-sharing fellows: Aitor, Ander, Araceli, Dani, Eneko, Fran, Mikel, Sara, and Unai.

Bidaia hau ezinezkoa izango zen nire adiskide minen babes ezean. Mila esker Asier eta Bruno zuen kidetasun ukaezinagatik. Esker aunitz unibertsitatea hasiz geroztik hortxe izan dudan Andoniri. Jon eta Imanol: eskerrik beroenak pisuko urte zoragarri horiengatik. Ezin ahaztu Kanadako lagunak, Jorge, Leire, Mikel eta Txiki, ezta Donostiako ubarroiak ere, Ekain, Jokin eta Paul. Zuekin bizitakoarengatik (eta datorrenarengatik!) eskerrak ematea besterik ez dut. Azken traka gisa, Aritz, Etxeni, Guille, Guti, Iker, Iñaki, Kennedy, Roque, Xabi eta Yeray: nire bihotzean beti izango duzue txoko bat. Eskerrik asko zeuei eta lerro eskas hauetan aipa ezin zaituztedan guztioi.

Muchas gracias, Cristóbal, Laura, Margarita y Myriam por vuestro apoyo y, sobre todo, Valle por acompañarme durante todo este tiempo. Debo decir que nada de esto habría sido posible sin el amor incondicional de mi familia. Tías, tíos, primos, Abuela, Abuelo, Aitona, Amona, Aita, Ama, Jon. No sería quien soy, ni estaría donde estoy, de no ser por vosotros.

Abstract

It was some kind of cosmic switching device, routing the traffic of the stars through unimaginable dimensions of space and time.

2001: A Space Odyssey
by Arthur C. Clarke.

We introduce a covariant effective theory for spherical loop quantum gravity. Quantum corrections in non-homogeneous spacetimes are required to be compatible with matter with local degrees of freedom, while the whole set-up remains explicitly covariant. The modifications are implemented at the Hamiltonian level [1–3], and they are then endowed with an unambiguous geometric description: different gauge choices on phase space correspond to particular charts of one same metric tensor. The Schwarzschild singularity is completely resolved [4, 5], and this result is generalised to nearly neutral black holes of large mass embedded in a universe with a small positive cosmological constant [6]. Therefore, the effective theory provides an entirely regular description of spherical astrophysical black holes.

Contents

Resumen

LOS DATOS SON TODAVÍA INSUFICIENTES PARA UNA RESPUESTA ESCLARECEDORA.

La última pregunta
de Isaac Asimov.

La teoría de la relatividad general de Einstein (1915) rompió con los conceptos clásicos de espacio y tiempo, esbozando la gravedad como una consecuencia de la geometría de un nuevo ente llamado «espacio-tiempo». Pero, sin lugar a dudas, la lección fundamental que nos legaron Einstein y sus coetáneos es el principio general de covariancia, que enuncia que las leyes físicas deben ser independientes de las coordenadas que utilice el observador. La dinámica einsteniana se resume de forma cualitativa como sigue: el contenido energético del universo moldea su forma y la curvatura resultante determina el movimiento subsiguiente. Sin embargo, la relatividad general posee una base matemática complicada y cualquier estudio más detallado exige lidiar con un sistema de ecuaciones diferenciales de segundo orden altamente acoplado.

Entre tal abrumadora complejidad emerge el concepto relativamente simple de agujero negro, el testimonio directo de la extrema voracidad de la gravedad. Los agujeros negros son cuerpos sin mácula, los objetos macroscópicos más sencillos que conocemos. Su comportamiento se encuentra completamente determinado por su masa, carga eléctrica y momento angular, sin importar cuál fuese el estado previo de sus componentes. No sorprende, por tanto, que sean también la mayor evidencia de las inconsistencias de la teoría de Einstein, entre las que se encuentran las singularidades en las que la relatividad general pierde todo su poder de predicción. Sin embargo, además de ser excelentes laboratorios para fenómenos de altas energías, se cree que los agujeros negros tienen un papel primordial en la formación y evolución de las galaxias. Al tratarse de los últimos retazos tras la muerte de las estrellas supermasivas, comprender en detalle el proceso autofágico al que sucumben las nebulosas estelares, y que finalmente desencadena la formación de los agujeros negros, es esencial para el estudio de la gravedad y del universo.

Tanto las bases como el desarrollo de la relatividad general se encuentran inextricablemente unidos a los agujeros negros. Tan solo unos meses después de que Einstein publicase sus ecuaciones, Schwarzschild (1916), en plena Primera Guerra Mundial, encontró una solución exacta bajo la suposición de simetría esférica en vacío. Dicha solución, que hoy en día lleva su nombre, ha sido objeto de múltiples e intensas investigaciones, arrojando luz sobre conceptos fundamentales como la causalidad y las propiedades del propio espacio-tiempo. Estudios actuales, respaldados por el teorema de unicidad de Jebsen (1921) y Birkhoff (1923), aportan todavía nuevas pistas en torno a la naturaleza de la gravedad y las singularidades.

Cabe recalcar que el profundo entendimiento de la geometría de Schwarzschild ha sido fruto de un arduo camino, no exento de controversia. De hecho, la métrica de Schwarzschild muestra un punto singular que ha sido objeto de extenso debate y, a pesar de la celeridad con la que se descubrieron coordenadas que incluyen esa región —Painlevé (1921), Gullstrand (1922) y Eddington (1923), entre otros—, no fue hasta la década de los sesenta cuando se aceptó de forma generalizada que dicho punto describe el horizonte de un agujero negro. Cuando Synge (1950), Szekeres (1960) y Kruskal (1960) encontraron la máxima extensión analítica del espacio-tiempo de Schwarzschild, se pudo demostrar que existe una singularidad real —donde la curvatura diverge y a la que un observador puede llegar tras un tiempo finito— más allá de la cual el espacio-tiempo es inextendible.

Los resultados de Schwarzschild fueron prontamente generalizados para incluir carga eléctrica y constante cosmológica, dando lugar a finales de la década de 1910 a los espacio-tiempos de Reissner-Nordström y Kottler, respectivamente. A pesar de que tanto el número de horizontes como la estructura asintótica de estas geometrías varían, una de las predicciones características de Schwarzschild prevalece: la inevitable singularidad central.

Friedmann y Lemaître en los años veinte, y Robertson y Walker en los treinta, fueron los primeros en emplear la relatividad general para describir el cosmos como un todo. De hecho, la solución homogénea e isótropa (FLRW) que encontraron, y que actualmente se sigue considerando una buena aproximación de nuestro universo, lleva por nombre sus iniciales. El propio Lemaître (1933) y Tolman (1934) extendieron el estudio a simetría esférica. Dicho trabajo fue más adelante investigado en detalle por Bondi (1947), por lo que actualmente se conoce como el modelo LTB. Aunque inicialmente se postuló como una teoría cosmológica, el origen privilegiado de la simetría esférica choca de lleno con nuestra visión del cosmos.

Sin embargo, el trabajo pionero de Oppenheimer y Snyder (1939) utilizó los resultados de Lemaître y Tolman para describir el colapso esférico de una estrella de densidad homogénea.

Sus cálculos demuestran que todos los componentes de la estrella convergen finalmente en una singularidad. A pesar de la excesiva simplificación del problema, estudios posteriores más complejos comprobaron que su intuición era correcta: la singularidad central tiene un origen dinámico. Todo ello queda resumido de forma precisa en los teoremas de singularidades, certificando así la incompletitud de la relatividad general. Por lo tanto, debemos ir más allá de las enseñanzas de Einstein para comprender los secretos más profundos de la gravedad.

Es aquí donde entra en juego la gravedad cuántica de lazos, una teoría no perturbativa basada en el formalismo hamiltoniano de la relatividad general. Al igual que la teoría de Einstein, su formulación carece de estructuras de fondo sobre las que establecer las leyes físicas y es, hoy en día, una de las candidatas principales para lograr una descripción cuántica de la gravedad. Entre sus principales predicciones se encuentra el espectro discreto de magnitudes geométricas tales como el área y el volumen, lo que se aplica en el cálculo de la entropía de agujeros negros y que también proporciona una resolución del Big Bang en modelos cosmológicos. Sin embargo, la teoría es aún incompleta; la formulación de la dinámica es un problema abierto en la gravedad cuántica de lazos. Por ello, se ha realizado un notable esfuerzo en lo referido a modelos efectivos que den cuenta de las principales características cuánticas de la gravedad y que ayuden a desentrañar los aspectos más oscuros de la teoría.

La elaboración de teorías efectivas va de la mano del desarrollo científico. Su propósito es analizar el comportamiento del sistema bajo estudio ignorando sus fuentes primordiales. De esta forma se pueden colegir ciertas predicciones de la teoría completa en los regímenes en los que esta deja de ser manejable o incluso cuando se desconoce la estructura subyacente. Un ejemplo ampliamente conocido es el modelo para la desintegración beta de Fermi, considerado el precursor de la teoría electrodébil. Su modelo supuso un hito no solo por su excelente armonía con los experimentos, sino porque el fenómeno del que da cuenta ocurre a energías mucho más altas (tres órdenes de magnitud) que las disponibles en los experimentos de la época. Cabe recalcar que, por desgracia, la brecha entre los experimentos actuales y las escalas energéticas de los efectos gravitatorio-cuánticos se estima en quince órdenes de magnitud.

La falta de pruebas observacionales es una barrera difícil de franquear a la hora de completar cualquier teoría efectiva, así como de la dinámica completa de la gravedad cuántica de lazos. Además, la extrema concordancia entre las predicciones de la relatividad general y los datos experimentales (desde la desviación de la luz medida en eclipses solares hasta la reciente observación directa de ondas gravitatorias) aflora descorazonadora, ya que no aporta

ningún hilo del que tirar. Las únicas líneas consistentes para el futuro desarrollo de modelos efectivos parecen ser la consistencia matemática y la resolución de las singularidades.

A pesar de todo, contamos con el respaldo de los modelos cosmológicos, en los que las teorías efectivas concuerdan con la descripción completa de la teoría cuántica de lazos. La generalización de dichas predicciones a escenarios menos simétricos confirmaría la resolución de las singularidades clásicas. En esta tesis daremos el paso lógico hacia los modelos esféricamente simétricos con materia. Aunque las restricciones de simetría son todavía notables, el salto que daremos es equivalente al que hay entre la mecánica cuántica y las teorías cuánticas de campos. Además, el papel fundamental de las soluciones esféricas en los orígenes de la relatividad general nos hace pensar que su descripción cuántica arrojará luz sobre el camino hacia un conocimiento más profundo de la gravedad. No obstante, como ya hemos comentado, las escalas energéticas en las que se podrían percibir fenómenos gravitatorio-cuánticos se restringen a los sucesos cósmicos más extremos del universo. De hecho, y al contrario de lo que ocurre en la cosmología cuántica, los profundos pozos gravitatorios en los que se esconden las singularidades de los agujeros negros las colocan muy lejos de nuestro alcance, por lo que contrastar la teoría con observaciones escapa a nuestras capacidades actuales.

La cuantización de los agujeros negros y la resolución de las singularidades son problemas abiertos en la gravedad cuántica de lazos. No sorprende, por tanto, la proliferación de modelos efectivos en tanto que el programa de cuantización llegue a buen puerto. Uno de los aspectos clave que se debe afrontar es la reconciliación del espacio-tiempo discreto predicho por la gravedad cuántica de lazos con la noción continua que aporta la simetría de difeomorfismos en relatividad general. Por ello, resulta inquietante que los estudios disponibles hasta la fecha violen consistentemente el principio de covariancia de la teoría de Einstein.

El procedimiento habitual para obtener una descripción efectiva radica en introducir correcciones cuánticas en el Hamiltoniano de la relatividad general y, de esta forma, derivar las modificaciones en la dinámica. Cabe destacar el caso específico de las correcciones por holonomías, ya que son las que suscitan mayor éxito en cosmología. Dichos efectos se deben a que ciertas cantidades no poseen un operador cuántico bien definido. En su lugar, se emplea su variación a lo largo de un circuito cerrado —un lazo—, lo que, matemáticamente, equivale a utilizar la exponencial imaginaria de dicha cantidad. A nivel efectivo, se espera que tales efectos se puedan codificar mediante funciones sinusoidales. Para determinar la escala a la que las correcciones deben entrar en juego, se suele introducir el llamado parámetro de «polimerización».

Este es el punto de partida de la tesis, siendo su principal objetivo elaborar una teoría matemáticamente consistente que describa los efectos fundamentales de la gravedad cuántica de lazos en simetría esférica y que cumpla los siguientes requisitos: ***(i)*** respeta el principio de covariancia general, ***(ii)*** tiene la relatividad general como un límite claro y ***(iii)*** las correcciones cuánticas son compatibles con la incorporación de materia. De esta forma, la teoría efectiva será invariante bajo cambios de coordenadas y, por tanto, sus predicciones serán independientes del observador en cuestión. En consecuencia, podremos dar un paso más para esclarecer si la resolución de singularidades es una propiedad connatural de la gravedad cuántica de lazos.

Para superar los obstáculos a los que se enfrentan los modelos efectivos de gravedad cuántica de lazos, realizamos un estudio sistemático y exhaustivo de todas las posibles modificaciones del Hamiltoniano de relatividad general que respetan su estructura de derivadas. El requisito de covariancia exige que las ligaduras del sistema formen un álgebra de primera clase y, además, que la función de estructura de dicho álgebra tenga unas propiedades de transformación características que permitan embeber la teoría efectiva en una variedad cuadridimensional. De esta forma, somos capaces de construir de forma unívoca el tensor métrico con correcciones cuánticas en términos de funciones del espacio de fases.

Los resultados positivos de este estudio son los primeros en la literatura. Por un lado, la obtención del Hamiltoniano más general en vacío que cumple con todos los requisitos y, por otro lado, la incorporación con éxito de grados de libertad locales en la teoría efectiva. El modelo presenta un parámetro libre directamente relacionado con la escala de «polimerización» de las correcciones por holonomías de la gravedad cuántica de lazos. Cuando dicho parámetro se desvanece, recuperamos las predicciones dadas por la relatividad general.

La construcción geométrica nos permite estudiar en detalle la teoría efectiva. En el modelo de vacío, demostramos que la singularidad de Schwarzschild es reemplazada por una superficie de transición, compuesta por esferas de área finita, dentro del horizonte. Un observador en caída libre atravesaría el horizonte, y también dicho mínimo, para emerger al exterior por un nuevo horizonte. Al incorporar carga eléctrica y constante cosmológica al estudio, comprobamos que las singularidades se resuelven mediante el mismo mecanismo anterior, al menos para valores realistas de los parámetros del modelo: poca carga eléctrica y constante cosmológica positiva y pequeña, ambas en comparación con la masa. Cabe destacar que las correcciones cuánticas también alteran la estructura asintótica de los espacio-tiempos con constante cosmológica no nula. De hecho, al igual que ocurre con las superficies de área mínima, la teoría predice superficies de área máxima finita. Los observadores que se alejasen

del centro no podrían huir indefinidamente. Por el contrario, llegarían al citado máximo y, al intentar ir más allá, se dirigirían paulatinamente hacia una región similar en un universo paralelo. La teoría también describe modelos cosmológicos, en los que el universo atraviesa fases sucesivas de expansión y contracción, oscilando entre mínimos y máximos finitos.

En conclusión, nuestra teoría efectiva con correcciones de gravedad cuántica de lazos es covariante y proporciona una descripción libre de singularidades para cualquier agujero negro esférico astrofísico, es decir, aquellos con masas relativamente grandes y prácticamente neutros sumergidos en un universo con una constante cosmológica positiva pequeña.

Introduction

THERE IS AS YET INSUFFICIENT DATA FOR A MEANINGFUL ANSWER.

The Last Question
by Isaac Asimov.

The theory of general relativity [7] forever broke the Newtonian notions of space and time, illustrating gravity as a consequence of the geometry of a novel entity: spacetime. In all likelihood, the most fundamental lesson encoded in Einstein's theory is the principle of general covariance, stating that physical laws are necessarily independent of the arbitrary coordinates employed to describe them. It is common to qualitatively summarise Einsteinian dynamics as follows: The energy content of the universe warps time and space with the resulting curvature determining matter's forthcoming evolution [8]. Notwithstanding, a deeper analysis requires dealing with a highly coupled system of ten second-order partial differential equations, revealing the underlying mathematical intricacy of general relativity.

Rising from those wells of complexity, one finds the yet simple concept of black holes, the most extreme representatives of gravitational attraction. They are the most seamless macroscopic objects in the universe and the simplest ones as well. Their mass, electric charge, and angular momentum determine their behaviour, regardless of the former state of their constituents. Not startlingly, black holes spark some inconsistencies in Einstein's theory, and, in the present thesis, we deal with one of such: the singularities where general relativity is ill-defined. But beyond fundamental physics, where they provide a unique arena to test Einstein's predictions in strong-field regimes, black holes are also of utmost importance in astrophysics, as they are thought to play a key role in the formation and evolution of galaxies. Being the final remnant of massive stars, the autophagic process of stellar nebulae that ultimately triggers the formation of black holes is essential for our understanding of gravity and the universe.

The foundations and development of general relativity are inextricably tied to black holes. Just in the dawn of the theory, Schwarzschild, and independently Droste months later, found an exact analytic solution under the assumption of spherical symmetry in vacuum [9, 10].

The Schwarzschild solution has been the subject of extensive research, raising deep questions about causality and the properties of spacetime itself. Ongoing studies continue to provide important insights into the nature of gravity and the singularities, enhanced by Jebsen's (1921) and Birkhoff's (1923) proofs on any asymptotically flat spacetimes outside a spherical configuration being static and described by the Schwarzschild geometry [11, 12]. The solution showed a singular point that was, after much controversy, identified as the horizon of the black hole. Different coordinates including that region were soon suggested [13–15] by Painlevé (1921), Gullstrand (1922), and Eddington (1923). However, acknowledging them as coordinate transformations of one same metric, and the final recognition of the Schwarzschild radius to be just a coordinate singularity, had to wait until the 1960s, the beginning of the golden age of general relativity. Synge (1950), Szekeres (1960), and Kruskal (1960) obtained the maximal analytic extension of the Schwarzschild spacetime [16–18]. Besides the horizon, the solution shows a true physical singularity where curvature scalars diverge. An infalling observer arrives at this singular point after a finite proper time, and the spacetime cannot be further extended in a smooth way. The fact that many years had to pass for a complete understanding of that metric, which nowadays bears Schwarzschild's name, should not tarnish, but rather laud, its weight and influence.

Schwarzschild's results were soon generalised to include charge and a cosmological constant while keeping the assumption of spherical symmetry, yielding in the late 1910s the Reissner-Nordström [19, 20] and Kottler [21] spacetimes, respectively. While the number of horizons and even the asymptotic structure of these solutions vary, one characteristic prediction remains: the ineludible central singularity.

Concerning the description of the cosmos as a whole, Friedmann [22] and Lemaître [23] in the 1920s, and Robertson [24] and Walker [25] in the 1930s, worked upon the assumption that the universe is homogeneous and spatially isotropic. These studies led to the well-known FLRW solution (after their initials), which is still a good approximation to describe current observations. Lemaître himself (1933) and Tolman (1934) incorporated a spherically symmetric pressureless perfect fluid to account for possible inhomogeneities. This was later thoroughly studied by Bondi (1947), and it is usually referred to as the LTB solution for its authors' last names [26–28]. Although first thought of as a generalisation of the homogeneous and spatially isotropic spacetime, the privileged origin of the spherical symmetry collides with our current notion of the cosmos.

All the same, the pioneering work of Oppenheimer and Snyder (1939) considered a star of homogeneous density and modelled its collapse using Lemaître's and Tolman's results. All

the matter within their assumptions eventually converges into a singularity [29]. Indeed, this was a first step towards describing the actual formation of black holes, and subsequent studies, loosening symmetry restrictions and with more realistic matter, proved their intuition to be true: the central singularity is dynamically generated. The outcome of these investigations, beautifully summarised in the singularity theorems [30–32], gloomily certifies the incompleteness of general relativity, and it is generally accepted that we must go beyond Einstein's teachings to understand gravity's most profound nature.

While it is firmly expected that a quantum description of gravity ought to cure these flaws, the unconcluded search for such a theory faces severe obstacles, with the absence of resilient quantum-gravity tests challenging its construction to a greater extent. A widespread thought is that gravity per se should be quantised in the same vein as the other fundamental interactions. Since general relativity describes the being of spacetime itself, that may lead to a quantised notion of time and space.

Loop quantum gravity [33–37] is a non-perturbative and background-independent theory based on the Hamiltonian description of general relativity. Nowadays it stands for one of the soundest candidates to achieve the quantisation of Einstein's theory. It is based on the idea that the fundamental building blocks of the universe are quanta of area and volume, providing a robust quantisation of the kinematical structures of general relativity. Although it has led to several significant results, such as discrete and finite spectra for geometric operators [38, 39] and the resolution of the Big Bang singularity in cosmological models [40–42], the formulation of the full dynamics of loop quantum gravity remains open.

To gain insight into the quantum realm of gravity, there has been a considerable effort to build effective approximations. Effective methods describe the behaviour of a given theory when it stops being tractable, while ignoring the underlying fundamental structure. Inferring the main predictions of the full framework in a semiclassical regime is their raison d'être. A well-known example is Fermi's description of beta decay [43]. The standard model of particle physics explains that a flavour-changing gauge boson mediates the process, and Fermi's effective theory is regarded as the low-energy precursor of the electroweak theory. It was a major milestone, not only due to its agreement with experiments, but also because the mass of the mediator was three orders of magnitude above all feasible energy scales at that time. This effective theory holds the honour of providing the tested result with the largest difference in energy scales between the effective and the full frameworks. In the case of quantum gravity, the energetic gap with respect to current experiments is expected to be around fifteen orders of magnitude.

The lack of observational evidence is a large hurdle towards the full dynamics and effective descriptions of quantum gravity. In addition, the extreme reliability of general relativity in all experimental tests (from the deflection of light in solar eclipses since 1919 to the latest measurements of gravitational waves) is somewhat discouraging, as the only steady guidelines for developing a quantum-gravity theory seem to be mathematical consistency and the alleviation of the problem of singularities.

The main reinforcement in our endeavour is that the homogeneous symmetry reduction of general relativity has been subject to a consistent loop quantisation [44–46]. Further, the effective models implementing key aspects of the theory have been shown to greatly agree with the full quantum dynamics [47, 48]. In particular, they both show the resolution of the initial singularity. The effective approach encodes loop-quantum-gravity predictions in the Hamiltonian to derive the expected corrected dynamics.

Extending those predictions to less symmetric scenarios should be a consistency check (or rejection) of the singularity resolution, and we take the natural step towards spherical symmetry. Although symmetry assumptions are still strong, the jump from homogeneous to spherically symmetric models with matter is equivalent to that of quantum mechanics to quantum field theories. Both the static and the dynamic spherically symmetric solutions were vital in the advent of general relativity, and they are still essential to understand the fundamental properties of gravity. Their (effective) quantum description will most probably enlighten the road to a deeper comprehension of gravity.

However, the energy scales where quantum-gravity phenomena should become noticeable are restricted to the most extreme events in the cosmos. In contrast to early-universe measurements, quantum effects must leak away from black holes to weigh them, and correlating the theory with observations is still beyond our current capabilities.

While a complete quantisation of black holes and the resolution of classical singularities are still open problems in loop quantum gravity [49–51], effective descriptions have proliferated in the literature, and the variety of their predictions is wide enough to exhibit conflicting results. But perhaps the most distressing point is to realise that (to the best of our knowledge) every effective implementation so far violates the covariance of Einstein's theory [52, 53], which also lies at the core of loop quantum gravity. With little room for doubt, the central question any effective model must face is how the underlying spacetime discreteness predicted by loop quantum gravity is reconciled with the continuous diffeomorphism symmetry of general relativity.

The usual approach to obtain effective models is to incorporate the expected quantum corrections at the Hamiltonian level and derive the modified dynamics. We will briefly review a small sample of the studies in the literature, particularly focusing on those implementing holonomy corrections. These modifications descend from the fact that the operator associated with the connection is not well defined in loop quantum gravity [35]. Instead, one considers the exponential form of parallel-transported connections, the so-called holonomies, with a definite operator counterpart. The effective approach replaces connections with periodic and bounded functions, usually sinusoidal ones. It is common to incorporate a "polymerisation parameter" to account for the scale of quantum effects.

The first attempts relied on the isometry between the homogeneous interior of spherical black holes and the Kantowski-Sachs universe [54–59]. Therefore, restricting to that region of the Schwarzschild spacetime, one could import the successful corrections of loop quantum cosmology. The motivation is that quantum effects should be relevant close to the singularity and negligible near the horizon. These models find bounces for the area of the spheres of spherical symmetry. Still, without further analysis, it is difficult to tell whether such predictions are a generic feature or just a coordinate artefact, as those area elements show the same bouncing behaviour when reaching the horizon. If no previous notion of "exterior" existed, one would conclude that the minima and maxima entailed the same physical meaning. In addition, these studies dismiss all factors arising from the lack of homogeneity.

When aiming to describe the complete spacetime, one has to deal with several problems, including those of the asymptotics, the slicing independence, and the smoothness of the solution across horizons. Some recent proposals predict either the formation of an inner horizon [60], the replacement of the singularity with a spacelike transition surface towards a white hole [61–65], or the formation of a Euclidean region in the deep quantum regime [66]. Nevertheless, a complete geometric study is mandatory to check whether those are enduring effects, independent of the specific coordinates or gauge choice.

In spherical symmetry, there are two connection components that could be promoted to sinusoidal functions. Whether both variables, or only the one related to the compact direction, should be subject to corrections [67] and whether the polymerisation scheme should depend on the scale or not [62] remain open questions.

For instance, a clever transformation from the usual triad and connection variables mimics scale-dependent holonomy corrections while implementing a constant polymerisation scheme [63, 64], analogous to its cosmological counterpart. Besides, the on-shell identification of the new momenta with curvature scalars and the area-radius function opens a

way to describe the exterior region of the modified Schwarzschild solution. A different study [61, 62, 65] foliates the exterior region of the Schwarzschild spacetime by level surfaces of constant radial coordinate and "evolves" the timelike homogeneous hypersurfaces along the radial direction. In that way, one gets a different set of variables and constraints — and, hence, solutions — which are analogous to those of the interior region. In this last work, the authors choose a polymerisation that remains constant on each trajectory on the phase space but changes in the space of solutions. In brief, it amounts to considering the polymerisation parameter to be a function of the constants of motion of the theory, which solves some problems related to other polymerisation schemes. While both models reproduce general relativity in asymptotic regions and predict a transition surface that replaces the Schwarzschild singularity, neither describes the horizon of the black hole. In addition, the black-hole masses differ in different exterior regions.

A related, though different, approach is based on the abelianisation of constraints [68–70], which may lead to a consistent theory of spherical loop quantum gravity, even under the presence of matter fields. This procedure relies on a redefinition of the Lagrange multipliers of the theory that transforms the hypersurface deformation algebra into a Lie algebra suitable for a Dirac quantisation. The authors also suggest an effective metric with bounded curvature scalars [71]. Most remarkably, the study incorporates scale-dependent holonomy modifications, making quantum corrections rapidly vanish in asymptotic regions. Although these coordinates cross the horizon, they do not cover the expected minimum surface.

In a similar work, scale-dependent holonomy modifications are implemented so that the algebra between constraints remains first class [60]. In this case, the drawback is that correction functions involving curvature components remain bounded only after a partial gauge fixing: The area-radius function is required to be the radial coordinate. These coordinates penetrate the horizon and shows a finite minimum beyond an inner horizon that changes the trapped nature of the hypersurfaces inside the black hole. Despite not being related by coordinate transformations, the study shows how the effective metric in Ref. [71] is obtained from this same Hamiltonian. But, just as in that previous work, one needs to contrast whether the minimum is a strong prediction or only a consequence of the choice of coordinates.

The program of consistent constraint deformations was considered in Refs. [66, 72–74], and aims to preserve the first-class nature of the hypersurface deformation algebra. The core idea is that since the first-class constraints encode both the dynamics and the diffeomorphism invariance of general relativity, only modifications that preserve that first-class nature should be allowed. Nonetheless, having a first-class algebra is a necessary but insufficient condi-

tion to recover a clear geometric picture because one also needs to embed the canonical theory in the four-dimensional spacetime manifold. In Ref. [66], the authors suggest that the metric should be deformed accordingly with the Hamiltonian, making a first attempt in that direction. The study concludes by suggesting the formation of a Euclidean region in the deep quantum regime, where all notion of causality would be lost. Nevertheless, the analysis omits the region nearby the signature change, and it needs to be clarified whether quantum effects would allow reaching the innermost Euclidean space.

Some of those works extend their predictions to include non-dynamical fields [75, 76] and even collapsing matter [77–79]. However, they suffer equally from the discussed lack of covariance as different solutions to the effective equations provide incompatible predictions.

With all the above, we are ready to unveil the primary goal of this thesis. We aim to construct a mathematically consistent effective theory that describes the main effects of loop quantum gravity in spherical symmetry, following three important requisites: ***(i)*** it respects general covariance, ***(ii)*** Einstein's theory is recovered in a clear limit, and ***(iii)*** the effective corrections are compatible with the addition of matter. The effective description will thus rely on a classical spacetime picture, and the first requirement will ensure that its predictions are not induced by any arbitrary choice of coordinates. The second one will hopefully provide some insight into the future development of loop quantum gravity, and it is a consistency check for the model. Finally, the third requirement is necessary to eventually describe spherical gravitational collapse. In this way, we will be able to check whether the theory provides an everywhere smooth description for classical black-hole singularities, and also for the dynamical process preventing their formation. These are key questions upon which quantum gravity is expected to shed light.

Before closing this introductory section, let us comment on the organisation of the thesis. We begin with some basic notions of loop quantum gravity and its spherical symmetry reduction in Chapter 1. We also highlight the process of constructing the spacetime metric from the phase space of canonical general relativity. In Chapter 2, we suggest covariant modifications of the Hamiltonian of general relativity. First, we find the most general framework in vacuum that admits a metric interpretation. Second, we incorporate propagating degrees of freedom with the same requirement. It turns out that demanding the former to be the vacuum limit of the latter further constrains possible modifications. Subsequent chapters study the singularity resolution of the effective model in vacuum (Chapter 3), and in the presence of a cosmological constant and an electromagnetic field (Chapter 4). Finally, we summarise the results and point out the main features of the effective theory.

1

Basic Notions for Spherical Loop Quantum Gravity

The board is set, the pieces are moving.
We come to it at last... The great battle of our time.

The Lord of the Rings
by J. R. R. Tolkien.

Loop quantum gravity (LQG) aims to reconcile the quantum world with general relativity (GR). The theory relies on a canonical quantisation of the gravitational interaction in terms of the Ashtekar variables, triads and connections, and their respective fluxes and holonomies.

The whole framework still being unravelled, one must stick to quantising symmetry reductions of GR. For instance, the homogeneous scenario leading to loop quantum cosmology (LQC) replaces the initial singularity with a quantum bounce at early times. Loosening symmetry restrictions increases difficulties in tracking the models, and it is unclear whether they may answer such critical defects of GR. Hence, there has been a considerable effort to build the spherical reduction of LQG to confirm whether singularity resolution is an enduring property of the theory. Extending mechanisms avoiding the Big Bang to spherical symmetry would be a robustness check of those predictions.

In this chapter, we briefly overview the foundations of LQG, sketching the primary steps towards its classical formulation (Sec. 1.1). A notorious prediction in this theory is the quantised notion of spacetime that presumably mends the unavoidable singularities of GR. Besides, it is based on a specific formulation of GR that allows writing it as a Yang-Mills theory. Finally, we will reconstruct the explicitly covariant metric picture from the phase space (Sec. 1.2) and introduce the framework and basic variables adapted to spherical symmetry (Sec. 1.3).

1.1 Loops: A concise journey

The starting point of this section is the four-dimensional spacetime $(\mathcal{M}, g)$. We first need to split spacetime into space and time to obtain a Hamiltonian formulation for GR. We will explicitly show that the proper way of doing this does not interfere with the covariance of Einstein's theory. The main references followed in this introductory section are [35, 80, 81].

1.1.1 On the 3+1 decomposition

Assuming global hyperbolicity, the spacetime $(\mathcal{M}, g)$ can be foliated by spacelike hypersurfaces defined as level surfaces of a smooth real-valued function t on $\mathcal{M}$. We define a leaf, $\Sigma_t := \{p \in \mathcal{M},\ t(p) = t\}$, of the foliation such that $\Sigma_{t_1} \cap \Sigma_{t_2} = \emptyset$ for $t_1 \neq t_2$, and we further assume that the set of all leaves, $\{\Sigma_t\}|_{\forall t \in \mathbb{R}}$, covers $\mathcal{M}$. When convenient, we will exploit the abstract index notation, where u^μ and u_μ stand for the components of the vector $u^\mu \partial_\mu$ and the covector $u_\mu dx^\mu$, respectively. We use lowercase Latin indices $(a, b \ldots)$ taking the values 1, 2 and 3, and Greek indices $(\mu, \nu \ldots)$ running from 0 to 3.

The notion of evolution is thence provided by the gradient of the function t. The one-form $dt \equiv (\nabla_\mu t) dx^\mu$ and its metric dual, the timelike vector field $(\nabla^\mu t)\partial_\mu$, are both orthogonal to the slices Σ_t. We define the unit normal as

$$n_\mu dx^\mu := -N dt, \tag{1.1a}$$

$$n^\mu \partial_\mu := -\big(N \nabla^\mu t\big)\partial_\mu, \tag{1.1b}$$

where

$$N := \big(- \nabla_\mu t \, \nabla^\mu t\big)^{-1/2} > 0, \tag{1.2}$$

is the ***lapse function***. The unit normal is unique up to its orientation, which we have chosen to be future-pointing for increasing t. That is, $n^\mu \partial_\mu t = 1/N$ is positive.

Besides t, we need three additional functions, x^a, on $\mathcal{M}$ to define a coordinate basis, which we say to be adapted to the foliation. We shall call ∂_t or, equivalently, $t^\mu \partial_\mu$ the time vector, which is tangent to the lines of constant x^a but not necessarily orthogonal to the hypersurfaces Σ_t. The natural basis of the tangent space is $\{\partial_t, \partial_a\} := \{\frac{\partial}{\partial t}, \frac{\partial}{\partial x^a}\}$, and its associated dual basis reads $\{dt, dx^a\}$. Note that the integral curve of the time vector through $p_1 \in \Sigma_{t_1}$ will intersect Σ_{t_2} once and only once provided $\partial_t t = 1$, which adapts the flow to the concept of time given by the function t. Therefore, we may identify that intersection, $p_2 \in \Sigma_{t_2}$, as the same spatial point at a different time, that is, $p(t_1) := p_1$ and $p(t_2) := p_2$.

In these coordinates, the unit normal reads $n^\mu \partial_\mu = N^{-1}\big(t^\mu \partial_\mu - N^a \partial_a\big)$, where

$$N^a := -N n^\mu \partial_\mu x^a \tag{1.3}$$

are the only trivially non-vanishing components of the ***shift vector***, $N^\mu \partial_\mu := (t^\mu - N n^\mu)\partial_\mu = 0\,\partial_t + N^a \partial_a$. One can check that $n_\mu N^\mu = 0$, so the shift vector is tangent to Σ_t, and thus a spatial vector. More precisely, it is the projection of the time vector on the leaf, and we can write its usual $3+1$ decomposition:

$$\partial_t = t^\mu \partial_\mu = N n^\mu \partial_\mu + N^\mu \partial_\mu. \tag{1.4}$$

We can explicitly compute the components of the metric tensor in the natural basis $\{dt, dx^a\}$,

$$ds^2 = g_{\mu\nu} dx^\mu dx^\nu = -N^2 dt^2 + q_{ab}\big(dx^a + N^a dt\big)\big(dx^b + N^b dt\big), \tag{1.5}$$

and find that all its information is encoded in the induced three-dimensional Riemannian metric $q_{ab}dx^a dx^b$, the lapse function N, and the shift vector $N^a \partial_a$. In particular, the determinant of the spacetime metric is $\det(g) = -N^2 \det(q)$. The projector $h_{\mu\nu} := g_{\mu\nu} + n_\mu n_\nu$ will allow us to decompose every spacetime object into orthogonal and tangential components to Σ_t, that is, to find the projection of every quantity onto the spacelike hypersurfaces. Note that the spatial components of the spacetime metric g_{ab} coincide with the induced spatial metric q_{ab} but, generically, the components of their inverses do not, i.e., $g^{ab} \neq q^{ab}$. In contrast, the projector's spatial part coincides with the induced three-dimensional metric for every index ordering: $h_{ab} = q_{ab}$, $h^{ab} = q^{ab}$, $h_a^{\ b} = q_a^{\ b}$, and $h^a_{\ b} = q^a_{\ b}$.

After some calculations, we can express the Einstein-Hilbert action — up to boundary terms (total derivatives) that we omit in the following — as three-dimensional quantities:

$$S_{EH} = \int d^4x \sqrt{-\det(g)}\ {}^{(4)}R = \int dt \int d^3x \sqrt{\det(q)} N \left(K_{ab}K^{ab} - (K_a^{\ a})^2 + {}^{(3)}R\right), \tag{1.6}$$

where ${}^{(4)}R$ and ${}^{(3)}R$ denote the four-dimensional and three-dimensional Ricci scalars, respectively, $K_{ab}dx^a dx^b$ is the extrinsic curvature of the three-dimensional surface embedded in spacetime, and $K_a^{\ a}$ stands for its trace. This second fundamental form is the variation of the spatial metric along the normal direction. It is a symmetric tensor, with components

$$K_{ab} := \frac{1}{2}\mathcal{L}_n q_{ab} = \frac{1}{2N}\left(\mathcal{L}_t q_{ab} - 2\,{}^{(q)}\nabla_{(a} N_{b)}\right), \tag{1.7}$$

where ${}^{(q)}\nabla$ is the covariant derivative compatible with the induced three-metric.

1.1.2 Hamiltonian formalism

To introduce the Hamiltonian formulation of GR, we start with the usual ADM approach [82] that takes the induced three-metric to be the configuration variable. One can check that its conjugate momentum

$$p^{ab} := \sqrt{\det(q)}\left(K^{ab} - K_c{}^c q^{ab}\right), \tag{1.8}$$

is directly related to the extrinsic curvature, with $\{q_{ab}(x_1), p^{cd}(x_2)\} = \delta^c_a \delta^d_b \delta(x_1, x_2)$. Note that all these three tensors are symmetric. The above relation is invertible, and we can perform a Legendre transformation on (1.6) to obtain the total Hamiltonian of the system,

$$\begin{aligned} H_{\text{TOT}} &= \int d^3x\, \mathcal{H}_{\text{TOT}} := \int d^3x \left(\dot{q}_{ab}p^{ab} - \sqrt{\det(q)}N\left(K_{ab}K^{ab} - (K_a{}^a)^2 + {}^{(3)}R\right)\right) \\ &= \int d^3x \sqrt{\det(q)}\left(N\left(\frac{2p_{ab}p^{ab} - (p_a{}^a)^2}{2\det(q)} - {}^{(3)}R\right) - 2N^{a(q)}\nabla_b\left(\frac{p_a^b}{\sqrt{\det(q)}}\right)\right), \end{aligned} \tag{1.9}$$

with p_a^a the trace of the momentum, and where we have integrated by parts to remove (spatial) derivatives of N^a. Notice that there are no time derivatives of the lapse N and the shift N^a; they are Lagrange multipliers. Their respective conjugate momenta, $\mathcal{P}$ and $\mathcal{P}_a$, are thus vanishing, and define primary constraints of the system. We can formally compute the evolution of the primary constraints,

$$\mathcal{C} := -\frac{\partial \mathcal{H}_{\text{TOT}}}{\partial N} = \sqrt{\det(q)}\,{}^{(3)}R - \frac{p_{ab}p^{ab}}{\sqrt{\det(q)}} + \frac{(p_a{}^a)^2}{2\sqrt{\det(q)}} \approx 0, \tag{1.10a}$$

$$\mathcal{C}_a := -\frac{\partial \mathcal{H}_{\text{TOT}}}{\partial N^a} = 2\sqrt{\det(q)}\,{}^{(q)}\nabla_b\left(\frac{p_a^b}{\sqrt{\det(q)}}\right) \approx 0, \tag{1.10b}$$

where we use "$\approx$" for equalities obeyed on-shell. These are secondary constraints, and they are called the Hamiltonian constraint and the diffeomorphism constraint, respectively. There are no further (tertiary) constraints, and the system is self-consistent. We now realise that the total Hamiltonian can be expressed as a linear combination of constraints,

$$H_{\text{TOT}} = \int d^3x \big(N\mathcal{C} + N^a\mathcal{C}_a\big) =: C[N] + C_a[N^a], \tag{1.11}$$

where we have additionally introduced on the right-hand side the notation of smeared constraints that will be employed in the following. In the Hamiltonian description of GR, the constraints play a crucial role: They restrict the initial data and generate gauge transformations, including time evolution. Indeed, the vanishing of $\mathcal{C}$ and $\mathcal{C}_a$, along with $\dot{q}_{ab} := \{q_{ab}, H_{\text{TOT}}\}$ and $\dot{p}_{ab} := \{p_{ab}, H_{\text{TOT}}\}$, is entirely equivalent to the Einstein vacuum equations. More pre-

cisely, the two constraints are just contractions of the Einstein tensor with the unit normal vector such that $\mathcal{C}_a = 0$ and $\mathcal{C} = 0$ imply $G_{0a} = 0$ and $G_{00} = 0$, respectively. The six remaining (second-order) differential equations, $G_{ab} = 0$, are encoded in the twelve (first-order) evolution equations for q_{ab} and p_{ab}.

Although the Hamiltonian formulation loses the manifest diffeomorphism invariance, the theory remains covariant only if the constraints are preserved under gauge transformations, which is guaranteed whenever those constraints are first class. That is precisely the case of GR, and the set of relations between constraints is known as the hypersurface deformation algebra:

$$\{C_a[s_1^a], C_b[s_2^b]\} = C_a[s_1^b \partial_b s_2^a - s_2^b \partial_b s_1^a], \tag{1.12a}$$

$$\{C_a[s_1^a], C[s_2]\} = C[s_1^a \partial_a s_2], \tag{1.12b}$$

$$\{C[s_1], C[s_2]\} = C_a[F^{ab}(s_1 \partial_b s_2 - s_2 \partial_b s_1)], \tag{1.12c}$$

with s and s^a suitable smearing functions, and $F^{ab} = q^{ab}$ in GR. The first bracket stands for the diffeomorphism symmetry on each hypersurface. The second one ensures that the Hamiltonian, as defined in (1.11), is a weight-one scalar density. The third bracket relates deformations of hypersurfaces as a set. When the structure function in that last bracket is the inverse of the spatial metric, that is, $F^{ab} = q^{ab}$, the set of three-dimensional spacelike hypersurfaces can be embedded in the spacetime manifold, thus providing a foliation with spatial leaves with metric q_{ab} [83, 84]. This is precisely the case in GR but not necessarily in modified Hamiltonian theories. For that reason, a careful analysis of the hypersurface deformation algebra is required to relate the phase-space and geometric descriptions.

Finally, a brief side note may be convenient. Note that, up to this point, we did not worry about matter sources, mainly because their incorporation into the analysis is formally trivial as long as they are minimally coupled to gravity. One only needs to add a generic Lagrangian density, $\mathcal{L}_m$, in (1.6), which, after the $3 + 1$ splitting and the Legendre transformation yielding (1.9), contributes with respective terms to the Hamiltonian and the diffeomorphism constraints. Then, the corresponding combinations of the vacuum and the matter contributions define the full constraints, which must vanish on-shell. In addition, those full constraints follow the algebra (1.12), with the same structure function as in vacuum. Since these matter sources do not provide further insight into the remaining subsections, we will omit them in the following. However, note that, when we write the constraints, they will only contain the vacuum contribution.

1.1.3 Connection formulation

The tetrad formalism maps the tangent space at each point of the manifold to the tangent space of the Minkowski space, and the spacetime metric is the pullback from that flat space to the tangent one. The projection of tetrads on a constant t hypersurface are the triads, e^a_i, which provide an alternative (and equivalent) description to that of the metric formulation [85].

Let (Σ_t, q) be a leaf of the spacetime foliation, (E, δ) a three-dimensional Euclidean space, and consider the map

$$\begin{aligned} e: \quad T\Sigma_t &\to TE \\ u^a\partial_a &\to u^a e^i_a \partial_i, \end{aligned} \tag{1.13}$$

and the function $\delta : TE \times TE \to \mathbb{R}$. Then, the metric $q : T\Sigma_t \times T\Sigma_t \to \mathbb{R}$ is just the pullback of δ by e at each point. That is, $\delta_{ij}(u^a e^i_a)(v^b e^j_b) = q_{ab}u^a u^b$, and thus $q_{ab} = \delta_{ij}e^i_a e^j_b$. We will label by i, j, k the flat indices running from 1 to 3. The position of these internal indices is not relevant, $u^i = u_i$, and we will write them conveniently opposed to spacetime indices.

Intuitively, the triads provide an orthonormal basis of the tangent space at each point,

$$q_{ab}e^a_i e^b_j = \delta_{ij}, \tag{1.14}$$

where e^a_i and e^b_j diagonalise the metric at each point. Note that $e^i_a e^a_j = \delta^i_j$ and $e^i_a e^b_i = \delta^b_a$, which define e^i_a as the inverse of the three orthonormal vector fields e^a_i.

In addition to the inherent Riemannian geometry, the triad formalism associates an internal Euclidean space to each point of the hypersurface, and one finds an additional local $SO(3)$ symmetry due to the rotational degrees of freedom in e^a_i that are not present in the metric q_{ab}. The addition of this internal space requires the extension of the covariant derivative in such a way that it obeys the Leibniz rule $\nabla_a(u_b v_i) = (\nabla_a u_b)v_i + u_b(\nabla_a v_i)$. Consider

$$\nabla_a e^b_i = \partial_a e^b_i + \Gamma^b{}_{ac} e^c_i + \Gamma^j{}_{ai} e^b_j, \tag{1.15}$$

where $\Gamma^b{}_{ac}$ are the Christoffel symbols, and when the above expression vanishes, that is, when the covariant derivative is compatible with the triad, $\Gamma^j{}_{ai}$ are the components of the so-called spin connection. We will denote this as ${}^{(e)}\nabla_a$. The Christoffel symbols are symmetric in the lower indices, $\Gamma^b_{ac} = \Gamma^b_{ca}$. In contrast, the spin connection is antisymmetric in the internal space, i.e., $\Gamma^j{}_{ai} = -\Gamma^i{}_{aj}$, as one can check from the symmetry $e^b_i = e^{bi}$.

Rather than the triad, we will use its densitized version,

$$E^a_i := \sqrt{\det(q)}\, e^a_i, \tag{1.16}$$

simply because it is a vector density of weight one and thus ${}^{(e)}\nabla_a E^b_i = \partial_a E^b_i + \Gamma^j{}_{ai} E^b_j$, which does not depend on the Christoffel symbols. Note that the positiveness of $\det(q)$, plus its smoothness, imposes a constant sign on the determinant of the triad. Indeed, this is the requirement for the hypersurface to be orientable. Taking now the divergence of the densitized triad,

$$0 = {}^{(e)}\nabla_a E^a_i = \partial_a E^a_i + \Gamma^j{}_{ai} E^a_j =: \partial_a E^a_i + \epsilon_{ijk}\Gamma^j_a E^a_k, \tag{1.17}$$

we can define Γ^j_a in the last step based on the antisymmetry of the spin connection in the internal indices. From the above expression, it is evident that Γ^j_a is a function of the densitized triad and its derivatives only.

In a similar fashion, one defines $K^i_a := e^b_i K_{ab}$, such that $K_{ab} = K^i_a e^j_b \delta_{ij}$. Since the extrinsic curvature is symmetric, K^i_a cannot be arbitrary, and it is constrained by $K^i_{[a} e^i_{b]} = 0$. After a contraction with $\sqrt{\det(q)}\, e^a_k e^b_j$, we may express this last relation as $K_{a[j} E^a_{k]} = 0$. This is equivalent to demanding the vanishing of

$$\mathcal{G}_i := \epsilon_{ijk} K^j_a E^a_k, \tag{1.18}$$

which is, in fact, the generator of the internal $SO(3)$ rotations within the triad formulation. Moreover, $\{K^i_a(x_1), E^b_j(x_2)\} = \delta^b_a \delta^i_j \delta(x_1, x_2)$ and $\{q_{ab}(x_1), p^{cd}(x_2)\} = \delta^c_a \delta^d_b \delta(x_1, x_2)$ define the same phase space precisely on the surface $\mathcal{G}_i \approx 0$. This constraint is usually referred to as the Gauss law. Let us illustrate this by expressing (1.18) as a total divergence.

For that purpose, we need to find a suitable generalised covariant derivative. Let us point out that the symplectic structure remains unaltered under the constant transformation $K^i_a \to \beta K^i_a$ and $E^b_j \to E^b_j/\beta$, where β is known as the Immirzi-Barbero parameter [86]. One can then check that the Christoffel symbols and the spin connection are invariant under this rescaling. Thus, the covariant derivative ${}^{(e)}\nabla_a$ is independent of the parameter β, and it is straightforward to see that $\mathcal{G}_i$ is also insensitive to this rescaling. We are finally in a position to write the rescaled form of (1.18) as a divergence, simply adding ${}^{(e)}\nabla_a E^a_i/\beta$, which is zero by (1.17):

$$\mathcal{G}_i = {}^{(e)}\nabla_a (E^a_i/\beta) + \epsilon_{ijk}(\beta K^j_a)(E^a_k/\beta) = \partial_a (E^a_i/\beta) + \epsilon_{ijk}\big(\Gamma^j_a + \beta K^j_a\big)(E^a_k/\beta). \tag{1.19}$$

Upon the definition of a new covariant derivative,

$$D_a E^a_i := \partial_a E^a_i + \epsilon_{ijk}\big(\Gamma^j_a + \beta K^j_a\big)E^a_k, \tag{1.20}$$

we can write $\mathcal{G}_i = \beta^{-1} D_a E^a_i$. The constraint surface $\mathcal{G}_i = 0$ is thus given by $D_a E^a_i = 0$, that is, the new derivative annihilates the densitized triad. Note that D_a acts as the usual covariant derivative on spacetime quantities, $D_a u_b = {}^{(q)}\nabla_a u_b$, and as a Yang-Mills $SU(2)$ derivative on the internal space, $D_a v_i = \partial_a v_i + \epsilon_{ijk} A^j_a v_k$, with connection components

$$A^j_a := \Gamma^j_a + \beta K^j_a, \tag{1.21}$$

which is usually referred to as the Ashtekar connection. This element plays a central role in loop quantum gravity as it forms a canonical pair with the densitized triad,

$$\{A^i_a(x_1), E^b_j(x_2)\} = \beta \delta^b_a \delta^i_j \delta(x_1, x_2). \tag{1.22}$$

In terms of these new variables, the total Hamiltonian reads [35]

$$H_{\text{TOT}} = \int d^3x \left(\Lambda^i \mathcal{G}_i + N^a \mathcal{C}_a + N\mathcal{C}\right) =: G[\Lambda] + C_a[N^a] + C[N], \tag{1.23}$$

with $\mathcal{G}_i = D_a E^a_i/\beta$ the Gauss constraint, $\mathcal{C}_a = F^i_{ab} E^b_i/\beta$ the diffeomorphism constraint and

$$\mathcal{C} = \frac{\epsilon_{ijk} E^a_j E^b_k}{\sqrt{\det(q)}} \left(F^i_{ab} - (1+\beta^2)\epsilon_{ilm} K^l_a K^m_b\right), \tag{1.24}$$

the Hamiltonian constraint. In the last expression, $F^i_{ab} := 2\partial_{[a} A^i_{b]} + \epsilon_{ilm} A^l_a A^m_b$ is the curvature of the connection, and $\det(q)$ and K^l_a must be taken as functionals of A^l_a and E^l_a. As a final remark, the enhanced constraint structure remains first-class but now with six relations (only five non-trivial ones, because $G[\Lambda]$ and $C[N]$ commute off-shell).

1.1.4 Towards the loop representation

We need to find a suitable smearing for the connection variables A^i_a to obtain a non-distributional behaviour of their Poisson bracket with the densitized triads E^b_j. Not all choices are acceptable, and the smearings must be such that they do not introduce a background metric (recall that LQG aims for a background-independent theory). In addition, there should be a direct relation to gauge-invariant objects since, eventually, one will be interested in tracking such quantities. This problem is common to non-abelian Yang-Mills theories, and we may import some valuable lessons from their study.

First, we need to define the concept of holonomy, which is a consequence of the curvature of a connection in a smooth manifold and measures the variation of geometric quantities along a closed path. More precisely, making use of the Ashtekar connection (1.21), and its associated covariant derivative (1.20), v^b is said to be parallel-transported along the curve γ, with tangent vector $\dot{\gamma}^a$, provided $\dot{\gamma}^a D_a v^b = 0$. This differential equation can be iteratively solved, and when the path is closed, $\gamma(t) = \gamma(0)$, the solution is $v^b(t) = h_\gamma(A)v^b(0)$, where

$$h_\gamma(A) := \mathcal{P}\left[\exp\left(-\frac{i}{2}\oint_\gamma \sigma_j \dot{\gamma}^a A_a^j\right)\right] \tag{1.25}$$

is the holonomy of the connection along that curve, the elements σ_j are Pauli matrices and $\mathcal{P}\big[x_2(t_2)x_1(t_1)\big] \equiv \mathcal{P}\big[x_1(t_1)x_2(t_2)\big] := x_2(t_2)x_1(t_1)$, for $t_2 > t_1$, is the path-ordering operator. The trace of a holonomy — also known as Wilson loop — is a gauge-invariant scalar quantity. Furthermore, the set of all possible Wilson loops forms a basis for any observable that is a function of the connection only.

Second, since the connection has been smeared in one dimension, we define the flux of the densitized triad across a two-dimensional surface, S,

$$\Phi_S(E, f) := \int_S u_a f^j E_j^a, \tag{1.26}$$

with u_a the normal one-form to the two-dimensional surface, which is independent of any background metrics, and $f := -if^j\sigma_j$ an $su(2)$-valued scalar smearing function. The Poisson bracket between holonomies and fluxes reads

$$\big\{h_\gamma(A), \Phi_S(E, f)\big\} = i\beta\delta(\gamma, S) f^j h_{\gamma_2}(A)\sigma_j h_{\gamma_1}(A). \tag{1.27}$$

The function $\delta(\gamma, S)$ vanishes whenever the curve γ does not intersect or is tangential to the surface S. When they do intersect, $\delta(\gamma, S)$ is positive (negative) if the orientation of the curve and that of the surface is the same (opposite). More precisely, it takes the values $\pm 1/2$ when the intersection point is either the starting or final point of γ. Otherwise, $\delta(\gamma, S) = \pm 1$ and S divides γ in two open paths, γ_1 and γ_2.

This Poisson structure can be promoted to a commutator algebra upon Dirac's quantisation procedure. Eventually, loop quantum gravity leads to geometric operators describing a quantised spacetime, and the geometry becomes discrete at the Planck level.

1.2 Construction of the metric

We started from a foliated spacetime with induced spatial metric q_{ab}. The Poisson brackets between constraints produced a structure function F^{ab}, which in GR is precisely the inverse of q_{ab}. The way back from the canonical representation to the spacetime picture is, therefore, trivial. In this section, we will consider some generic $\mathcal{C}$, $\mathcal{C}_a$, and F^{ab} satisfying (1.12), and construct the corresponding metric tensor, without assuming prior knowledge of a spacetime. That is, indeed, the situation we will be facing when modifying the GR Hamiltonian.

The intuition about how to obtain a geometric description associated with the Hamiltonian formulation lies at the core of this thesis because we will introduce corrections on the phase space. Those changes will modify the structure functions in the algebra between constraints, and the geometry described by the new Hamiltonian will not be generically the same as the one described by GR.

For the theory to be covariant, diffeomorphism invariance must be read from the gauge freedom of the phase space. To deduce the form of the metric associated with the Hamiltonian, we suggest a generic ansatz,

$$d\widetilde{s}^2 = -\widetilde{N}^2 d\widetilde{t}^{\,2} + \widetilde{q}_{ab}\left(\widetilde{N}^a d\widetilde{t} + d\widetilde{x}^a\right)\left(\widetilde{N}^b d\widetilde{t} + d\widetilde{x}^b\right), \tag{1.28}$$

and proceed to express the metric components in terms of phase-space quantities. For that purpose, we need to identify objects that change accordingly under coordinate and gauge transformations.

Observe that the time function employed for the $3+1$ decomposition remains unaltered when deriving the Hamiltonian formulation. It is thus reasonable to request that the inverse process preserves the definition of time. Therefore, we will assume that the metric formulation inherits the notion of time from the Hamiltonian formalism, and thus the lapse and the shift are defined in the same way as in (1.2) and (1.3), respectively. Demanding the function $\widetilde{t} = t$ to define the foliation will lead to $\widetilde{N} = N$. In addition, choosing $\widetilde{x}^a = x^a$ for the generic spatial coordinates fixes $\widetilde{N}^a = N^a$, and only $\widetilde{q}_{ab}$ remains to be specified.

First, we compute the Lie derivative of the metric (1.28) along a generic vector field $\xi^\mu\partial_\mu$:

$$\mathcal{L}_\xi N = \partial_t(\xi^t N) + \xi^a\partial_a N - N N^a\partial_a\xi^t, \tag{1.29a}$$

$$\mathcal{L}_\xi N^a = \partial_t(\xi^t N^a + \xi^a) + \xi^b\partial_b N^a - N^b\partial_b\xi^a - \left(N^a N^b + N^2\widetilde{q}^{ab}\right)\partial_b\xi^t, \tag{1.29b}$$

$$\mathcal{L}_\xi \widetilde{q}_{ab} = \xi^t\partial_t\widetilde{q}_{ab} + \xi^c\partial_c\widetilde{q}_{ab} + 2\widetilde{q}_{ac}\left(N^c\partial_b\xi^t + \partial_b\xi^c\right). \tag{1.29c}$$

Second, we study gauge transformations. For a phase-space function Φ, the gauge flow is generated by the total Hamiltonian with four arbitrary gauge parameters ϵ and ϵ^a, that is,

$$\delta_\epsilon \Phi := \{\Phi, C[\epsilon] + C_a[\epsilon^a]\}. \tag{1.30}$$

In order to relate both transformations, this bracket should describe the coordinate change defined by the vector field $\xi^\mu \partial_\mu$ above, provided that the gauge parameters are its components in the normal-tangential basis, i.e.,

$$\xi^\mu \partial_\mu = \xi^t \partial_t + \xi^a \partial_a = \xi^t N n^\mu \partial_\mu + (\xi^t N^a + \xi^a)\partial_a \quad \Rightarrow \quad \begin{cases} \epsilon := \xi^t N, \\ \epsilon^a := \xi^t N^a + \xi^a, \end{cases} \tag{1.31}$$

where we have used (1.4), and $n^\mu \partial_\mu$ stands for the unit vector orthogonal to the hypersurfaces of constant t. Then, (1.30) coincides with the Lie derivative of Φ along $\xi^\mu \partial_\mu$, i.e.,

$$\delta_\epsilon \Phi = \mathcal{L}_\xi \Phi. \tag{1.32}$$

As a side remark, note that time evolution is pure gauge: it stands for the particular choice $\xi^\mu = t^\mu$. In that case, ϵ and ϵ^a are precisely the lapse and the shift:

$$\dot{\Phi} := \{\Phi, C[N] + C_a[N^a]\} = \mathcal{L}_t \Phi. \tag{1.33}$$

The expression (1.30) is valid for all canonical variables, their conjugate momenta, and any functions constructed from them, but not for the Lagrange multipliers. Hence, one still needs to study the gauge transformations of N and N^a.

For instance, a way of computing them is given in Ref. [87]. The procedure is as follows. Recall that at the beginning of Sec. 1.1.2, we said that the momenta conjugate to the lapse N and the shift N^a, $\mathcal{P}$ and $\mathcal{P}_a$, define primary constraints. First, we need to restore those constraints by plugging them in the Hamiltonian with their respective Lagrange multipliers, η and η^a, so that the lapse and the shift become canonical variables. The smeared form of these constraints are $P[\eta]$ and $P[\eta^a]$. The dynamics do not change because the additional terms vanish on-shell. Second, we need to find the diffeomorphism-induced gauge generators, providing the gauge transformations for any functions on this extended phase space [87],

$$\delta_\epsilon \Phi := \Big\{\Phi, P_A\big[\dot{\epsilon}^A + \{C_B[\epsilon^B], C_D[N^D]\}\big] + C_A[\epsilon^A]\Big\}, \tag{1.34}$$

where capital Latin indices take values $\{0,1,2,3\}$, and one should understand $N^0 := N$, $\epsilon^0 := \epsilon$, $C_0 := C$, and $P_0 := P$. Clearly, enforcing $\mathcal{P} = 0$ and $\mathcal{P}_a = 0$ reduces (1.34) to (1.30).

To obtain the gauge variations of the lapse and the shift, we substitute Φ by N^A in (1.34). The only relevant term is the first one on the right-hand side of the Poisson bracket, yielding

$$\delta_\epsilon N^A = \dot{\epsilon}^A + \{C_B[\epsilon^B], C_D[N^D]\}. \tag{1.35}$$

The last bracket is obtained through the commutation relations (1.12). If we split now the expression to read the transformations for the lapse and the shift, we find

$$\delta_\epsilon N = \dot{\epsilon} + \epsilon^b \partial_b N - N^b \partial_b \epsilon, \tag{1.36a}$$
$$\delta_\epsilon N^a = \dot{\epsilon}^a + \epsilon^b \partial_b N^a - N^b \partial_b \epsilon^a + F^{ab}(\epsilon \partial_b N - N \partial_b \epsilon). \tag{1.36b}$$

Now, to make contact with their transformation under an infinitesimal coordinate change, we proceed to substitute the values of ϵ and ϵ^a as given in (1.31),

$$\delta_\epsilon N = \partial_t(\xi^t N) + \xi^a \partial_a N - N N^a \partial_a \xi^t, \tag{1.37a}$$
$$\delta_\epsilon N^a = \partial_t(\xi^t N^a + \xi^a) + \xi^b \partial_b N^a - N^b \partial_b \xi^a - (N^a N^b + N^2 F^{ab}) \partial_b \xi^t, \tag{1.37b}$$

We can immediately identify (1.37a) with (1.29a), and see that $\delta_\epsilon N = \mathcal{L}_\xi N$. Comparing (1.37b) with (1.29b) we find

$$\mathcal{L}_\xi N^a - \delta_\epsilon N^a = \left(F^{ab} - \widetilde{q}^{ab}\right) N^2 \partial_b \xi^t. \tag{1.38}$$

Therefore, since the left-hand side must be vanishing, we deduce that the structure function F^{ab} must be equal to the inverse of the spatial metric $\widetilde{q}_{ab}$. In fact, coming from any Hamiltonian formulation, with canonical brackets (1.12), we may consider this identity as the definition of the spatial metric, $\widetilde{q}_{ab} := F_{ab}$. However, this definition is not always possible. For F_{ab} to be understood as the spatial metric, it must transform accordingly to (1.29c), that is, $\delta_\epsilon F_{ab} = \mathcal{L}_\xi \widetilde{q}_{ab}$. In such a case, the metric

$$ds^2 = -N^2 dt^2 + F_{ab}\left(dx^a + N^a dt\right)\left(dx^b + N^b dt\right), \tag{1.39}$$

associated with the Hamiltonian satisfying (1.12) will meet the principle of general covariance in the sense that gauge variations on phase space describe coordinate transformations.

A necessary condition for a modified theory to remain covariant is thus that the metric is changed accordingly to the algebraic deformation. If the inverse of the structure function did not satisfy the transformation rule (1.29c), we would not be able to recover a consistent metric description as prescribed here.

1.3 Spherical symmetry reduction

The Riemannian space (Σ_t, q) is said to be spherically symmetric when the rotation group $SO(3)$ acts by isometry, and its orbits on Σ_t are two-dimensional spheres. In that case, one can introduce a function x on Σ_t to be constant on the orbits of $SO(3)$. Outside the fixed points of the rotation group, x defines a radial direction, with dx vanishing nowhere.

Taking this adapted coordinate, the only trivially non-vanishing component of the shift vector is the radial one, $N^x := -Nn^\mu \partial_\mu x = -Nn^x$, and with no need of specifying the angular coordinates on the symmetry orbits, we get

$$ds^2 = -N^2 dt^2 + q_{xx}\big(dx + N^x dt\big)^2 + q_{\theta\theta} d\Omega^2, \tag{1.40}$$

where the functions $N(t,x)$, $N^x(t,x)$, $q_{xx}(t,x)$, and $q_{\theta\theta}(t,x)$ are independent of the angular coordinates, and $d\Omega^2$ is the metric of the two-sphere mentioned above.

The spherical symmetry reduction in terms of triads and connections was studied in detail in Ref. [88]. Here we only summarise the most relevant results. The difference with respect to metric variables, where the symmetry reduction yields two independent components q_{xx} and $q_{\theta\theta}$, is that the spherical symmetry reduction of connections and triads leaves three non-trivial components for each. However, the Gauss law still has a residual $U(1)$ gauge freedom, and we may work only with elements invariant under the action of that group. That is, the gauge-invariant quantities will be (A_x, A_φ) for the connection and (E^x, E^φ) for the triad. Similarly, one can decompose the extrinsic curvature and obtain the gauge-invariant pair (K_x, K_φ). One can check that the conjugate variable of E^φ is K_φ, rather than A_φ. Interestingly, A_x and K_x turn out to be proportional after solving the reduced Gauss law.

Therefore, the symplectic structure of the phase space is given by the canonical pairs

$$\{K_x(x_1), E^x(x_2)\} = \{K_\varphi(x_1), E^\varphi(x_2)\} = \delta(x_1, x_2). \tag{1.41}$$

The constant sign of E^x determines the orientation of the triad, and we choose it as positive.

Now, since the two angular components of the diffeomorphism constraint are identically vanishing, at this point we introduce a new notation for the constraints. We denote with a prime the derivative with respect to x, and, in terms of the above variables, we are left with the radial diffeomorphism constraint,

$$\mathcal{D}_g := -E^{x\prime} K_x + K'_\varphi E^\varphi, \tag{1.42a}$$

and the Hamiltonian constraint,

$$\mathcal{H}_g^{(0)} := -\frac{E^\varphi}{2\sqrt{E^x}}\left(1+K_\varphi^2\right) - 2\sqrt{E^x}K_xK_\varphi + \frac{(E^{x\prime})^2}{8\sqrt{E^x}E^\varphi} - \frac{\sqrt{E^x}}{2E^{\varphi 2}}E^{x\prime}E^{\varphi\prime} + \frac{\sqrt{E^x}}{2E^\varphi}E^{x\prime\prime}, \quad (1.42b)$$

as introduced in Ref. [89]. We now recall that the GR Hamiltonian is the sum of the vacuum constraints (1.42) and the corresponding matter contribution,

$$\mathcal{D} := \mathcal{D}_g + \mathcal{D}_m, \quad (1.43a)$$

$$\mathcal{H}^{(0)} := \mathcal{H}_g^{(0)} + \mathcal{H}_m^{(0)}. \quad (1.43b)$$

As we want to study dynamical scenarios, we will consider a spherically symmetric matter field described by a third pair of canonical variables

$$\{\phi(x_1), P_\phi(x_2)\} = \delta(x_1, x_2). \quad (1.44)$$

This includes the two cases that we will have in mind for this thesis: a scalar field and a dust field. Their contribution to the diffeomorphism constraint has the same form,

$$\mathcal{D}_m := \phi' P_\phi, \quad (1.45)$$

while the contributions of the scalar field and the dust field to the Hamiltonian constraint are given by

$$\mathcal{H}_m^{(0)} := \frac{P_\phi^2}{2\sqrt{E^x}E^\varphi} + \frac{(E^x)^{3/2}}{2E^\varphi}(\phi')^2 + \sqrt{E^x}E^\varphi V(E^x,\phi), \quad (1.46a)$$

$$\mathcal{H}_m^{(0)} := P_\phi\sqrt{1+\frac{E^x}{(E^\varphi)^2}(\phi')^2}\,, \quad (1.46b)$$

respectively. Both sets of constraints, in vacuum (1.42) and with matter (1.43), obey the hypersurface deformation algebra,

$$\left\{D[s_1], D[s_2]\right\} = D\left[s_1s_2' - s_1's_2\right], \quad (1.47a)$$

$$\left\{D[s_1], H^{(0)}[s_2]\right\} = H^{(0)}\left[s_1s_2'\right], \quad (1.47b)$$

$$\left\{H^{(0)}[s_1], H^{(0)}[s_2]\right\} = D\left[F(s_1s_2' - s_1's_2)\right], \quad (1.47c)$$

with the structure function F having only one component after the symmetry reduction. As a result of the symmetry reduction, the angular sector is now trivial and the algebra does not provide any information about the angular components of the metric tensor.

In the particular case of GR,

$$F = \frac{E^x}{(E^\varphi)^2}, \tag{1.48}$$

and the corresponding metric reads

$$ds^2 = -N^2 dt^2 + \frac{(E^\varphi)^2}{E^x}\big(dx + N^x dt\big)^2 + E^x d\Omega^2. \tag{1.49}$$

As we will show in the next chapter, the modifications performed at the Hamiltonian level will deform the commutation relations between constraints and thus the metric, if any, describing such corrections. As commented above, the angular part of the metric is insensitive to these changes due to the symmetry reduction, so we can only fix its Lorentzian part. Hence, the metric will generically read

$$ds^2 = -N(t,x)^2 dt^2 + \frac{1}{F(t,x)}\big(dx + N^x(t,x)dt\big)^2 + r(t,x)^2 d\Omega^2, \tag{1.50}$$

with $r(t,x)$ being a spacetime scalar function.

In principle, any such scalar is eligible, but different functions will lead to different geometries. Our choice is simple: As we did for the lapse and the shift, we will assume that the modifications do not affect the angular part of the metric. In other words, the effective corrections preserve the foliation (the time function) and the area of the orbits of the rotation group (the area-radius function). Therefore, and as long as E^x keeps transforming as a scalar under general gauge transformations generated by $H[\epsilon] + D[\epsilon^x]$, we will define $r(t,x) := \sqrt{E^x}(t,x)$.

2

Covariant Deformations of General Relativity

I tested the brackets by hitting them with rocks. This kind of sophistication is what we interplanetary scientists are known for.

The Martian
by Andy Weir.

We devote this chapter to the construction of the effective theory. We will incorporate modifications to the spherically symmetric GR Hamiltonian (1.43), in such a way that it remains covariant, in the sense that it has an associated geometric picture. We will explicitly show this by constructing the metric tensor from phase-space functions, as explained in Sec. 1.2.

In Sec. 2.1, we provide a brief review of the successful mechanism inducing singularity resolution in effective homogeneous and isotropic cosmological models, and we comment on some previous attempts to incorporate holonomy corrections in spherical symmetry. The main body of this chapter is divided in two sections, Sec. 2.2 and Sec. 2.3. The former studies the vacuum case while the latter incorporates matter. Their structure is very similar: We start from a generic Hamiltonian constraint and demand that it generates an anomaly-free algebra. After that, we explicitly construct its associated metric. These two conditions heavily restrict the form of the Hamiltonian. In fact, in Sec. 2.4, we obtain a particular family of Hamiltonians, which depends only on one free function, that satisfies all our requirements. The final section (Sec. 2.5) is devoted to relate the effective model with GR.

2.1 Background and motivation

We depict an effective cosmology, and the unfruitful extension to spherical symmetry.

2.1.1 Homogeneous and isotropic cosmology

The usual variables that are used in the literature to describe homogeneous and isotropic cosmological models in the context of loop quantum cosmology are b and v, satisfying the

Poisson bracket $\{b, v\} = 1$. The variable b is directly related to the Hubble parameter, and v describes the volume of the universe. Considering a scalar field ϕ, with conjugate momentum P_ϕ, as the matter content, the homogeneous and isotropic Hamiltonian reads

$$\mathcal{C}^{(0)} = -c_1|v|b^2 + c_2\frac{P_\phi^2}{|v|} \approx 0. \tag{2.1}$$

All c_k in this section are constants that do not affect the generic derivation presented here. The energy density for the field is defined as

$$\rho := c_3\frac{P_\phi^2}{v^2} \approx \frac{c_1c_3}{c_2}b^2, \tag{2.2}$$

where the last equality holds on-shell, i.e., when $\mathcal{C}^{(0)}$ vanishes. Since v corresponds to the volume, the Hubble parameter $\mathbb{H}_0$ is proportional to $\dot{v}/|v|$, that is,

$$\mathbb{H}_0^2 = c_4\frac{\dot{v}^2}{v^2} \approx 4\frac{c_1c_2c_4}{c_3}\rho, \tag{2.3}$$

where we have used $\dot{v} = \{v, \mathcal{C}^{(0)}\} = 2c_1|v|b$ and the definition (2.2). Therefore, the Hubble parameter is not bounded from above and it only vanishes for $\rho = 0$.

The "usual" polymerisation replaces b by $\sin(\lambda b)/\lambda$, and defines the effective Hamiltonian

$$\mathcal{C}^{(\mathrm{pol})} = -c_1|v|\frac{\sin^2(\lambda b)}{\lambda^2} + c_2\frac{P_\phi^2}{|v|} \approx 0. \tag{2.4}$$

By definition, the energy density (2.2) is still the same, but its on-shell value in terms of b is also polymerised as it now corresponds to the vanishing of $\mathcal{C}^{(\mathrm{pol})}$. Hence, it is different to its classical form, that is,

$$\rho = c_3\frac{P_\phi^2}{v^2} \approx \frac{c_1c_3}{c_2}\frac{\sin^2(\lambda b)}{\lambda^2}. \tag{2.5}$$

The effective dynamics, $\dot{v} = \{v, \mathcal{C}^{(\mathrm{pol})}\} = c_1|v|\lambda^{-1}\sin(2\lambda b)$, yield the Hubble parameter

$$\mathbb{H}_{\mathrm{pol}}^2 = c_4\frac{(\dot{v})^2}{v^2} = c_1\frac{\sin^2(2\lambda b)}{\lambda^2} \approx 4\frac{c_1c_2c_4}{c_3}\rho\left(1 - \frac{\rho}{\rho_{\mathrm{max}}}\right) = \left(1 - \frac{\rho}{\rho_{\mathrm{max}}}\right)\mathbb{H}_0^2, \tag{2.6}$$

with $\rho_{\mathrm{max}} := c_1c_3/(c_2\lambda^2)$. This finite value provides the energy density $\rho = \rho_{\mathrm{max}}$ where the Hubble rate vanishes, which corresponds to a minimum value of v (because $\dot{v} = 0$ and $\ddot{v} > 0$ there). This means that the scale factor in this model experiences a bounce when reaching the critical density ρ_{max}, and the Big-Bang singularity is thus avoided.

2.1.2 First contact with spherical holonomy modifications

Motivated by the fact that simple effective models, such as the one just presented, agree with the full quantum dynamics of loop quantum cosmology, there has been a huge effort to build effective spherical models implementing key attributes of LQG so as to confirm whether singularity resolution is an enduring property of the theory. The extension of the mechanisms avoiding the Big Bang to spherical symmetry would be a robustness check of those predictions. Here, we briefly review known results on holonomy corrections that explicitly respect the first-class nature of the hypersurface deformation algebra.

Following the standard procedure found in the literature [66, 73, 75], let us replace the terms K_φ and K_φ^2 in (1.42b) by $f_1(K_\varphi)$ and $f_2(K_\varphi)$, respectively, and define the holonomy-modified vacuum Hamiltonian constraint,

$$\begin{aligned}\mathcal{H}_g^{(h)} :=& -\frac{E^\varphi}{2\sqrt{E^x}}\Big(1+f_2(K_\varphi)\Big) - 2\sqrt{E^x}K_x f_1(K_\varphi)\\ &+\frac{(E^{x\prime})^2}{8\sqrt{E^x}E^\varphi} - \frac{\sqrt{E^x}}{2E^{\varphi 2}}E^{x\prime}E^{\varphi\prime} + \frac{\sqrt{E^x}}{2E^\varphi}E^{x\prime\prime},\end{aligned} \tag{2.7}$$

along with its smeared form $H_g^{(h)}[s] := \int s\mathcal{H}_g^{(h)}dx$. Considering this deformed Hamiltonian in combination with the classical diffeomorphism constraint (1.42a), one can check that the first two brackets of the hypersurface deformation algebra, (1.47a) and (1.47b), remain unaltered. In turn, the third bracket (1.47c) generates an anomalous term,

$$\begin{aligned}\Big\{H_g^{(h)}[s_1], H_g^{(h)}[s_2]\Big\} =& D_g\big[F(s_1s_2' - s_1's_2)\big]\\ &+\int\frac{E^{x\prime}}{4E^\varphi}\left(2f_1 - \frac{\partial f_2}{\partial K_\varphi}\right)(s_1s_2' - s_1's_2)dx.\end{aligned} \tag{2.8}$$

In order to remove it, one must simply enforce the relation $2f_1 = \partial f_2/\partial K_\varphi$, which leaves f_2 as the only free function of the model. The usual choice for this function is $f_2 = \sin^2(\lambda K_\varphi)/\lambda^2$, which is interpreted as parametrising the holonomy corrections, so that (2.7) reads

$$\begin{aligned}\mathcal{H}_g^{(h)} =& -\frac{E^\varphi}{2\sqrt{E^x}}\left(1+\frac{\sin^2(\lambda K_\varphi)}{\lambda^2}\right) - \sqrt{E^x}K_x\frac{\sin(2\lambda K_\varphi)}{\lambda}\\ &+\frac{(E^{x\prime})^2}{8\sqrt{E^x}E^\varphi} - \frac{\sqrt{E^x}}{2E^{\varphi 2}}E^{x\prime}E^{\varphi\prime} + \frac{\sqrt{E^x}}{2E^\varphi}E^{x\prime\prime}.\end{aligned} \tag{2.9}$$

The structure function in (2.8) is then

$$F = \frac{1}{2}\frac{\partial^2 f_2}{\partial K_\varphi^2}\frac{E^x}{E^{\varphi 2}} = \cos(2\lambda K_\varphi)\frac{E^x}{E^{\varphi 2}}. \tag{2.10}$$

Although providing an algebra, the above Hamiltonian faces some conceptual problems.

First, the inverse of the structure function (2.10) does not transform adequately as required by (1.29c), and there is not a metric associated with the Hamiltonian (2.9) as derived in Sec. 1.2.

Second, the above modification is inconsistent with the addition of (minimally coupled) matter with local degrees of freedom [73]. To prove it, let us consider a minimally coupled matter model of the form $\mathcal{D} = \mathcal{D}_g + \mathcal{D}_m$ and $\mathcal{H}^{(h)} = \mathcal{H}_g^{(h)} + \mathcal{H}_m$, where $\mathcal{H}_m$ depends on the matter variables and their derivatives, and on the triad components, but does not depend on derivatives of the triad nor on curvature components. Due to these restrictions, one can check that the bracket $\{H_g^{(h)}[s_1], H_m[s_2]\}$ is antisymmetric under the change $s_1 \leftrightarrow s_2$, and

$$\left\{H^{(h)}[s_1], H^{(h)}[s_2]\right\} = \left\{H_g^{(h)}[s_1], H_g^{(h)}[s_2]\right\} + \left\{H_m[s_1], H_m[s_2]\right\}. \tag{2.11}$$

Since the bracket between vacuum Hamiltonian constraints is (2.8), anomaly-freedom demands $\left\{H_m[s_1], H_m[s_2]\right\} = D_m[F(s_1 s_2' - s_1' s_2)]$. That is, the bracket between matter Hamiltonian constraints must be proportional to the matter diffeomorphism constraint. Recall now that our assumptions for $\mathcal{H}_m$ mean, in particular, that F must be independent of K_φ. As a result, the vacuum Hamiltonian constraint is, at most, quadratic in that variable [see (2.10)], ruling out the holonomy corrections that were allowed in vacuum.

Hence, we must conclude that there is no known way to render the usual holonomy corrections in non-homogeneous vacuum models. And, even if there was, these modifications turn out to be incompatible with the addition of minimally coupled local degrees of freedom. If one seeks a consistent notion of holonomy effects, further changes in the Hamiltonian are needed.

A possible way out to these no-go results for holonomy corrections in non-homogeneous spacetimes would be that matter and geometric degrees of freedom developed non-minimal couplings when approaching the quantum regime, which, far from being discarded, seems a plausible circumstance in the quantum world of gravitation. But, in addition, the vacuum Hamiltonian must be further deformed because no covariant notion of holonomy correction exists. Such modifications could involve, for instance, higher powers of curvature components, higher derivative terms, and/or couplings between the curvature and derivatives of the triad (that is, couplings between spatial and time derivatives of the metric).

2.1.3 Outline

The goal of this chapter is twofold, as we want to find all possible covariant modifications that can be interpreted as holonomy corrections, but also to learn how those could be made compatible with matter with local degrees of freedom. For that purpose, we begin with a general Hamiltonian constraint and impose the following requirements,

i. The derivative structure is the same as in GR.

ii. The constraints must form an anomaly-free algebra.

iii. The model must be embeddable in a four-dimensional manifold as explained in Sec. 1.2. That is, the structure functions in the algebra must transform adequately in order to define a metric associated to the Hamiltonian.

iv. The GR Hamiltonian (1.43) ought to be recovered in a suitable limit.

v. There has to be an explicit vacuum limit.

Our initial ansatz will thus assume that the derivative structure of the Hamiltonian constraint is the same as in GR, i.e., it is linear in second-order radial derivatives and quadratic in first-order radial derivatives of the momenta. Every other combination of canonical variables will be allowed, both on their own and coupled to derivative terms. The main body of the computations in this chapter has been performed with computer algebra tools.

Along the whole chapter, we will use the expression "canonical form of the algebra" to refer to the commutation relations between constraints that read as (1.47), that is,

$$\{D[s_1], D[s_2]\} = D\left[s_1 s_2' - s_1' s_2\right], \tag{2.12a}$$

$$\{D[s_1], H[s_2]\} = H\left[s_1 s_2'\right], \tag{2.12b}$$

$$\{H[s_1], H[s_2]\} = D\left[F(s_1 s_2' - s_1' s_2)\right], \tag{2.12c}$$

with any structure function F that does not vanish identically.

In Sec.2.2, we will present the construction for vacuum, and we will find the most general Hamiltonian that satisfies all requirements above. In Sec. 2.3, we will consider an additional couple of conjugate variables to describe matter with local degrees of freedom, and we will find the most general Hamiltonian that fulfils (i) and (ii). In Sec. 2.4, we will obtain a particular solution meeting the five conditions (i)–(v).

2.2 Covariant holonomy corrections in vacuum

In order to have a compact notation, we define a new set of canonical pairs of variables,

$$\{q_i(x_1), p_j(x_2)\} = \delta_{ij}\delta(x_1, x_2), \tag{2.13}$$

with the subindices i, j being 1 or 2. We consider now the most general Hamiltonian constraint with two pairs of conjugate variables which is quadratic in radial derivatives of the momenta and linear in a second-order derivative term:

$$\mathcal{H}_g = a_0 + (p_1')^2 a_1 + p_1' p_2' a_2 + (p_2')^2 a_3 + p_1'' a_4, \tag{2.14}$$

where $a_k = a_k(q_1, q_2, p_1, p_2)$, for $k = 0, 1, 2, 3, 4$. Recall that the prime denotes the derivative with respect to x. Regarding the diffeomorphism constraint, we will consider its classical form (1.42a),

$$\mathcal{D}_g = -q_1 p_1' + q_2' p_2. \tag{2.15}$$

where the primed momentum coincides with that of the second-order derivative in $\mathcal{H}_g$. The GR Hamiltonian (1.42) is clearly included in the above ansatz for the specific choice

$$a_0 = -2\sqrt{p_1} q_1 q_2 - \frac{p_2}{2\sqrt{p_1}}\left(1 + q_2^2\right), \quad a_1 = \frac{1}{8 p_1 p_2}, \quad a_2 = -\frac{\sqrt{p_1}}{2{p_2}^2}, \quad a_4 = \frac{\sqrt{p_1}}{2p_2}, \tag{2.16}$$

and $a_3 = 0$, along with the identification

$$q_1 = K_x, \qquad p_1 = E^x, \qquad q_2 = K_\varphi, \qquad \text{and} \qquad p_2 = E^\varphi. \tag{2.17}$$

In the construction that will be performed in the following subsection, we assume that only the function a_3 can be set to zero. Otherwise, we would not have GR as a limit of the model. The remaining free functions a_0, a_1, a_2, and a_4, along with the variables q_1 and q_2, and the momenta p_1 and p_2 cannot be identically vanishing.

Recall also that the Hamiltonian must be a weight-one density on the spatial leave, as ensured by the bracket (2.12b). In this symmetry-reduced model, one variable of each conjugate couple is a scalar (on the spatial leave), whereas the other one is a weight-one density [88]. To

check this, we compute their gauge transformations generated by the constraint $D_g[v]$,

$$\{q_1, D_g[v]\} = vq_1' + v'q_1, \qquad \{p_1, D_g[v]\} = vp_1', \tag{2.18a}$$

$$\{q_2, D_g[v]\} = vq_2', \qquad \{p_2, D_g[v]\} = vp_2' + v'p_2, \tag{2.18b}$$

and we compare them with the Lie derivatives along the vector field $v^x\partial_x$, i.e., $\mathcal{L}_v q_1$, $\mathcal{L}_v p_1$, $\mathcal{L}_v q_2$, and $\mathcal{L}_v p_2$, respectively. We see that p_1 and q_2 are scalars, while q_1 and p_2 are necessarily scalar densities of weight one. Therefore, the primed variables in (2.15) are the scalars and their conjugate momenta retain the weight. Also notice that every radial derivative adds a density weight one.

2.2.1 Anomaly freedom

Let us define the concept of anomaly. Any terms that prevent the algebra between constraints being first class are considered anomalous. We now compute the commutation relations between the above constraints, (2.14) and (2.15), and read the conditions for anomaly freedom.

On the one hand, the bracket of the diffeomorphism constraint with itself still follows,

$$\{D_g[s_1], D_g[s_2]\} = D_g[s_1 s_2' - s_1' s_2], \tag{2.19}$$

because the functional form of the diffeomorphism constraint (2.15) remains unaltered. On the other hand, the remaining two commutation relations in the algebra between constraints are modified.

We first compute $\{D_g[s_1], H_g[s_2]\}$, and we remove derivatives of s_1 by integration by parts, until getting an expression of the form

$$\{D_g[s_1], H_g[s_2]\} = \int dx\, s_1 \left(s_2 F_0 + s_2' F_1 + s_2'' F_2\right), \tag{2.20}$$

to sistematically find all anomalous terms. Here, F_0, F_1, and F_2 encode expressions that depend on the five a_k functions and their partial derivatives, and also of the canonical variables and momenta, and their radial derivatives (up to third order). To set apart anomalies from terms vanishing on-shell, we isolate p_1'' and q_2 from the constraints (2.14) and (2.15), that is,

$$q_2' = \frac{1}{q_2}\left(\mathcal{D}_g + q_1 p_1'\right), \tag{2.21a}$$

$$p_1'' = \frac{1}{a_4}\left(\mathcal{H}_g - a_0 - (p_1')^2 a_1 - p_1' p_2' a_2 - (p_2')^2 a_3\right), \tag{2.21b}$$

and we replace these values in F_0, F_1, and F_2. Recall that the constraints vanish on-shell, $\mathcal{D}_g \approx 0$ and $\mathcal{H}_g \approx 0$, so we need the right-hand side of (2.20) to vanish on-shell to obtain a first-class algebra. That is,

$$s_2 F_0 + s_2' F_1 + s_2'' F_2 \approx 0. \tag{2.22}$$

Clearly, the terms F_0, F_1, and F_2 do not depend on s_2 nor its derivatives, so the above gives rise to three independent equations,

$$F_0 \approx 0, \qquad F_1 \approx 0, \qquad \text{and} \qquad F_2 \approx 0. \tag{2.23}$$

But, further, the free functions a_k do not depend on radial derivatives. Therefore, each coefficient going with any combinations of radial derivatives must vanish by itself off-shell. This allows us to further split the anomalies into different expressions that must vanish independently.

For instance, F_2 is given on-shell by

$$F_2 \approx -\left(a_4 + p_2 a_2\right) p_1' - 2 p_2 a_3 p_2', \tag{2.24}$$

and, thus, it produces two independent conditions

$$a_2 = -\frac{a_4}{p_2} \qquad \text{and} \qquad a_3 = 0. \tag{2.25}$$

We can now enforce these two conditions to simplify F_0 and F_1. Let us first focus on F_1, which reads on-shell

$$F_1 \approx -2a_0 + a_0 \left[q_1 \frac{\partial}{\partial q_1} + p_2 \frac{\partial}{\partial p_2} \right] \log\left(\frac{a_0}{a_4}\right) + (p_1')^2 a_1 \left[q_1 \frac{\partial}{\partial q_1} + p_2 \frac{\partial}{\partial p_2} \right] \log\left(\frac{a_1}{a_4}\right). \tag{2.26}$$

Therefore, $F_1 \approx 0$ provides two independent requirements: the vanishing of the coefficient of $(p_1')^2$, and the vanishing of the remaining terms, that is,

$$a_0 \left[q_1 \frac{\partial}{\partial q_1} + p_2 \frac{\partial}{\partial p_2} \right] \log\left(\frac{a_0}{a_4}\right) = 2a_0 \tag{2.27a}$$

$$a_1 \left[q_1 \frac{\partial}{\partial q_1} + p_2 \frac{\partial}{\partial p_2} \right] \log\left(\frac{a_1}{a_4}\right) = 0. \tag{2.27b}$$

The general solution for these equations is

$$a_0 = p_2^2 a_4(q_1, q_2, p_1, p_2)\, b_0\!\left(\frac{q_1}{p_2}, q_2, p_1\right), \tag{2.28a}$$

$$a_1 = a_4(q_1, q_2, p_1, p_2)\, b_1\!\left(\frac{q_1}{p_2}, q_2, p_1\right). \tag{2.28b}$$

The above conditions turn out to be already sufficient to solve all anomalies from the bracket (2.20). It is convenient to redefine $a_4 = \tilde{a}_4/p_2$ so that the Hamiltonian constraint reads

$$\mathcal{H}_g = \tilde{a}_4 \left(p_2 b_0 + \frac{(p_1')^2}{p_2} b_1 - \frac{p_1' p_2'}{p_2^2} + \frac{p_1''}{p_2}\right), \tag{2.29}$$

with $b_k = b_k(q_1/p_2, q_2, p_1)$, for $k = 0, 1$, and $\tilde{a}_4 = \tilde{a}_4(q_1, q_2, p_1, p_2)$. Then, any Hamiltonian of the form (2.29) commutes on-shell with the diffeomorphism constraint (2.15),

$$\{D_g[s_1], H_g[s_2]\} = H_g\left[s_1 s_2' + s_1' s_2 \left(\frac{q_1}{\tilde{a}_4}\frac{\partial \tilde{a}_4}{\partial q_1} + \frac{p_2}{\tilde{a}_4}\frac{\partial \tilde{a}_4}{\partial p_2}\right)\right]. \tag{2.30}$$

Note that anomaly freedom excludes the term $(p_2')^2$ from the Hamiltonian, and also requires the coefficients of $p_1' p_2'$ and p_1'' to be proportional. The term $s_1' s_2$ on the right-hand side of (2.30) tells us that the density weight of the Hamiltonian constraint $\mathcal{H}_g$ is not correct. Recall that it must be a weight-one scalar density on the leaf, and thus follow (2.12b). Further imposing the coefficient of $s_1' s_2$ on the right-hand side to vanish requires that all the arguments in $\tilde{a}_4$ are scalar combinations of the variables and momenta, i.e., $\tilde{a}_4 = b_4(q_1/p_2, q_2, p_1)$,

$$\{D_g[s_1], H_g[s_2]\} = H_g[s_1 s_2']. \tag{2.31}$$

At this point, there are only three free functions b_0, b_1, and b_4, which only depend on the scalar combinations of variables q_1/p_2, q_2, and p_1.

Now, we turn our attention to the bracket $\{H_g[s_1], H_g[s_2]\}$. Defining $s := s_1 s_2' - s_1' s_2$, we first remove all derivatives of s through integration by parts to write

$$\{H_g[s_1], H_g[s_2]\} = \int dx\, (s_1 s_2' - s_1' s_2) F_3. \tag{2.32}$$

We can replace (2.21) in F_3, and express it as a combination of radial derivatives (up to first order) of the canonical variables and their conjugate momenta,

$$F_3 \approx \sum_{l,n} \mathcal{A}^{l_1 l_2}_{n_1 n_2} \prod_{j=1}^{2} (q_j')^{l_j} (p_j')^{n_j}, \tag{2.33}$$

where the sum is for every non-negative integer l_j and n_j, with $j = 1, 2$. In this way, the conditions for anomaly freedom are translated to the vanishing of every coefficient on the right-hand side. That is,

$$F_3 \approx 0 \qquad \Longleftrightarrow \qquad \mathcal{A}^{l_1 l_2}_{n_1 n_2} = 0 \qquad \forall \quad l_1, l_2, n_1, n_2. \tag{2.34}$$

The simplest conditions are

$$0 = \mathcal{A}^{00}_{01} = a_4^2 \frac{q_1}{p_2} \frac{\partial^2 b_0}{\partial q_1^2}, \tag{2.35a}$$

$$0 = \mathcal{A}^{00}_{21} = a_4^2 \frac{q_1}{p_2^3} \frac{\partial^2 b_1}{\partial q_1^2}, \tag{2.35b}$$

meaning that b_0 and b_1 must be at most linear in q_1, that is,

$$b_0 = c_{00}(p_1, q_2) + \frac{q_1}{p_2} c_{01}(p_1, q_2), \tag{2.36a}$$

$$b_1 = c_{10}(p_1, q_2) + \frac{q_1}{p_2} c_{11}(p_1, q_2). \tag{2.36b}$$

This fixes the dependence on all scalar densities but those of the global factor b_4. After enforcing these conditions, the remaining anomalies simplify, and we find that only two equations remain, namely,

$$0 = \mathcal{A}^{00}_{30} = \frac{a_4^2}{p_2^3} \left(\frac{\partial c_{10}}{\partial q_2} - \frac{\partial c_{11}}{\partial p_1} \right), \tag{2.37a}$$

$$0 = \mathcal{A}^{00}_{10} = \frac{a_4^2}{p_2} \left(\frac{\partial c_{00}}{\partial q_2} + 2(c_{00} c_{11} - c_{01} c_{10}) - \frac{\partial c_{01}}{\partial p_1} \right). \tag{2.37b}$$

The general solution to this system of equations can be written in terms of two free functions of two variables, $f(p_1, q_2)$ and $g(p_1, q_2)$, and two additional functions which only depend on the moment p_1, $U(p_1)$ and $V(p_1)$, as follows,

$$c_{00} = \frac{1}{g(q_2, p_1)} \left(\frac{1}{2p_1} \Big(1 + \sqrt{p_1}\, V(p_1) + U(p_1) f(q_2, p_1) \Big) + \frac{\partial f(q_2, p_1)}{\partial p_1} \right), \tag{2.38a}$$

$$c_{01} = \frac{1}{g(q_2, p_1)} \frac{\partial f(q_2, p_1)}{\partial q_2}, \tag{2.38b}$$

$$c_{10} = \frac{U(p_1)}{4p_1} + \frac{1}{2} \frac{\partial}{\partial p_1} \Big[\log \big(g(q_2, p_1) \big) \Big], \tag{2.38c}$$

$$c_{11} = \frac{1}{2} \frac{\partial}{\partial q_2} \Big[\log \big(g(q_2, p_1) \big) \Big]. \tag{2.38d}$$

The Hamiltonian reads

$$\mathcal{H}_g = b_4\Bigg(\frac{p_2}{g}\left(\frac{1}{2p_1}\left(1+\sqrt{p_1}\,V+Uf\right)+\frac{\partial f}{\partial p_1}+\frac{q_1}{p_2}\frac{\partial f}{\partial q_2}\right) + \frac{(p_1')^2}{p_2}\left(\frac{U}{4p_1}+\frac{1}{2g}\left(\frac{\partial g}{\partial p_1}+\frac{q_1}{p_2}\frac{\partial g}{\partial q_2}\right)\right)-\frac{p_1'p_2'}{p_2^2}+\frac{p_1''}{p_2}\Bigg) \tag{2.39}$$

Note that the function $U(p_1)$ is redundant. This is straightforward to check because $U(p_1)$ can be absorbed in a redefiniton of f, g, and V. In brief, the rescalings $f \to u(p_1)f$, $g \to u(p_1)g$, and $1+\sqrt{p_1}V(p_1) \to (1+\sqrt{p_1}V(p_1))u(p_1)$, with the function $u(p_1)$ satisfying

$$U+\frac{2p_1}{u}\frac{\partial u}{\partial p_1}=1, \tag{2.40}$$

remove U from the Hamiltonian. Equivalently, we fix $U(p_1)=1$ in (2.39) with no loss of generality.

With all the above, $\{H_g[s_1], H_g[s_2]\} \approx 0$, which ensures that we have the same number of degrees of freedom as in GR: four canonical variables plus two first-class constraints. That is, there are no propagating degrees of freedom.

2.2.2 Spacetime embedding

Although the above Hamiltonian constraint commutes weakly with itself, the off-shell form of the Poisson bracket is rather complicated. Schematically,

$$\{\mathcal{H}_g, \mathcal{H}_g\} = F_4\mathcal{D}_g + F_5\mathcal{H}_g + F_6\mathcal{H}_g' + F_7\mathcal{D}_g\mathcal{H}_g. \tag{2.41}$$

Our purpose is to construct the metric associated to the Hamiltonian theory. To apply the procedure explained in Sec. 1.2, we need to find the canonical form of the algebra (2.12). First, one can check that the coefficients F_6 and F_7 in (2.41) are both linear in $\partial b_4/\partial q_1$, so we get rid of them only when removing the dependence of the global factor b_4 on the scalar densities q_1 and p_2. Thus, we fix $b_4 = c_4(q_2, p_1)$. In this way, the bracket reads

$$\{H_g[s_1], H_g[s_2]\} = H_g\left[(s_1s_2'-s_1's_2)\frac{c_4p_1'}{p_2^2}\left(\frac{\partial c_4}{\partial q_2}-\frac{\partial g}{\partial q_2}\right)\right] + D_g\left[(s_1s_2'-s_1's_2)\frac{c_4^2}{g^2p_2^2}\left(\frac{\partial f}{\partial q_2}\frac{\partial g}{\partial q_2}-g\frac{\partial^2 f}{\partial q_2^2}+\left(\frac{p_1'}{p_2}\right)^2\left(\left(\frac{\partial g}{\partial q_2}\right)^2-g\frac{\partial^2 g}{\partial q_2^2}\right)\right)\right]. \tag{2.42}$$

Second, we want to cancel the H_g term on the right-hand side. This means that the partial derivatives of c_4 and g with respect to q_2 must be equal. The general solution is

$$c_4 = -\sqrt{p_1}\mathfrak{g}(p_1)g(q_2,p_1), \tag{2.43}$$

for a generic function $\mathfrak{g}$. Then, the most general Hamiltonian constraint of the form (2.14) following the canonical algebra (2.12) with the diffeomorphism constraint (2.15) is

$$\begin{aligned}\mathcal{H}_g = -\sqrt{p_1}\mathfrak{g}(p_1)\Bigg(&\frac{p_2}{2p_1}\left(1-\sqrt{p_1}\,V(p_1)+f(q_2,p_1)\right)+p_2\frac{\partial f(q_2,p_1)}{\partial p_1}\\&+\frac{(p_1')^2}{2p_2}\left(\frac{g(q_2,p_1)}{2p_1}+\frac{\partial g(q_2,p_1)}{\partial p_1}+\frac{q_1}{p_2}\frac{\partial g(q_2,p_1)}{\partial q_2}\right)\\&+q_1\frac{\partial f(q_2,p_1)}{\partial q_2}-\frac{p_1'p_2'}{p_2^2}g(q_2,p_1)+\frac{p_1''}{p_2}g(q_2,p_1)\Bigg).\end{aligned} \tag{2.44}$$

with the yet free functions $f(p_1,q_2)$, $g(p_1,q_2)$, and $V(p_1)$. The algebra reads

$$\left\{D_g[s_1],D_g[s_2]\right\} = D_g\left[s_1s_2'-s_1's_2\right], \tag{2.45}$$

$$\left\{D_g[s_1],H_g[s_2]\right\} = H_g\left[s_1s_2'\right], \tag{2.46}$$

$$\left\{H_g[s_1],H_g[s_2]\right\} = D_g\left[F(s_1s_2'-s_1's_2)\right], \tag{2.47}$$

with the structure function

$$F = -\mathfrak{g}^2g^2\frac{p_1}{p_2^2}\frac{\partial}{\partial q_2}\left[\frac{1}{g}\frac{\partial f}{\partial q_2}+\frac{1}{2g}\left(\frac{p_1'}{p_2}\right)^2\frac{\partial g}{\partial q_2}\right]. \tag{2.48}$$

Following Sec. 1.2, we still need to check whether the inverse of this structure function qualifies for being the radial-radial component of the metric. Thence, we must compare the coordinate transformations of $q_{xx} := 1/F$ along a generic vector field, $\xi^\mu\partial_\mu = \xi^t\partial_t+\xi^x\partial_x$, given by [see (1.29c)]

$$\mathcal{L}_\xi\left(\frac{1}{F}\right) = \xi^t\partial_t\left(\frac{1}{F}\right)+\xi^x\partial_x\left(\frac{1}{F}\right)+2\left(\frac{1}{F}\right)\left(N^x\partial_x\xi^t+\partial_x\xi^x\right), \tag{2.49a}$$

with the gauge transformations of $1/F$ [see (1.30)],

$$\delta_\epsilon\left(\frac{1}{F}\right) = \left\{\left(\frac{1}{F}\right),H[\epsilon]+D[\epsilon^x]\right\} = \left\{\left(\frac{1}{F}\right),H\left[\xi^tN\right]+D\left[\xi^tN^x+\xi^x\right]\right\}. \tag{2.49b}$$

As specified in (1.31) and (1.32), when the gauge parameters of the transformation, ϵ and ϵ^x, and the coefficients ξ^t and ξ^x are components of the same vector field (in different basis), we

must have:

$$\mathcal{L}_\xi\left(\frac{1}{F}\right) = \delta_\epsilon\left(\frac{1}{F}\right). \tag{2.50}$$

We will be able to construct the metric associated to the Hamiltonian only when this condition is satisfied. In the spherically symmetric configuration, the relations between ϵ, ϵ^x, ξ^t, and ξ^x are $\epsilon = \xi^t N$ and $\epsilon^x = \xi^t N^x + \xi^x$.

Equation (2.50) is not generically satisfied by F as given in (2.48), and this condition restricts even more the form of the free functions in the Hamiltonian. Just in the same way as when solving anomalies, the fact that f, g, V, and $\mathfrak{g}$ do not depend on derivatives of the canonical variables, nor the momenta, allows us to find two independent equations. In fact, the above relation holds only when both

$$g^2\frac{\partial^3 f}{\partial q_2^3} - \left(2g\frac{\partial^2 g}{\partial q_2^2} - \left(\frac{\partial g}{\partial q_2}\right)^2\right)\frac{\partial f}{\partial q_2} = 0, \tag{2.51a}$$

$$g^2\frac{\partial^3 g}{\partial q_2^3} - \left(2g\frac{\partial^2 g}{\partial q_2^2} - \left(\frac{\partial g}{\partial q_2}\right)^2\right)\frac{\partial g}{\partial q_2} = 0, \tag{2.51b}$$

are satisfied. Most remarkably, these equations completely fix the dependence of the Hamiltonian on q_2. The general solution to these two equations is

$$f = \frac{A_f}{\omega^2}\sin^2\left(\omega(q_2+\varphi_f)\right) + \chi, \tag{2.52a}$$

$$g = -\frac{1}{2}A_g\cos^2\left(\omega(q_2+\varphi_g)\right), \tag{2.52b}$$

with the six integration functions $A_f(p_1)$, $A_g(p_1)$, $\varphi_f(p_1)$, $\varphi_g(p_1)$, $\omega(p_1)$ and $\chi(p_1)$ being completely free (note, in particular, that the integration functions might be complex, thus making the trigonometric functions hyperbolic). Notice that we may set $\chi = 0$ with no loss of generality because it can be absorbed in $V(p_1)$ inside the expression of the Hamiltonian (2.44). The most remarkable property of the solutions for f and g is that their "frequency" ω must be the same.

We thus find that

$$\begin{aligned}\mathcal{H}_g = &-\sqrt{p_1}\mathfrak{g}\Bigg(q_1\left(\frac{A_f}{\omega}-\left(\frac{p_1'}{2p_2}\right)^2 A_g\omega\right)\sin\left(2\omega(q_2+\varphi_f)\right)\\ &+\frac{p_2}{2p_1}\left(1-\sqrt{p_1}\,V+\frac{A_f}{\omega^2}\sin^2\left(\omega(q_2+\varphi_f)\right)+2p_1\frac{\partial}{\partial p_1}\left[\frac{A_f}{\omega^2}\sin^2\left(\omega(q_2+\varphi_f)\right)\right]\right)\\ &-\frac{(p_1')^2}{4p_2}\frac{\partial}{\partial p_1}\left[A_g\cos^2\left(\omega(q_2+\varphi_g)\right)\right]-\frac{A_g}{2}\left(\frac{p_1''}{p_2}-\frac{p_1'p_2'}{p_2^2}+\frac{(p_1')^2}{4p_1p_2}\right)\cos^2\left(\omega(q_2+\varphi_g)\right)\Bigg),\end{aligned} \tag{2.53}$$

where $\mathfrak{g}$, ω, A_f, A_g, φ_f, φ_g, and V are free functions of p_1, is the most general Hamiltonian within our initial assumptions that admits a covariant metric interpretation.

The GR Hamiltonian constraint (1.42b) is recovered for the specific choices $q_1 = K_x$, $q_2 = K_\varphi$, $p_1 = E^x$, and $p_2 = E^\varphi$, along with

$$\mathfrak{g}=1, \qquad A_f=1, \qquad A_g=1, \qquad \varphi_f=1, \qquad \varphi_g=0, \qquad \text{and} \qquad \omega\to 0, \tag{2.54}$$

and we consider these values to be the "GR limit" in the following. The function $V(p_1)$ (or $V(E^x)$ in the GR limit) stands for a "scalar potential" term in the Hamiltonian. For instance, it may describe a cosmological constant, in which case $V = \sqrt{E^x}\Lambda$ in GR, as it will be studied in detail in Chapter 4.

2.2.3 The mass

Note that since q_1 appears only linearly in both $\mathcal{H}_g$ and $\mathcal{D}_g$, we may define the abelianised constraint (see Refs. [68, 69] for further details on the abelianisation of constraints),

$$\mathcal{C}_g := -\frac{1}{2\mathfrak{g}p_2}\left(p_1'\mathcal{H}_g+\mathcal{D}_g\frac{\partial\mathcal{H}_g}{\partial q_1}\right), \tag{2.55}$$

such that its bracket with itself is zero off-shell, $\{C_g[s_1], C_g[s_2]\} = 0$. A key property of this constraint is that it does not contain any q_1. Its primitive,

$$M := \int \mathcal{C}_g\,dx = \frac{\sqrt{p_1}}{2}\left(1+f+2g\left(\frac{p_1'}{2p_2}\right)^2\right)-\frac{1}{4}\int V(p_1)dp_1, \tag{2.56}$$

is also independent of q_1, and it can be checked that it is a Dirac observable,

$$\begin{aligned}\dot{M} &= \{M, D_g[N^x]+H_g[N]\}\\ &= -H_g\left[N^x\frac{p_1'}{2\mathfrak{g}p_2}\right]+D_g\left[\frac{N^x}{p_2}\frac{\partial M}{\partial q_2}+N\mathfrak{g}g^2\frac{\sqrt{p_1}p_1'}{p_2^3}\frac{\partial}{\partial q_2}\left(\frac{1}{g}\frac{\partial M}{\partial q_2}\right)\right]\approx 0.\end{aligned} \tag{2.57}$$

Let us point out that this result is independent of the specific forms of $f(q_2, p_1)$ and $g(q_2, p_1)$.

It turns out convenient to define

$$m := \frac{\sqrt{p_1}}{2}\left(1 + f + 2g\left(\frac{p_1'}{2p_2}\right)^2\right), \tag{2.58}$$

because it is the Hawking mass in the GR limit. To prove it, we compute the Hawking mass for a spherically symmetric vacuum configuration using the GR metric (1.49), and check that it coincides with (2.58) when imposing conditions (2.54), which define the GR limit. That is,

$$M_H^{(0)} := \frac{\sqrt{E^x}}{2}\left(1 - \frac{\partial^\mu E^x \partial_\mu E^x}{4E^x}\right) = \frac{\sqrt{E^x}}{2}\left(1 + K_\varphi^2 - \left(\frac{E^{x\prime}}{2E^\varphi}\right)^2\right), \tag{2.59}$$

where one needs to use the Einstein equations for $\dot{E}^x$ in the last step. Therefore, we will interpret the quantity (2.58) as the mass of the deformed model. Finally, note that $m = M$ provided $V = 0$ in the Hamiltonian (2.53), and m is thus a constant of motion.

The quantity m turns out to be extremely useful to express the structure function because it allows to remove all derivative terms. Then, the Hamiltonian (2.53) follows the canonical form of the algebra (2.12), with the structure function being

$$F = \mathfrak{g}^2 A_g\left(A_f \cos^2\left(\omega(\varphi_f - \varphi_g)\right) + \omega^2\left(1 - \frac{2m}{\sqrt{p_1}}\right)\right)\frac{p_1}{p_2^2}, \tag{2.60}$$

and m defined in (2.58) along with (2.52). It is straightforward to compute the GR limit (2.54) and recover the GR result $F = E^x/(E^\varphi)^2$.

As prescribed in Sec. 1.2, the metric associated to this Hamiltonian is

$$ds^2 = -N(t,x)^2 dt^2 + \frac{1}{F(t,x)}\big(dx + N^x(t,x)dt\big)^2 + r(t,x)^2 d\Omega^2, \tag{2.61}$$

where $r(t,x)$ is a scalar function still to be determined (see Sec. 2.5).

It is remarkable how the requirement of covariance heavily restricts the form of the Hamiltonian. We started from five functions a_k of four variables each, and retain only freedom in terms of six functions of one single variable p_1. The dependence of the Hamiltonian on the other three variables, q_1, q_2, and p_2, is completely fixed.

2.3 Covariant holonomy corrections coupled to matter

Adding local degrees of freedom makes anomaly resolution much harder to track, and also restricts more the freedom to modify the Hamiltonian. Making contact with the previous section, we begin with the ansatz

$$\mathcal{D} = -p_1' q_1 + p_2 q_2' - p_3' q_3, \tag{2.62a}$$

$$\mathcal{H} = a_0 + (p_1')^2 a_1 + p_1' p_2' a_2 + (p_2')^2 a_3 + p_1'' a_4 + p_1' p_3' a_5 + p_2' p_3' a_6 + (p_3')^2 a_7, \tag{2.62b}$$

where all quadratic combinations of radial derivatives of the three momenta (and one second-order derivative) are included, each multiplied by a free function $a_k = a_k(q_1, q_2, q_3, p_1, p_2, p_3)$, with k running from 0 to 7. The symplectic structure is given by

$$\{q_i(x_1), p_j(x_2)\} = \delta_{ij}\delta(x_1, x_2), \tag{2.63}$$

with the subindices i, j running from 1 to 3.

The particular case of GR corresponds to

$$\begin{aligned} a_0 &= -2\sqrt{p_1} q_1 q_2 - \frac{p_2}{2\sqrt{p_1}}\left(1 + q_2^2\right) + \frac{q_3^2}{2\sqrt{p_1} p_2} + \sqrt{p_1} p_2 V(p_1, p_3), \\ a_1 &= \frac{1}{8 p_1 p_2}, \qquad a_2 = -\frac{\sqrt{p_1}}{2 {p_2}^2}, \qquad a_4 = \frac{\sqrt{p_1}}{2 p_2}, \qquad a_7 = \frac{p_1^{3/2}}{2 p_2}, \end{aligned} \tag{2.64}$$

and $a_3 = a_5 = a_6 = 0$, along with

$$q_1 = K_x, \quad p_1 = E^x, \quad q_2 = K_\varphi, \quad p_2 = E^\varphi, \quad q_3 = P_\phi, \quad \text{and} \quad p_3 = -\phi. \tag{2.65}$$

Once again, the bracket between two diffeomorphism constraints (2.62a) is given by (1.47a), and we thus start with the Poisson bracket between (2.62a) and (2.62b). After integrating by parts to remove the derivatives of the smearing function of the diffeomorphism constraint, one gets

$$\left\{D[s_1], H[s_2]\right\} = \int dx\, s_1 \left(s_2 F_0 + s_2' F_1 + s_2'' F_2\right), \tag{2.66}$$

where F_0, F_1, and F_2 are independent of the smearing functions s_1 and s_2, and must vanish on-shell. Since the free functions a_k do not depend on derivatives of the variables, every coefficient going with any combination of radial derivatives must be zero on its own. To know which terms survive after setting the constraints to zero, we replace p_1'' and q_2' by using (2.21), with $\mathcal{D}$ and $\mathcal{H}$ as given in (2.62) instead of the vacuum constraints $\mathcal{D}_g$ and $\mathcal{H}_g$.

As in the previous section, F_0 and F_1 are long expressions, but we can readily solve

$$F_2 \approx -\left(a_4 + p_2 a_2\right) p_1' - 2p_2 a_3 p_2' - p_2 a_6 p_3'. \tag{2.67}$$

Setting $F_2 \approx 0$, and since the coefficients of p_1', p_2', and p_3' must vanish independently, one gets

$$a_2 = \frac{a_4}{p_2}, \qquad a_3 = 0, \qquad \text{and} \qquad a_6 = 0. \tag{2.68}$$

Once these conditions are imposed, the remaining anomalies are greatly simplified. In fact, similarly to what happened in the vacuum case, the vanishing of F_1 leads to four independent equations, namely,

$$\left[q_1 \frac{\partial}{\partial q_1} + p_2 \frac{\partial}{\partial p_2} + q_3 \frac{\partial}{\partial q_3}\right] \log\left(\frac{a_0}{a_4}\right) = 2a_0, \tag{2.69a}$$

and

$$\left[q_1 \frac{\partial}{\partial q_1} + p_2 \frac{\partial}{\partial p_2} + q_3 \frac{\partial}{\partial q_3}\right] \log\left(\frac{a_k}{a_4}\right) = 0, \tag{2.69b}$$

for $k = 1, 5, 7$. These correspond to the coefficients of the free term (with no derivatives), and the coefficients of $(p_1')^2$, $p_1' p_3'$, and $(p_3')^2$, respectively, of F_1. After solving the equations, we can express the Hamiltonian constraint as

$$\mathcal{H} = a_4 \left(p_2 b_0 + \frac{(p_1')^2}{p_2} b_1 + \frac{p_1' p_3'}{p_2} b_5 + \frac{(p_3')^2}{p_2} b_7 - \frac{p_1' p_2'}{p_2^2} + \frac{p_1''}{p_2}\right), \tag{2.70}$$

with $b_k = b_k(q_1/p_2, q_3/p_2, q_2, p_1, p_3)$ for $k = 0, 1, 5, 7$. As in vacuum, the bracket of (2.70) with the diffeomorphism constraint is given by (2.30). In order to recover the canonical form of the algebra, we must set $a_4 = b_4(q_1/p_2, q_3/p_2, q_2, p_1, p_3)$, which is equivalent to demanding that a_4 is also a scalar function. In that way,

$$\left\{D[s_1], H[s_2]\right\} = H\left[s_1 s_2'\right]. \tag{2.71}$$

We continue the study by computing the Poisson bracket of the constraint (2.70), with $a_4 = b_4$, with itself. If we define the combination $s := s_1 s_2' - s_1' s_2$, all derivatives of s can be removed through integration by parts, and we can express

$$\left\{H[s_1], H[s_2]\right\} = \int dx \, (s_1 s_2' - s_1' s_2) F_3 \,, \tag{2.72}$$

where F_3 does not depend on the smearing functions. After replacing (2.21) with $\mathcal{D}$ and $\mathcal{H}$, instead of $\mathcal{D}_g$ and $\mathcal{H}_g$, and setting the constraints to zero, each coefficient in front of a radial derivative must vanish by itself. We find that the highest derivative order of F_3 is two, so

$$F_3 \approx \sum_{l,m,n,o} \mathcal{A}^{l_1 l_2 l_3 m_1 m_2 m_3}_{n_1 n_2 n_3 o_1 o_2 o_3} \prod_{j=1}^{3} (q_j')^{l_j} (p_j')^{n_j} (q_j'')^{m_j} (p_j'')^{o_j}, \tag{2.73}$$

where the sum is for every non-negative integer l_j, m_j, n_j, and o_j, with $j = 1, 2, 3$. The problem of anomaly resolution is thus translated to the vanishing of every $\mathcal{A}$:

$$F_3 \approx 0 \quad \Longleftrightarrow \quad \mathcal{A}^{l_1 l_2 l_3 m_1 m_2 m_3}_{n_1 n_2 n_3 o_1 o_2 o_3} = 0 \quad \forall \;\; l_1, l_2, l_3, m_1, m_2, m_3, n_1, n_2, n_3, o_1, o_2, o_3. \tag{2.74}$$

We sistematically solve the anomalies, starting from the simplest ones, and we replace those conditions into the more complicated ones. We first read the equations

$$0 = \mathcal{A}^{100000}_{000000} = -\frac{b_4^2}{p_2^2} \frac{\partial^2 b_0}{\partial q_1^2}, \tag{2.75a}$$

$$0 = \mathcal{A}^{001000}_{000000} = -\frac{b_4^2}{p_2^2} \frac{\partial^2 b_0}{\partial q_1 \partial q_3}, \tag{2.75b}$$

$$0 = \mathcal{A}^{100000}_{200000} = -\frac{b_4^2}{p_2^2} \frac{\partial^2 b_1}{\partial q_1^2}, \tag{2.75c}$$

$$0 = \mathcal{A}^{001000}_{200000} = -\frac{b_4^2}{p_2^2} \frac{\partial^2 b_1}{\partial q_1 \partial q_3}, \tag{2.75d}$$

$$0 = \mathcal{A}^{000000}_{100001} = -\frac{b_4^2}{p_2} \frac{\partial b_5}{\partial q_1}, \tag{2.75e}$$

$$0 = \mathcal{A}^{000000}_{001001} = -\frac{2b_4^2}{p_2} \frac{\partial b_7}{\partial q_1}. \tag{2.75f}$$

Enforcing these relations, we can reduce the functions b_0, b_1, b_5, and b_7 to

$$b_0 = c_0(p_1, q_2, q_3/p_2, p_3) + \frac{q_1}{p_2} d_{0a}(p_1, q_2, p_3), \tag{2.76a}$$

$$b_1 = c_1(p_1, q_2, q_3/p_2, p_3) + \frac{q_1}{p_2} d_{1a}(p_1, q_2, p_3), \tag{2.76b}$$

$$b_5 = c_5(p_1, q_2, q_3/p_2, p_3), \tag{2.76c}$$

$$b_7 = c_7(p_1, q_2, q_3/p_2, p_3). \tag{2.76d}$$

We also find the following equations,

$$0 = \mathcal{A}^{000000}_{003000} = -\frac{2b_4^2}{p_2^2} c_7 \frac{\partial c_7}{\partial q_3}, \tag{2.77a}$$

$$0 = \mathcal{A}^{000000}_{102000} = \frac{b_4^2}{p_2^3}\left(2d_{1a}c_7 + \frac{\partial c_7}{\partial q_2} - 2p_2 c_7 \frac{\partial c_5}{\partial q_3} - p_2 c_5 \frac{\partial c_7}{\partial q_3}\right), \tag{2.77b}$$

$$0 = \mathcal{A}^{000000}_{201000} = \frac{b_4^2}{p_2^3}\left(d_{1a}c_5 - \frac{p_2}{2}\frac{\partial c_5^2}{\partial q_3} - \frac{\partial d_{1a}}{\partial p_3} - \frac{q_3}{p_2}\frac{\partial d_{1a}}{\partial q_2} + \frac{\partial c_5}{\partial q_2} - 2p_2 c_7 \frac{\partial c_1}{\partial q_3}\right), \tag{2.77c}$$

$$0 = \mathcal{A}^{000000}_{001000} = \frac{b_4^2}{p_2}\left(d_{0a}c_5 + \frac{\partial d_{0a}}{\partial p_3} + \frac{q_3}{p_2}\frac{\partial d_{0a}}{\partial q_2} + 2p_2 c_7 \frac{\partial c_0}{\partial q_3}\right). \tag{2.77d}$$

Therefore, c_7 is independent of q_3; c_5 is, at most, linear in q_3; while c_0 and c_1 are, at most, quadratic in that variable. These equations fix the dependence of the Hamiltonian on all the densities (q_1, p_2, q_3), except in the global factor $b_4 = b_4(q_1/p_2, q_3/p_2, q_2, p_1, p_3)$, i.e.,

$$\begin{aligned}\mathcal{H} = b_4\Bigg(& p_2\left(\frac{q_1}{p_2}d_{0a} + d_{0b} + \frac{q_3}{p_2}d_{0c} + \frac{q_3^2}{p_2^2}d_{0d}\right) - \frac{p_1' p_2'}{p_2^2} + \frac{p_1''}{p_2} + \frac{(p_3')^2}{p_2}d_{7b} \\ & + \frac{(p_1')^2}{p_2}\left(\frac{q_1}{p_2}d_{1a} + d_{1b} + \frac{q_3}{p_2}d_{1c} + \frac{q_3^2}{p_2^2}d_{1d}\right) + \frac{p_1' p_3'}{p_2}\left(d_{5b} + \frac{q_3}{p_2}d_{5c}\right)\Bigg),\end{aligned} \tag{2.78}$$

where $d_{ij} = d_{ij}(q_2, p_1, p_3)$, for $i = 0, 1, 5, 7$ and the corresponding $j = a, b, c, d$. Now, the remaining equations $\mathcal{A} = 0$ can be further split because the free functions d_{ij} do not depend on the weight-one scalar densities (q_1, p_2, q_3). This means that each function $\mathcal{A}$ is a polynomial on those variables, and the coefficient of every term of the form $q_1^n p_2^m q_3^o$, with non-negative integers n, m, and o, in each $\mathcal{A}$ must vanish independently. In this way, we can translate the requirement of anomaly freedom to the following eleven partial differential equations:

$$\frac{\partial d_{0a}}{\partial q_2} = -d_{0a}d_{5c} - 4d_{0d}d_{7b}, \tag{2.79a}$$

$$\frac{\partial d_{0b}}{\partial q_2} = -2d_{0b}d_{1a} + 2d_{0a}d_{1b} + d_{0c}d_{5b} + \frac{\partial d_{0a}}{\partial p_1}, \tag{2.79b}$$

$$\frac{\partial d_{0c}}{\partial q_2} = -2d_{0c}d_{1a} + 2d_{0a}d_{1c} + 2d_{0d}d_{5b} + d_{0c}d_{5c}, \tag{2.79c}$$

$$\frac{\partial d_{0d}}{\partial q_2} = -2(d_{0d}d_{1a} - d_{0a}d_{1d} - d_{0d}d_{5c}), \tag{2.79d}$$

$$\frac{\partial d_{1b}}{\partial q_2} = d_{1c}d_{5b} + \frac{\partial d_{1a}}{\partial p_1}, \tag{2.79e}$$

$$\frac{\partial d_{1c}}{\partial q_2} = 2d_{1d}d_{5b} + d_{1c}d_{5c}, \tag{2.79f}$$

$$\frac{\partial d_{1d}}{\partial q_2} = 2d_{1d}d_{5c}, \tag{2.79g}$$

$$\frac{\partial d_{5b}}{\partial q_2} = -d_{1a}d_{5b} + d_{5b}d_{5c} + 2d_{1c}d_{7b} + \frac{\partial d_{1a}}{\partial p_3}, \tag{2.79h}$$

$$\frac{\partial d_{5c}}{\partial q_2} = -d_{1a}d_{5c} + (d_{5c})^2 + 4d_{1d}d_{7b} + \frac{\partial d_{1a}}{\partial q_2}, \tag{2.79i}$$

$$\frac{\partial d_{7b}}{\partial q_2} = -2(d_{1a}d_{7b} - d_{5c}d_{7b}), \tag{2.79j}$$

$$\frac{\partial d_{0a}}{\partial p_3} = -d_{0a}d_{5b} - 2d_{0c}d_{7b}. \tag{2.79k}$$

A general solution of this system is elusive because it is highly coupled but, since almost all equations contain derivatives with respect to q_2, the dependence on this variable will clearly be severely restricted. In particular, the choice $d_{1a} = 0$, thoroughly studied in Ref. [1], showed that $\mathcal{H}$ is at most quadratic in q_2 in that case.

When the above relations (2.79) are satisfied, the constraint (2.78) commutes weakly with itself, $\{H[s_1], H[s_2]\} \approx 0$, but, as in the vacuum case, it is schematically given by $\{\mathcal{H}, \mathcal{H}\} = F_4\mathcal{D} + F_5\mathcal{H} + F_6\mathcal{H}' + F_7\mathcal{D}\mathcal{H}$ off-shell. In order to remove the last two terms, the global factor must be independent of the scalar densities (q_1, p_2, q_3). More precisely, $F_6 = 0$ and $F_7 = 0$ only when $b_4(q_1/p_2, q_3/p_2, q_2, p_1, p_3)$ is independent of q_1. Under this condition the bracket reads

$$\begin{aligned}\{H[s_1], H[s_2]\} = D\left[(s_1s_2' - s_1's_2)\frac{b_4^2}{p_2^2}\left(d_{0a}d_{5c} + 4d_{0d}d_{7b} - \left(\frac{p_1'}{p_2}\right)^2\frac{\partial d_{1a}}{\partial q_2}\right)\right] \\ - H\left[(s_1s_2' - s_1's_2)\left(\frac{p_1'}{p_2^2}\left(2b_4d_{1a} - \frac{\partial b_4}{\partial q_2}\right) + \frac{1}{p_2}\frac{\partial b_4}{\partial q_3}\left(2p_3'd_{7b} + p_1'\left(d_{5b} + \frac{q_3}{p_2}d_{5c}\right)\right)\right)\right].\end{aligned} \tag{2.80}$$

To remove the H-term on the right-hand side, we first need $\partial b_4/\partial q_3 = 0$ because the free functions do not depend on derivatives of the momenta, nor on p_2 and q_3. Recall that this, along with the independence of q_1, makes b_4 to be also independent of p_2. We choose the specific form $b_4 = -\sqrt{p_1}\mathfrak{g}(p_1, p_3)g(q_2, p_1, p_3)$. In this way, the above bracket reads

$$\begin{aligned}\{H[s_1], H[s_2]\} = &- D\left[(s_1s_2' - s_1's_2)\mathfrak{g}^2g^2\frac{p_1}{p_2^2}\left(\frac{\partial d_{0a}}{\partial q_2} + \left(\frac{p_1'}{p_2}\right)^2\frac{\partial d_{1a}}{\partial q_2}\right)\right] \\ &- H\left[(s_1s_2' - s_1's_2)\mathfrak{g}\frac{\sqrt{p_1}p_1'}{p_2^2}\left(\frac{\partial g}{\partial q_2} - 2d_{1a}g\right)\right],\end{aligned} \tag{2.81}$$

where we have used relation (2.79a) to simplify the coefficient going with the diffeomorphism constraint. To recover the canonical form of the constraint algebra, we must further impose that the expression inside the last round brackets vanishes, which leads to

$$d_{1a} = \frac{1}{2g}\frac{\partial g}{\partial q_2}. \tag{2.82}$$

In summary, the most general generator of infinitesimal normal transformations that satisfies our initial requirements (i) and (ii) is

$$\begin{aligned}\mathcal{H} = -\sqrt{p_1}\mathfrak{g}g\Bigg(p_2\left(\frac{q_1}{p_2}d_{0a}+d_{0b}+\frac{q_3}{p_2}d_{0c}+\frac{q_3^2}{p_2^2}d_{0d}\right)-\frac{p_1'p_2'}{p_2^2}+\frac{p_1''}{p_2}+\frac{(p_3')^2}{p_2}d_{7b}\\ +\frac{(p_1')^2}{p_2}\left(\frac{q_1}{2p_2}\frac{1}{g}\frac{\partial g}{\partial q_2}+d_{1b}+\frac{q_3}{p_2}d_{1c}+\frac{q_3^2}{p_2^2}d_{1d}\right)+\frac{p_1'p_3'}{p_2}\left(d_{5b}+\frac{q_3}{p_2}d_{5c}\right)\Bigg),\end{aligned} \tag{2.83}$$

under the condition that the functions $d_{ij}(q_2,p_1,p_3)$ satisfy the anomaly equations (2.79), with d_{1a} as given in (2.82). The resulting bracket reads

$$\{H[s_1],H[s_2]\} = -D\left[\mathfrak{g}^2g^2\frac{p_1}{p_2^2}\left(\frac{\partial d_{0a}}{\partial q_2}+\frac{1}{2}\left(\frac{p_1'}{p_2}\right)^2\frac{\partial^2\log(g)}{\partial q_2^2}\right)(s_1s_2'-s_1's_2)\right]. \tag{2.84}$$

The structure function that can be read from this relation resembles its vacuum counterpart (2.48). In fact, renaming

$$d_{0a} = \frac{1}{g}\frac{\partial f}{\partial q_2}, \tag{2.85}$$

with $f = f(q_2,p_1,p_3)$, we see that they both have the same formal expression.

2.4 The effective model

In this section, we seek a particular solution to the anomaly equations (2.79) that allows for covariant holonomy modifications coupled to matter with local degrees of freedom. Recall that the above Hamiltonian satisfies the initial requirements (i) and (ii). Therefore, we still need to impose conditions (iii), (iv), and (v). The former ensures the embeddability of the model in a four-dimensional manifold to allow for a metric description. The last one demands an explicit vacuum limit which must be necessarily included in the family of vacuum Hamiltonians (2.53) derived in Sec. 2.2. Recall now the GR Hamiltonian (1.43). Upon identification (2.65), we see that neither d_{0d} nor d_{7b} can be identically vanishing in order to fulfill the fourth requirement. If we tried to set to zero the functions coupled to either q_3 or p_3, then d_{1a} would become independent of q_2, as one can read from (2.79i), which does not reproduce the required vacuum limit (2.53) for any choices of the remaining free functions. Therefore, we need at least either d_{1d} or d_{5c} to be non-vanishing.

To obtain a solution to the system (2.79), we make certain particular choices. A careful inspection shows that setting $d_{1d}=0$ slightly decouples the system because d_{5c} always multiplies the function whose derivative appears on the left-hand side of the equations.

Setting $d_{0c}=0$, $d_{1c}=0$, $d_{1d}=0$, and $d_{5b}=0$, we find a consistent non-trivial system:

$$\frac{\partial d_{0a}}{\partial q_2} = -d_{0a}d_{5c} - 4d_{0d}d_{7b}, \tag{2.86a}$$
$$\frac{\partial d_{0b}}{\partial q_2} = 2(d_{0a}d_{1b} - d_{0b}d_{1a}) + \frac{\partial d_{0a}}{\partial p_1}, \tag{2.86b}$$
$$\frac{\partial d_{0d}}{\partial q_2} = 2d_{0d}(d_{5c} - d_{1a}), \tag{2.86c}$$
$$\frac{\partial d_{1b}}{\partial q_2} = \frac{\partial d_{1a}}{\partial p_1}, \tag{2.86d}$$
$$\frac{\partial d_{5c}}{\partial q_2} - \frac{\partial d_{1a}}{\partial q_2} = d_{5c}(d_{5c} - d_{1a}), \tag{2.86e}$$
$$\frac{\partial d_{7b}}{\partial q_2} = 2d_{7b}(d_{5c} - d_{1a}), \tag{2.86f}$$
$$\frac{\partial d_{0a}}{\partial p_3} = \frac{\partial d_{1a}}{\partial p_3} = 0. \tag{2.86g}$$

Then, it is clear that $d_{1a}=d_{5c}$ solves three of the equations provided the matter coefficients d_{0d} and d_{7b} do not depend on q_2. The functions d_{0a} and d_{1a} are independent of p_3.

We see that equations (2.86b) and (2.86d) are decoupled from the matter contribution, and they correspond to vacuum equations (2.37) with the identification $d_{0b}=c_{00}$, $d_{0a}=c_{01}$, $d_{1b}=c_{10}$, and $d_{1a}=c_{11}$. The only difference is that now d_{0b} and d_{1b} — and thus U and V in (2.38) — may also depend on p_3. The incorporation of matter generates the additional condition (2.86a), which after using (2.82) and (2.85), reads

$$\frac{1}{2}\frac{\partial f}{\partial q_2}\frac{\partial g}{\partial q_2} - g\frac{\partial^2 f}{\partial q_2^2} = 4g^2 d_{0d}d_{7b}. \tag{2.87}$$

Since d_{0a} and d_{1a} are independent of p_3, the product $d_{0d}d_{7b}$ only depends on p_1, and thus the above equation can be integrated in q_2, leading to

$$g = -\frac{(f-\chi)^{-1}}{8d_{0d}d_{7b}}\left(\frac{\partial f}{\partial q_2}\right)^2, \tag{2.88}$$

with $\chi=\chi(p_1,p_3)$ a free integration function. At this point, all anomalies are vanishing, leaving free $d_{0d}(p_1,p_3)$ and $d_{7b}(p_1,p_3)$. The easiest choice is to consider that both these functions retain their classical form. In summary, we obtain the particular solution of the system (2.79),

$$d_{0a} = \frac{1}{g}\frac{\partial f}{\partial q_2}, \tag{2.89a}$$
$$d_{0b} = \frac{1}{g}\left(\frac{1+Uf}{2p_1} - \frac{V}{2\sqrt{p_1}} + \frac{\partial f}{\partial p_1}\right), \tag{2.89b}$$

$$d_{1a} = d_{5c} = \frac{1}{2g}\frac{\partial g}{\partial q_2}, \tag{2.89c}$$

$$d_{1b} = \frac{U}{4p_1} + \frac{1}{2g}\frac{\partial g}{\partial p_1}, \tag{2.89d}$$

$$d_{7b} = (d_{0d})^{-1} = p_1, \tag{2.89e}$$

$$d_{0c} = d_{1c} = d_{1d} = d_{5b} = 0, \tag{2.89f}$$

with $U = U(p_1, p_3)$ and $V = V(p_1, p_3)$. The solution has been written in a form which trivially shows that all the dependence on p_3 of f can be absorbed in U and V. Therefore, let us consider $f = f(q_2, p_1)$. Combining this with (2.89e), we find $g = g(q_2, p_1)$ and $\chi(p_1)$ in (2.88). But, in addition, a shift $f \to f + \chi$ amounts to a redefinition of V. As a result, let us fix $\chi = 0$. Moreover, we can absorb U by a suitable rescaling of $\mathfrak{g}$, V, f, and g, just in the same way as we did in vacuum. Equivalently, we take the above solution with $U = 1$. In that case, the Hamiltonian constraint reads

$$\begin{aligned}\mathcal{H} = -\sqrt{p_1}\mathfrak{g}\Bigg(& q_1\frac{\partial f}{\partial q_2} + p_2\left(\frac{1+f}{2p_1} - \frac{V}{2\sqrt{p_1}} + \frac{\partial f}{\partial p_1}\right) - g\frac{p_1' p_2'}{p_2^2} + g\frac{p_1''}{p_2} + g\frac{p_1 (p_3')^2}{p_2} \\ & + \frac{(p_1')^2}{2p_2}\left(\frac{q_1}{p_2}\frac{\partial g}{\partial q_2} + \frac{g}{2p_1} + \frac{\partial g}{\partial p_1}\right) + \frac{q_3}{2p_2^2}\frac{\partial g}{\partial q_2}p_1' p_3' + g\frac{q_3^2}{p_1 p_2}\Bigg),\end{aligned} \tag{2.90}$$

which reduces to the vacuum constraint (2.44) when removing all terms that depend on the matter degrees of freedom (q_3, p_3). The Poisson bracket takes the same formal expression as in vacuum, namely, $\{H[s_1], H[s_2]\} = D[F(s_1 s_2' - s_1' s_2)]$, with

$$F = -\mathfrak{g}^2 g^2 \frac{p_1}{p_2^2}\frac{\partial}{\partial q_2}\left[\frac{1}{g}\frac{\partial f}{\partial q_2} + \frac{1}{2g}\left(\frac{p_1'}{p_2}\right)^2\frac{\partial g}{\partial q_2}\right]. \tag{2.91}$$

In order to analyse the embeddability of the dynamics defined by the above Hamiltonian in spacetime [requirement (iii)], one needs to check the condition (2.50), i.e., $\mathcal{L}_\xi(1/F) = \delta_\epsilon(1/F)$. In this case, this is straightforward as we obtain the same two equations (2.51) as in vacuum. Nevertheless, since g is no longer free, and it is now given in terms of f by relation (2.88), those two equations are no longer independent, and the solution

$$f = \frac{A}{\omega^2}\sin^2\big(\omega(q_2 + \varphi)\big) + \chi, \tag{2.92a}$$

with $A = A(p_1), \omega = \omega(p_1)$, and $\varphi = \varphi(p_1)$ which, in turn, implies

$$g = -\frac{1}{2}A\cos^2\big(\omega(q_2 + \varphi)\big), \tag{2.92b}$$

satisfies the equations (2.51). Note that χ in (2.92a) and (2.88) must be the same function, and

we already showed that it can be absorbed trivially in V. In addition, it is easy to see that, since the coefficient A is the same in f and g, it can be absorbed in a redefinition of the global factor $\mathfrak{g}$ and V. Therefore, we set $A = 1$ with no loss of generality.

The embedabbility condition (iii) is necessary for the covariance of the theory, and, from this point on, the model univocally defines a spacetime.

Note that the incorporation of matter with local degrees of freedom imposes an additional restriction, and f and g are no longer independent. Besides, the vacuum limit of (2.90) with (2.92) is straightforward and given by (2.53), upon the choice $A_f = A_g = 1$ and $\varphi := \varphi_f = \varphi_g$. Further, the canonical transformation

$$q_2 \to q_2 - \varphi \qquad \text{and} \qquad q_1 \to q_1 - p_2 \frac{\partial \varphi}{\partial p_1}, \tag{2.93}$$

removes $\varphi(p_1)$, and thus we can set it to zero with no loss of generality. In this way, we obtain a family of Hamiltonians satisfying all five conditions (i) to (v),

$$\begin{aligned}\mathcal{H} = \mathfrak{g}\Bigg(& -\frac{p_2}{2\sqrt{p_1}}\left(1+\frac{\sin^2(\omega q_2)}{\omega^2}\right) - \sqrt{p_1}q_1\frac{\sin(2\omega q_2)}{\omega}\left(1+\left(\frac{\omega p_1'}{2p_2}\right)^2\right) \\ & + \left(\frac{(p_1')^2}{8\sqrt{p_1}p_2} - \frac{\sqrt{p_1}}{2p_2^2}p_1'p_2' + \frac{\sqrt{p_1}}{2p_2}p_1'' + \frac{q_3^2}{2\sqrt{p_1}p_2} + \frac{(p_1)^{3/2}(p_3')^2}{2p_2}\right)\cos^2(\omega q_2) \\ & + 2\sqrt{p_1}p_2\frac{\sin(\omega q_2)}{\omega}\left(\frac{\sin(\omega q_2)}{\omega} - q_2\left(1+\left(\frac{\omega p_1'}{2p_2}\right)^2\right)\cos(\omega q_2)\right)\frac{\partial\log(\omega)}{\partial p_1} \\ & + \sqrt{p_1}p_2 V(p_1,p_3) - \frac{\sqrt{p_1}q_3 p_1' p_3'}{4p_2^2}\omega\sin(2\omega p_2)\Bigg),\end{aligned} \tag{2.94}$$

in terms of a free function $\omega(p_1)$. Conditions (i), (ii), and (iii) are satisfied by construction. Also note that the GR Hamiltonian corresponds to the vanishing of ω. Although the limit $\omega \to 0$ is non-trivial, it is well-defined within this family of solutions, and thus satisfies condition (iv). The vacuum Hamiltonian (2.53), with $A_f = A_g = 1$ and $\varphi_f = \varphi_g = 0$, is straightforwardly obtained by removing all the terms with q_3 or p_3, ensuring that requirement (v) is satisfied.

The only remaining free function is the scalar global factor $\mathfrak{g}$. However, this freedom is present in GR, where one can rescale N and $\mathcal{H}$ by scalar functions without changing the total Hamiltonian. Recall that it is 1 in the GR limit specified above. Regarding $V(p_1, p_3)$, we see that it can be interpreted as the potential of a scalar field by looking at the GR constraint (1.43b).

For this family of Hamiltonians, the bracket reads $\{H[s_1], H[s_2]\} = D[F(s_1 s_2' - s_1' s_2)]$, with the everywhere non-negative structure function

$$F = \mathfrak{g}^2 \cos^2(\omega q_2) \left(1 + \left(\frac{\omega p_1'}{2p_2}\right)^2\right) \frac{p_1}{p_2^2}. \tag{2.95}$$

At this point, it is interesting to recall the mass function (2.58), which allows us to simplify the structure function:

$$F = \mathfrak{g}^2 (1+\omega^2) \left(1 - \frac{2\omega^2 m}{(1+\omega^2)\sqrt{p_1}}\right) \frac{p_1}{p_2^2}. \tag{2.96}$$

For simplicity, we fix the global factor as

$$\mathfrak{g} = \frac{1}{\sqrt{1+\omega^2}}, \tag{2.97}$$

which automatically satisfies the GR limit (2.54), i.e., $\mathfrak{g} \to 1$ as $\omega \to 0$.

The family of Hamiltonians (2.94) describes scale-dependent holonomy corrections. This is, on its own, a relevant result because it is the first time that spherical holonomy corrections are implemented in a covariant way, and also consistently coupled to matter in spherical symmetry. Note that the polymerised variable q_2 appears outside the argument of trigonometric functions whenever ω is not constant, which agrees with previous studies in the literature [75]. For simplicity, we will consider a constant polymerisation function $\omega \equiv \lambda \in \mathbb{R}$ to account for quantum effects, thus ensuring that the Hamiltonian constraint is bounded and periodic regarding q_2. In addition, the Hamiltonian is greatly simplified when $\partial\omega/\partial p_1 = 0$.

2.5 Metric interpretation

The metric associated to the Hamiltonian (2.94) is

$$ds^2 = -N(t,x)^2 dt^2 + \frac{1}{F}\left(dx^2 + N^x(t,x)dt^2\right) + r(t,x)^2 d\Omega^2, \tag{2.98}$$

with F given in (2.96), which has the same formal expression as in vacuum (2.61).

Therefore, to complete the geometric interpretation of the model, we only need to specify the area-radius function $r(t,x)$. Recall that the algebra does not provide any information about that component of the metric due to the spherical symmetry reduction. But we demand the modifications to preserve the area of the orbits of the spherical symmetry, just in the same way as we require them to keep the definition of time (the foliation).

The constraint (2.94) is tightly related to the GR Hamiltonian (1.43). In fact, it is possible to find (2.94) from the classical set-up by means of a non-bijective canonical transformation and a linear combination of the Hamiltonian and the diffeomorphism constraints. The coefficients of that combination are phase-space dependent functions, and they become ill-defined at the same points where the canonical transformation breaks down. Although it is possible to perform these changes with a non-constant function $\omega(p_1)$ — see equation (42) in Ref. [2] —, it is more illustrative to consider $\omega \equiv \lambda \in \mathbb{R}$, matching also the simplicity requirement stated above. In this way, the expressions are less complicated, and there is a welcome byproduct: When the polymerisation function is constant, the canonical transformation only affects one pair of conjugate variables.

More precisely, let us perform the canonical transformation

$$K_x = q_1 \qquad \text{and} \qquad E^x = p_1, \tag{2.99a}$$

$$K_\varphi = \frac{\sin(\lambda q_2)}{\lambda} \qquad \text{and} \qquad E^\varphi = \frac{p_2}{\cos(\lambda q_2)}, \tag{2.99b}$$

$$P_\phi = q_3 \qquad \text{and} \qquad \phi = -p_3. \tag{2.99c}$$

It is clear that two degrees of freedom remain unaltered, as compared to GR, while the angular components of the triad and the curvature retain all the changes. Based on the resemblance of the effective model with the GR Hamiltonian, we rename $\mathcal{K}_\varphi := q_2$ and $\mathcal{E}^\varphi := p_2$, such that

$$K_\varphi = \frac{\sin(\lambda \mathcal{K}_\varphi)}{\lambda} \qquad \text{and} \qquad E^\varphi = \frac{\mathcal{E}^\varphi}{\cos(\lambda \mathcal{K}_\varphi)}, \tag{2.100}$$

and we use the following three pairs of variables:

$$\{K_x(x_1), E^x(x_2)\} = \{\mathcal{K}_\varphi(x_1), \mathcal{E}^\varphi(x_2)\} = \{\phi(x_1), P_\phi(x_2)\} = \delta(x_1, x_2). \tag{2.101}$$

We will now show that the Hamiltonian (2.94) with $\omega = \lambda \in \mathbb{R}$, and $p_1 = K_x$, $p_2 = \mathcal{K}_\varphi$, $p_3 = -\phi$, $q_1 = E^x$, $q_2 = \mathcal{E}^\varphi$, and $q_3 = P_\phi$ can indeed be obtained from the GR Hamiltonian (1.43) with (1.46a).

Let us first perform the canonical transformation (2.100). Note that this canonical transformation leaves invariant the diffeomorphism constraint (1.43a). On the one hand, the bracket between the transformed GR Hamiltonian constraint, $\mathcal{H}^{(0)} \xrightarrow{\text{c.t.}} \overline{\mathcal{H}}^{(0)}$, and the unchanged diffeomorphism constraint, $\mathcal{D}$, remains unaltered, that is, $\{D[s_1], \overline{H}^{(0)}[s_2]\} = \overline{H}^{(0)}[s_1 s_2']$. On the other hand, due to the presence of phase-space variables in the structure function, the

bracket between two transformed Hamiltonian constraints changes accordingly,

$$\left\{\overline{H}^{(0)}[s_1],\overline{H}^{(0)}[s_2]\right\} = D\left[\frac{E^x}{(\mathcal{E}^\varphi)^2}\cos^2(\lambda\mathcal{K}_\varphi)(s_1s_2'-s_1's_2)\right]. \tag{2.102}$$

Notice now that, since the GR Hamiltonian (1.42b) is linear in E^φ and K_x, the new constraint $\overline{\mathcal{H}}^{(0)}$ acquires explicit poles at $\cos(\lambda\mathcal{K}_\varphi) = 0$, which correspond to the surfaces where the canonical transformation (2.100) is not valid. As we want to regularise those potential infinities, we define a rescaled Hamiltonian $\widetilde{\mathcal{H}} := \overline{\mathcal{H}}^{(0)}\cos(\lambda\mathcal{K}_\varphi)$. However, that new constraint is not the canonical generator of normal deformations since

$$\begin{aligned}\{\widetilde{H}[s_1],\widetilde{H}[s_2]\} = {}& D\left[\frac{E^x}{\mathcal{E}^{\varphi 2}}\cos^4(\lambda\mathcal{K}_\varphi)(s_1s_2'-s_1's_2)\right]\\ & - \widetilde{H}\left[\frac{\sqrt{E^x}E^{x\prime}}{4(\mathcal{E}^\varphi)^2}\lambda\sin(2\lambda\mathcal{K}_\varphi)(s_1s_2'-s_1's_2)\right].\end{aligned} \tag{2.103}$$

In order to obtain a geometric interpretation, we are forced to find the normal projection of $\widetilde{H}$, that is, to find the form $\{H[s_1],H[s_2]\} = D[F(s_1s_2'-s_1's_2)]$. One can check that the suitable combination $H[N] := \widetilde{H}[N] - D[NF_{\widetilde{H}}]$, with $F_{\widetilde{H}}$ the smearing function in the $\widetilde{H}$ term on the right-hand side of (2.103), produces the canonical form of the bracket.

More explicitly, the regularised Hamiltonian is defined as

$$\mathcal{H} := \widetilde{\mathcal{H}} + \lambda\sin(2\lambda\mathcal{K}_\varphi)\frac{\sqrt{E^x}E^{x\prime}}{4(\mathcal{E}^\varphi)^2}\mathcal{D} = \left(\overline{\mathcal{H}}^{(0)} + \lambda\sin(\lambda\mathcal{K}_\varphi)\frac{\sqrt{E^x}E^{x\prime}}{2(\mathcal{E}^\varphi)^2}\mathcal{D}\right)\cos(\lambda\mathcal{K}_\varphi). \tag{2.104}$$

This last expression turns out to be exactly the same as the Hamiltonian constraint (2.94) with $\omega = \lambda \in \mathbb{R}$, and $p_1 = K_x$, $p_2 = \mathcal{K}_\varphi$, $p_3 = -\phi$, $q_1 = E^x$, $q_2 = \mathcal{E}^\varphi$, and $q_3 = P_\phi$. Explicitly, the Hamiltonian with scale-invariant covariant holonomy corrections reads

$$\mathcal{D} = -K_xE^{x\prime} + \mathcal{K}_\varphi'\mathcal{E}^\varphi + \phi' P_\phi, \tag{2.105a}$$

$$\begin{aligned}\mathcal{H} = {}& \frac{1}{\sqrt{1+\lambda^2}}\left(-\frac{\mathcal{E}^\varphi}{2\sqrt{E^x}}\left(1+\frac{\sin^2(\lambda\mathcal{K}_\varphi)}{\lambda^2}\right) - \sqrt{E^x}K_x\frac{\sin(2\lambda\mathcal{K}_\varphi)}{\lambda}\left(1+\left(\frac{\lambda E^{x\prime}}{2\mathcal{E}^\varphi}\right)^2\right)\right.\\ & + \left(\frac{(E^{x\prime})^2}{8\sqrt{E^x}\mathcal{E}^\varphi} - \frac{\sqrt{E^x}}{2\mathcal{E}^{\varphi 2}}E^{x\prime}\mathcal{E}^{\varphi\prime} + \frac{\sqrt{E^x}}{2\mathcal{E}^\varphi}E^{x\prime\prime} + \frac{P_\phi^2}{2\sqrt{E^x}\mathcal{E}^\varphi} + \frac{E^{x3/2}(\phi')^2}{2\mathcal{E}^\varphi}\right)\cos^2(\lambda\mathcal{K}_\varphi)\\ & \left. + \sqrt{E^x}\mathcal{E}^\varphi V(E^x,\phi) + \frac{\sqrt{E^x}}{4\mathcal{E}^{\varphi 2}}E^{x\prime}\phi' P_\phi\lambda\sin(2\lambda\mathcal{K}_\varphi)\right).\end{aligned} \tag{2.105b}$$

Note that the Hamiltonian constraint is periodic in $\mathcal{K}_\varphi$, with period π/λ, and that leading-order corrections go as λ^2.

It is straightforward to compute that the constraints (2.105) satisfy the canonical form of the algebra,

$$\{D[s_1], D[s_2]\} = D[s_1 s_2' - s_1' s_2], \tag{2.106a}$$

$$\{D[s_1], H[s_2]\} = H[s_1 s_2'], \tag{2.106b}$$

$$\{H[s_1], H[s_2]\} = D[F(s_1 s_2' - s_1' s_2)], \tag{2.106c}$$

with the everywhere non-negative structure function

$$F = \frac{\cos^2(\lambda \mathcal{K}_\varphi)}{1+\lambda^2}\left(1 + \left(\frac{\lambda E^{x\prime}}{2\mathcal{E}^\varphi}\right)^2\right)\frac{E^x}{\mathcal{E}^{\varphi 2}}. \tag{2.107}$$

As we did before, we can use the mass function (2.58), which now reads

$$m := \frac{\sqrt{E^x}}{2}\left(1 + \frac{\sin^2(\lambda \mathcal{K}_\varphi)}{\lambda^2} - \left(\frac{E^{x\prime}}{2\mathcal{E}^\varphi}\right)^2 \cos^2(\lambda \mathcal{K}_\varphi)\right), \tag{2.108}$$

to simplify the structure function:

$$F = \left(1 - \frac{2\lambda m}{\sqrt{E^x}}\right)\frac{E^x}{\mathcal{E}^{\varphi 2}}. \tag{2.109}$$

In addition, we have defined the new parameter

$$\lambda := \frac{\lambda^2}{1+\lambda^2}. \tag{2.110}$$

Note that, by definition, this constant is bounded, and it takes values in the range $(0, 1)$. Indeed, this is the physically meaningful constant of the model, and it measures the geometric scale of quantum effects. The limit $\lambda \to 0$ corresponds to GR, since the canonical transformation (2.100) is the identity, $\mathcal{H} = \mathcal{H}^{(0)}$, and $F = E^x/E^{\varphi 2}$. Hence, we expect the effective regime to be valid for $\lambda \ll 1$, while the limit $\lambda \to 1$ would represent the maximum departure from the classical theory.

As commented before, anomaly freedom is not a sufficient condition for the Hamiltonian to have a direct geometric interpretation. The transformation properties of the structure function in the algebra are also constrained if one wants to embed the $3+1$ theory in a four-dimensional manifold. By construction, we already have the radial component of the metric, the inverse of the structure function (2.107). We also know the coefficients of the dt^2 and the $dtdx$ elements of the metric because we required the lapse and the shift to be defined in the same way as in GR. Therefore, we only need to specify the angular component of the met-

ric. However, since the canonical transformation leaves invariant the pair (K_x, E^x), and E^x transforms as a scalar quantity, we also argue that the area of the orbits of the rotation group should still be determined by this variable. That is, we will fix $r(t,x) := \sqrt{E^x}(t,x)$. Gathering all the above, the metric associated to the Hamiltonian (2.105) is

$$ds^2 = -N^2dt^2 + \left(1 - \frac{2\lambda m}{\sqrt{E^x}}\right)^{-1} \frac{\mathcal{E}^{\varphi 2}}{E^x}\left(dx + N^x dt\right)^2 + E^x d\Omega^2, \tag{2.111}$$

with the functions $N(t,x)$, $N^x(t,x)$, $E^x(t,x)$, $\mathcal{E}^\varphi(t,x)$ and $m(t,x)$ satisfying the two constraint equations, $\mathcal{D} = 0$ and $\mathcal{H} = 0$, plus the six Hamiltonian equations of motion.

As we did obtain the Hamiltonian (2.105) in two independent ways, the poles $\cos(\lambda\mathcal{K}_\varphi) = 0$ are shown to be consistently regularised and potential ill-definitions at those points are absent. Moreover, the process consisting of the canonical transformation (2.100) plus the regularisation (2.104) provides a very simple and systematic way to reach the effective Hamiltonian, and it is not restricted to the case of a scalar field. For instance, we can consider non-rotating dust as the matter component [recall (1.46b)], and implement (2.100) along with (2.104) to obtain an anomaly-free Hamiltonian with the same structure function (2.95).

3

The Effective Quantum Schwarzschild Black Hole

Remember, the enemy's gate is down.

Ender's Game
by Orson Scott Card.

The Schwarzschild spacetime is a fundamental exact solution of the equations of general relativity. It describes the gravitational field in vacuum outside a spherically symmetric massive object in an asymptotically flat spacetime. This solution shows a physical singularity where curvature scalars diverge. An infalling observer arrives there in finite proper time, and the spacetime cannot be further extended in a smooth way.

In this chapter, we study the vacuum reduction of our effective model and examine the geometric properties of the resulting spacetime, comparing them with those of Schwarzschild. In Sec. 3.1, we obtain solutions for the equations of motion in different gauges and show how the corresponding line elements are related through coordinate transformations. This fact is ensured by our covariant construction, and thus different gauge choices just provide different charts of one same metric tensor. In particular, we obtain a chart that covers the whole spacetime. This is the starting point to study the global structure of the solution in Sec. 3.2, which eventually provides the maximal analytic extension of the spacetime. The main properties of the solution are studied in Sec. 3.3. Our analysis shows that the singularity in the Schwarzschild solution is fully resolved and replaced by a minimal spacelike hypersurface. This separates a trapped and an anti-trapped region within a completely regular and geodesically complete homogeneous region. We also characterise the area of the spheres in that transition surface, both globally and quasi-locally. Finally, in Sec. 3.4, we show that Minkowski is a solution of the effective theory, and also that the Schwarzschild spacetime is recovered in a particular limit of the model. All figures in this chapter were published in Ref. [5].

Removing the matter field from the Hamiltonian (2.105), one obtains

$$\mathcal{D}_g = - K_x E^{x\prime} + \mathcal{K}'_\varphi \mathcal{E}^\varphi, \tag{3.1a}$$

$$\begin{aligned}\mathcal{H}_g =& \frac{-1}{\sqrt{1+\lambda^2}}\left(\frac{\mathcal{E}^\varphi}{2\sqrt{E^x}}\left(1+\frac{\sin^2(\lambda\mathcal{K}_\varphi)}{\lambda^2}\right)+\sqrt{E^x}K_x\frac{\sin(2\lambda\mathcal{K}_\varphi)}{\lambda}\left(1+\left(\frac{\lambda E^{x\prime}}{2\mathcal{E}^\varphi}\right)^2\right)\right.\\ &\left.-\left(\frac{(E^{x\prime})^2}{8\sqrt{E^x}\mathcal{E}^\varphi}-\frac{\sqrt{E^x}}{2\mathcal{E}^{\varphi 2}}E^{x\prime}\mathcal{E}^{\varphi\prime}+\frac{\sqrt{E^x}}{2\mathcal{E}^\varphi}E^{x\prime\prime}\right)\cos^2(\lambda\mathcal{K}_\varphi)\right),\end{aligned} \tag{3.1b}$$

with $\lambda \in \mathbb{R}$. These constraints form the algebra

$$\{D_g[s_1], D_g[s_2]\} = D_g[s_1 s_2' - s_1' s_2], \tag{3.2a}$$

$$\{D_g[s_1], H_g[s_2]\} = H_g[s_1 s_2'], \tag{3.2b}$$

$$\{H_g[s_1], H_g[s_2]\} = D_g[F(s_1 s_2' - s_1' s_2)], \tag{3.2c}$$

where the everywhere non-negative structure function F is given by (2.107), that is,

$$F = \left(1 - \frac{2\lambda m}{\sqrt{E^x}}\right)\frac{E^x}{\mathcal{E}^{\varphi 2}} \geq 0. \tag{3.3}$$

Recall the definition of the bounded parameter $\lambda := \lambda^2/(1+\lambda^2) \in (0,1)$, which measures the departure of the effective theory from GR. Indeed, the limit $\lambda \to 0$ corresponds to GR. As we pointed out before, m, as defined in (2.108), is a constant of motion in vacuum,

$$\begin{aligned}\dot{m} =& \{m, D_g[N^x] + H_g[N]\} = -H_g\left[\sqrt{1+\lambda^2}\frac{N^x E^{x\prime}}{2\mathcal{E}^\varphi}\right]\\ &+ D_g\left[\frac{\sqrt{E^x}}{2\mathcal{E}^\varphi}\left(1+\left(\frac{\lambda E^{x\prime}}{2\mathcal{E}^\varphi}\right)^2\right)\left(\frac{N^x\sin(2\lambda\mathcal{K}_\varphi)}{\lambda}-\frac{N\sqrt{E^x}E^{x\prime}\cos^2(\lambda\mathcal{K}_\varphi)}{2\sqrt{1+\lambda^2}\mathcal{E}^{\varphi 2}}\right)\right] \approx 0,\end{aligned} \tag{3.4}$$

so let us define $M \in \mathbb{R}$ as the constant value of the mass function, that is,

$$M = \frac{\sqrt{E^x}}{2}\left(1+\frac{\sin^2(\lambda\mathcal{K}_\varphi)}{\lambda^2}-\left(\frac{E^{x\prime}}{2\mathcal{E}^\varphi}\right)^2\cos^2(\lambda\mathcal{K}_\varphi)\right). \tag{3.5}$$

Note that for positive values of M, the function $\sqrt{E^x}$ has a positive lower bound. The underlying reason is that the structure function (3.3) is non-negative, forbidding the ranges of $\sqrt{E^x}$ for which F would attain negative values. We will restrict to non-negative values of M, and leave the cases $M < 0$ for the next chapter. As it will be shown below, from the geometric point of view, the vanishing of F at the critical values $\sqrt{E^x} = 2\lambda M$ translates to the appearance of a minimum for the area of the orbits of the spherical symmetry.

The length

$$r_0 := 2\lambda M, \tag{3.6}$$

will denote those critical values.

Recall that the metric is

$$ds^2 = -N^2 dt^2 + \left(1 - \frac{2\lambda M}{\sqrt{E^x}}\right)^{-1} \frac{\mathcal{E}^{\varphi 2}}{E^x}\left(dx + N^x dt\right)^2 + E^x d\Omega^2, \tag{3.7}$$

where M and λ are constant, and the functions $N(t,x)$, $N^x(t,x)$, $E^x(t,x)$ and $\mathcal{E}^\varphi(t,x)$ follow

$$\dot{E}^x = \{E^x, D_g[N^x] + H_g[N]\} = N^x E^{x\prime} + N\sqrt{E^x}\frac{\sin(2\lambda\mathcal{K}_\varphi)}{\lambda\sqrt{1+\lambda^2}}\left(1 + \left(\frac{\lambda E^{x\prime}}{2\mathcal{E}^\varphi}\right)^2\right), \tag{3.8a}$$

$$\begin{aligned}\dot{\mathcal{E}}^\varphi =& \{\mathcal{E}^\varphi, D_g[N^x] + H_g[N]\} = (N^x\mathcal{E}^\varphi)' + 2N\sqrt{E^x}K_x\frac{\cos(2\lambda\mathcal{K}_\varphi)}{\sqrt{1+\lambda^2}}\left(1 + \left(\frac{\lambda E^{x\prime}}{2\mathcal{E}^\varphi}\right)^2\right)\\ &+ N\frac{\sin(2\lambda\mathcal{K}_\varphi)}{\lambda\sqrt{1+\lambda^2}}\left(\frac{\mathcal{E}^\varphi}{2\sqrt{E^x}} + \frac{\lambda^2}{2}\left(\frac{E^{x\prime}}{2\mathcal{E}^\varphi}\left(\sqrt{E^x}\right)' + \sqrt{E^x}\left(\frac{E^{x\prime}}{\mathcal{E}^\varphi}\right)'\right)\right),\end{aligned} \tag{3.8b}$$

$$\begin{aligned}\dot{K}_x =& \{K_x, D_g[N^x] + H_g[N]\} = (N^x K_x)' + N''\frac{\sqrt{E^x}\cos^2(\lambda\mathcal{K}_\varphi)}{2\sqrt{1+\lambda^2}\mathcal{E}^\varphi}\\ &+ \frac{N'\sqrt{E^x}}{2\sqrt{1+\lambda^2}\mathcal{E}^{\varphi 2}}\left(\lambda\sin(2\lambda\mathcal{K}_\varphi)\left(E^{x\prime}K_x - 2\mathcal{E}^\varphi\mathcal{K}_\varphi'\right) + \cos^2(\lambda\mathcal{K}_\varphi)\left(\frac{\mathcal{E}^\varphi E^{x\prime}}{2E^x} - \mathcal{E}^{\varphi\prime}\right)\right)\\ &+ \frac{N}{\sqrt{1+\lambda^2}}\left(\frac{\mathcal{E}^\varphi(\sin^2(\lambda\mathcal{K}_\varphi) + \lambda^2)}{4\lambda^2 E^{x3/2}} + \frac{\cos^2(\lambda\mathcal{K}_\varphi)}{4\sqrt{E^x}\mathcal{E}^\varphi}\left(E^{x\prime\prime} - \frac{(E^{x\prime})^2}{4E^x} - \frac{E^{x\prime}\mathcal{E}^{\varphi\prime}}{\mathcal{E}^\varphi}\right)\right.\\ &\left. - \frac{K_x\sin(2\lambda\mathcal{K}_\varphi)}{2\lambda\sqrt{E^x}}\left(1 + \left(\frac{\lambda E^{x\prime}}{2\mathcal{E}^\varphi}\right)^2\right) - \left[\sin(2\lambda\mathcal{K}_\varphi)\frac{\lambda\sqrt{E^x}}{2\mathcal{E}^{\varphi 2}}\mathcal{D}_g\right]'\right),\end{aligned} \tag{3.8c}$$

$$\begin{aligned}\dot{\mathcal{K}}_\varphi =& \{\mathcal{K}_\varphi, D_g[N^x] + H_g[N]\} = N^x\mathcal{K}_\varphi' + N'\frac{\sqrt{E^x}E^{x\prime}}{2\mathcal{E}^{\varphi 2}}\frac{\cos^2(\lambda\mathcal{K}_\varphi)}{\sqrt{1+\lambda^2}} - N\frac{\sin^2(\lambda\mathcal{K}_\varphi) + \lambda^2}{2\lambda^2\sqrt{E^x}\sqrt{1+\lambda^2}}\\ &+ N\frac{(E^{x\prime})^2}{8\sqrt{E^x}\mathcal{E}^{\varphi 2}}\frac{\cos^2(\lambda\mathcal{K}_\varphi)}{\sqrt{1+\lambda^2}} - N\frac{\sin(2\lambda\mathcal{K}_\varphi)}{\sqrt{1+\lambda^2}}\frac{\lambda\sqrt{E^x}E^{x\prime}}{2\mathcal{E}^{\varphi 3}}\mathcal{D}_g,\end{aligned} \tag{3.8d}$$

in addition to the constraint equations $\mathcal{D}_g = 0$ and $\mathcal{H}_g = 0$, as given in (3.1).

3.1 The spacetime solution

We begin with the chart $\Psi^A = \{t, x\}$ (plus the angular coordinates, which we omit in the following) on some domain D_A of the spacetime manifold $\mathcal{M}$, with metric tensor (3.7). From now on, $\{\cdot,\cdot\}$ will denote charts and not Poisson brackets. The allowed ranges of the coordinates define a patch on $\mathbb{R}^2$ which is the preimage of the domain $D_A \subset \mathcal{M}$.

There is an inherent gauge freedom in the model that allows to fix two among the four phase-space functions. Since the construction of the metric has been carried out so that coordinate transformations correspond to gauge changes on phase space, each consistent gauge choice will lead to a solution of the above system of equations and produce the same metric tensor in the corresponding chart and domain of definition. The spacetime solution is thus unique.

Although proven in the previous chapter, we will illustrate this by considering different gauge choices and by seeing how the corresponding line elements are related through coordinate transformations, thus defining the same geometry. In order to avoid confusion, we will re-label t and x in a different way for each chart. For the moment, we will exclude degenerate solutions with identically vanishing N or $\mathcal{E}^\varphi$.

3.1.1 Static region

We start with the gauge-fixing conditions

$$\sqrt{E^x} = x \qquad \text{and} \qquad \mathcal{K}_\varphi = 0, \tag{3.9}$$

which restrict the range of the radial coordinate to $x \geq 0$. Recall that we already have a first integral of the system, the constant of motion (3.5), from where we obtain

$$\mathcal{E}^\varphi = \varepsilon_1 x \left(1 - \frac{2M}{x}\right)^{-1/2}, \tag{3.10}$$

with $\varepsilon_1^2 = 1$. In this gauge, the constraints and the dynamical equations are greatly simplified. The diffeomorphism constraint imposes a vanishing K_x,

$$0 = \mathcal{D}_g = -2xK_x, , \tag{3.11}$$

and the conservation of the two gauge conditions (3.9),

$$0 = \dot{E}^x = 2xN^x, \tag{3.12a}$$

$$0 = \dot{\mathcal{K}}_\varphi = \frac{N'}{\sqrt{1+\lambda^2}}\left(1 - \frac{2M}{x}\right) - \frac{mN}{\sqrt{1+\lambda^2 x^2}}, \tag{3.12b}$$

require, respectively,

$$N^x = 0 \qquad \text{and} \qquad N = c_1\sqrt{1 - \frac{2M}{x}}, \tag{3.13}$$

where the constant $c_1 \neq 0$ can be trivially absorbed in a time redefinition. We thus set $c_1 = 1$.

The remaining equations, (3.8b), (3.8c), and the vanishing of (3.1b), are automatically satisfied.

We now relabel (t, x) as the pair of real functions $(\tilde{t}, \tilde{r})$ on $D_S \subset \mathcal{M}$ that defines the static chart $\Psi^S = \{\tilde{t}, \tilde{r}\}$ on $\mathbb{R}^2$, with the ranges of coordinates specified by the existence of the above solutions. Then, the domain D_S is only restricted by $\tilde{r} > 2M$, and the metric reads

$$ds^2 = -\left(1 - \frac{2M}{\tilde{r}}\right) d\tilde{t}^2 + \left(1 - \frac{2\lambda M}{\tilde{r}}\right)^{-1} \left(1 - \frac{2M}{\tilde{r}}\right)^{-1} d\tilde{r}^2 + \tilde{r}^2 d\Omega^2. \tag{3.14}$$

Before focusing on the study of this geometry, we will obtain additional charts and domains of definition for that same metric tensor, but we point out that neither $\tilde{r} = 2\lambda M$ nor $\tilde{r} = 2M$ (which are not included in the above chart) will describe a physical singularity, as one can check by computing the curvature scalars (see Sec. 3.3.2).

3.1.2 Homogeneous region

In this case, we demand the partial gauge fixing

$$E^{x\prime} = 0 \qquad \text{and} \qquad \mathcal{E}^{\varphi\prime} = 0. \tag{3.15}$$

It is straightforward to see that the vanishing of the diffeomorphism constraint,

$$0 = \mathcal{D}_g = \mathcal{K}'_\varphi \mathcal{E}^\varphi, \tag{3.16}$$

fixes $\mathcal{K}'_\varphi = 0$, and since the radial derivative of $\mathcal{H}_g$ must also vanish,

$$0 = \mathcal{H}_g \quad \to \quad 0 = \mathcal{H}'_g = \sqrt{E^x} K'_x \frac{\sin(2\lambda \mathcal{K}_\varphi)}{\lambda}, \tag{3.17}$$

we obtain $K'_x = 0$ because a constant $\mathcal{K}_\varphi$ is inconsistent with our assumption $N \neq 0$ [see (3.8d)]. Taking now the time derivative of the gauge-fixing conditions (3.15), we obtain two equations to solve for the lapse and the shift:

$$0 = (\dot{E}^x)' = N' \frac{\sin(2\lambda \mathcal{K}_\varphi)}{\lambda\sqrt{1+\lambda^2}} \qquad \to \qquad N' = 0, \tag{3.18a}$$

$$0 = (\dot{\mathcal{E}}^\varphi)' = N^{x\prime\prime} \mathcal{E}^\varphi + 2N' \sqrt{E^x} K_x \frac{\cos(2\lambda \mathcal{K}_\varphi)}{\sqrt{1+\lambda^2}} \qquad \to \qquad N^{x\prime\prime} = 0. \tag{3.18b}$$

With these results, we use part of the remaining gauge freedom to set a vanishing shift,

$$N^x = 0, \tag{3.19}$$

which is consistent with the above condition.

From the geometric point of view, this represents a diagonalisation of the metric, because $N^{x\prime\prime} = 0 \leftrightarrow N^x = a(t)x + b(t)$ implies that one can always find a function y such that $dx + N^x dt = \exp(-\int a(t)dt)dy$.

Imposing the commented conditions, the remaining equations of motion are thus

$$\dot{E^x} = N\sqrt{E^x}\frac{\sin(2\lambda\mathcal{K}_\varphi)}{\lambda\sqrt{1+\lambda^2}}, \tag{3.20a}$$

$$\dot{\mathcal{E}^\varphi} = \frac{N}{\sqrt{1+\lambda^2}}\left(2\sqrt{E^x}K_x\cos(2\lambda\mathcal{K}_\varphi) + \frac{\mathcal{E}^\varphi\sin(2\lambda\mathcal{K}_\varphi)}{2\lambda\sqrt{E^x}}\right), \tag{3.20b}$$

$$\dot{K_x} = \frac{N}{2\sqrt{E^x}\sqrt{1+\lambda^2}}\left(\frac{\mathcal{E}^\varphi}{2E^x}\left(1+\frac{\sin^2(\lambda\mathcal{K}_\varphi)}{\lambda^2}\right) - K_x\frac{\sin(2\lambda\mathcal{K}_\varphi)}{\lambda}\right), \tag{3.20c}$$

$$\dot{\mathcal{K}_\varphi} = -\frac{N}{2\sqrt{E^x}\sqrt{1+\lambda^2}}\left(1+\frac{\sin^2(\lambda\mathcal{K}_\varphi)}{\lambda^2}\right), \tag{3.20d}$$

$$0 = \mathcal{H} = -\frac{\mathcal{E}^\varphi}{2\sqrt{E^x}\sqrt{1+\lambda^2}}\left(1+\frac{\sin^2(\lambda\mathcal{K}_\varphi)}{\lambda^2}\right) - \sqrt{E^x}K_x\frac{\sin(2\lambda\mathcal{K}_\varphi)}{\lambda\sqrt{1+\lambda^2}}. \tag{3.20e}$$

We still retain certain gauge freedom since we have not specified completely the form of $E^x(t)$ and $\mathcal{E}^\varphi(t)$, which we will use in the following to express the metric in two different coordinate patches.

Half of the homogeneous region

First, we consider

$$E^x = t^2, \tag{3.21}$$

and, just as in the previous section, we use the constant of motion,

$$M = \frac{t}{2}\left(1+\frac{\sin(\lambda\mathcal{K}_\varphi)}{\lambda}\right), \tag{3.22}$$

to solve for one of the variables. In this case,

$$\frac{\sin(\lambda\mathcal{K}_\varphi)}{\lambda} = \varepsilon_2\sqrt{\frac{2M}{t}-1}, \tag{3.23}$$

where $\varepsilon_2^2 = 1$. Note that this relation imposes the condition $t \leq 2M$ for the domain of the coordinate t. We can obtain the lapse from equation (3.20a),

$$N = \varepsilon_3\left(1-\frac{2\lambda M}{t}\right)^{-1/2}\left(\frac{2M}{t}-1\right)^{-1/2}, \tag{3.24}$$

with $\varepsilon_3^2 = 1$, which further restricts the range of t to $2\lambda M < t < 2M$.

Equation (3.20b) is now

$$\dot{\mathcal{E}^\varphi} = \mathcal{E}^\varphi \frac{M(1+\lambda) - t}{(2M-t)(t-2\lambda M)}, \tag{3.25}$$

and, upon integration, we find

$$\mathcal{E}^\varphi = c_2 \sqrt{2M-t}\sqrt{t-2\lambda M}, \tag{3.26}$$

with a non-vanishing constant c_2. The only variable left, K_x, might be directly obtained from the homogeneous Hamiltonian constraint (3.20e), yielding

$$K_x = -\varepsilon_3 c_2 \sqrt{1-\lambda}\,\frac{M}{2t^2}. \tag{3.27}$$

With all the above, one can check that both (3.20c) and (3.20d) are satisfied. We consider the pair of real functions (T, X) on $D_h \subset \mathcal{M}$ relabelling (t, x) to define the chart $\Psi^h = \{T, X\}$ on $\mathbb{R}^2$, restricted by $T \in (2\lambda M, 2M)$. The metric (3.7) in that chart is

$$ds^2 = -\left(1 - \frac{2\lambda M}{T}\right)^{-1}\left(\frac{2M}{T} - 1\right)^{-1} dT^2 + \left(\frac{2M}{T} - 1\right) dX^2 + T^2 d\Omega^2, \tag{3.28}$$

where we have trivially set $c_2 = 1$.

The complete homogeneous region

In this occasion we use the remaining gauge freedom in (3.20) to choose

$$\mathcal{K}_\varphi = \frac{t}{\lambda} \tag{3.29}$$

as our time. The constant of motion (3.5) now yields

$$E^x = \left(\frac{2M\lambda^2}{\lambda^2 + \sin^2 t}\right)^2, \tag{3.30}$$

and we can solve either (3.20a) or (3.20d) for the lapse,

$$N = -\frac{\sqrt{1+\lambda^2}}{M\lambda}\left(\frac{2M\lambda^2}{\lambda^2 + \sin^2 t}\right)^2. \tag{3.31}$$

Finally, combining (3.20b) and (3.20e) we find

$$\mathcal{E}^\varphi = \frac{c_3 \lambda M \sin(2t)}{\sqrt{1+\lambda^2}(\lambda^2 + \sin^2 t)} \qquad \text{and} \qquad K_x = \frac{(\lambda^2 + \sin^2 t)^2}{8M\lambda^4\sqrt{1+\lambda^2}}, \tag{3.32}$$

with $c_3 \neq 0$. As in previous occasions, we can set $c_3 = 1$ with no loss of generality.

We now identify (t, x) with the pair of real functions $(\overline{T}, \overline{X})$ on $D_H \subset \mathcal{M}$ defining the homogeneous chart $\Psi^H = \{\overline{T}, \overline{X}\}$. Due to the periodicity of the solution, the domain D_H is the preimage of the stripe $\overline{T} \in (0, \pi)$ in $\mathbb{R}^2$. Using definition (3.6), we write the metric,

$$ds^2 = -\frac{16M^2\lambda^3}{\left(\lambda + (1-\lambda)\sin^2\overline{T}\right)^4} d\overline{T}^2 + \frac{1-\lambda}{\lambda}\sin^2\overline{T}\, d\overline{X}^2 + \frac{4\lambda^2M^2}{\left(\lambda + (1-\lambda)\sin^2\overline{T}\right)^2} d\Omega^2. \quad (3.33)$$

It is enlightening to express the above in terms of the area-radius function,

$$r(\overline{T}) := \sqrt{E^x} = \frac{2\lambda M}{\lambda + (1-\lambda)\sin^2\overline{T}}, \quad (3.34)$$

yielding

$$ds^2 = -\frac{r(\overline{T})^4}{\lambda M^2} d\overline{T}^2 + \left(\frac{2M}{r(\overline{T})} - 1\right) d\overline{X}^2 + r(\overline{T})^2 d\Omega^2, \quad (3.35)$$

with the area-radius function being restricted to the range $r(\overline{T}) \in [2\lambda M, 2M)$, corresponding to $\sin^2\overline{T} = 1$ and $\sin^2\overline{T} \to 0$, respectively. Recall that this last value lies outside the allowed region but the spacelike hypersurface $r(\overline{T} = \pi/2) = 2\lambda M$ is contained within it.

3.1.3 The covering domain

We impose time-independence on the functions E^x and $\mathcal{E}^\varphi$ but still leave some gauge freedom:

$$\dot{E}^x = 0 \qquad \text{and} \qquad \dot{\mathcal{E}}^\varphi = 0. \quad (3.36)$$

Note that if E^x was everywhere constant, and since we assumed a non-vanishing $\mathcal{E}^\varphi$, the Hamiltonian constraint, $\mathcal{H}_g = 0$, would require $K_x \neq 0$ and $\sin(2\lambda\mathcal{K}_\varphi) \neq 0$. In such a case, (3.8a) for $\dot{E}^x = 0$ would yield $N = 0$, which would not meet our initial assumption for an identically non-vanishing lapse. Therefore, conditions (3.36) also imply an identically non-vanishing $E^{x\prime}$. Moreover, the constant of motion (3.5) can be expressed as

$$M = \frac{\sqrt{E^x}}{2\lambda^2}\left(1 + \lambda^2 - \left(1 + \left(\frac{\lambda E^{x\prime}}{2\mathcal{E}^\varphi}\right)^2\right)\cos^2(\lambda\mathcal{K}_\varphi)\right), \quad (3.37)$$

and we see that when $E^{x\prime} \neq 0$, the term $\cos(\lambda\mathcal{K}_\varphi)$ cannot vanish identically or m would not be constant. Since the case $\sin(\lambda\mathcal{K}_\varphi) = 0$ was studied in Sec. 3.1.1, we shall further assume

a non-vanishing $\sin(2\lambda\mathcal{K}_\varphi)$. We solve the above relation to write

$$\cos^2(\lambda\mathcal{K}_\varphi) = \left(1+\left(\frac{\lambda E^{x\prime}}{2\mathcal{E}^\varphi}\right)^2\right)^{-1}\left(1+\lambda^2-\frac{2M\lambda^2}{\sqrt{E^x}}\right), \tag{3.38}$$

and we read, from the vanishing of the diffeomorphism constraint (3.1a),

$$K_x = \frac{\mathcal{E}^\varphi \mathcal{K}'_\varphi}{E^{x\prime}}. \tag{3.39}$$

The lapse and the shift are given by the vanishing of equations (3.8a) and (3.8b). First, we solve $\dot{E^x}=0$ for the shift. Inserting that in $\dot{\mathcal{E}^\varphi}=0$, we obtain

$$\sin(2\lambda\mathcal{K}_\varphi)E^x\left(1+\left(\frac{\lambda E^{x\prime}}{2\mathcal{E}^\varphi}\right)^2\right)\left(N'E^{x\prime}\mathcal{E}^\varphi + N(\mathcal{E}^{\varphi\prime}E^{x\prime}-\mathcal{E}^\varphi E^{x\prime\prime})\right)=0. \tag{3.40}$$

Since all the other factors cannot vanish, we find a first-order differential equation for the lapse. The general solution is

$$N = \frac{c_4}{2}\frac{E^{x\prime}}{\mathcal{E}^\varphi}, \tag{3.41}$$

for some non-zero constant c_4. Then, (3.8a) yields

$$N^x = \varepsilon_4 c_4 \frac{\sqrt{E^x}}{\mathcal{E}^\varphi}\sqrt{1-\frac{2\lambda M}{\sqrt{E^x}}}\sqrt{\frac{2M}{\sqrt{E^x}}-1+\left(\frac{E^{x\prime}}{2\mathcal{E}^\varphi}\right)^2}, \tag{3.42}$$

where $\varepsilon_4 = -\operatorname{sgn}\left(\sin(2\lambda\mathcal{K}_\varphi)\right)$, and we can fix $c_4=-1$ with no loss of generality.

At this point, all the constraints and the evolution equations are satisfied, and we obtain a family of line elements in terms of the free functions $E^x(x)$ and $\mathcal{E}^\varphi(x)$:

$$\begin{aligned} ds^2 = &-\left(1-\frac{2M}{\sqrt{E^x}}\right)dt^2 + 2\left(1-\frac{2\lambda M}{\sqrt{E^x}}\right)^{-1/2}\frac{\mathcal{E}^\varphi}{\sqrt{E^x}}\sqrt{\frac{2M}{\sqrt{E^x}}-1+\left(\frac{E^{x\prime}}{2\mathcal{E}^\varphi}\right)^2}\,dtdx \\ &+\left(1-\frac{2\lambda M}{\sqrt{E^x}}\right)^{-1}\frac{\mathcal{E}^{\varphi 2}}{E^x}dx^2 + E^x d\Omega^2\,. \end{aligned} \tag{3.43}$$

The possible values of x will be restricted by the specific forms of $E^x(x)$ and $\mathcal{E}^\varphi(x)$, and also by the condition that all the solutions are real, that is, (3.38) and (3.42) must be real. Observe that the function $\mathcal{E}^\varphi(x)$ may be absorbed through the change of coordinates $\mathcal{E}^\varphi(x)dx=dy$, but it is convenient to keep that freedom to find the most convenient chart. Now, we must fix the gauge for $E^x(x)$ and $\mathcal{E}^\varphi(x)$. Let us present two possibilities.

Horizon-crossing domains

One of the simplest choices is $E^x = x^2$ and $\mathcal{E}^\varphi = x$, which, after relabelling (t, x) as $(\tilde{\tau}, \tilde{\rho})$, yields the line element

$$ds^2 = -\left(1 - \frac{2M}{\tilde{\rho}}\right) d\tilde{\tau}^2 + 2\sqrt{\frac{2M}{\tilde{\rho} - 2\lambda M}}\, d\tilde{\tau} d\tilde{\rho} + \left(1 - \frac{2\lambda M}{\tilde{\rho}}\right)^{-1} d\tilde{\rho}^2 + \tilde{\rho}^2 d\Omega^2. \tag{3.44}$$

Besides, we notice that the limit $\mathcal{E}^\varphi \to 0$ of the above family of line elements (3.43) is well-defined, so taking instead $E^x = x^2$ and $\mathcal{E}^\varphi = 0$, and relabelling (t, x) as $(\tilde{U}, \tilde{X})$, we obtain the alternative element

$$ds^2 = -\left(1 - \frac{2M}{\tilde{X}}\right) d\tilde{U}^2 + 2\left(1 - \frac{2\lambda M}{\tilde{X}}\right)^{-1/2} d\tilde{U} d\tilde{X} + \tilde{X}^2 d\Omega^2, \tag{3.45}$$

with $\tilde{U}$ a null coordinate (see next section for more details).

These charts of the domain D_{EF} are the equivalents to Gullstrand-Painlevé and Eddington-Finkelstein coordinates in GR, respectively. Both cross the surface $\sqrt{E^x} = 2M$, but none of them includes the points where $\sqrt{E^x} = 2\lambda M$.

The whole covering domain $\mathcal{U}$

Let us now use the definition of the area-radius function $r := \sqrt{E^x}$ on $\mathcal{M}$, and use it to denote E^x in the following. Notice that we already have static (3.14) and homogeneous (3.28) non-intersecting charts, covering $r \in (2M, \infty)$ and $r \in (2\lambda M, 2M)$, respectively. We also found the complete homogeneous solution (3.35) that describes the region with $r \in [2\lambda M, 2M)$. In addition, the two last line elements, (3.44) and (3.45), are valid for $r \in (2\lambda M, \infty)$. Our purpose is to find a chart covering all the above.

From the family (3.43), it is clear that $r = 2\lambda M$ presents divergences. Therefore, to reach those points we must cancel the diverging terms. Let us try, for instance, to set

$$\mathcal{E}^\varphi = r(x)\sqrt{1 - \frac{2\lambda M}{r(x)}}. \tag{3.46}$$

In this way, divergences coming from the coefficient of dx^2 are removed, but there is still one possible infinity hidden in the shift. Replacing now (3.46) in (3.42), we find

$$N^x = \sqrt{\frac{2M}{r(x)} - 1 + \left(1 - \frac{2\lambda M}{r(x)}\right)^{-1} r'(x)^2}. \tag{3.47}$$

In order to remove the divergence at $r = 2\lambda M$, we fix the remaining gauge freedom as

$$r'(x)^2 = \left(1 - \frac{2\lambda M}{r(x)}\right). \tag{3.48}$$

Now, we relabel (t, x) as (τ, z) and we complete the gauge choice by setting

$$\frac{dr(z)}{dz} = \mathrm{sgn}(z)\sqrt{1 - \frac{2\lambda M}{r(z)}}, \qquad \text{with} \qquad r(0) = r_0 := 2\lambda M. \tag{3.49}$$

Defined in this way, $r(z)$ is an analytic function on $\mathbb{R}$, it is even, $r(-z) = r(z)$, it attains its minimum value r_0 at $z = 0$, and $r \to |z|$ as $z \to \pm\infty$. Note that we employ the usual definition of the sign function sgn, i.e., $\mathrm{sgn}(z = 0) = 0$. Since the sign function is not differentiable there, we consider $\mathrm{sgn}(z)^2 = 1$ in a distributional sense, so that higher derivatives of $r(z)$ are continuously defined at $z = 0$.

In fact, one can integrate (3.49) and define $r(z)$ implicitly as

$$z = \sqrt{r(z)}\sqrt{r(z) - r_0} + r_0 \log\left(\sqrt{\frac{r(z)}{r_0}} + \sqrt{\frac{r(z)}{r_0} - 1}\right), \qquad \text{for} \quad z > 0. \tag{3.50}$$

In this chart, the metric reads

$$ds^2 = -\left(1 - \frac{2M}{r(z)}\right)d\tau^2 + 2\sqrt{\frac{2M}{r(z)}}\, d\tau dz + dz^2 + r(z)^2\, d\Omega^2, \tag{3.51}$$

and the image of the domain $\mathcal{U}$ through the chart $\Psi^{\mathcal{U}}_{\tau z} = \{\tau, z\}$ is the whole real plane, that is, the ranges of coordinates are $(\tau, z) \in \mathbb{R}^2$. Let us remark that the function r on $\mathcal{U}$, i.e., $r : \mathcal{U} \to \mathbb{R}$, is bounded from below by $r_0 > 0$.

3.1.4 Coordinate transformations

We have thoroughly said that different gauge choices on phase space yield the same spacetime geometry, but did not provide yet any specific example. In the next section, we shall study the global structure of the domain $\mathcal{U}$ and compute its Penrose diagram. On the way, we will explicitly show the diffeomorphisms that relate all the above line elements.

In the meanwhile, and since the forthcoming derivation shall result difficult to tackle, we perform the change of coordinates from (3.50) to (3.14) in two steps.

First, recall the range of the chart $\Psi^{EF} = \{\tilde\tau, \tilde\rho\}$, defined on $D_{EF} \subset \mathcal{M}$, is given by $\tilde\rho > 2\lambda M$. If one performs the change $(\tilde\tau, \tilde\rho) \to (\tau, z)$ in (3.44) defined by $\tilde\tau(\tau) = \tau$ and $\tilde\rho(z) = r(z)$,

with $r(z)$ given by (3.49), and taking, for instance, the positive branch so that z is restricted by $z > 0$, one obtains (3.51) restricted to the half plane $z > 0$. The domain D_{EF} is thus isometric to the subdomain $\mathcal{U}|_{z>0}$, which does not contain $r = 2\lambda M$.

Second, the change $\{\tilde{\tau}, \tilde{\rho}\} \to \{\tilde{t}, \tilde{r}\}$ defined by $\tilde{\rho} = \tilde{r}$ and

$$\tilde{t} = \tau + 2\sqrt{2M}\sqrt{\tilde{r} - 2\lambda M} + \frac{2M}{\sqrt{1-\lambda}} \log\left(\frac{\sqrt{2M}\sqrt{1-\lambda} - \sqrt{\tilde{r} - 2\lambda M}}{\sqrt{2M}\sqrt{1-\lambda} + \sqrt{\tilde{r} - 2\lambda M}}\right), \tag{3.52}$$

which is valid only for $\tilde{\rho} = \tilde{r} > 2M$, transforms (3.44) into (3.14), and the subdomain $D_{EF}|_{\tilde{\rho}>2M}$ is therefore isometric to D_S. As a result, D_{EF} completely covers D_S and, in turn, $\mathcal{U}$ completely covers D_{EF}. That is, $D_S \subset D_{EF} \subset \mathcal{U}$.

3.2 Global structure

In this section, we will analyse in detail the spherically symmetric spacetime solution $(\mathcal{M}, g)$. Recall we have a chart $\Psi^{\mathcal{U}}_{\tau z} = \{\tau, z\}$ defined over the domain $\mathcal{U} \subset \mathcal{M}$, where the line element is given by (3.51) and the area-radius function $r(z)$ satisfies (3.49). The domain $\mathcal{U}$ is foliated by the level surfaces of τ, which are spacelike hypersurfaces, and we take the unit normal (1.1) as the representative of the future-pointing direction on $\mathcal{U}$. In these coordinates,

$$n^\mu \partial_\mu = -(N \nabla^\mu \tau)\partial_\mu = \partial_\tau - \sqrt{\frac{2M}{r}}\partial_z. \tag{3.53}$$

Looking for the global structure of $(\mathcal{U}, g)$, we will first produce appropriate coordinate transformations from (τ, z) to null coordinates so that the metric takes a conformally flat form on the (τ, z) plane. On the way, we will show that $\mathcal{U}$ covers any static D_S, homogeneous D_h and D_H, and Eddington-Finkelstein D_{EF} regions. More precisely, the procedure will show that $\mathcal{U}$ contains exactly one globally hyperbolic interior homogeneous domain, isometric to a region D_H, and two static exterior regions, both isometric to a region D_S. The study will end by obtaining the maximal analytic extension of the solution.

Before continuing, we define the relevant subsets of $\mathcal{U}$ by taking their restrictions under the values of the area-radius function r on $\mathcal{M}$. In the following, for any set $D \subset \mathcal{U}$, we will also use the name D for the image of that domain on $\mathbb{R}^2$ under any chart. In addition, we introduce the auxiliary variable σ, with possible values $+1$ and -1, or just $+$ and $-$ when used as a subindex. Since $r(z) = r(-z)$, we define two non-intersecting subsets of D as $D_\sigma := D|_{\mathrm{sgn}(z)=\sigma}$.

Recall that $r_0 = 2\lambda M$ by definition. We will use r_0 to emphasise that we refer to the positive lower bound of the area-radius function, but we will keep $2\lambda M$ in the metric.

First, we define the following subsets of $\mathcal{U}$,

- $E := \{r > 2M\} \cap \mathcal{U}$,
- $\mathcal{Z} := \{r = 2M\} \cap \mathcal{U}$,
- $I := \{r < 2M\} \cap \mathcal{U}$,
- $\mathcal{T} := \{r = r_0\} \cap \mathcal{U}$.

Splitting now the above sets by restricting them under the sign of z, we find

- $E = E_+ \cup E_-$,
- $\mathcal{Z} = \mathcal{Z}_+ \cup \mathcal{Z}_-$,
- $I = I_+ \cup \mathcal{T} \cup I_-$.

We see that I is a connected domain in $\mathcal{U}$, mapped by the chart $\Psi^{\mathcal{U}}_{\tau z}$ to the stripe $(-z_s, z_s)$ in $\mathbb{R}^2$, with z_s being the positive root of $r(z_s) = 2M$. The other two regions, E and $\mathcal{Z}$, are disconnected, with E_+ corresponding to $z \in (z_s, \infty)$, E_- to $z \in (-\infty, -z_s)$, $\mathcal{Z}_+$ to $z = z_s$, and $\mathcal{Z}_-$ to $z = -z_s$. As anticipated by their names, the domains E and I will correspond to the "exterior and interior regions of the black hole", respectively. They are separated by the null hypersurfaces $\mathcal{Z}$, standing for the horizon, and the connected set $\mathcal{T}$ mapped to $z = 0$ denotes the transition surface that, as we will show, replaces the central singularity.

3.2.1 Radial geodesics

The radial geodesics of the metric (3.51), parametrised as $\big(\tau(s), z(s)\big)$, are determined by

$$\gamma = -\left(1 - \frac{2M}{r(z)}\right)\left(\frac{d\tau}{ds}\right)^2 + 2\sqrt{\frac{2M}{r(z)}}\frac{d\tau}{ds}\frac{dz}{ds} + \left(\frac{dz}{ds}\right)^2, \tag{3.54a}$$

$$\mathcal{E} = -\left(1 - \frac{2M}{r(z)}\right)\frac{d\tau}{ds} + \sqrt{\frac{2M}{r(z)}}\frac{dz}{ds}, \tag{3.54b}$$

with s the affine parameter, $\gamma = 0, 1, -1$ for null, spacelike and timelike geodesics, respectively, and $\mathcal{E}$ the conserved quantity associated with the timelike Killing vector field ∂_τ (i.e., the energy). These two equations may be combined to remove $d\tau/ds$, and obtain

$$\left(\frac{dz}{ds}\right)^2 = \mathcal{E}^2 + \gamma\left(1 - \frac{2M}{r(z)}\right). \tag{3.55}$$

In order to find the transformations to null coordinates, we focus on the case $\gamma = 0$. When $\mathcal{E} \neq 0$, the affine parameter is proportional to the coordinate z, and we choose $dz/ds = \varepsilon$,

with $\varepsilon = \pm 1$. The two possible values of ε produce the "outgoing" and "ingoing" geodesic vectors,

$$l^\mu \partial_\mu = \left(1 + \sqrt{\frac{2M}{r}}\right)^{-1} \partial_\tau - \partial_z, \tag{3.56a}$$

$$k^\mu \partial_\mu = \left(1 - \sqrt{\frac{2M}{r}}\right)^{-1} \partial_\tau + \partial_z. \tag{3.56b}$$

Observe that $l^\mu \partial_\mu$ is future-pointing everywhere ($n_\mu l^\mu < 0$), while $k^\mu \partial_\mu$ is future-pointing on E (with $n_\mu k^\mu < 0$), past-pointing on I (with $n_\mu k^\mu > 0$), and it is not defined at $r = 2M$. In the case $\mathcal{E} = 0$, $d\tau/ds$ cannot be vanishing, and the radial geodesics lie on the horizon (they are parametrised as $z = \pm z_s$). Their tangent vector, $\partial_\tau|_{r=2M}$, is null there.

Clearly, null radial geodesics with $\mathcal{E} \neq 0$ take a finite amount of affine parameter to cross the interior domain I. It will be further checked (see Sec. 3.3.1) that timelike curves also take a finite amount of proper time when going from $z = z_s$ to $z = -z_s$.

3.2.2 Null coordinates

The affine parametrisation implies that the one-forms associated with $l^\mu \partial_\mu$ and $k^\mu \partial_\mu$ are exact, and we can use the former to define coordinates all over $\mathcal{U}$. With this in mind, we perform the change $(\tau, z) \to (U, X)$, defined by $dX := dz$ and

$$dU := -l_\mu dx^\mu = d\tau + \left(1 + \sqrt{\frac{2M}{r(z)}}\right)^{-1} dz. \tag{3.57}$$

More precisely, the new coordinate U is determined from

$$\frac{\partial U}{\partial \tau} = 1, \tag{3.58a}$$

$$\frac{\partial U}{\partial z} = \left(1 + \sqrt{\frac{2M}{r(z)}}\right)^{-1}. \tag{3.58b}$$

Using now relation (3.49), we find that U in terms of τ and z reads

$$U(\tau, z) = \tau + \mathrm{sgn}(z) R_U\big(r(z)\big), \tag{3.59}$$

where the auxiliary function R_U is the integral

$$R_U(r) = \int_{r_0}^{r} \left(\sqrt{1 - \frac{2\lambda M}{s}}\left(1 + \sqrt{\frac{2M}{s}}\right)\right)^{-1} ds. \tag{3.60}$$

Note that R_U vanishes at r_0, i.e., $R_U(r_0) = R_U\big(r(0)\big) = 0$, and it provides a function $U(\tau, z)$ that is analytic on the whole plane $(\tau, z) \in \mathbb{R}^2$. We can explicitly perform the above integral,

$$\begin{aligned} R_U(r) =& \frac{4M}{\sqrt{1-\lambda}} \log\left(\sqrt{\lambda}\frac{\sqrt{r-2\lambda M}+\sqrt{2M}\sqrt{1-\lambda}}{\sqrt{r-2\lambda M}+\sqrt{r}\sqrt{1-\lambda}}\right) \\ &+ \left(\sqrt{r}-2\sqrt{2M}\right)\sqrt{r-2\lambda M} + 2M(1+\lambda)\log\left(\sqrt{\frac{r}{2\lambda M}}+\sqrt{\frac{r}{2\lambda M}-1}\right). \end{aligned} \tag{3.61}$$

and check that $\lim_{r\to\infty} R_U(r)/r = 1$. Furthermore, $R_U(r)$ is strictly increasing. Therefore, the change of coordinates from (τ, z) to (U, X),

$$\Phi^{\mathcal{U}} = \Big\{X(\tau, z) = z, \quad U(\tau, z) = \tau + \mathrm{sgn}(z) R_U(z)\Big\}, \tag{3.62}$$

provides a diffeomorphism from $\mathbb{R}^2$ to $\mathbb{R}^2$, and the new chart $\Psi^{\mathcal{U}}_{UX} = \{U, X\}$, also given by $\Psi^{\mathcal{U}}_{UX} = \Phi^{\mathcal{U}} \circ \Psi^{\mathcal{U}}_{\tau z}$ is defined all over $\mathcal{U}$. The metric (3.51) in that chart reads

$$ds^2 = -\left(1 - \frac{2M}{r(X)}\right) dU^2 + 2dU dX + r(X)^2 d\Omega^2, \tag{3.63}$$

where $r(X)$ is $r(z)$ as given by (3.50), just replacing z by X. This also provides a direct identification with the line element (3.45), showing that the gauge choices $\mathcal{E}^\varphi = 0$ and $E^x = r(x)^2$, with $r(x)$ defined in (3.50), yield the metric in the form (3.63). The hypersurfaces of constant U are clearly null, while those of constant X are timelike on E, null on $\mathcal{Z}$, and spacelike on I.

To produce the Penrose diagram for $\mathcal{U}$, we need to express the metric in the (double) null chart. Therefore, we need to define a second null coordinate V such that it provides, along with U, the line element in a conformally flat form. Just as $l_\mu dx^\mu$ defined U, the one-form $k_\mu dx^\mu$ will define V. However, since it is not defined at $r = 2M$, we need to analyse each disjoint domain E_+, E_-, and I separately.

Exterior domain

We start with the two exterior regions. For each E_σ, we need to construct the diffeomorphism $\widehat{\Phi}_\sigma : (\tau, z)|_{E_\sigma} \to (U_\sigma, V_\sigma)$, where $z|_{E_+} = (z_s, \infty)$ and $z|_{E_-} = (-\infty, -z_s)$, and U_σ is the restriction of (3.59) on E_σ, that is, $U_\sigma = U|_{E_\sigma}$ or, explicitly,

$$U_\sigma(\tau, z) = \tau + \sigma R_U(r(z)). \tag{3.64}$$

In addition, we define V_σ on each E_σ as

$$dV_\sigma := -k_\mu dx^\mu|_{E_\sigma} = d\tau - \left(1 - \sqrt{\frac{2M}{r(z)}}\right)^{-1} dz|_{E_\sigma}. \tag{3.65}$$

We can directly integrate this relation, and we find

$$V_\sigma(\tau, z) = \tau - \sigma R_V^{(E)}(r(z)), \tag{3.66}$$

where

$$R_V^{(E)}(r) = \int \left(\sqrt{1 - \frac{2\lambda M}{r}}\left(1 - \sqrt{\frac{2M}{r}}\right)\right)^{-1} dr + C_V. \tag{3.67}$$

A convenient choice of the integration constant C_V yields

$$\begin{aligned} R_V^{(E)}(r) =& \frac{4M}{\sqrt{1-\lambda}} \log\left(\sqrt{\lambda}\frac{\sqrt{r-2\lambda M} - \sqrt{2M}\sqrt{1-\lambda}}{\sqrt{r-2\lambda M} + \sqrt{r}\sqrt{1-\lambda}}\right) \\ &+ \left(\sqrt{r} + 2\sqrt{2M}\right)\sqrt{r-2\lambda M} + 2M(2+\lambda)\log\left(\sqrt{\frac{r}{2\lambda M}} + \sqrt{\frac{r}{2\lambda M} - 1}\right), \end{aligned} \tag{3.68}$$

which is analytic and strictly increasing in its domain of definition $r \in (2M, \infty)$. This can be clearly seen in (3.67), where the integrand is regular and positive on the whole domain. The limits $\lim_{r\to\infty} R_V^{(E)}(r)/r = 1$ and $\lim_{r\to 2M} R_V^{(E)}(r) = -\infty$ are also straightforward to check. Therefore, each diffeomorphism $\widehat{\Phi}_\sigma$ maps the half plane $r \in (2M, \infty) \in \mathbb{R}^2$ to the whole real plane, and the images of the charts $\widehat{\Psi}_\sigma^E = \{U_\sigma, V_\sigma\}$, given by $\widehat{\Psi}_\sigma^E = \widehat{\Phi}_\sigma \circ \Psi_{\tau z}^{\mathcal{U}}|_{E_\sigma}$, cover $\mathbb{R}^2$.

Regarding the asymptotic structure, null infinity $\mathcal{J}$ is reached as $r \to \infty$ (thus as $z \to \pm\infty$). Considering the different orientations of $l^\mu\partial_\mu$ and $k^\mu\partial_\mu$ on each E_σ, we find:

- On E_+, $\mathcal{J}^+$ is reached as $U_+ \to +\infty$ with fixed V_+.
- On E_+, $\mathcal{J}^-$ is reached as $V_+ \to -\infty$ with fixed U_+.
- On E_-, $\mathcal{J}^+$ is reached as $V_- \to +\infty$ with fixed U_-.
- On E_-, $\mathcal{J}^-$ is reached as $U_- \to -\infty$ with fixed V_-.

In addition, spatial infinity i^0 is reached as $|z| \to \infty$ with fixed τ, i.e., for $(U_+, V_+) \to (\infty, -\infty)$ on E_+ and for $(U_-, V_-) \to (-\infty, \infty)$ on E_-. Finally, timelike infinities $i^\pm$ are reached as $\tau \to \pm\infty$ with fixed z, and correspond to $(U_\sigma, V_\sigma) \to (\pm\infty, \pm\infty)$, respectively.

Interior domain

We now turn our attention to I. In order to construct the change $\widehat{\Phi}^I : (\tau, z)|_I \to (U^I, V^I)$, with $z|_I = (-z_s, z_s)$, we define U^I as the restriction of (3.59) to the domain under consideration,

$$U^I(\tau, z) := U|_I = \tau + \mathrm{sgn}(z) R_U(r(z)), \tag{3.69}$$

while we demand V^I to satisfy

$$dV^I = k_\mu dx^\mu|_I = -d\tau + \left(1 - \sqrt{\frac{2M}{r(z)}}\right)^{-1} dz|_I. \tag{3.70}$$

Note the different sign when comparing this expression with (3.65). This choice was taken because the null vector field $k^\mu \partial_\mu$ is past-pointing on I. We thus have that

$$V^I(\tau, z) = -\tau + \mathrm{sgn}(z) R_V^{(I)}(r(z)), \tag{3.71}$$

on I, with $R_V^{(I)}(r)$ given by

$$R_V^{(I)}(r) = \int_{r_0}^{r} \left(\sqrt{1 - \frac{2\lambda M}{s}}\left(1 - \sqrt{\frac{2M}{s}}\right)\right)^{-1} ds, \tag{3.72}$$

so that its domain is $r \in [2\lambda M, 2M)$, and it vanishes at the lower bound, i.e., $R_V^{(I)}(r_0) = 0$. In this way, $V^I(\tau, z)$ is analytic on the whole domain of definition $z \in (-z_s, z_s)$ because

$$\begin{aligned} R_V^{(I)}(r) =& \frac{4M}{\sqrt{1-\lambda}} \log\left(\sqrt{\lambda}\frac{\sqrt{2M}\sqrt{1-\lambda} - \sqrt{r - 2\lambda M}}{\sqrt{r - 2\lambda M} + \sqrt{r}\sqrt{1-\lambda}}\right) \\ &+ \left(\sqrt{r} + 2\sqrt{2M}\right)\sqrt{r - 2\lambda M} + 2M(2+\lambda)\log\left(\sqrt{\frac{r}{2\lambda M}} + \sqrt{\frac{r}{2\lambda M} - 1}\right) \end{aligned} \tag{3.73}$$

is strictly decreasing, with $R_V^{(I)}(r_0) = 0$ and $\lim_{r\to 2M} R_V^{(I)}(r) = -\infty$.

As one approaches $z \to \pm z_s$ for finite τ, the function U^I remains bounded while V^I diverges as $V^I \to \mp\infty$. Also for finite values of τ, the function U^I is bounded, as can be read from the boundedness of $R_U(r)$ on $r \in (2\lambda M, 2M)$, and the limits $U^I \to \pm\infty$ correspond to $\tau \to \pm\infty$, respectively. Therefore, the diffeomorphism $\widehat{\Phi}^I$ maps the stripe $z \in (-z_s, z_s)$ to $\mathbb{R}$, and the chart $\widehat{\Psi}^I = \{U^I, V^I\}$, given by $\widehat{\Psi}^I = \widehat{\Phi}^I \circ \Psi^{\mathcal{U}}_{\tau z}|_I$, thus maps I to the whole real plane.

So far, we have obtained three coordinate changes producing the charts $\widehat{\Psi}^E_\sigma = \{U_\sigma, V_\sigma\}$ and $\widehat{\Psi}^I = \{U^I, V^I\}$. Each of them maps its corresponding disjoint domain to $\mathbb{R}^2$.

Dropping the indices of U and V, the metric in all these charts takes the form

$$ds^2 = -\left|1 - \frac{2M}{r(U,V)}\right| dU dV + r(U,V)^2 d\Omega^2, \tag{3.74}$$

where the area-radius function $r(U,V)$ is implicitly given by

$$\begin{aligned} U_\sigma - V_\sigma &= \sigma(R_U(r) + R_V^{(E)}(r)) \\ &= \sigma\left\{ \frac{4M}{\sqrt{1-\lambda}} \left[\log\left(\frac{r}{2M} - 1\right) - 2\log\left(\sqrt{\frac{r}{2\lambda M} - 1} + \sqrt{1-\lambda}\sqrt{\frac{r}{2\lambda M}}\right) \right] \right. \\ &\quad \left. + 2\sqrt{r}\sqrt{r - 2\lambda M} + 4M(2+\lambda)\log\left(\sqrt{\frac{r}{2\lambda M}} + \sqrt{\frac{r}{2\lambda M} - 1}\right) \right\}, \end{aligned} \tag{3.75}$$

in the exterior E_σ domains, and by

$$\begin{aligned} U^I + V^I &= \mathrm{sgn}(z)(R_U(r) + R_V^{(I)}(r)) \\ &= \mathrm{sgn}(z)\left\{ \frac{4M}{\sqrt{1-\lambda}} \left[\log\left(1 - \frac{r}{2M}\right) - 2\log\left(\sqrt{\frac{r}{2\lambda M} - 1} + \sqrt{1-\lambda}\sqrt{\frac{r}{2\lambda M}}\right) \right] \right. \\ &\quad \left. + 2\sqrt{r}\sqrt{r - 2\lambda M} + 4M(2+\lambda)\log\left(\sqrt{\frac{r}{2\lambda M}} + \sqrt{\frac{r}{2\lambda M} - 1}\right) \right\}, \end{aligned} \tag{3.76}$$

in the interior I domain.

Both combinations $R_U + R_V^{(E)}$ and $R_U + R_V^{(I)}$ satisfy the differential equation

$$\frac{1}{2}\frac{d(R_U + R_V)}{dr} = \left(1 - \frac{2\lambda M}{r}\right)^{-1/2} \left(1 - \frac{2M}{r}\right)^{-1} \tag{3.77}$$

on their domains of definition, where we have removed the superindices $^{(E)}$ and $^{(I)}$. It is straightforward to see that the combination $R_U + R_V^{(I)}$ is a strictly decreasing function of r on its domain $(2\lambda M, 2M)$, with $\left(R_U(r) + R_V^{(I)}(r)\right)|_{r=2\lambda M} = 0$, and it is thus negative. Therefore, $\mathrm{sgn}(U^I + V^I) = -\mathrm{sgn}(z)$. Conversely, $R_U + R_V^{(E)}$ is strictly increasing on $r \in (2M, \infty)$, and its image covers the real line. It is interesting to point out that the above differential equation defines the tortoise coordinate of the modified geometry, and we conveniently denote

$$r_* := \frac{1}{2}\left(R_U + R_V^{(E)}\right), \tag{3.78}$$

on E, which reduces to the usual tortoise coordinate in the GR limit,

$$\lim_{\lambda \to 0} r_* = r + 2M\log\left(\frac{r}{2M} - 1\right). \tag{3.79}$$

3.2.3 Conformal compactification

In this section, we proceed to find a convenient compactification for each of the three charts $\widehat{\Psi}^E_\sigma$ and $\widehat{\Psi}^I$ by following the standard procedure (see, e.g., Ref. [90]).

Compactification of the exterior domain

For the two exterior regions E_σ, we perform the changes $\Theta_\sigma : \{U_\sigma, V_\sigma\} \to \{u_\sigma, v_\sigma\}$, with

$$\Theta_\sigma = \left\{ \begin{array}{l} u_\sigma = \sigma \arctan\exp\left[\dfrac{\sigma}{4M}\sqrt{1-\lambda}\,U_\sigma\right], \\ \\ v_\sigma = -\sigma \arctan\exp\left[-\dfrac{\sigma}{4M}\sqrt{1-\lambda}\,V_\sigma\right] \end{array} \right\}. \tag{3.80}$$

These maps take $\mathbb{R}^2$ to the (open) squares $A_+ := \{(u_+, v_+); u_+ \in (0, \pi/2), v_+ \in (-\pi/2, 0)\}$ and $A_- := \{(u_-, v_-); u_- \in (-\pi/2, 0), v_- \in (0, \pi/2)\}$, for the corresponding value of σ. The metric in each chart $\Psi^E_\sigma = \{u_\sigma, v_\sigma\}$, given by $\Psi^E_\sigma = \Theta_\sigma \circ \widehat{\Psi}^E_\sigma$, reads

$$ds^2 = \frac{\Gamma\big(r(u_\sigma, v_\sigma)\big)}{\cos^2 u_\sigma \cos^2 v_\sigma} du_\sigma dv_\sigma + r(u_\sigma, v_\sigma)^2 d\Omega^2, \tag{3.81}$$

with

$$\begin{aligned} \Gamma(r) :=& -\frac{16M^2}{1-\lambda}\left(1-\frac{2M}{r}\right)\exp\left[-\frac{\sqrt{1-\lambda}}{2M}\,r_*(r)\right] \\ =& -\frac{32M^3}{(1-\lambda)r}\left(\sqrt{1-\frac{2\lambda M}{r}}+\sqrt{1-\lambda}\right)^2 \exp\left[-\frac{\sqrt{1-\lambda}}{2M}\sqrt{1-\frac{2\lambda M}{r}}\,r\right] \\ &\times\left(1+\sqrt{1-\frac{2\lambda M}{r}}\right)^{-\sqrt{1-\lambda}(2+\lambda)} \sqrt{\frac{2\lambda M}{r}}^{\sqrt{1-\lambda}(2+\lambda)-2}, \end{aligned} \tag{3.82}$$

and where $r = r(u_\sigma, v_\sigma)$ is implicitly determined by

$$\Upsilon(r) := -\exp\left[\frac{\sqrt{1-\lambda}}{2M}\,r_*(r)\right] = \tan u_\sigma \tan v_\sigma. \tag{3.83}$$

It is important to point out that, although we have obtained the functions $\Gamma(r)$ and $\Upsilon(r)$ only on E, definition (3.82), and thus (3.83), can be trivially extended all over $\mathcal{U}$ because they are valid for $r \in [r_0, \infty)$, as it will be shown in the next section. A direct computation yields

$$\Gamma\Upsilon = \frac{16M^2}{1-\lambda}\left(1-\frac{2M}{r}\right), \tag{3.84a}$$

$$1 = \sqrt{1-\lambda}\sqrt{1-\frac{2\lambda M}{r}}\,\frac{\Gamma}{8M}\,\frac{d\Upsilon}{dr}. \tag{3.84b}$$

Since the function $\Gamma(r)$ is always negative, we conclude from (3.84b) that $\Upsilon(r)$ is a strictly decreasing function. In addition, we see in (3.84a) that $\Upsilon(2M) = 0$. As a result, $\Upsilon(r)$ is positive for $r \in [2\lambda M, 2M)$ and negative for $r \in (2M, \infty)$.

To see the explicit analogy with GR, we take the limit

$$\lim_{\lambda \to 0} \Gamma(r) = -\frac{32M^3}{r} e^{-r/2M}, \tag{3.85}$$

which yields (3.81) into the usual Kruskal-Szekeres line element of Schwarzschild.

Given relation (3.83), it is easy to see that the sets of constant r have a one-to-one correspondence with the constant values of the product $\tan u_\sigma \tan v_\sigma$, which is negative in both exterior regions ($r > 2M$) for both σ. The horizon, located at $r = 2M$, corresponds to the limit $\tan u_\sigma \tan v_\sigma = 0$, that is, to the boundaries $u_\sigma = 0$ and $v_\sigma = 0$ of the open squares $A_\pm$ that are the image of the charts Ψ^E_σ given above (see Fig. 3.1).

As done before, we find the following characterisations of the null infinities in terms of (u_σ, v_σ):

- On A_+, $\mathcal{J}^+$ corresponds to the segment $u_+ = \pi/2$.
- On A_+, $\mathcal{J}^-$ corresponds to the segment $v_+ = -\pi/2$.
- On A_-, $\mathcal{J}^+$ corresponds to the segment $v_- = \pi/2$.
- On A_-, $\mathcal{J}^-$ corresponds to the segment $u_- = -\pi/2$.

The spatial infinity i^0 is the point $(u_+, v_+) = (\pi/2, -\pi/2)$ on A_+ and $(u_-, v_-) = (-\pi/2, \pi/2)$ on A_-. The future timelike infinity i^+ is located at $(u_+, v_+) = (\pi/2, 0)$ and $(u_-, v_-) = (0, \pi/2)$ on A_+ and A_-, respectively. The past timelike infinity i^- corresponds to $(u_+, v_+) = (0, -\pi/2)$ on A_+ and to $(u_-, v_-) = (-\pi/2, 0)$ on A_-.

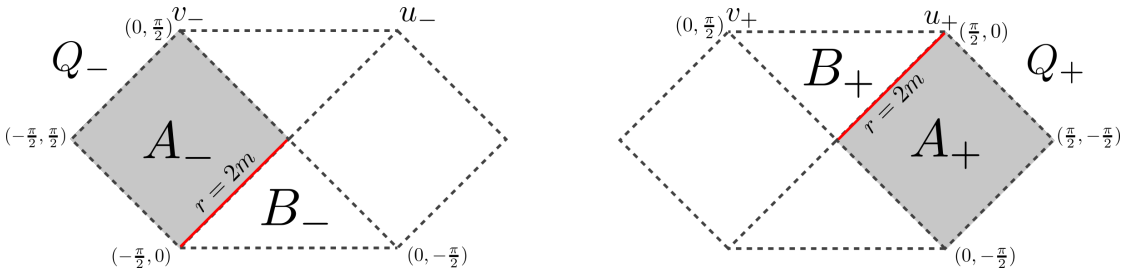

Figure 3.1: Penrose diagrams of E_- and E_+ through the charts Ψ^E_σ. The extensions (dotted lines) correspond to Q_- and Q_+, the images of the extended charts $\Psi^{\mathcal{V}_\sigma}$ (see Sec. 3.2.4).

On each exterior region E_σ, the full change of coordinates from $(\tau, z)|_{E_\sigma}$ to (u_σ, v_σ), defined as $\Phi_\sigma := \Psi^E_\sigma \circ (\Psi^{\mathcal{U}}_{\tau z})^{-1}|_{E_\sigma} = \Theta_\sigma \circ \widehat{\Phi}_\sigma$, reads

$$\Phi_\sigma = \left\{ \begin{array}{l} u_\sigma = \sigma \arctan \exp \left[\dfrac{\sqrt{1-\lambda\!\!\!^{-}}}{4M} \Big(\sigma\tau + R_U\big(r(z)\big) \Big) \right], \\ \\ v_\sigma = -\sigma \arctan \exp \left[\dfrac{\sqrt{1-\lambda\!\!\!^{-}}}{4M} \Big(-\sigma\tau + R^{(E)}_V\big(r(z)\big) \Big) \right] \end{array} \right\}. \tag{3.86}$$

By computing the product of the vector fields ∂_{u_σ} and ∂_{v_σ} with $n^\mu \partial_\mu$, one can check that the above maps preserve the time orientation. This concludes the construction of the Penrose diagram for the regions E_σ (see Fig.3.1). Both are asymptotically flat in the sense that their compactified domains A_σ have the same boundary structure (at infinity) as Minkowski.

As we anticipated at the beginning of the section, it is now straightforward to check that the change $(\tau, z)|_{E_\sigma} \to (\tilde{t}, \tilde{r})$, given by

$$\tilde{r} = \tilde{r}(z), \tag{3.87a}$$

$$\tilde{t} = \tau + \frac{\sigma}{2} \Big(R_U\big(r(z)\big) - R^{(E)}_V\big(r(z)\big) \Big), \tag{3.87b}$$

transforms the line element (3.51), restricted to $r > 2M$, into (3.14), showing that both E_+ and E_- are isometric to D_S. Therefore, the domain $\mathcal{U}$ covers two regions that are isometric to a static domain D_S.

Compactification of the interior domain

We now turn our attention to the interior domain I. A convenient compact form of the chart $\widehat{\Psi}^I$ is given by $\Theta^I : (U^I, V^I) \to (\bar{u}, \bar{v})$ such that

$$\Theta^I = \left\{ \bar{u} = \tanh\left(\sqrt{1-\lambda\!\!\!^{-}}\, \frac{U^I}{8M} \right), \quad \bar{v} = \tanh\left(\sqrt{1-\lambda\!\!\!^{-}}\, \frac{V^I}{8M} \right) \right\}. \tag{3.88}$$

This map takes the whole real plane that is the image of I under the chart $\widehat{\Psi}^I$ to the open square $C := \{(\bar{u}, \bar{v}); \bar{u}, \bar{v} \in (-1, 1)\}$.

The metric in the chart $\Psi^I = \{\bar{u}, \bar{v}\}$, given by $\Psi^I = \Theta^I \circ \widehat{\Psi}^I = \Theta^I \circ \widehat{\Phi}^I \circ \Psi^{\mathcal{U}}_{\tau z}|_I$, is

$$ds^2 = -\frac{64M^2}{1-\lambda\!\!\!^{-}} \left(\frac{2M}{r(\bar{u}, \bar{v})} - 1 \right) \frac{1}{(1-\bar{u}^2)(1-\bar{v}^2)} d\bar{u} d\bar{v} + r(\bar{u}, \bar{v})^2 d\Omega^2, \tag{3.89}$$

with $r(\bar{u}, \bar{v})$ satisfying

$$-\left| \frac{\bar{u} + \bar{v}}{1 + \bar{u}\bar{v}} \right| = \tanh\left[\frac{\sqrt{1-\lambda\!\!\!^{-}}}{8M} \Big(R_U(r) + R^{(I)}_V(r) \Big) \right], \tag{3.90}$$

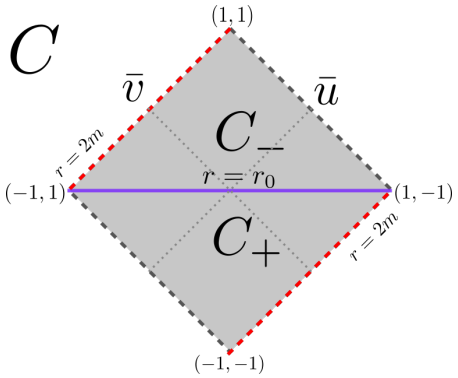

Figure 3.2: Penrose diagram of the domain I under the chart $\widehat{\Psi}^I$.

and where R_U and $R_V^{(I)}$ are given in (3.61) and (3.73), respectively. Let us study some properties of these coordinates. First, $R_U(r_0) = 0$ and $R_V^{(I)}(r_0) = 0$, so the curve $r = r_0$ corresponds to the segment $\bar{u} + \bar{v} = 0$. Second, $\mathrm{sgn}(\bar{u} + \bar{v}) = \mathrm{sgn}(U^I + V^I) = -\mathrm{sgn}(z)$, and the curves of constant $r \in (r_0, 2M)$ satisfy $\bar{u}\bar{v} < 1$. There are thus two curves of constant r going from $(\bar{u}, \bar{v}) = (-1, 1)$ to $(\bar{u}, \bar{v}) = (1, -1)$: one through positive values of $\bar{u} + \bar{v}$ and the other through negative values of $\bar{u} + \bar{v}$, that is, one for each sign of z. Then, we can take each C_σ to be the image of Ψ^I under the corresponding restriction of the sign of z. Explicitly, $\Psi^I|_{I_\sigma} : I_\sigma \to C_\sigma$, which are given by $C_+ = \{C \,|\, \bar{u} + \bar{v} < 0\}$ and $C_- = \{C \,|\, \bar{u} + \bar{v} > 0\}$.

Recall now that as $r \to 2M$, the function R_U remains bounded while $R_V^{(I)} \to -\infty$ for finite values of τ. This is achieved for a bounded $\bar{u}$ and $\bar{v} \to -\mathrm{sgn}(z)$, and, as a result, $\mathcal{Z}_+$ and $\mathcal{Z}_-$ are part of the boundary of C, and correspond to $\bar{v} = -1$ and $\bar{v} = +1$, respectively, with $\bar{u} \in (-1, 1)$. Similarly, the limits $\tau \to \pm\infty$ are located at $\bar{u} = \pm 1$ (see Fig.3.2).

The full change of coordinates $\Phi^I := \Psi^I \circ (\Psi^{\mathcal{U}}_{\tau z})^{-1}|_I = \Theta^I \circ \widehat{\Phi}^I : (\tau, z)|_I \to (\bar{u}, \bar{v})$, reads

$$\Phi^I = \left\{ \begin{array}{l} \bar{u} = \tanh\left[\dfrac{\sqrt{1-\lambda}}{8M}\Big(\tau + \mathrm{sgn}(z) R_U\big(r(z)\big)\Big)\right], \\ \bar{v} = \tanh\left[\dfrac{\sqrt{1-\lambda}}{8M}\Big(-\tau + \mathrm{sgn}(z) R_V^{(I)}\big(r(z)\big)\Big)\right] \end{array} \right\}. \tag{3.91}$$

The products of $\partial_{\bar{u}}$ and $\partial_{\bar{v}}$ with the unit normal $n^\mu \partial_\mu$ are negative on I, showing that these two vector fields are future-pointing. In other words, Φ^I preserves the time orientation.

The coordinate transformation $\{\tau, z\}|_I \to \{\overline{T}, \overline{X}\}$ is now given by

$$r(\overline{T}) = r(z) \tag{3.92a}$$

$$\tau = \overline{X} - \frac{\mathrm{sgn}(z)}{2}\Big(R_U\big(r(\overline{T})\big) - R_V^{(I)}\big(r(\overline{T})\big)\Big) \tag{3.92b}$$

with $r(\overline{T})$ given by relation (3.34). More explicitly,

$$\tau = \overline{X} - \frac{4M}{\sqrt{1-\lambda}}\operatorname{artanh}\left[\sqrt{\frac{r(\overline{T})}{2M}}\cos\overline{T}\right] + 4M\sqrt{1-\lambda}\sqrt{\frac{r(\overline{T})}{2M}}\cos\overline{T}, \tag{3.93a}$$

$$z = 2\lambda M \operatorname{artanh}\left[\sqrt{1-\lambda}\cos\overline{T}\right] + \frac{r(\overline{T})\cos\overline{T}}{2M\sqrt{1-\lambda}}, \tag{3.93b}$$

which implies $\operatorname{sgn}(z) = \operatorname{sgn}(\cos\overline{T})$. This diffeomorphism between the stripes $z \in (-z_s, z_s)$ and $\overline{T} \in (0,\pi)$ on $\mathbb{R}^2$ transforms the metric (3.51) into the form (3.35), showing that the region $I \subset \mathcal{U}$ is isometric to a homogeneous domain D_H. In addition, $\mathcal{Z}_+$, $\mathcal{Z}_-$, and $\mathcal{T}$ correspond to $z = z_s$ or $\overline{T} = 0$, $z = -z_s$ or $\overline{T} = \pi$, and $z = 0$ or $\overline{T} = \pi/2$, respectively.

Finally, the change $(\tau, z)|_{I_\sigma} \to (T, X)$ on each interior domain I_σ, which is given by

$$T = r(z), \tag{3.94a}$$

$$X = \tau + \frac{\sigma}{2}\left(R_U\big(r(z)\big) - R_V^{(I)}\big(r(z)\big)\right), \tag{3.94b}$$

brings (3.51), on each I_σ, to the form (3.28). Therefore, I and $\mathcal{U}$ cover two interior regions isometric to D_h. We must be careful with these transformations because whereas the change for $\sigma = 1$ preserves the time orientation, the change for $\sigma = -1$ does not.

3.2.4 Maximal analytic extension

Up to this point, we have constructed the Penrose diagram of the disjoint domains E_σ and I. On the way, we have shown that both E_σ are isometric to a static domain D_S, that each one of I_σ is isometric to a homogeneous region D_h, and that the connected domain $I = I_+ \cup \mathcal{T} \cup I_-$ is isometric to the full homogeneous domain D_H. To obtain now the complete diagram for $\mathcal{U}$, and also its maximal analytic extension, we need to extend the compactified charts of E_σ.

As already commented above, we can do this because $\Gamma(r)$ and $\Upsilon(r)$, defined in (3.82) and (3.83), respectively, are valid all over $r \in [r_0, \infty)$. Given their properties, $\Upsilon(r) = \tan u_\sigma \tan v_\sigma$ has a solution $r(u_\sigma, v_\sigma)$ for all pairs (u_σ, v_σ) on $\mathbb{R}^2$ that satisfy $r \geq r_0$. Since $\Upsilon(r_0) = 1$, then, necessarily, $(u_\sigma + v_\sigma)|_{r=r_0} = \pm\pi/2$, and since $\Upsilon(2M) = 0$, we can extend the domains of the charts Ψ_σ^E across the segments $r = 2M$ in the plane (u_σ, v_σ). The extended domains $\mathcal{V}_\sigma \subset M$ are the preimages of two charts $\Psi^{\mathcal{V}_\sigma} : \mathcal{V}_\sigma \to Q_\sigma \subset \mathbb{R}^2$, where $Q_\sigma = \{(u_\sigma, v_\sigma); u_\sigma, v_\sigma \in (-\pi/2, \pi/2), |u_\sigma + v_\sigma| < \pi/2\}$. The boundaries $|u_\sigma + v_\sigma| = \pi/2$ correspond to the points $r = r_0$, as stated above. It turns convenient to define the open triangles $B_\sigma \subset Q_\sigma$ such that $B_+ := \{(u_+, v_+); u_+, v_+ \in (0, \pi/2), u_+ + v_+ < \pi/2\}$ and $B_- := \{(u_-, v_-); u_-, v_- \in (-\pi/2, 0), u_- + v_- > -\pi/2\}$. This is depicted in Fig. 3.1.

Now, we need to identify the relevant parts of the extensions of E_σ with some region of I. In particular, we request that $\mathcal{V}_\sigma \cap I = I_\sigma$, so that the Penrose diagram for $\mathcal{U}$ consists of the conformal diagram for I patched to the exterior part of the diagrams for $\mathcal{V}_+$ and $\mathcal{V}_-$ (see Fig. 3.4). With exterior we refer to regions where $r > 2M$. This identification is done through the diffeomorphisms $\Lambda_\sigma : C_\sigma \to B_\sigma$, defined by

$$\Lambda_\sigma = \left\{ u_\sigma = \sigma \arctan\left(\frac{1+\bar{u}_\sigma}{1-\bar{u}_\sigma}\right)^\sigma, \quad v_\sigma = \sigma \arctan\left(\frac{1+\bar{v}_\sigma}{1-\bar{v}_\sigma}\right)^\sigma \right\}, \tag{3.95}$$

where $\bar{u}_\sigma := \bar{u}|_{I_\sigma}$ and $\bar{v}_\sigma := \bar{v}|_{I_\sigma}$. We now build the charts $\Psi^{\mathcal{V}_\sigma}$ as $\Psi^{\mathcal{V}_\sigma}(p) = \Lambda_\sigma \circ \Psi^I(p)$ for any $p \in I_\sigma$, and, by construction, the coordinate transformations from the charts $\Psi^I|_{I_\sigma}$ to $\Psi^{\mathcal{V}_\sigma}|_{I_\sigma}$ are described by Λ_σ. In this way, the image of I_σ is the corresponding B_σ.

Regarding the horizons $\mathcal{Z}_\sigma$, they are clearly included by continuity in the domains $\mathcal{V}_\sigma$, and we can extend the chart Ψ^I to include these sets by mapping them to $\bar{v} = -\sigma$ at the boundary of C. Defining the diffeomorphisms Λ_σ as (3.95), plus the relations $\{v_\sigma = \sigma\pi/2 \Leftrightarrow \bar{v}_\sigma = -\sigma\}$, we see that they are mapped to the corresponding boundaries of B_σ.

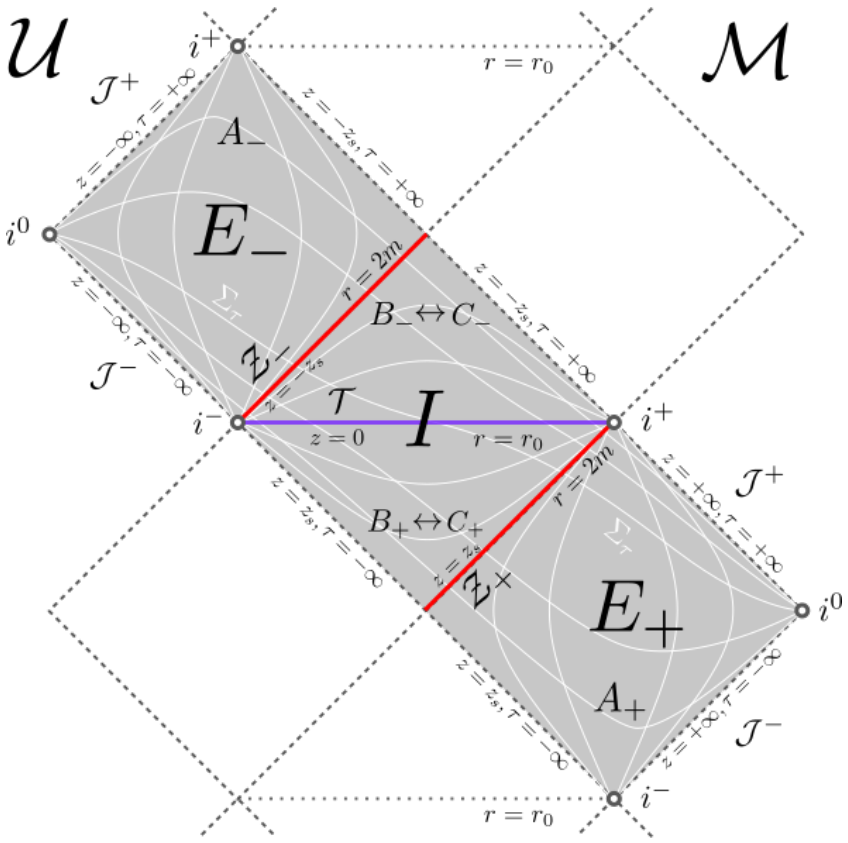

Figure 3.3: Penrose diagram of $(\mathcal{U}, g)$ (shaded), and the maximal extension $(\mathcal{M}, g)$ (outlined). The curves of constant z and constant τ are drawn in white. The latter denote the hypersurfaces Σ_τ, going from i^0 to i^0.

With all the above, we have ended the construction of the Penrose diagram for the domain $\mathcal{U}$, depicted in Fig. 3.3, and shown that it covers exactly one homogeneous region D_H and two static regions D_S.

To end this section, we consider the Kruskal-Szekeres-type extensions Q_σ to analytically extend $\mathcal{U}$ to the two domains $\mathcal{V}_\sigma$. Any such domain constitutes the fundamental domain of the maximal analytic extension $\mathcal{M}$, which is built following the usual periodic construction. Finally, given that the boundary of the Penrose diagram for $\mathcal{M}$ is completely composed by sets of the type i^0, $i^\pm$, and $\mathcal{J}^\pm$, we conclude that $\mathcal{M}$ is geodesically complete.

3.2.5 Conformally flat line elements from phase space

A final consistency check of the model is to see that the above expressions for the metric solve Hamilton's equations. With that in mind, let us search for a metric of the form

$$ds^2 = \Psi(u,v)dudv + r(u,v)^2 d\Omega^2. \tag{3.96}$$

In the Hamiltonian formulation, which is based on a $3+1$ decomposition, it is convenient to find instead

$$ds^2 = \Psi(t,x)\left(dt^2 - dx^2\right) + r(t,x)^2 d\Omega^2, \tag{3.97}$$

with $2t = u + v$ and $2x = u - v$. Comparing this with (3.7), the above ansatz translates to $\Psi = -N^2, r = \sqrt{E^x}, N^x = 0$, and

$$\mathcal{E}^\varphi = \varepsilon_5 \sqrt{-\Psi}\, r \sqrt{1 - \frac{2\lambda M}{r}}, \tag{3.98}$$

with $\varepsilon_5^2 = 1$.

The diffeomorphism constraint (3.1a) then fixes K_x,

$$K_x = \frac{\mathcal{E}^{\varphi\prime}\mathcal{K}_\varphi}{2rr'}, \tag{3.99}$$

and we use (3.5) to determine $\mathcal{K}_\varphi$:

$$\cos(\lambda\mathcal{K}_\varphi) = \varepsilon_6 \sqrt{1 - \frac{2\lambda M}{r}} \left(1 - \lambda\left(1 - \left(\frac{rr'}{\mathcal{E}^\varphi}\right)^2\right)\right)^{-1/2}, \tag{3.100}$$

with $\varepsilon_6^2 = 1$.

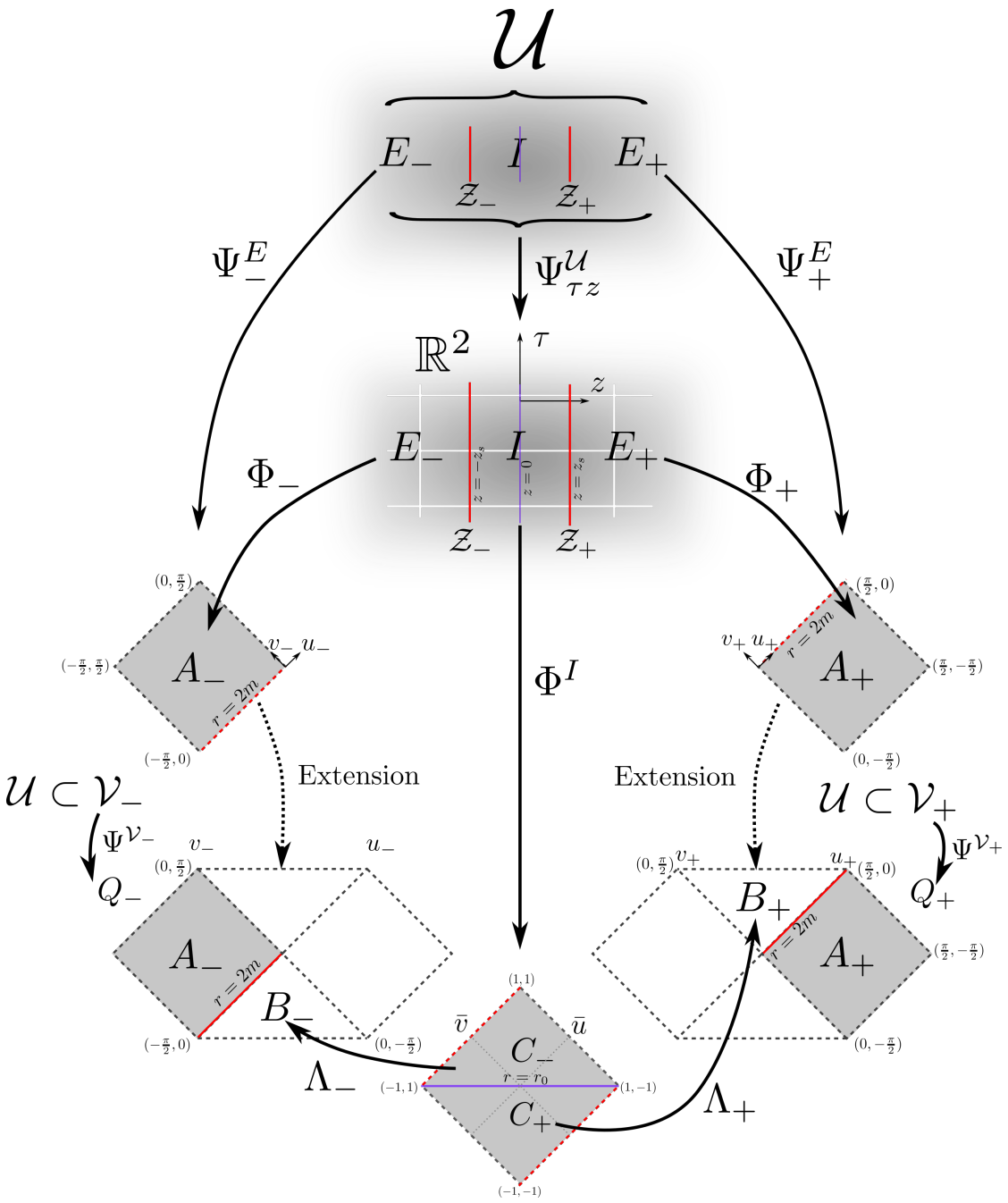

Figure 3.4: Sketch of the construction of the conformal diagram of $(\mathcal{U}, g)$. We first divide the domain $\mathcal{U}$ in subsets (E and I) restricted by the values of the area-radius function r. In addition, we further split them under the sign of the radial coordinate z. We then find the suitable charts that bring E_+, E_-, I_+, and I_- into a compactified form A_+, A_-, C_+, and C_-, respectively. Finally, we identify the convenient extended regions of A_+ and A_- with C_+ and C_-. In this way, we obtain the Penrose diagram as given in Fig. 3.3.

The evolution equations for E^x and E^φ, namely (3.8a) and (3.8b), restrict the form of these functions, and we find an expression for Ψ in terms of r and its first-order derivatives, namely,

$$\Psi(t,x) = \left(1 - \frac{2\lambda M}{r}\right)^{-1} \left(1 - \frac{2M}{r}\right)^{-1} \left(\left(\frac{\partial r}{\partial t}\right)^2 - \left(\frac{\partial r}{\partial x}\right)^2\right). \tag{3.101a}$$

When the metric is static, no further restrictions arise, and all the equations of motion are satisfied. However, when $\partial r/\partial t \neq 0$, one also finds the condition

$$\frac{\partial^2 r}{\partial t^2} - \frac{\partial^2 r}{\partial x^2} = \left(1 + \frac{\lambda}{2} - \frac{3\lambda M}{r}\right) \frac{2M\Gamma}{r^2}. \tag{3.101b}$$

This allows us to check whether the above line elements (3.74), (3.81), and (3.90) solve Hamilton's equations.

First, taking $x = r^*$, and thus $\partial r/\partial t = 0$, we find $\Psi = -(1 - 2M/r)$, leading to (3.74) on E_σ.

Second, considering $\Upsilon(r) = \tan(t+x)\tan(t-x)$, with Υ defined in (3.83), we get, from (3.101a), $\Psi = \Gamma(r)\cos^{-2}(t+x)\cos^{-2}(t-x)$, with Γ given by (3.82), eventually yielding (3.81). One can check that $r(t,x)$, as implicitly given by (3.84a), and this $\Psi(t,x)$ satisfy (3.101b).

Third, taking r defined by (3.90), one gets (3.89) by following the same procedure as above.

3.3 Geometric properties

In this section we analyse some relevant properties of the spacetime solution $(\mathcal{M}, g)$. We start with a review of its causal structure (Sec. 3.3.1), study the curvature (Sec. 3.3.2), compare different definitions for the mass (Sec. 3.3.3), and compute the effects on the dynamics of a test scalar field propagating on the exterior region (Sec. 3.3.4).

3.3.1 Causal structure

The components of the mean curvature vector of the spheres of constant time and radial coordinates are defined as

$$H^\mu := \frac{2}{r}\nabla^\mu r = \frac{2}{r} g^{\mu\nu}\partial_\nu r, \tag{3.102}$$

and they encode all the information regarding the causal structure of each region. In the chart $\Psi^{\mathcal{U}}_{\tau z} = \{\tau, z\}$, the mean curvature vector reads

$$H^\mu \partial_\mu = \mathrm{sgn}(z)\frac{2}{r}\sqrt{1 - \frac{2\lambda M}{r}} \left(\sqrt{\frac{2M}{r}}\partial_\tau + \left(1 - \frac{2M}{r}\right)\partial_z\right). \tag{3.103}$$

Notice that the mean curvature vector is identically vanishing at the hypersurface $\mathcal{T}$ with $r = 2\lambda M$, meaning that it is minimal (it has zero extrinsic curvature). More precisely, $\mathcal{T}$ has topology $\mathbb{R} \times S^2$ with metric $ds^2 = (\lambda - 1)/\lambda d\tau^2 + r_0^2 d\Omega^2$ and, therefore, it is foliated by totally geodesic surfaces of area $4\pi r_0^2 > 0$. The existence of such a positive minimal area for the orbits of the spherical symmetry group is the key difference between the spacetime $(\mathcal{M}, g)$ and the Schwarzschild geometry.

We may compute the norm of the mean curvature vector,

$$H_\mu H^\mu = \frac{4}{r^2}\left(1 - \frac{2\lambda M}{r}\right)\left(1 - \frac{2M}{r}\right), \tag{3.104a}$$

to see that it is spacelike for $r > 2M$, timelike for $2\lambda M < r < 2M$, and null at $r = 2M$. Additionally, its product with the unit normal vector,

$$n_\mu H^\mu = -\operatorname{sgn}(z)\frac{2}{r^2}\sqrt{1 - \frac{2\lambda M}{r}}\sqrt{\frac{2M}{r}}, \tag{3.104b}$$

shows that it is future-pointing for $z > 0$ and past-pointing for $z < 0$. Combining (3.104a) and (3.104b), we deduce that the spheres of constant τ and z are:

- Non-trapped for $r > 2M$, independently of the sign of z, that is, on E_+ and E_-.
- Trapped to the future (or just trapped) for $r_0 = 2\lambda M < r < 2M$ and $z > 0$, i.e., on I_+.
- Trapped to the past (or anti-trapped) for $r_0 = 2\lambda M < r < 2M$ and $z < 0$, i.e., on I_-.
- Marginally trapped at the apparent horizons $r = 2M$, that is, on $\mathcal{Z}_+$ and $\mathcal{Z}_-$.

An additional check of the regularity of this spacetime relies on radial geodesics traversing the interior homogeneous region in a finite proper time. First, recall that the affine parameter of radial null geodesics is proportional to z (see Sec. 3.2.1), and it is trivial to see that the amount of affine distance Δs between the horizons $\mathcal{Z}_+$ and $\mathcal{Z}_-$ is proportional to $2z_s$. Second, for timelike geodesics, let us compute the proper time of a free-falling observer that was at rest at infinity. That is, we set $\gamma = -1$ and $\mathcal{E} = -1$ in (3.54), yielding the equation

$$\frac{dz}{ds} = -\sqrt{\frac{2M}{r(z)}}, \tag{3.105}$$

where we have chosen the minus sign so that z decreases with s. Then, the amount of proper

time Δs spent to go from $r(z_s) = 2M$ to $r(-z_s) = 2M$ can be explicitly computed as follows

$$\begin{aligned}\Delta s &= \int_{z_s}^{-z_s} ds = \int_{-z_s}^{z_s} \sqrt{\frac{r(z)}{2M}} dz = 2\int_0^{z_s} \sqrt{\frac{r(z)}{2M}} dz \\ &= 2\int_{r_0}^{2M} \sqrt{\frac{r}{2M}} \left(1 - \frac{2\lambda M}{r}\right)^{-1/2} dr = \frac{8M}{3}(1+2\lambda)\sqrt{1-\lambda},\end{aligned} \tag{3.106}$$

where we have used $r(-z) = r(z)$ in the third equality and (3.49) in the fourth. The analogous calculation for Schwarzschild yields a proper time of $4M/3$ for an observer to fall from the horizon to the singularity. The computed proper time Δs is larger than twice such time.

3.3.2 Curvature

Since the present geometry is free of singularities, from the singularity theorems [30, 31], we know that some of the eigenvalues of the Einstein tensor become negative in some region of the trapped black-hole interior I_+. In the chart $\Psi^{\mathcal{U}}_{\tau z}$, the Einstein tensor reads

$$G_{\mu\nu}dx^\mu dx^\nu = 4\lambda M^2 \left(\frac{r-2M}{r^5}d\tau^2 - \frac{2\sqrt{2M}}{r^{9/2}}d\tau dz - \frac{r+2M}{2Mr^4}dz^2 + \frac{r-M}{4Mr^2}d\Omega^2\right). \tag{3.107}$$

Its eigenvalues at the Lorentzian part (defined by the coordinates τ and z) are $\mu_0 = -4\lambda M^2/r^4$ and $\mu_1 = -2\lambda M/r^3$, with respective eigenvectors $v_0^\mu\partial_\mu = \partial_\tau$ and $v_1^\mu\partial_\mu = \sqrt{2M/r}\,\partial_\tau + (1-2M/r)\,\partial_z$. The moduli of v_0 and v_1 are $(2M/r-1)$ and $(1-2M/r)$, respectively. In the angular sector, there is a double eigenvalue $\mu_\theta = \lambda M(r-M)/r^4$. Hence, when interpreting the Einstein tensor as an effective energy-momentum tensor, one finds that the energy, the radial pressure, and the angular pressure are, respectively,

$$\rho^{(E)} := -\mu_0 = \frac{4\lambda M^2}{r^4}, \quad p_r^{(E)} := \mu_1 = -\frac{2\lambda M}{r^3}, \quad \text{and} \quad p_\theta := \mu_\theta = \frac{\lambda M}{r^4}(r-M), \tag{3.108a}$$

on the exterior region $r > 2M$, and

$$\rho^{(I)} := -\mu_1 = \frac{2\lambda M}{r^3}, \quad p_r^{(I)} := \mu_0 = -\frac{4\lambda M^2}{r^4}, \quad \text{and} \quad p_\theta := \mu_\theta = \frac{\lambda M}{r^4}(r-M), \tag{3.108b}$$

on the interior region $r_0 \leq r < 2M$. The energy conditions for such an anisotropic fluid read:

- Null energy condition: $\rho + p_r \geq 0$ and $\rho + p_\theta \geq 0$.
- Weak energy condition: $\rho + p_r \geq 0$, $\rho + p_\theta \geq 0$, and $\rho \geq 0$.
- Dominant energy condition: $\rho \geq |p_r|$ and $\rho \geq |p_\theta|$.
- Strong energy condition: $\rho + p_r \geq 0$, $\rho + p_\theta \geq 0$, and $\rho + p_r + 2p_\theta \geq 0$.

Therefore, all the effective energy conditions are violated both inside and outside the horizon. It is straightforward to check this statement by computing

$$\rho + p_r = \rho - |p_r| = -\frac{2\lambda M}{r^4}\,|r - 2M|\,, \tag{3.109}$$

which is always negative except at $r = 2M$, where it vanishes. This is because the Einstein tensor has a double eigenvalue along the null direction $\partial_\tau|_{r=2M}$, given by $\mu_0|_{r=2M} = \mu_1|_{r=2M} = -\lambda/(4M^2)$. Since $\mu_\theta|_{r=2M} > 0$, all the effective energy conditions are satisfied on the horizon. In addition, they are also fulfilled at infinity (but not in a neighbourhood) because the four eigenvalues decay at least as $\mathcal{O}(1/r^3)$.

The relevant curvature scalars are the ***Ricci scalar***,

$$\mathcal{R} = \frac{6\lambda M^2}{r^4}, \tag{3.110}$$

and the only non-vanishing component of the ***Weyl tensor***, the "Coulomb" term

$$\Psi_2 = -\frac{M}{r^3}\left(1 + \frac{\lambda}{2}\right) + \frac{5\lambda M^2}{2r^4}, \tag{3.111}$$

in the usual null frame adapted to the spherical symmetry.

Note that both $\mathcal{R}$ and Ψ_2 are bounded from above because $r \geq r_0$ and, in particular, the Ricci scalar is everywhere positive. It attains its maximum at $r = r_0$, with the value $R|_{\mathcal{T}} = 3/(8\lambda^3 M^2)$.

To compare with the Schwarzschild geometry, we compute the ***Kretschmann scalar***,

$$\mathcal{R}_{\mu\nu\sigma\rho}\mathcal{R}^{\mu\nu\sigma\rho} = \frac{48M^2}{r^6}\left(1 + \lambda - \frac{5\lambda M}{r}\right) + \frac{24\lambda^2 M^2}{r^6}\left(1 - \frac{16M}{3r} + \frac{27M^2}{2r^2}\right), \tag{3.112}$$

which is also always positive and reaches its maximum value at the critical surface $\mathcal{T}$.

3.3.3 Mass

We have referred to M as the mass of the model for it being a constant of motion and because it is the Schwarzschild mass in the GR limit. Nevertheless, infinitely many combinations of M and r_0 satisfy such requirements. Hence, a more comprehensive analysis of some usual notions of mass turns out mandatory in order to attain a proper understanding of both constants. Certainly, there is not a unique concept of mass in GR [91–93], and one finds several geometric definitions, both local and global, that we now compute for the spacetime $(\mathcal{M}, g)$.

Komar mass

The Komar mass is defined in any exterior region $r > 2M$, and can be intuitively understood as a quantity proportional to the force an observer at infinity should exert to keep a test particle in place.

Since this geometric notion is only defined for the exterior static regions, we may employ the line element (3.14) to compute the Komar mass on any sphere of radius $\tilde{r} = r|_E > 2M$ and time $\tilde{t}$, as specified in Ref. [81].

For that purpose, we need to consider the vectors normal to the surfaces of constant $\tilde{t}$ and $\tilde{r}$. They are just the metric conjugates to $d\tilde{t}$ and $d\tilde{r}$, that is, $\tilde{t}^\mu\partial_\mu$ and $\tilde{r}^\mu\partial_\mu$, respectively.

Then, the Komar mass reads

$$M_K := \frac{1}{4\pi}\int_{\mathcal{S}} \frac{\tilde{t}^\mu}{\sqrt{-\tilde{t}_\rho\tilde{t}^\rho}}\frac{\tilde{r}^\nu}{\sqrt{\tilde{r}_\sigma\tilde{r}^\sigma}}\nabla_\mu\tilde{t}_\nu\, d\mathcal{S}, \tag{3.113}$$

and, in this particular case, it takes the form

$$\begin{aligned} M_K(\tilde{r}) &= \tilde{r}^2\sqrt{1-\frac{2\lambda M}{\tilde{r}}}\tilde{t}^\mu\tilde{r}^\nu g_{\nu\alpha}\nabla_\mu\tilde{t}^\alpha = \tilde{r}^2\sqrt{1-\frac{2\lambda M}{\tilde{r}}}\tilde{t}^\mu\tilde{r}^\nu g_{\nu\alpha}\left(\partial_\mu\tilde{t}^\alpha + \Gamma^\alpha_{\mu\beta}\tilde{t}^\beta\right) \\ &= \tilde{r}^2\sqrt{1-\frac{2\lambda M}{\tilde{r}}}g_{11}\Gamma^1_{00} = M\sqrt{1-\frac{2\lambda M}{\tilde{r}}}. \end{aligned} \tag{3.114}$$

The explicit dependence of M_K on the area-radius function descends from $R_{\mu\nu}$ not being zero, and more precisely from its part normal to the spheres S^2. It is interesting to point out that the limit for large radii tends to the constant M, that is,

$$\lim_{r\to\infty} M_K(r) = M. \tag{3.115}$$

We may also compute the surface gravity, κ, defined on each component $\mathcal{Z}_\sigma$ of the horizon, $\kappa\tau^\mu := \tau^\nu\nabla_\nu\tau^\mu$, with the Killing vector field $\tau^\mu\partial_\mu$. This yields

$$\kappa = \frac{\sigma}{4M}\sqrt{1-\lambda}. \tag{3.116}$$

Note that the usual relation $|\kappa| = r^{-2}M_K|_{r=2M}$ is satisfied [81]. In the limit $\lambda \to 1$, which represents the maximum departure of the effective model from GR, one would get a vanishing surface gravity, in analogy with the extremal Reissner-Nordström spacetime. However, this limit is out of the scope of the present model since, by definition, $\lambda < 1$.

Hawking mass

The Hawking mass — or, equivalently in spherical symmetry, the Misner-Sharp mass — shall be computed on any sphere of radius $r \geq r_0$. It is given by

$$M_H(r) := \frac{r}{2}\left(1 - \nabla_\mu r \nabla^\mu r\right) = \frac{r}{2}\left(1 - \frac{r^2}{4} H_\mu H^\mu\right) = M\left(1 + \lambda - \frac{2\lambda M}{r}\right), \tag{3.117}$$

which is always positive and, further, monotonically increasing. The minimum is attained at

$$M_H|_{\mathcal{T}} := \lim_{r \to r_0} M_H(r) = M\lambda. \tag{3.118}$$

In addition, note that the Hawking mass coincides with M at the horizon,

$$M_H|_{\mathcal{Z}} := \lim_{r \to 2M} M_H(r) = M. \tag{3.119}$$

Besides, it is interesting to point out the following relation between the values of the Hawking mass evaluated at different points,

$$M_H|_{i^0} = M_H|_{\mathcal{Z}} + M_H|_{\mathcal{T}}. \tag{3.120}$$

It should be remarked that the Komar and Hawking masses coincide in GR. But, since the spacetime $(\mathcal{M}, g)$ does not satisfy Einstein's equations, that is no longer true. In fact, we have checked that a non-vanishing Ricci tensor in vacuum affects both masses in a different way.

ADM mass

The Arnowitt-Deser-Misner (ADM) mass is defined on any spacelike hypersurface. First, we consider the slicing generated by constant values of the time coordinate $\tilde{t}$ on any exterior region described by the line element (3.14). It is clear that the corresponding slices $\Sigma_{\tilde{t}}$ have topology $(2M, \infty) \times S^2$, while their metric is given by $d\sigma^2_{\tilde{t}} = (1-2\lambda M/\tilde{r})^{-1}(1-2M/\tilde{r})^{-1} d\tilde{r}^2 + \tilde{r}^2 d\Omega^2$. The Ricci scalar of these slices, ${}^{(3)}\mathcal{R}_{\tilde{t}} = 8\lambda m^2/r^4$, is integrable and, since they have vanishing extrinsic curvature, they satisfy the proper fall-off conditions for asymptotic flatness. Thus, the ADM mass is a geometric invariant [93], and it corresponds to the Hawking mass at i^0 [92],

$$M^{(\tilde{t})}_{ADM} \equiv M_H|_{i^0} := \lim_{r \to \infty} M_H(r) = (1 + \lambda)M. \tag{3.121}$$

Second, we study the slicing of constant τ on $\mathcal{U}$. The hypersurfaces $\Sigma_\tau \sim \mathbb{R} \times S^2$ start and end on i^0 (see Fig. 3.3), and their metric is $d\sigma^2_\tau = dz^2 + r(z)^2 d\Omega^2$. Despite having a vanishing Ricci scalar, ${}^{(3)}\mathcal{R}_\tau = 0$, these hypersurfaces do not satisfy the conditions for being asymptotically flat (their extrinsic curvature goes as $r^{-3/2}$ at infinity), and, therefore, their ADM mass will not

be the limit of the Hawking mass. Note that in the GR limit these hypersurfaces are defined by a constant time in Painlevé-Gullstrand coordinates. In that case, they are flat [94], and, hence, have zero ADM mass.

To compute explicitly $M_{ADM}^{(\tau)}$, we express the metric of the hypersurfaces Σ_τ in asymptotically Euclidean coordinates, i.e.,

$$d\sigma_\tau^2 = dz^2 + r(z)^2 d\Omega^2 = \Psi(\rho)^2 (d\rho^2 + \rho^2 d\Omega^2) = \Psi^2 \delta_{ij} dx^i dx^j, \tag{3.122}$$

with $\rho^2 = \delta_{ij} x^i x^j$ and $\Psi^2 = 1 + \mathcal{O}(1/\rho)$. A direct inspection shows that $\mathrm{sgn}(z) dz = \Psi d\rho$ and $r = \Psi\rho$, from where

$$\frac{d\rho}{\rho} = \mathrm{sgn}(z) \frac{dz}{r(z)} = \mathrm{sgn}(z) \frac{dr}{r(z)} \left(\frac{dr}{dz}\right)^{-1} = \left(1 - \frac{2\lambda M}{r}\right)^{-1/2} \frac{dr}{r}. \tag{3.123}$$

We can integrate this equation and write $r(\rho) = 2\lambda M \left(1 + c\rho\right)^2 / (4c\rho)$, with an integration constant c. Then, the conformal factor reads

$$\Psi = \frac{r}{\rho} = \frac{\lambda M}{2c\rho^2} \left(1 + c\rho\right)^2, \tag{3.124}$$

and, due to the required fall-off conditions, we find $c = 2/(\lambda M)$, i.e.,

$$\Psi = \left(1 + \frac{\lambda M}{2\rho}\right)^2 = 1 + \frac{\lambda M}{\rho} + \mathcal{O}\left(\rho^{-2}\right). \tag{3.125}$$

Making use of the Cartesian coordinates x^i, the ADM mass reads

$$M_{ADM} := \frac{1}{16\pi} \lim_{\rho\to\infty} \oint_{\mathcal{S}} \sum_{i,j} \left(\frac{\partial q_{ij}}{\partial x^j} - \frac{\partial q_{jj}}{\partial x^i}\right) n^i d\mathcal{S}, \tag{3.126}$$

with $q_{ij} = \Psi^2 \delta_{ij}$, $n^i = x^i/(\Psi\rho)$ and $\oint_{\mathcal{S}} d\mathcal{S} = 4\pi\Psi^2\rho^2$. The integrand vanishes for $i = j$ and, therefore,

$$M_{ADM} = -\frac{1}{2} \lim_{\rho\to\infty} \Psi^2 \rho^2 \sum_i \frac{\partial \Psi^2}{\partial \rho} \frac{\partial \rho}{\partial x^i} \frac{x^i}{\Psi\rho} = -\lim_{\rho\to\infty} \Psi^2 \rho^2 \frac{\partial \Psi}{\partial \rho}, \tag{3.127}$$

with the additional 2 factor coming from the fact that one needs to sum over $i \neq j$. In the last step, we used the relations $\partial\rho/\partial x^i = x^i/\rho$ and $\sum_i (x^i/\rho)^2 \equiv 1$. Replacing in the last expression the form of the conformal factor (3.125), one finally gets

$$M_{ADM}^{(\tau)} = \lambda M. \tag{3.128}$$

Geroch mass

Recall that the Hawking mass (3.117) on some closed co-dimension two-surface $\mathcal{S}$ in $\mathcal{M}$ (which we take to be the orbits of the spherical symmetry group) depends only on the module of the mean curvature vector. Then, assuming $\mathcal{S}$ can be embedded in a spacelike hypersurface Σ, the Hawking mass can be rewritten as

$$M_H(r) = \frac{r}{2}\left(1 - \frac{r^2}{4}\left(k^2 - K^2\right)\right), \tag{3.129}$$

where k and K stand for the traces of the respective extrinsic curvatures of $\mathcal{S}$ on Σ and of Σ on $\mathcal{M}$. The Geroch energy thence provides a positive lower bound for the Hawking mass,

$$M_G(r) := \frac{r}{2}\left(1 - \frac{r^2}{4}k^2\right) \leq M_H(r). \tag{3.130}$$

Since the hypersurfaces $\Sigma_{\tilde{t}}$ are minimal ($K_{ab}dx^a dx^b = 0$), the Geroch and Hawking masses coincide. It is more interesting to consider those spheres embedded in Σ_τ, which have metric $r(z)^2 d\Omega^2$ and extrinsic curvature $r(z)r'(z)d\Omega^2$. Then, $k = 2r'(z)/r(z)$ and

$$M_G^{(\tau)} = \lambda M, \tag{3.131}$$

that is, one obtains a constant Geroch energy, which is equal to the ADM mass of Σ_τ. Most remarkably, the Geroch mass being a quasi-local quantity, it does not depend on global properties (for instance, the asymptotic behaviour) of the specific hypersurface Σ. For that reason, a constant $M_G^{(\tau)}$ provides a quasi-local characterisation of λM, playing an analogous role to that of M on the asymptotically flat hypersurfaces in Schwarzschild.

Additional remarks

The most important aspect to highlight from this section is that, regardless which notion of mass one considers, the mass has the same exact value in all exterior regions of the maximal extension $\mathcal{M}$. Of course, this means there is no mass (de)amplification when crossing the transition surface $\mathcal{T}$.

In addition, all spacelike slicings in $\mathcal{M}$ share the same topology $\mathbb{R} \times S^2$. This applies, in particular, to the level surfaces of the function τ on $\mathcal{U}$ that cross the transition hypersurface $\mathcal{T}$, as opposed to other nonsingular black-hole constructions [32, 95, 96].

We have thoroughly said that the constant λ measures the departure of the effective theory from GR. With the different definitions of mass, we have also found several characterisations (both global and quasi-local) for that parameter.

For instance, one can write

$$\lambda\!\!\!^{-} = \lim_{r\to\infty} \frac{M_H}{M_K} - 1. \tag{3.132}$$

An equivalent and interesting result is that the minimum area of the orbits of the spherical symmetry, r_0, is just twice the difference between the Hawking and the Komar masses:

$$r_0 = 2 \lim_{r\to\infty} \left(M_H - M_K\right). \tag{3.133}$$

As a final consistency check, one can see that if Einstein's equations are satisfied, the right-hand side in the last two equations vanishes and, thus, $\lambda\!\!\!^{-}$ and r_0 are necessarily zero in GR.

3.3.4 Measurable imprints

Although the transition surface $\mathcal{T}$ is always inside the horizon, the effective theory modifies the spacetime at every point. Of course, that is due to the non-vanishing of the Ricci tensor and, as we explicitly showed in the previous section, it leaves traces in the asymptotic regions. Therefore, quantum corrections are measurable by an observer outside the black hole, and thus the model is testable; that is, future observations could, in principle, constrain the actual value of $\lambda\!\!\!^{-}$.

One may consider additional test fields propagating on this background spacetime to read deviations from the Schwarzschild geometry. Let us consider the particular simple example of a massless scalar field. Its dynamics is given by the Klein-Gordon equation, $\Box\Phi = 0$, which using the coordinates $\tilde{t}$ and r_* (3.78) in some exterior region D_S can be expressed as

$$\frac{\partial^2\psi_l}{\partial r_*^2} - \frac{\partial^2\psi_l}{\partial \tilde{t}^2} = V(r(r_*))\psi_l, \tag{3.134}$$

where the scalar field has been decomposed in spherical harmonics,

$$\Phi(\tilde{t}, r_*) = \frac{1}{r(r_*)} \sum_{l,m} \psi_l(\tilde{t}, r_*) Y_{lm}(\theta, \phi). \tag{3.135}$$

The main point here is that the potential term,

$$\begin{aligned} V(r) &= \left(1 - \frac{2M}{r}\right) \frac{l(l+1)}{r^2} + \frac{1}{r}\frac{d^2 r}{dr_*^2} = \left(1 - \frac{2M}{r}\right)\left(\frac{l(l+1)}{r^2} - \frac{R}{6} - 2\Psi_2\right) \\ &= \left(1 - \frac{2M}{r}\right)\left(\frac{l(l+1)}{r^2} + \frac{(2+\lambda\!\!\!^{-})M}{r^3} - \frac{6\lambda\!\!\!^{-}M^2}{r^4}\right), \end{aligned} \tag{3.136}$$

differs from that of Schwarzschild. Their difference,

$$V(r) - V_{Sch}(r) = V(r) - V(r)|_{\lambda=0} = \frac{2\lambda M}{r^3}\left(1 - \frac{2M}{r}\right)\left(\frac{1}{2} - \frac{3M}{r}\right), \tag{3.137}$$

is independent of the angular-momentum number l, and thus all the modes are affected in the same way. In addition, it decays asymptotically as $\lambda M/r^3$. Such measurable imprints on the behaviour of the scalar field are also expected for more general fields.

3.4 Limiting spacetimes

As already shown in the previous chapter, the case $\lambda = 0$ corresponds to GR. This is trivial on phase space, where the Hamiltonian (3.1) reduces to its GR form (1.42b) as $\lambda \to 0$. But here we explicitly show that the limit $\lambda \to 0$ of $(\mathcal{M}, g)$ also corresponds to the Schwarzschild spacetime.

Furthermore, Minkowski is the $M = 0$ limit of the spacetime $(\mathcal{M}, g)$, just in the same way as it is the limit of Schwarzschild in GR.

Schwarzschild

When $\lambda = 0$, the minimum for the area-radius r_0 is zero by definition. Conversely, $\lambda = 0$ is required for an identically vanishing Ricci tensor. Thus, $\lambda = 0$ if and only if the spacetime solves the vacuum Einstein equations in spherical symmetry, and the limit $\lambda \to 0$ of the spacetime $(\mathcal{M}, g)$ is clearly the Schwarzschild solution with mass M.

Checking this statement in the regions not including the transition surface $\mathcal{T}$ is trivial, as one can directly set $\lambda = 0$.

For the covering domain $\mathcal{U}$, however, one should note that (3.50) reduces to $r(z) = |z|$ when $\lambda = 0$, and that equation is no longer differentiable at $z = 0$. Then, $r(0)$ is ill-defined. But, furthermore, the area-radius function now reaches $r = 0$, where the curvature diverges. Therefore, the transition hypersurface $\mathcal{T}$ emerges as the Schwarzschild singularity, and we must split $\mathcal{U}$ in two disconnected domains, one for each sign of z. These correspond to two time-reversed Eddington-Finkelstein-like domains.

Regarding the global structure, the Kruskal-type "building blocks" are now the maximal analytic extension of the spacetime, which is no longer geodesically complete.

Minkowski

The limit $M \to 0$ implies $r_0 \to 0$ for any λ. In view of the above, the limit $M \to 0$ of the spacetime $(\mathcal{M}, g)$ corresponds to that of Schwarzschild. But, in addition, we see that the limit $M \to 0$ holds for any value of the polymerisation parameter, and thus Minkowski is always a solution of the effective Hamiltonian model.

4

Regular Charged Black Holes in Cosmological Backgrounds

In my experience, milady, we can never get back to exactly where we started, no matter how hard we try.

Cetaganda
by Lois McMaster Bujold.

Simple matter models with no local of freedom are of great relevance in general relativity, and the historical and conceptual importance of the exact solutions of Reissner-Nordström and Kottler are beyond any doubts. Although in effective theories of loop quantum gravity these spacetimes are usually regarded as intermediate steps between modified Schwarzschild-like and collapsing models, and they are rarely studied, a comprehensive analysis of these solutions may well give insight into the limits and validity of holonomy corrections.

In general relativity, the incorporation of charge or a cosmological constant changes the global structure of the spacetime. The former may introduce an inner Cauchy horizon inside the black-hole horizon. The latter prevents the spacetime from being asymptotically flat, and may also generate additional (cosmological) horizons. It is remarkable that, in both cases, the singularity at the center is always present. In this chapter, we will analyse in detail the effects of holonomy corrections for charged black holes embedded in cosmological (anti-)de Sitter backgrounds, extending the previous results in vacuum and checking whether singularity resolution remains a strong prediction of the effective theory.

After a brief review of the Hamiltonian formulation of these models in GR (Sec. 4.1), we obtain the metric in different charts for the corresponding gauge choices on phase space in Sec. 4.2. The effective theory does not show a direct resolution of singularities, and we devote Sec. 4.3 to find the ranges of the parameters of the model in which the singularity is avoided. Finally, in Sec. 4.4 we study the global structure of the singularity-free spacetimes, and compute their corresponding conformal diagrams. All figures in this chapter were published in Ref. [6].

4.1 Non-dynamical scalar fields

The cosmological constant Λ may be thought of as a non-dynamical scalar field, and it only contributes with a potential term of the form $V = \Lambda/2$ to the Hamiltonian constraint. Nevertheless, as already mentioned above, it drastically changes the asymptotic structure of the spacetime and also its horizon structure.

Coupling a Maxwell field is a bit more complicated. However, we will show that, in the end, its contribution is also in the form of a non-dynamical spherical scalar field. Electromagnetism is described in terms of the vector potential, which has only two non-trivial components, A_0 and A_x, in spherical symmetry. The former is not a dynamical variable because its conjugate momentum, p^0, is identically vanishing, and thus defines a primary constraint. This fact descends directly from the antisymmetry of the electromagnetic field tensor, $F_{\mu\nu} = 2\partial_{[\mu}A_{\nu]}$. Hence, a spherical electromagnetic field is described by a single pair of conjugate variables,

$$\{A_x(x_1), p^x(x_2)\} = \delta(x_1 - x_2). \tag{4.1}$$

The contributions of the electromagnetic field to the constraints are [72]

$$D_{\text{em}}[N^x] = \int N^x \mathcal{D}_{\text{em}} dx = \int N^x A_x (p^x)' dx, \tag{4.2a}$$

$$H_{\text{em}}[N] = \int N \mathcal{H}_{\text{em}} dx = \int N \left(\frac{E^\varphi (p^x)^2}{2(E^x)^{3/2}} - (p^x)' A_0 \right) dx. \tag{4.2b}$$

Since A_0 only appears in this last component, and knowing that the total Hamiltonian is the sum of the vacuum part and the matter contribution, it is straightforward to see that the conservation of the primary constraint $p^0 = 0$ leads to

$$\mathcal{G}_{\text{em}} := \frac{1}{N}\{p^0, H_{\text{em}}[N]\} = (p^x)' \approx 0, \tag{4.3}$$

which is the electromagnetic Gauss constraint. Let $G_{\text{em}}[\widetilde{\beta}] = \int \widetilde{\beta}\mathcal{G}_{\text{em}} dx$ be its smeared form. Since there are three first-class constraints, and only three pairs of conjugate variables, there are no propagating degrees of freedom. In addition, the matter contribution decouples from the vacuum part and it is possible to fix the gauge for the electromagnetic variables with no loss of generality. Since the vacuum part of the constraints does not have any dependence on the matter variables (that is, the matter contribution is decoupled), the equations for the

pair (A_x, p^x) read

$$\dot{A}_x = \{A_x, H_{\text{em}}[N] + D_{\text{em}}[N^x] + G_{\text{em}}[\beta + A_0 N - A_x N^x]\} = \frac{N E^\varphi p^x}{(E^x)^{3/2}} - \beta', \tag{4.4}$$

$$\dot{p^x} = \{p^x, H_{\text{em}}[N] + D_{\text{em}}[N^x] + G_{\text{em}}[\beta + A_0 N - A_x N^x]\} = N^x (p^x)', \tag{4.5}$$

where we have trivially absorbed in the Lagrange multiplier of $\mathcal{G}_{\text{em}}$ all the coefficients of $(p_x)'$ coming from (4.2). We immediately see that the second equation is proportional to the Gauss constraint, and, hence, p^x is a conserved quantity. More precisely, it denotes the charge of the spacetime,

$$Q := p^x. \tag{4.6}$$

This solution strongly enforces the Gauss constraint, and any gauge-fixing condition of the form $A_x = \Phi(p^x, K_x, K_\varphi, E^x, E^\varphi)$ provides the Lagrange multiplier β through the conservation of that condition, $\dot{A}_x = \dot{\Phi}$. Since neither A_x nor β appears in the remaining equations of motion, their specific forms do not affect the evolution of the geometric variables, which are thus insensitive to such a partial gauge fixing. This partial gauge fixing makes the electromagnetic diffeomorphism constraint identically vanishing while its contribution to the Hamiltonian constraint is simplified to only one term of the form $N E^\varphi Q^2/(2(E^x)^{3/2})$.

Therefore, both sources (the cosmological constant and the charge) can be described simultaneously by the addition of

$$\mathcal{H}_m = \frac{1}{2}\sqrt{E^x} E^\varphi \left(\Lambda + \frac{Q^2}{(E^x)^2}\right) \tag{4.7}$$

to the Hamiltonian constraint, and both can be thus understood as a potential term for a non-dynamical scalar field in this spherically symmetric configuration [see (1.46a)]. Therefore, these matter components are included in the analysis performed in Chapter 2, and the results obtained there apply [see (2.105)]. That is, the effective spherically symmetric model with holonomy corrections including charge and a cosmological constant is described by the following diffeomorphism and Hamiltonian constraints:

$$\mathcal{D} = -K_x E^{x\prime} + \mathcal{K}_\varphi' \mathcal{E}^\varphi, \tag{4.8a}$$

$$\begin{aligned}\mathcal{H} = &-\frac{\mathcal{E}^\varphi}{2\sqrt{1+\lambda^2}\sqrt{E^x}}\left(1 + \frac{\sin^2(\lambda\mathcal{K}_\varphi)}{\lambda^2}\right) - \sqrt{E^x} K_x \frac{\sin(2\lambda\mathcal{K}_\varphi)}{\sqrt{1+\lambda^2}\lambda}\left(1 + \left(\frac{\lambda E^{x\prime}}{2\mathcal{E}^\varphi}\right)^2\right) \\ &+ \left(\frac{(E^{x\prime})^2}{8\sqrt{E^x}\mathcal{E}^\varphi} - \frac{\sqrt{E^x}}{2\mathcal{E}^{\varphi 2}} E^{x\prime}\mathcal{E}^{\varphi\prime} + \frac{\sqrt{E^x}}{2\mathcal{E}^\varphi} E^{x\prime\prime}\right)\frac{\cos^2(\lambda\mathcal{K}_\varphi)}{\sqrt{1+\lambda^2}} + \frac{\sqrt{E^x}\mathcal{E}^\varphi}{2\sqrt{1+\lambda^2}}\left(\Lambda + \frac{Q^2}{(E^x)^2}\right)\Bigg).\end{aligned} \tag{4.8b}$$

that satisfy the algebra (2.106), with the everywhere non-negative structure function (2.107). Recall that $\lambda := \lambda^2/(1+\lambda^2)$ is a constant taking values in $(0,1)$, with $\lambda \to 0$ corresponding to GR, and that the mass function m, c.f., (2.108), although no longer constant, is still a scalar function that simplifies some computations. In particular, due to the spherical symmetry, m will be a sole function of E^x. The metric constructed from the effective Hamiltonian is

$$ds^2 = -N^2dt^2 + \left(1 - \frac{2\lambda m}{\sqrt{E^x}}\right)^{-1} \frac{(\mathcal{E}^\varphi)^2}{E^x}\left(dx + N^x dt\right)^2 + E^x d\Omega^2, \tag{4.9}$$

with $N(t,x)$, $N^x(t,x)$, $E^x(t,x)$, $\mathcal{E}^\varphi(t,x)$, and $m(t,x)$ satisfying the two constraint equations, $\mathcal{D}=0$ and $\mathcal{H}=0$, plus the four first-order Hamilton equations

$$\dot{E}^x = \{E^x, D[N^x] + H[N]\} = N^x E^{x\prime} + N\sqrt{E^x}\frac{\sin(2\lambda\mathcal{K}_\varphi)}{\lambda\sqrt{1+\lambda^2}}\left(1 + \left(\frac{\lambda E^{x\prime}}{2\mathcal{E}^\varphi}\right)^2\right), \tag{4.10a}$$

$$\begin{aligned}\dot{\mathcal{E}}^\varphi =& \{\mathcal{E}^\varphi, D[N^x] + H[N]\} = (N^x\mathcal{E}^\varphi)' + 2N\sqrt{E^x}K_x\frac{\cos(2\lambda\mathcal{K}_\varphi)}{\sqrt{1+\lambda^2}}\left(1 + \left(\frac{\lambda E^{x\prime}}{2\mathcal{E}^\varphi}\right)^2\right)\\ &+ N\frac{\sin(2\lambda\mathcal{K}_\varphi)}{\lambda\sqrt{1+\lambda^2}}\left(\frac{\mathcal{E}^\varphi}{2\sqrt{E^x}} + \frac{\lambda^2}{2}\left(\frac{E^{x\prime}}{2\mathcal{E}^\varphi}\left(\sqrt{E^x}\right)' + \sqrt{E^x}\left(\frac{E^{x\prime}}{\mathcal{E}^\varphi}\right)'\right)\right),\end{aligned} \tag{4.10b}$$

$$\begin{aligned}\dot{K}_x =& \{K_x, D[N^x] + H[N]\} = (N^xK_x)' + N''\frac{\sqrt{E^x}\cos^2(\lambda\mathcal{K}_\varphi)}{2\sqrt{1+\lambda^2}\mathcal{E}^\varphi} + \frac{N\mathcal{E}^\varphi(\Lambda - 3Q^2/(E^x)^2)}{4\sqrt{1+\lambda^2}\sqrt{E^x}}\\ &+ \frac{N'\sqrt{E^x}}{2\sqrt{1+\lambda^2}\mathcal{E}^{\varphi 2}}\left(\lambda\sin(2\lambda\mathcal{K}_\varphi)\left(E^{x\prime}K_x - 2\mathcal{E}^\varphi\mathcal{K}'_\varphi\right) + \cos^2(\lambda\mathcal{K}_\varphi)\left(\frac{\mathcal{E}^\varphi E^{x\prime}}{2E^x} - \mathcal{E}^{\varphi\prime}\right)\right)\\ &+ \frac{N}{\sqrt{1+\lambda^2}}\left(\frac{\mathcal{E}^\varphi(\sin^2(\lambda\mathcal{K}_\varphi)+\lambda^2)}{4\lambda^2E^{x3/2}} + \frac{\cos^2(\lambda\mathcal{K}_\varphi)}{4\sqrt{E^x}\mathcal{E}^\varphi}\left(E^{x\prime\prime} - \frac{(E^{x\prime})^2}{4E^x} - \frac{E^{x\prime}\mathcal{E}^{\varphi\prime}}{\mathcal{E}^\varphi}\right)\right.\\ &\left. - \frac{K_x\sin(2\lambda\mathcal{K}_\varphi)}{2\lambda\sqrt{E^x}}\left(1 + \left(\frac{\lambda E^{x\prime}}{2\mathcal{E}^\varphi}\right)^2\right) - \left[\sin(2\lambda\mathcal{K}_\varphi)\frac{\lambda\sqrt{E^x}}{2\mathcal{E}^{\varphi 2}}\mathcal{D}\right]'\right),\end{aligned} \tag{4.10c}$$

$$\begin{aligned}\dot{\mathcal{K}}_\varphi =& \{\mathcal{K}_\varphi, D[N^x] + H[N]\} = N^x\mathcal{K}'_\varphi + N'\frac{\sqrt{E^x}E^{x\prime}}{2\mathcal{E}^{\varphi 2}}\frac{\cos^2(\lambda\mathcal{K}_\varphi)}{\sqrt{1+\lambda^2}} - N\frac{\sin^2(\lambda\mathcal{K}_\varphi)+\lambda^2}{2\lambda^2\sqrt{E^x}\sqrt{1+\lambda^2}}\\ &+ \frac{N(E^{x\prime})^2\cos^2(\lambda\mathcal{K}_\varphi)}{8\sqrt{1+\lambda^2}\sqrt{E^x}\mathcal{E}^{\varphi 2}} - \frac{N\lambda\sqrt{E^x}E^{x\prime}\sin(2\lambda\mathcal{K}_\varphi)}{2\sqrt{1+\lambda^2}\mathcal{E}^{\varphi 3}}\mathcal{D} + \frac{N\sqrt{E^x}(\Lambda + Q^2/(E^x)^2)}{2\sqrt{1+\lambda^2}}.\end{aligned} \tag{4.10d}$$

By construction, E^x is defined over the whole positive real line. However, the possible values that it can attain will be, in general, restricted as we will find forbidden ranges for the scalar E^x where F would be negative. The critical values $\sqrt{E^x} = 2\lambda m$ for which F vanishes, and which are only attainable for positive m, will denote the boundaries of the allowed regions.

We will show this by solving the above equations of motion.

Let us recall that, in order to follow the standard notation, we will use $r := \sqrt{E^x}$ when convenient. That is, the scalar E^x, as a function on the manifold, is the square of the area-radius function. We will also see that the charge and the cosmological constant appear in the metric just in the same way as in GR, that is, we could take the vacuum solution in Chapter 3 and simply replace M by $m(r)$. However, let us explicitly derive the solution of the equations of motion in certain gauges, leading to the corresponding charts and domains for the metric tensor.

4.2 The spacetime solutions

As in the vacuum case, the charts of the spacetime solutions are composed by two coordinates on the spheres S^2, which we do not specify, and two coordinates on the Lorentzian space L_2 orthogonal to the spheres, corresponding to the pair (t, x), which we shall conveniently rename as functions on the manifold for each gauge choice on phase space.

Knowing beforehand that the spacetime will be composed by static and homogeneous regions, we suggest one gauge choice for each. Further, we will show that these non-overlapping domains are part of the same spacetime by considering a third gauge that includes the horizons and thus overlaps with both kinds of regions. Finally, we also study the near-horizon geometries. These particular solutions are free of singularities in GR and also in this effective model.

4.2.1 Static regions

We partially fix the gauge freedom by choosing $\dot{E}^x = 0$ and $\sin(\lambda\mathcal{K}_\varphi) = 0$, and assume that $E^{x\prime}$ does not vanish identically. This means that $N^x = 0$ necessarily, and the vanishing of the diffeomorphism constraint further demands $K_x = 0$. The remaining equations are

$$0 = \dot{\mathcal{E}}^\varphi, \tag{4.11a}$$

$$0 = \dot{K}_x = \frac{N}{2\sqrt{1+\lambda^2}\sqrt{E^x}}\left(\left(\frac{E^{x\prime}}{2\mathcal{E}^\varphi}\right)' - \frac{(E^{x\prime})^2}{8E^x\mathcal{E}^\varphi} + \frac{\mathcal{E}^\varphi}{2}\left(\frac{1}{E^x} + \Lambda - 3\left(\frac{Q}{E^x}\right)^2\right)\right) + \left(\frac{N'\sqrt{E^x}}{2\sqrt{1+\lambda^2}\mathcal{E}^\varphi}\right)', \tag{4.11b}$$

$$0 = \dot{\mathcal{K}}_\varphi = \frac{N'\sqrt{E^x}E^{x\prime}}{2\sqrt{1+\lambda^2}\mathcal{E}^{\varphi 2}} - \frac{N}{2\sqrt{1+\lambda^2}\sqrt{E^x}}\left(1 - \left(\frac{E^{x\prime}}{2\mathcal{E}^\varphi}\right)^2\right) + \frac{\sqrt{E^x}N}{2\sqrt{1+\lambda^2}}\left(\Lambda + \left(\frac{Q}{E^x}\right)^2\right), \tag{4.11c}$$

$$0 = \mathcal{H} = \frac{1}{\sqrt{1+\lambda^2}}\Bigg[-\frac{\mathcal{E}^\varphi}{2\sqrt{E^x}} + \frac{1}{2}\left(\frac{E^{x\prime}}{2\mathcal{E}^\varphi}\left(\sqrt{E^x}\right)' + \sqrt{E^x}\left(\frac{E^{x\prime}}{\mathcal{E}^\varphi}\right)'\right) + \frac{1}{2}\sqrt{E^x}E^\varphi\left(\Lambda + \left(\frac{Q}{E^x}\right)^2\right)\Bigg]. \tag{4.11d}$$

The last equation can be solved for $\mathcal{E}^\varphi$, yielding

$$\mathcal{E}^\varphi = \varepsilon_1 \frac{E^{x\prime}}{2}\left(1 - \frac{2M}{\sqrt{E^x}} + \frac{Q^2}{E^x} - \frac{\Lambda}{3}E^x\right)^{-1/2}, \tag{4.12}$$

with $\varepsilon_1^2 = 1$ and $M \in \mathbb{R}$ an integration constant. The range of E^x is thus restricted so that the radicand above is positive. This solution automatically satisfies (4.11a), and integrating now (4.11c), we obtain the lapse up to a trivial non-zero constant:

$$N = c_1\left(1 - \frac{2M}{\sqrt{E^x}} + \frac{Q^2}{E^x} - \frac{\Lambda}{3}E^x\right)^{1/2}. \tag{4.13}$$

With all this, equation (4.11b) is satisfied. As a result, the gauge will be completely fixed by prescribing $E^x(x)$. The easiest choice would be $\sqrt{E^x}(x) = x$, yielding a line element of the form (3.14), upon the identification $(t, x) \to (\tilde{t}/c_1, \tilde{r})$ and the substitution $M \to m(\tilde{r})$, with m as defined below in (4.16).

Although the novel pole at $\tilde{r} = 2\lambda m(\tilde{r})$ is of little relevance as it is not included in such static regions (note that $\tilde{r} > 2m$ implies, necessarily, $\tilde{r} > 2\lambda m$), it is convenient to try a different $E^x(x)$ so that the explicit pole is removed. We do so by fixing

$$(E^{x\prime})^2 = 4E^x\left(1 - \lambda\left(\frac{2M}{\sqrt{E^x}} - \frac{Q^2}{E^x} + \frac{\Lambda}{3}E^x\right)\right). \tag{4.14}$$

Renaming $\sqrt{E^x} =: r$, and (t, x) as the pair of real functions $(T/c_1, z)$ on $\mathcal{M}$, the metric is

$$ds^2 = -\left(1 - \frac{2m\big(r(z)\big)}{r(z)}\right)dT^2 + \left(1 - \frac{2m\big(r(z)\big)}{r(z)}\right)^{-1}dz^2 + r(z)^2 d\Omega^2. \tag{4.15}$$

In terms of the scalar r, the function m defined in (2.108) takes the form

$$m(r) := M - \frac{Q^2}{2r} + \frac{\Lambda}{6}r^3. \tag{4.16}$$

After the above relabelling, equation (4.14) implicitly defines $r(z)$ as

$$\left(\frac{dr(z)}{dz}\right)^2 = 1 - \frac{2\lambda m\big(r(z)\big)}{r(z)}. \tag{4.17}$$

These coordinates are valid for all $T \in \mathbb{R}$, while z is restricted by those values that satisfy $2m\big(r(z)\big) < r(z)$ and also, by construction, by $r(z) > 0$. Once $2m\big(r(z)\big) < r(z)$ holds, we have $2\lambda m\big(r(z)\big) < r(z)$ (because $\lambda < 1$) and, hence, the right-hand side of equation (4.17) is always positive in this domain.

4.2.2 Homogeneous regions

We now consider $E^{x\prime} = 0$ and $\mathcal{E}^{\varphi\prime} = 0$, with a non-constant E^x. The vanishing of $\mathcal{D}$ and $\mathcal{H}'$ implies $\mathcal{K}'_\varphi = 0$ and $K'_x \sin(2\lambda\mathcal{K}_\varphi) = 0$, respectively. The second equation means that $K'_x = 0$, because having $\sin(2\lambda\mathcal{K}_\varphi) = 0$ would entail either $\cos(\lambda\mathcal{K}_\varphi) = 0$ or $\sin(\lambda\mathcal{K}_\varphi) = 0$. The former generates an identically vanishing structure function F, with no associated geometry. The latter requires $\dot{E}^x = 0$ because of (4.10a), that is, a constant E^x, which collides with our initial assumption. Now, the radial derivatives of (4.10a) and (4.10b) guarantee that $N' = 0$ and $N^{x\prime\prime} = 0$, respectively, and we can use part of the remaining gauge freedom to set $N^x = 0$. Recall that this can be understood as a coordinate transformation that diagonalises the metric since the specific form $N^x = a(t)x + b(t)$ ensures the existence of a function y such that $dx + N^x dt = \exp(-\int a(t)dt)dy$.

The remaining equations then read

$$\dot{E}^x = N\sqrt{E^x}\frac{\sin(2\lambda\mathcal{K}_\varphi)}{\lambda\sqrt{1+\lambda^2}}, \tag{4.18a}$$

$$\dot{\mathcal{E}}^\varphi = \frac{N}{\sqrt{1+\lambda^2}}\left(2\sqrt{E^x}K_x\cos(2\lambda\mathcal{K}_\varphi) + \frac{\mathcal{E}^\varphi\sin(2\lambda\mathcal{K}_\varphi)}{2\lambda\sqrt{E^x}}\right), \tag{4.18b}$$

$$\dot{K}_x = \frac{N}{2\sqrt{E^x}\sqrt{1+\lambda^2}}\left(\frac{\mathcal{E}^\varphi}{2}\left(\Lambda - 3\left(\frac{Q}{E^x}\right)^2\right) + \frac{\mathcal{E}^\varphi}{2E^x}\left(1+\frac{\sin^2(\lambda\mathcal{K}_\varphi)}{\lambda^2}\right) - K_x\frac{\sin(2\lambda\mathcal{K}_\varphi)}{\lambda}\right), \tag{4.18c}$$

$$\dot{\mathcal{K}}_\varphi = \frac{N}{2\sqrt{1+\lambda^2}}\left(\sqrt{E^x}\left(\Lambda + \left(\frac{Q}{E^x}\right)^2\right) - \frac{1}{2\sqrt{E^x}}\left(1+\frac{\sin^2(\lambda\mathcal{K}_\varphi)}{\lambda^2}\right)\right), \tag{4.18d}$$

$$0 = \mathcal{H} = \frac{1}{\sqrt{1+\lambda^2}}\left(\frac{1}{2}\sqrt{E^x}E^\varphi\left(\Lambda + \left(\frac{Q}{E^x}\right)^2\right) - \frac{\mathcal{E}^\varphi}{2\sqrt{E^x}}\left(1+\frac{\sin^2(\lambda\mathcal{K}_\varphi)}{\lambda^2}\right) - \sqrt{E^x}K_x\frac{\sin(2\lambda\mathcal{K}_\varphi)}{\lambda}\right). \tag{4.18e}$$

We isolate K_x from the last equation,

$$K_x = \frac{\mathcal{E}^\varphi\left(2\lambda^2\Lambda E^{x2} - 2E^x\left(\lambda^2+\sin^2(\lambda\mathcal{K}_\varphi)\right) + 2\lambda^2Q^2\right)}{4\lambda E^{x2}\sin(2\lambda\mathcal{K}_\varphi)}, \tag{4.19}$$

and we use (4.18a) to obtain the lapse, i.e.,

$$N = \frac{\lambda\sqrt{1+\lambda^2}\dot{E^x}}{\sqrt{E^x}\sin(2\lambda\mathcal{K}_\varphi)}. \tag{4.20}$$

Inserting this last result in (4.18d) we get, after integration,

$$\frac{\sin(\lambda\mathcal{K}_\varphi)}{\lambda} = \varepsilon_2\sqrt{\frac{2M}{\sqrt{E^x}} - \frac{Q^2}{E^x} + \frac{\Lambda}{3}E^x - 1}, \tag{4.21}$$

with $\varepsilon_2^2 = 1$ and $M \in \mathbb{R}$ an integration constant. Finally, we plug (4.19) and (4.21) in (4.18b), and integrate it to obtain

$$\mathcal{E}^\varphi = c_2\sqrt{E^x}\sqrt{1-\lambda\left(\frac{2M}{\sqrt{E^x}} - \frac{Q^2}{E^x} + \frac{\Lambda}{3}E^x\right)}\sqrt{\frac{2M}{\sqrt{E^x}} - \frac{Q^2}{E^x} + \frac{\Lambda}{3}E^x - 1}, \tag{4.22}$$

with some constant $c_2 \neq 0$. With these relations, all the equations of motion are obeyed. As in the static regions, the gauge will be completely fixed by choosing $\sqrt{E^x}(t)$.

In analogy with the vacuum case, we could consider $\sqrt{E^x}(t) = t$. If we relabelled (t, x) as the pair of real functions $(T, X/c_2)$ on $\mathcal{M}$, the metric would be (3.28) just replacing M with $m(T)$ as defined in (4.16). The coordinate T would be restricted by $2\lambda m(T) < T < 2m(T)$, and contrary to what happens in the static domains, the explicit pole of the metric at $2\lambda m(T)$ would restrict the range of T. To remove it and include those surfaces in the analysis, we make yet another choice of gauge. We fix $E^x(t)$ through its derivative by

$$(\dot{E^x})^2 = 4E^x\left(1 - \frac{2\lambda m(E^x)}{\sqrt{E^x}}\right). \tag{4.23}$$

Renaming $\sqrt{E^x}(t) =: r(t)$ and the pair (t, x) as (z, T)[1] as real functions on $\mathcal{M}$, the metric in this chart reads

$$ds^2 = -\left(\frac{2m\big(r(z)\big)}{r(z)} - 1\right)^{-1} dz^2 + \left(\frac{2m\big(r(z)\big)}{r(z)} - 1\right) dT^2 + r(z)^2 d\Omega^2, \tag{4.24}$$

with $m(r)$ given in (4.16), and the function $r(z)$ satisfying (4.17). The range of these coordinates is $T \in \mathbb{R}$ and z constrained by the conditions $r(z) > 0$ and $r(z) < 2m(r(z))$, and also by the domain of existence of the solution of (4.17), i.e., $2\lambda m\big(r(z)\big) \leq r(z)$.

[1] Mind the order! Note that we use the same names as in the static region above (although in a different order) just for notational convenience, as it will become clear in the following

4.2.3 The covering domain

We yet need to find a chart that covers the surfaces $r = 2\lambda m(r)$ to look for the global structure of the solution, so we produce an additional gauge providing a coordinate system that overlaps static and homogeneous regions.

We partially fix the gauge by requiring $\dot{E}^x = 0$ and $\dot{\mathcal{E}}^\varphi = 0$, and further assume $E^{x\prime}$ does not vanish identically. From $\mathcal{D} = 0$, we obtain

$$K_x = \frac{\mathcal{E}^\varphi \mathcal{K}'_\varphi}{E^{x\prime}}. \tag{4.25}$$

We now solve (4.10a) for N^x, and introduce it in (4.10b),

$$\mathcal{E}^\varphi E^x \sin(2\lambda\mathcal{K}_\varphi)\left(1+\left(\frac{\lambda E^{x\prime}}{2\mathcal{E}^\varphi}\right)^2\right)\left(N'E^{x\prime}\mathcal{E}^\varphi + N(\mathcal{E}^{\varphi\prime}E^{x\prime} - \mathcal{E}^\varphi E^{x\prime\prime})\right) = 0. \tag{4.26}$$

The case $\sin(\lambda\mathcal{K}_\varphi) = 0$ corresponds to the analysis in Sec. 4.2.1. If $\cos(\lambda\mathcal{K}_\varphi)$ was zero, the vanishing of the Hamiltonian constraint would demand $\mathcal{E}^\varphi = 0$, thus making the metric degenerate. Hence, we need to enforce the vanishing of the last factor in (4.26), which integrates to

$$N = \frac{c_3}{2}\frac{E^{x\prime}}{\mathcal{E}^\varphi}, \tag{4.27}$$

for some $c_3 \neq 0$. Using (4.25) the integration of $\mathcal{H} = 0$ yields

$$\frac{\sin(\lambda\mathcal{K}_\varphi)}{\lambda} = \varepsilon_3\left(1+\left(\frac{\lambda E^{x\prime}}{2\mathcal{E}^\varphi}\right)^2\right)^{-1/2}\sqrt{\left(\frac{E^{x\prime}}{2\mathcal{E}^\varphi}\right)^2 - \left(1 - \frac{2M}{\sqrt{E^x}} - \frac{Q^2}{E^x} + \frac{\Lambda}{3}E^x\right)}, \tag{4.28}$$

with $\varepsilon_3^2 = 1$ and M an integration constant. In terms of the above, the shift isolated from (4.10a) reads

$$\begin{aligned} N^x = {}& \varepsilon_4 c_3 \frac{\sqrt{E^x}}{\mathcal{E}^\varphi}\sqrt{1 - \lambda\left(\frac{2M}{\sqrt{E^x}} - \frac{Q^2}{E^x} + \frac{\Lambda}{3}E^x\right)} \\ & \times \sqrt{\left(\frac{E^{x\prime}}{2\mathcal{E}^\varphi}\right)^2 + \frac{2M}{\sqrt{E^x}} - \frac{Q^2}{E^x} + \frac{\Lambda}{3}E^x - 1}, \end{aligned} \tag{4.29}$$

where $\varepsilon_4 = -\operatorname{sgn}\left(\sin(2\lambda\mathcal{K}_\varphi)\right)$. With this, the last equations, (4.10c) and (4.10d), are satisfied.

Let us rename the remaining free functions $\sqrt{E^x}(x) =: r(x)$ and $\mathcal{E}^\varphi(x) =: s(x)$ so that the metric reads

$$ds^2 = -\left(1-\frac{2m(r(x))}{r(x)}\right)dt^2 + \left(1-\frac{2\lambda m(r(x))}{r(x)}\right)^{-1}\left(\frac{s(x)}{r(x)}\right)^2 dx^2 + r(x)^2 d\Omega^2$$
$$+2\left(1-\frac{2\lambda m(r(x))}{r(x)}\right)^{-1/2}\frac{s(x)}{r(x)}\sqrt{\left(\frac{r(x)r'(x)}{s(x)}\right)^2+\frac{2m(r(x))}{r(x)}-1}\,dtdx, \qquad (4.30)$$

after setting $\varepsilon_4 c_3 = 1$ with no loss of generality. The function $m(r)$ is defined in (4.16).

Note that, as in the vacuum case, $s(x)$ may be absorbed through a coordinate transformation $dy = s(x)dx$. Although several choices are possible, we fix

$$s = \sqrt{r^2 - 2\lambda r m(r)} \qquad (4.31)$$

to remove explicit divergences in the coefficient of dx^2 in the metric. Once again, the gauge will be completely fixed after choosing the specific form of $r(x)$. Note that the choice of $s(x)$ introduces explicit poles in the argument of the second square root of the shift (4.29), so we set

$$\big(r'(x)\big)^2 = 1-\frac{2\lambda m(r(x))}{r(x)}. \qquad (4.32)$$

In this way, $r(x)$ is implicitly defined up to its sign. We now rename (t,x) as the pair of real functions (τ,z) on $\mathcal{M}$. The metric reads

$$ds^2 = -\left(1-\frac{2m\big(r(z)\big)}{r(z)}\right)d\tau^2 + 2\sqrt{\frac{2m\big(r(z)\big)}{r(z)}}\,d\tau dz + dz^2 + r(z)^2 d\Omega^2, \qquad (4.33)$$

with the range of z being the domain of existence of the solution of (4.17) plus the requirement $m(r(z)) \geq 0$, while τ covers the real line. Note that any hypersurfaces defined by $m\big(r(z)\big) = 0$ must be located in static regions because $r(z) < m\big(r(z)\big)$ holds in homogeneous regions. Most remarkably, the boundaries $r(z) = 2m(r(z))$ of the static and homogeneous regions that define the horizons are included here. Note that this metric would be the same as its vacuum analog (3.44) just replacing M by $m(r)$.

In all the three cases above, (4.15), (4.24), and (4.33), the coordinate z can be freely shifted by a constant, and the allowed intervals of z will be determined by the zeros of $r(z) = 2\lambda m\big(r(z)\big)$ and $r(z) = 0$, which will be studied in detail in next sections.

4.2.4 Coordinate transformations

Observe that although the static and homogeneous regions do not overlap, the coordinates (τ, z) cover them at least partially, and include always the finite boundaries (horizons) of those regions. Where $m(r) \geq 0$ and $2m\big(r(z)\big) \neq r(z)$, the change from τ to T, given by

$$d\tau = dT + \left(1 - \frac{2m\big(r(z)\big)}{r(z)}\right)^{-1} \sqrt{\frac{2m\big(r(z)\big)}{r(z)}}\, dz, \tag{4.34}$$

is a coordinate transformation from the region $2m\big(r(z)\big) < r(z)$ of (4.33), to any static regions with $m(r) \geq 0$, where (4.15) holds. Besides, that same transformation from the region $r(z) < 2m\big(r(z)\big)$ of (4.33) leads to the whole homogeneous domain where the metric is (4.24). This, along with the fact that $m(r(z)) = 0$ cannot exist in homogeneous regions, proves that the coordinates (τ, z) cover at least one complete homogeneous region and part of one static region, depending on whether some surface $m(r(z)) = 0$ exists.

4.2.5 Near-horizon geometries

In the starting point of the static and covering domains, we set $\dot{E}^x = 0$, $\dot{E}^\varphi = 0$, and $E^{x\prime} \neq 0$. We now deal with the case in which $\sqrt{E^x} = r_a$ is a positive constant. In either case, equation (4.10a) requires $\sin(2\lambda K_\varphi) = 0$. From relation (2.108), the immediate consequence is that

$$m = \frac{r_a}{2}. \tag{4.35}$$

The constraint $\mathcal{D} = 0$ is automatically satisfied and $\mathcal{H} = 0$ provides an equation for r_a, namely

$$r_a^4 \Lambda - r_a^2 + Q^2 = 0, \tag{4.36}$$

with two possible solutions:

$$r_a = \sqrt{\frac{1 \pm \sqrt{1 - 4\Lambda Q^2}}{2\Lambda}} \tag{4.37}$$

provided $4\Lambda Q^2 \leq 1$ and $\Lambda > 0$. Note that the case $\Lambda = 0$ yields $r_a = |Q|$. The case of vanishing Q also leads to a unique solution, given by $r_a = 1/\sqrt{\Lambda}$.

The above solution also satisfies (4.10d). Further, we can obtain K_x from (4.10b), and, after introducing it in (4.10c), we find a partial differential equation for the remaining three functions N, N^x, and $\mathcal{E}^\varphi$. This equation ensures that the reduced two-dimensional Lorentzian

metric (t, x), explicitly given by

$$ds^2|_{L_2} = -N(t,x)^2 dt^2 + \left(\frac{\mathcal{E}^{\varphi}(t,x)}{r_a\sqrt{1-\lambda\ell}}\right)^2 \left(dx + N^x(t,x)dt\right)^2, \tag{4.38}$$

is of constant curvature. More precisely, its Gaussian curvature is

$$k = (1-\lambda\ell)\left(\Lambda - \frac{Q^2}{r_a^4}\right). \tag{4.39}$$

To sum up, this gauge choice leads to the spacetime $\mathcal{M} = L_2 \times S^2$, where L_2 is a Lorentzian space of constant curvature k and S^2 is the sphere of radius r_a. These correspond to the so-called near-horizon geometries [97]. Any consistent choice for $N(t,x)$, $N^x(t,x)$ and $\mathcal{E}^{\varphi}(t,x)$ just provides a different chart for these solutions. Let us show three particular choices: the spatially flat gauge, the symmetric gauge, and the half-null gauge.

Spatially flat gauge

The simplest choice is the diagonal, static, and spatially flat metric with $N^x = 0$, $\dot{N} = 0$, and $\mathcal{E}^{\varphi} = r_a\sqrt{1-\lambda\ell}$. The equation mentioned above reduces to

$$N'' + kN = 0. \tag{4.40}$$

The general solution clearly depends on the sign of k, and it will have two integration constants, c_1 and c_2, that can be absorbed by convenient constant shifts on the coordinates. Relabelling (t, x) as (T, z), the metric is

$$ds^2 = -\sin^2(\sqrt{k}z)dT^2 + dz^2 + r_a^2 d\Omega^2, \tag{4.41a}$$

for $k > 0$, and

$$ds^2 = -|k|^{-1}\sinh^2(\sqrt{|k|}z)dT^2 + dz^2 + r_a^2 d\Omega^2, \tag{4.41b}$$

for $k \leq 0$. Note that the limit $k = 0$ defines a flat L_2. The coordinate z may take values on the whole real line when $k \leq 0$, and it is restricted to the interval $z \in (0, \pi/\sqrt{k})$ when $k > 0$.

Most remarkably, the value of r_a does not depend on $\lambda\ell$, and the effective modifications only affect the curvature of the Lorentzian part k by a global constant factor.

Symmetric gauge

Alternatively, we can consider $N^x = 0, \dot{\mathcal{E}^\varphi} = 0$, and $N^2 = (1-\lambda)a^2/\mathcal{E}^{\varphi 2}$, so that the remaining equation now reads

$$\mathcal{E}^{\varphi\prime\prime}\mathcal{E}^\varphi - 3\mathcal{E}^{\varphi\prime 2} - \frac{k\mathcal{E}^{\varphi 4}}{r_a^2(1-\lambda)} = 0, \tag{4.42}$$

where we have used (4.36). The general solution is

$$\mathcal{E}^\varphi = \varepsilon_5 \left(-\frac{k}{r_a^2(1-\lambda)}(x+c_1)^2 + c_2 \right)^{-1/2}, \tag{4.43}$$

with $\varepsilon_5^2 = 1$. Once again, the arbitrary constants c_1 and c_2 are absorbed by a convenient rescaling of the coordinates $(t, x) \to (T, z)$, and the metric reads

$$ds^2 = -(\epsilon - kz^2)dT^2 + \frac{1}{\epsilon - kz^2}dz^2 + r_a^2 d\Omega^2, \tag{4.44}$$

where the range of z is just restricted by $\epsilon - kz^2 > 0$.

Half-null gauge

We produce a third gauge that will be useful to understand these geometries as limiting cases (with degenerate horizons) of the spacetimes above. The choice is $\mathcal{E}^{\varphi\prime} = 0$, $N^x = N^2$, and

$$N = \sqrt{1-\lambda}\frac{r_a}{\mathcal{E}^\varphi}. \tag{4.45}$$

The equation for the above variables now reduces to

$$\ddot{\mathcal{E}^\varphi}\mathcal{E}^\varphi + (\dot{\mathcal{E}^\varphi})^2 = (1-\lambda)^2\left(1 - \frac{2Q^2}{r_a^2}\right). \tag{4.46}$$

The solution for this equation is

$$\mathcal{E}^\varphi = \varepsilon_6(1-\lambda)\sqrt{1 - \frac{2Q^2}{r_a^2}}\sqrt{(t+c_1)^2 + c_2}, \tag{4.47}$$

with $\varepsilon_6^2 = 1$. Let us rename (t, x) by $(Y - c_1, \zeta)$, and use (4.36) to express $1 - 2Q^2/r_a^2 = 2\Lambda r_a^2 - 1$, so that the metric turns to

$$ds^2 = -\frac{1}{r_a^2}(1 - 2\Lambda r_a^2)(1-\lambda)(Y^2 + c_2)d\zeta^2 + 2dY d\zeta + r_a^2 d\Omega^2. \tag{4.48}$$

Note that we have left the constant c_2, which does not change the geometry but provides different patches [97]. Convenient rescalings of the coordinates allow us to set $c_2 = \{-1, 0, 1\}$.

Near-horizon geometries as limits

Let us check that, just as in GR, the near-horizon geometries can be obtained as a limit of the general family of spacetime solutions. Starting from (4.33), we perform the change of coordinates $(\tau, z) \to (\zeta, Y)$, given by

$$\tau = \frac{1}{\epsilon}\zeta, \tag{4.49a}$$

$$z = z_a + \epsilon Y, \tag{4.49b}$$

where z_a satisfies $r(z_a) = r_a$, and ϵ is an arbitrary parameter. If we now expand $r\big(z(Y)\big)$ in ϵ, i.e., around $z = z_a$, and using (4.17), we find

$$r(z(Y)) = r(z_a) + r'(z_a)(z - z_a) + O((z - z_a)^2) = r_a + \sigma\epsilon\sqrt{1 - \lambda}Y + O(\epsilon^2), \tag{4.50}$$

with $\sigma^2 = 1$. Recall (4.36) and (4.16), where we need to replace r by $r(z(Y))$. Further using (4.51), as specified below, it is a straightforward calculation to insert the above changes in (4.33) so that the limit $\epsilon \to 0$ yields (4.48) with $c_2 = 0$.

Special cases

We have shown that the near-horizon geometries are achievable through a convenient limit of the whole family of spacetimes parametrised by M, Q, and Λ. We now study some particular cases.

First, reading $m(r_a)$ from (4.16) for $r = r_a$, we can obtain

$$M = \frac{r_a}{2} + \frac{Q^2}{2r_a} - \frac{\Lambda}{6}r_a^3 = r_a\left(1 - \frac{2}{3}r_a^2\Lambda\right), \tag{4.51}$$

which, along with (4.37), provides a relation between the parameters M, Q, and Λ. Since neither of those relations depends on λ, they are exactly the same as in GR. In particular, if $\Lambda = 0$,

$$r_a = M = |Q| \qquad \Longrightarrow \qquad k = -\frac{1 - \lambda}{r_a^2}, \tag{4.52}$$

and, if $Q = 0$, which implies necessarily a positive value of Λ,

$$r_a = 3M = \frac{1}{\sqrt{\Lambda}} \qquad \Longrightarrow \qquad k = \frac{1 - \lambda}{r_a^2}, \tag{4.53}$$

which in GR correspond to the Bertotti-Robinson and Nariai spacetimes, that is, to the limits of Reissner-Nordström and Schwarzschild-de Sitter, respectively.

For completeness, we include the ultra-extreme case (see Ref. [98]), which can be seen as the limit where the three horizons coincide, and it is given by

$$r_a = \sqrt{2}|Q| = \frac{3}{2}M = \frac{1}{2\sqrt{\Lambda}} \qquad \Longrightarrow \qquad k = 0, \tag{4.54}$$

and also requires $\Lambda > 0$.

4.2.6 Curvature invariants

In GR, the family of spherically symmetric solutions of the Einstein-Maxwell equations coupled to a cosmological constant Λ have singularities except the near-horizon geometries and the maximally symmetric cases with $M = 0$ and $Q = 0$, that is, Minkowski ($\Lambda = 0$), de Sitter ($\Lambda > 0$), and anti-de Sitter ($\Lambda < 0$). As expected, the limit $\lambda\!\!\!^{-} \to 0$ reproduces all these geometries.

Using the metric in any of the forms (4.15), (4.24), or (4.33), we can compute the ***Ricci scalar***,

$$\mathcal{R} = 4\Lambda\left(1+\frac{\lambda\!\!\!^{-}}{2}\right) + 2\lambda\!\!\!^{-}\left(\frac{3M^2}{r^4} + \frac{Q^2}{r^4}\left(1-\frac{4M}{r}+\frac{Q^2}{r^2}\right) - \Lambda\left(\frac{4M}{r}+\Lambda r^2\right) + \frac{4\Lambda Q^2}{3r^2}\right), \tag{4.55}$$

and the ***Kretschmann scalar***,

$$\begin{aligned}\mathcal{R}_{abcd}\mathcal{R}^{abcd} = {}& \frac{8\Lambda^2}{3}(1+\lambda\!\!\!^{-}) + \frac{48M^2}{r^6} - \frac{96MQ^2}{r^7} + \frac{56Q^4}{r^8} \\ & - \lambda\!\!\!^{-}\left(\frac{8}{3}\Lambda^3 r^2 - \frac{152Q^6}{r^{10}} - \frac{240M^3}{r^7} + \frac{P_8(r)}{r^9}\right) \\ & + \lambda\!\!\!^{-2}\left(\frac{20}{27}\Lambda^4 r^4 - \frac{40}{27}\Lambda^3 r^2 + \frac{16}{3}M\Lambda^3 r + \frac{108Q^8}{r^{12}} + \frac{324M^4}{r^8} + \frac{P_{10}(r)}{r^{11}}\right),\end{aligned} \tag{4.56}$$

with $P_8(r)$ and $P_{10}(r)$ being polynomials of degree 8 and 10 in r, whose specific form is of no further relevance. Both polynomials depend on the parameters M, Q, and Λ, but not on $\lambda\!\!\!^{-}$.

Therefore, and just as in GR, the curvature diverges if points where $r = 0$ are reached. Moreover, and in contrast to GR, where the Ricci scalar is always constant, it diverges for all the cases except for $M = 0$ and $Q = 0$. In addition, the Kretschmann scalar diverges faster than in GR (just compare the inverse powers of r with the case $\lambda\!\!\!^{-} \to 0$). In addition, note that the modified model introduces diverging values of the curvature as $r \to \infty$ for all the cases with $\Lambda \neq 0$, which deviates also from the GR predictions. Therefore, at first sight, the model seems worse than its GR counterpart.

For the sake of completeness, we check that the Ricci scalar of the near-horizon geometries computed from (4.41), and given by

$$\mathcal{R} = 2\left(k + \frac{1}{r_a^2}\right), \tag{4.57}$$

coincides indeed with (4.55) at $r = r_a$ [see (4.37)] using (4.39) and (4.51). Note that in the particular cases $\Lambda = 0$ and $Q = 0$ this reduces to $\mathcal{R} = 2\lambda/Q^2$ and $\mathcal{R} = 4\Lambda(1 - \lambda/2)$, respectively. This can be also obtained as the direct addition of the curvatures of L_2 and S^2 [99].

4.3 Study of singularity resolution

As in GR, non-vanishing values of the mass and the charge make curvature invariants divergent at $r = 0$. But, in addition, a non-vanishing cosmological constant Λ also produces an infinite curvature as $r \to \infty$. However, recall now the singularity-resolution mechanism in vacuum, where curvature divergences were removed by the appearance of a positive lower bound for the area-radius function (r_0), thus making the points $r = 0$ unreachable. In the same way, and to avoid the divergences at $r \to \infty$, the existence of a finite maximum (r_∞) will also be necessary in this case.

The appearance of such bounds is not as straightforward as in vacuum, and it heavily relies on the specific values of the parameters M, Q, Λ, and λ of the solution. In the following, we will comprehensively analyse the ranges of these parameters for which singularities are resolved.

4.3.1 Allowed regions

In addition to $r \geq 0$, which is required by construction, the domain of $r(z)$ is restricted by its defining equation (4.17), which is a nonlinear autonomous differential equation of the form

$$\frac{1}{2}(r')^2 + V(r) = 0, \tag{4.58}$$

with the prime denoting the derivative with respect to the coordinate z. This equation is formally the same as that for the Hamiltonian of a one-dimensional Newtonian particle submerged in the potential $V(r)$ with zero total energy. In this analog model, r would denote the position of the particle at a certain time z. Since the particle can only move in regions where $V(r) \leq 0$, the roots of the potential define the extremes of $r(z)$. There might be several allowed non-overlapping intervals where the lower boundary of each interval is either a root of $V(r)$ or 0. Correspondingly, the upper boundary is either a root of $V(r)$ or infinity.

To study the existence and behaviour of the solution $r(z)$ as an analytic function, we first take the derivative with respect to z of (4.58), and obtain the usual equation for the acceleration,

$$r'' = -\frac{\partial V}{\partial r}, \tag{4.59}$$

at all points where $r'(z) \neq 0$. Besides, by continuity, the expression for the acceleration is satisfied at $r'(z) = 0$.

In contrast to the sign of the velocity $r'(z)$, the acceleration $r''(z)$ is unambiguously defined. Consequently, if $r_\alpha = r(z_\alpha)$ is a simple root of $V(r)$, the continuity of r'' at r_α demands that:

$$\text{If} \quad \frac{\partial V}{\partial r} < 0, \quad \text{then} \quad r'(z) = \operatorname{sgn}(z - z_\alpha)\sqrt{|V(r(z))|} \quad \text{around } z_\alpha. \tag{4.60a}$$

$$\text{If} \quad \frac{\partial V}{\partial r} > 0, \quad \text{then} \quad r'(z) = -\operatorname{sgn}(z - z_\alpha)\sqrt{|V(r(z))|} \quad \text{around } z_\alpha. \tag{4.60b}$$

In the former case, r_α will correspond to a lower bound of the domain of definition of r, whereas it will be an upper bound in the latter. From these relations, one also deduces that the function $r(z)$ will always be symmetric around any such simple roots, i.e., $r(z - z_\alpha) = r(z_\alpha - z)$.

An additional consequence of (4.59) is that if there exists a root r_α of the potential $V(r)$ with multiplicity higher than one, both r' and r'' vanish there. In fact, by recursively deriving (4.59), one sees that all the derivatives of $r(z)$ must be vanishing at that point, and r_α is thus an equilibrium point. Now, consider $n > 1$ to be the smallest integer for which $V^{(n)}(r_\alpha) \neq 0$. On the one hand, if n is odd, r_α is an inflection point and $V(r)$ changes sign there. In such a case, r_α determines the lower — if $V^{(n)}(r_\alpha) < 0$ — or upper — if $V^{(n)}(r_\alpha) > 0$ — bound of some allowed interval, but the particle reaches r_α only for infinite values of z. On the other hand, if n is even, then the potential $V(r)$ has a local minimum — when $V^{(n)}(r_\alpha) > 0$ — or maximum — when $V^{(n)}(r_\alpha) < 0$ — at r_α. In the former case, r_α is a stable equilibrium point, and the particle stays always at $r(z) = r_\alpha$. Therefore, it does not define a finite interval of r. In the latter case, $r(z) = r_\alpha$ is an unstable equilibrium point. The particle takes infinite time z to reach it from either side, and it defines simultaneously a lower and an upper bound of two disjoint intervals of $r(z)$.

Summing up, simple roots of $V(r)$ are turning points of $r(z)$ and define also fixed points of a reflection symmetry. Roots of multiplicity higher than one are only reached at asymptotic values of z and have no associated symmetry. Each of these last intervals in r thus describes an independent spacetime.

In the particular case under study, the potential stands for the rational function

$$V(r) = -\frac{1}{2}\left(1 - \frac{2\lambda m(r)}{r}\right). \tag{4.61}$$

The analysis of singularity resolution is thus reduced to the classification of the roots of $V(r)$, and the behaviour of $V(r)$ there. This will strongly depend on the specific values of M, Q, Λ, and λ. We will focus on the cases in which the solution avoids curvature divergences, that is, those in which a positive lower bound r_0 for $r(z)$ exists. This will be accomplished if there exists a $r_0 > 0$, such that $V(r_0) = 0$ and $V(r)$ is negative on some interval for which r_0 is infimum. Locally, this means that $V(r_0) = 0$ and that the first non-vanishing derivative of $V(r)$ at $r = r_0$ is negative. In addition, as commented above, we must restrict ourselves to cases with a finite upper bound r_∞ whenever the behaviour at $r \to \infty$ is divergent.

Lemma 4.1. *Critical hypersurfaces*. Let

$$P(r,s) := \begin{cases} \dfrac{s\Lambda}{3}r^4 - r^2 + 2sMr - sQ^2, & \text{if } Q \neq 0, \\ \dfrac{s\Lambda}{3}r^3 - r + 2sM, & \text{if } Q = 0, \end{cases} \tag{4.62}$$

so that P is always a polynomial in r with a nonvanishing free term, and fix $s \in (0,1]$. It is straightforward to identify

$$V(r) = \frac{P(r,\lambda)}{2r^\ell}, \tag{4.63}$$

with $\ell = 2$ and $\ell = 1$, for $Q \neq 0$ and $Q = 0$, respectively. A given $r_\alpha > 0$ is a root of $V(r)$ if and only if $P(r_\alpha, \lambda) = 0$. Besides, the sign of the gradient $dV/dr|_{r=r_\alpha}$ is the same as that of $P'(r_\alpha, \lambda)$. By iteration, the first n derivatives of $V(r)$ are vanishing at r_α if and only if the first n derivatives of $P(r,\lambda)$ with respect to its first argument vanish there, that is,

$$\left.\frac{d^n V}{dr^n}\right|_{r=r_\alpha} = 0 \quad \Leftrightarrow \quad P^{(n)}(r_\alpha, \lambda) = 0. \tag{4.64}$$

In addition, the signs of the subsequent derivatives of both functions coincide. The convenience of having introduced the second argument s is evident as $P(r,1) = \big(2m(r) - r\big)r^{\ell-1}$, with $\ell = 1, 2$ for $Q = 0$ and $Q \neq 0$, respectively, will provide the relevant information for the existence of horizons (see (4.33), for instance). Note, in particular, that $P(r,1) \geq 0$ implies, necessarily, $m(r) > 0$. The converse is not true.

From now on, whenever speaking about the roots and derivatives of $P(r,s)$, we will refer to the real roots on and the derivatives with respect to its first argument, respectively. The following results are independent of the specific value of $s \in (0,1]$. A value $r_0(M,Q,\Lambda,s) > 0$ such that $P(r_0,s) = 0$ and either

(a) $P'(r_0,s) < 0$,

(b) $P'(r_0,s) = 0, P''(r_0,s) < 0$,

(c) $P'(r_0,s) = P''(r_0,s) = 0, P'''(r_0,s) < 0$,

(d) $P'(r_0,s) = P''(r_0,s) = P'''(r_0,s) = 0, P''''(r_0,s) < 0$,

exists only in the following cases:

1. $\Lambda > 0, Q \neq 0, M > 0$, with $8Q^2 < 9sM^2$ and $\Lambda \in (\Lambda_-(s), \Lambda_+(s)) \cap (0, \Lambda_+(s))$, and (a) holds.

1D. $\Lambda > 0, Q \neq 0, M > 0$, with $8Q^2 < 9sM^2 < 9Q^2$ and $\Lambda = \Lambda_-(s)$, and (b) holds.

2. $\Lambda > 0, Q = 0$, and $0 < s^{3/2} 3\sqrt{\Lambda} M < 1$, and (a) holds.

3. $\Lambda = 0$ and $\sqrt{s}M > |Q|$ and (a) holds.

3D. $\Lambda = 0$ and $\sqrt{s}M = |Q| > 0$ and (b) holds.

4. $\Lambda < 0, Q \neq 0, \sqrt{s}M > |Q|$ and $\Lambda \in (\Lambda_-(s), 0)$ and (a) holds.

4D. $\Lambda < 0, Q \neq 0, \sqrt{s}M > |Q|$ and $\Lambda = \Lambda_-(s)$ and (b) holds.

5. $\Lambda < 0, Q = 0$, and $M > 0$ and (a) holds.

The bounds for Λ are

$$\Lambda_\pm(s) := \frac{1}{32 s^2 Q^6} \left(8Q^4 - \beta(\beta + 4Q^2) \pm 3\sqrt{sM^2\beta^3} \right), \quad \text{with} \quad \beta := 9sM^2 - 8Q^2. \tag{4.65}$$

Remark 4.1.1 When $\beta > 0$, both $\Lambda_\pm(s)$ are real and distinct. Furthermore, $\Lambda_+(s)$ is always positive while $\Lambda_-(s)$ is negative, vanishing, or positive when $sM^2 - Q^2$ is greater, equal, or smaller than zero, respectively. The limit $\beta = 0$ corresponds to $\Lambda_+(s) = \Lambda_-(s) = (2sQ)^{-2}$. Therefore, the conditions in the first case can be expressed as

1. $\Lambda > 0,\ Q \neq 0,\ M > 0,$ with either $\begin{cases} Q^2 \leq sM^2 \text{ and } \Lambda \in (0, \Lambda_+(s)), & \text{or} \\ 8Q^2 < 9sM^2 < 9Q^2 \text{ and } \Lambda \in (\Lambda_-(s), \Lambda_+(s)). \end{cases}$

Remark 4.1.2 Any b such that $P(b,s) < 0$ and $P'(b,s) < 0$ belongs to the interval where $P(r,s) \leq 0$ with infimum r_0.

Remark 4.1.3 In cases 1, 1D, and 2, the interval where $P(r,s) \leq 0$ with infimum r_0 is also bounded from above. The supremum $r_\infty(M,Q,\Lambda,s)$ satisfies $r_0 \leq r_\infty$, $P(r_\infty,s) = 0$, and $P'(r_\infty,s) > 0$. In addition, the limiting cases in which the largest root of $P(r,s)$ is a double root (say $r_0 = r_\infty$ in that limit), is given by $\Lambda = \Lambda_+(s)$, and then $P'(r_0,s) = 0$ with $P''(r_0,s) > 0$. In the remaining cases, the set $P(r,s) \leq 0$ with infimum r_0 is unbounded from above.

Remark 4.1.4 When $Q \neq 0$ there exists a $R(M,Q,\Lambda,s) > 0$ such that $R \leq r_0$ and $P(r,s) \leq 0$ in $r \in [0,R]$. The limit $R = r_0$, with $P'(r_0,s) = 0$ and $P''(r_0,s) < 0$, corresponds to the double root cases 1D, 3D, and 4D, while $R < r_0$ and $P'(R,s) > 0$ in the rest of cases. When $Q = 0$, no positive roots smaller than r_0 exist.

Remark 4.1.5 If either R, r_0, or r_∞ exists, then $P(r,1) \geq 0$ at those points. As a result, $m(r)$ is positive there.

Remark 4.1.6 When $\Lambda \geq 0$, the function $m(r)$ defined in (4.16) is always positive in the interval where $P(r,s) \leq 0$ with infimum r_0.

Proof. First, we compute the discriminant of the fourth-order polynomial $P(r,s)$:

$$\Delta = \frac{16}{27}s^2\Lambda\left[-16s^4\Lambda^2Q^6 - 3s^2\Lambda\left(27s^2M^4 - 36sM^2Q^2 + 8Q^4\right) + 9(sM^2 - Q^2)\right]. \quad (4.66)$$

We have $\Delta = 0$ if and only if at least two roots are equal. In that case, there are at most two equal roots if and only if

$$-1 < -4s^2\Lambda Q^2 < 3. \quad (4.67)$$

When $\Delta > 0$, there are either four roots or none. If there are four distinct roots, then $\Delta > 0$ necessarily. When $\Delta < 0$, there are only two roots.

Case 1. Assume $\Lambda > 0$ and $Q \neq 0$. For a pictorial representation, see Fig. 4.1.

Since $P(0,s) < 0$ and $P(r,s) > 0$ as $r \to \pm\infty$, then $P(r,s)$ has at least two roots of different sign. We denote the positive one as $r_{1+} > 0$ and the negative one as $r_{1-} < 0$. They satisfy $P'(r_{1-},s) \leq 0$ and $P'(r_{1+},s) \geq 0$. Therefore, r_{1+} cannot be a local maximum. As a result, for r_0 to exist in this case, we need at least a third positive root. In addition, if more roots exist, they must be contained in the interval (r_{1-}, r_{1+}). If $\Delta < 0$, there are no more roots, and no r_0

exists. Let $\Delta > 0$, in which case there are necessarily two more roots. Since the product of the four roots is $-3Q^2/\Lambda$, the two additional roots cannot be zero, and, further, they must have the same sign. Since r_{1+} does not qualify for being r_0, we need the additional two roots to be positive. When $\Delta = 0$, and knowing that we need a third positive root and that the product of all the roots is negative, we find only two cases where r_0 might appear: either the additional positive root is simple, r_{1s}, and r_{1+} is a double root, or it is double, r_{1d}, and r_{1+} is simple. In the former case, $P(r,s) = s\Lambda(r-r_{1+})^2(r-r_{1-})(r-r_{1s})/3$ and $P'(r_{1s},s) > 0$. Thence, r_{1s} does not satisfy the requirements of r_0. In the latter case, $P(r,s) = s\Lambda(r-r_{1+})(r-r_{1-})(r-r_{1d})^2/3$, $P'(r_{1d},s) = 0$, and $P''(r_{1d},s) < 0$. Therefore, r_{1d} is a local maximum.

Assume that $M > 0$. If there is a local maximum of $P(r,s)$, it must be for $r > 0$. Thence, r_{1d} (if $\Delta = 0$ and it exists) and the two additional roots (if $\Delta > 0$) are positive. Let a such that $P'(a,s) = 0$, i.e., $2s\Lambda a^3/3 - a + sM = 0$. Then, $a(3 - 2a^2 s\Lambda) > 0$. If $a < 0$, we must have $3 - 2a^2 s\Lambda < 0$, and, as a result, $P''(a,s) = -2(1 - 2a^2 s\Lambda) > 0$. A local maximum thus needs $a > 0$ necessarily. Besides, there is at most one local maximum of $P(r,s)$. Therefore, if $\Delta = 0$ then r_{1d}, if it exists, is positive, and if $\Delta > 0$, three roots are positive, and the fourth one is negative. In the former case, $r_0 = r_{1d}$ satisfies the requirements [with (b)], and the intervals in $r \geq 0$ where $P(r,s) \leq 0$ are $[0, r_{1d}]$ and $[r_{1d}, r_{1+}]$. In the latter case, let us denote the three positive roots as $0 < r_{1a} < r_{1b} < r_{1+}$. Clearly, only $P'(r_{1b},s) < 0$ and thus $r_0 = r_{1b}$ satisfies the requirements [with (a)]. The ranges where $P(r,s) \leq 0$ in $r \geq 0$ are $[0, r_{1a}]$ and $[r_{1b}, r_{1+}]$. Moreover, since $P'(0,s) = 2sM > 0$, and a local minimum must be located at $a < 0$ (see above), if $b > 0$ satisfies $P(b,s) < 0$ and $P'(b,s) < 0$, then b belongs to the interval (r_0, r_{1+}).

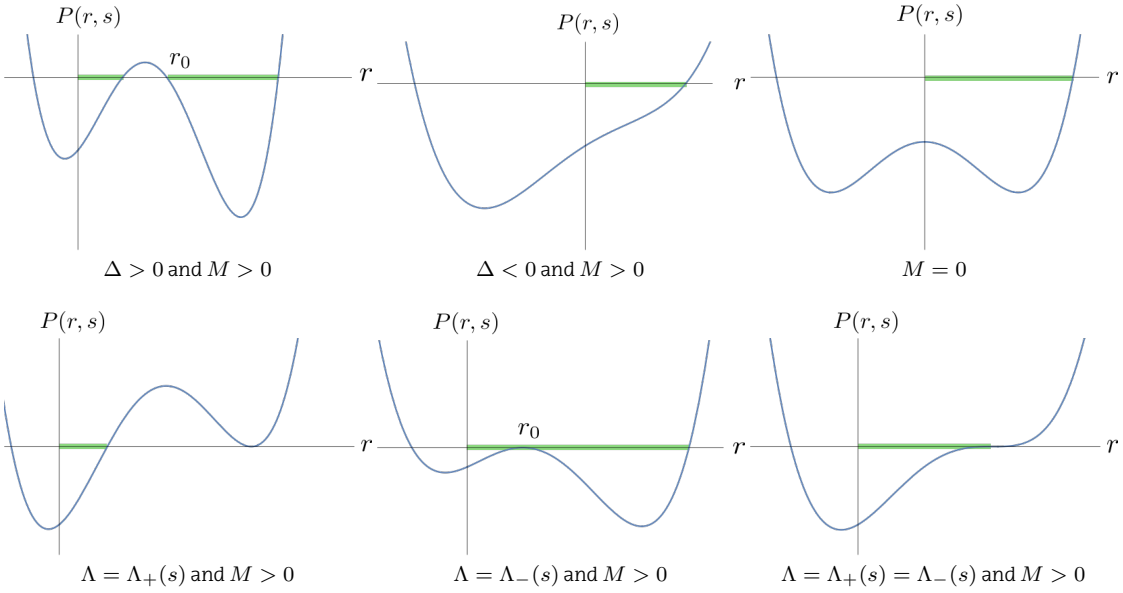

Figure 4.1: Graphical representation of $P(r,s)$ for $\Lambda > 0$, $Q \neq 0$, and $M \geq 0$, with the allowed intervals highlighted in green, and r_0 marked when it exists. For $M < 0$, no r_0 appears since $P(r,s)|_{M=-A} = P(-r,s)|_{M=A}$.

If $M = 0$, the polynomial is even with only one local maximum at $r = 0$, and $P(0, s) < 0$. Therefore, only r_{1+} is a positive root, and none of them can satisfy the requirements of r_0.

Finally, let $M < 0$. Since $P(r, s)$ is invariant under the change $\{M \to -M, r \to -r\}$, and using that r_{1-} cannot be a local maximum either, one needs a third positive root. However, using the same arguments above under the change $r \to -r$, we see that none of the possible roots satisfies the requirements, and thus no r_0 exists.

Case 2. Take $\Lambda > 0$ and $Q = 0$. For a pictorial representation, see Fig. 4.2.

In this case, $P(r, s)$ is a third-order polynomial and has at least one root, r_{2o}. In addition, $P(0, s) = 2sM$, $P'(0, s) = -1$, and the points $a_- = -\sqrt{1/(s\Lambda)}$ and $a_+ = \sqrt{1/(s\Lambda)}$ are a local maximum and a local minimum, respectively. If $M \neq 0$, the root r_{2o} must have the opposite sign of M, and if there are additional roots, their sign is that of M because the product of all of them must equal $2sM$.

Let $M > 0$. Then, $r_{2o} < 0$, and we need more roots to have a positive one. That condition is fulfilled when $P(a_+, s) \leq 0$, i.e., when the local minimum is not positive. Since $P''(r, s) > 0$ for all $r > 0$, we must also ask $P'(r, s) < 0$ at one root. This implies that we need two more distinct roots, and hence, $P(a_+, s) < 0$. These two roots are positive, $0 < r_{2a} < r_{2+}$, and clearly the smallest of the two, $r_0 = r_{2a}$, (and only that) satisfies $P'(r_{2a}, s) < 0$ [i.e., with (a)]. The domain where $P(r, s) \leq 0$ is restricted to the bounded interval $[r_0, r_{2+}]$, and since $a_+ < r_{2+}$ we have $P'(r_{2+}, s) > 0$. Of course, there are no more roots.

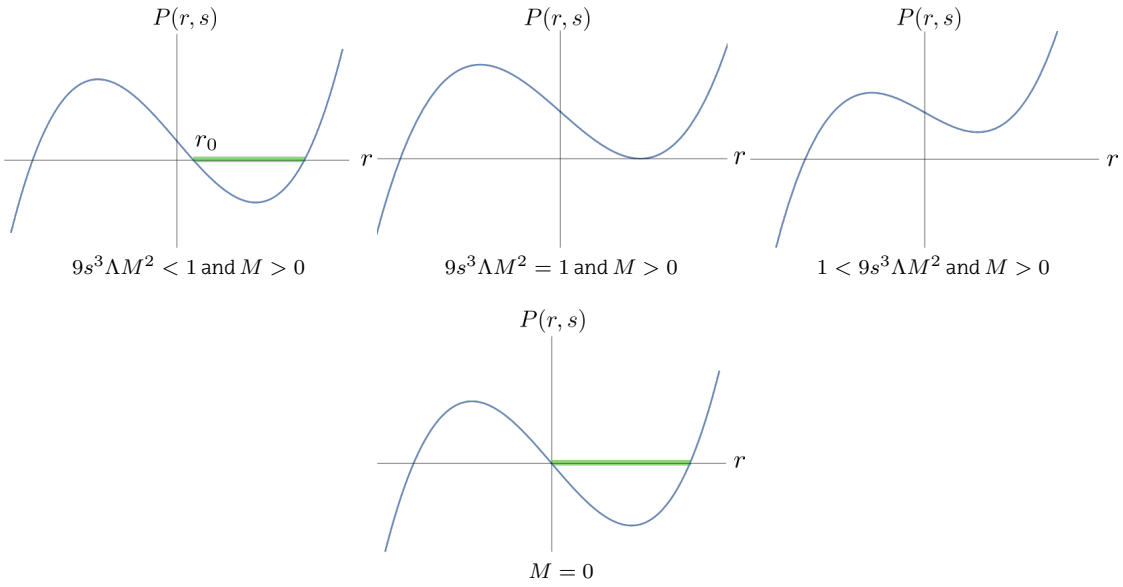

Figure 4.2: Graphical representation of $P(r, s)$ for $\Lambda > 0$, $Q = 0$, and $M \geq 0$. The allowed intervals are highlighted in green, and r_0 is marked when it exists. The cases with $M < 0$ satisfy $P(r, s)|_{M=-A} = -P(-r, s)|_{M=A}$, and thus no r_0 appears.

If $M = 0$, the three roots of the polynomial are $r = 0, \pm\sqrt{3/(s\Lambda)}$, with $P'(r,s) > 0$ at the positive root. Assume now that $M < 0$. Then, $r_{2o} > 0$ is the only possible positive root, with $P'(r_{2o}, s) > 0$. Therefore, no root fulfills the requirements of r_0.

Case 3. Let $\Lambda = 0$. For a pictorial representation, see Fig. 4.3.

When $Q \neq 0$, $P(r,s)$ is just a second-order polynomial in r. The two possible roots are $r_{3\pm} = sM \pm \sqrt{s^2M^2 - sQ^2}$, and the necessary and sufficient condition for their existence is $sM^2 - Q^2 \geq 0$. In particular, this demands $M \neq 0$. Further, when they exist, the roots have the same sign as M. Assume $M > 0$. If $sM^2 - Q^2 > 0$, we have $0 < r_{3-} < r_{3+}$, and the largest of them clearly satisfies the requirements [with (a)]. In this case, the interval where $P(r,s) \leq 0$ with infimum $r_0 = r_{3+}$ is unbounded from above. When $sM^2 - Q^2 = 0$, r_{3-} and r_{3+} degenerate into a double root, $r_d = sM$, with $P'(r_d, s) = 0$. Note that $P''(r,s) < 0$ everywhere, and thus r_d meets the requirements [with (b)] of r_0. Since $P(0,s) < 0$, there are two intervals where $P(r,s) \leq 0$, given by $[0, r_0]$ and $[r_0, \infty)$ with $r_0 = r_d$. Finally, when $M \leq 0$, no root satisfies the requirements because they are negative (if they exist).

When $Q = 0$ the polynomial is $P(r,s) = -r + 2sM$, and we only have one simple root $r_{3s} = 2sM$, with $P'(r,s) = -1$ everywhere. Thus, $r_0 = r_{3s}$ satisfies the requirements [with (a)] if and only if $M > 0$. Further, $P(r,s) < 0$ only for $r > r_{3s}$.

Clearly, if b satisfies $P(b,s) < 0$ and $P'(b,s) < 0$, then $b \in (r_0, \infty)$ in either case.

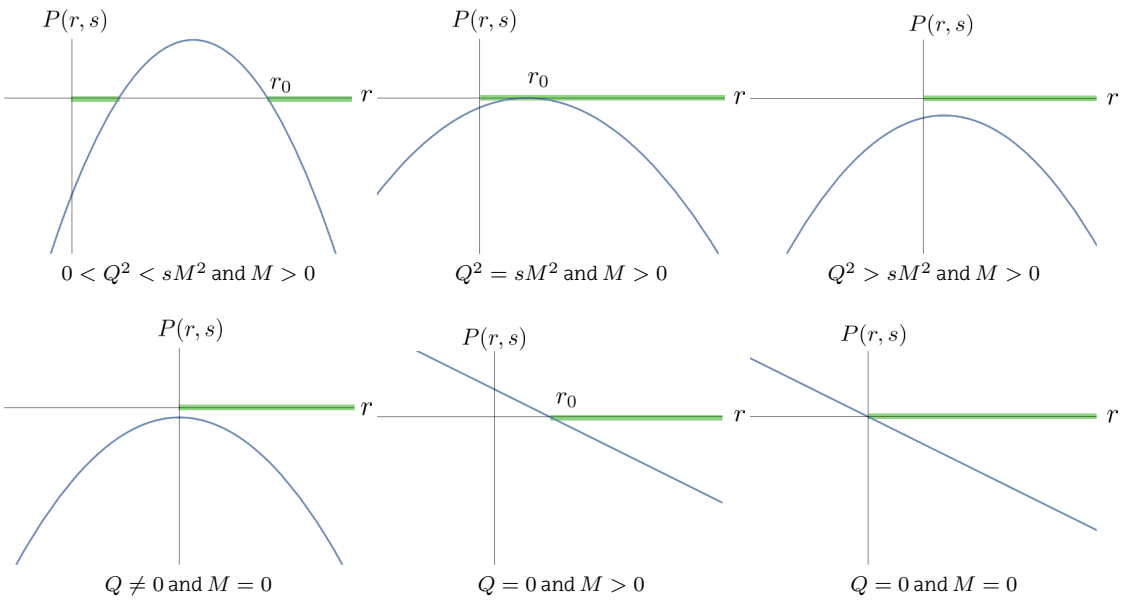

Figure 4.3: Graphical representation of $P(r,s)$ for $\Lambda = 0$ and $M \geq 0$. The allowed intervals are highlighted in green, and r_0 is marked when it exists. For the cases with $M < 0$ no r_0 appears because they satisfy $P(r,s)|_{M=-A} = P(-r,s)|_{M=A}$.

Case 4. Consider $\Lambda < 0$ and $Q \neq 0$. For a pictorial representation, see Fig. 4.4.

Since $P''(r,s) < 0$ for all r and $P(r,s) < 0$ as $r \to \pm\infty$, either there are no roots, there is a double one, or there are two simple roots. In addition, $P(r,s)$ has one and only one maximum in r.

Assume $M > 0$. Then, $P'(0,s) > 0$, and the maximum is located at positive values of r. Since $P(0,s) < 0$, the roots (if any) must be positive. To have a root fulfilling the requirements of r_0, we need either $P'(r_0,s) = 0$ and have a double root r_{4d} (recall $P''(r,s) < 0$), or $P'(r_0,s) < 0$ so that there are two distinct roots $0 < r_{4a} < r_{4b}$. In the former case, we need $\Delta = 0$, while the latter is only possible when $\Delta < 0$. The double root $r_0 = r_{4d}$ satisfies the requirements [with (b)]. When $\Delta < 0$, we have $r_0 = r_{4b}$ satisfying the requirements with (a). In both cases, the interval where $P(r,s) \leq 0$ with infimum r_0 is unbounded from above. Moreover, there is a second interval where $P(r,s) \leq 0$. In the double root case, the interval is $r \in [0, r_0]$ while it is $r \in [0, r_{4a}]$ in the two-simple-root case. In either case if b satisfies $P(b,s) < 0$ and $P'(b,s) < 0$, then $b \in (r_0, \infty)$.

Just as before, the case $M < 0$ can be treated accordingly by changing $r \to -r$. Then, we stick to the previous analysis to see that the roots, if any, are negative. Therefore, $P(r,s) < 0$ for all $r \geq 0$.

Similarly, $P(r,s) < 0$ for all $r \geq 0$ when $M = 0$.

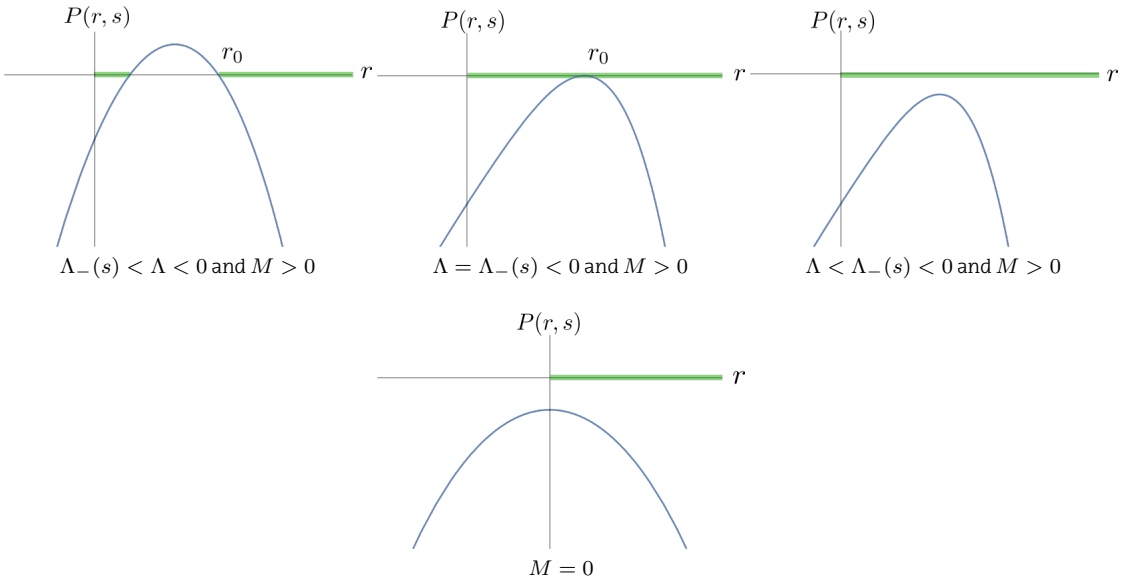

Figure 4.4: Graphical representation of $P(r,s)$ for $\Lambda < 0$, $Q \neq 0$, and $M \geq 0$. The allowed intervals are highlighted in green, and r_0 is marked when it exists. The cases with $M < 0$ satisfy $P(r,s)|_{M=-A} = P(-r,s)|_{M=A}$, and thus no r_0 appears.

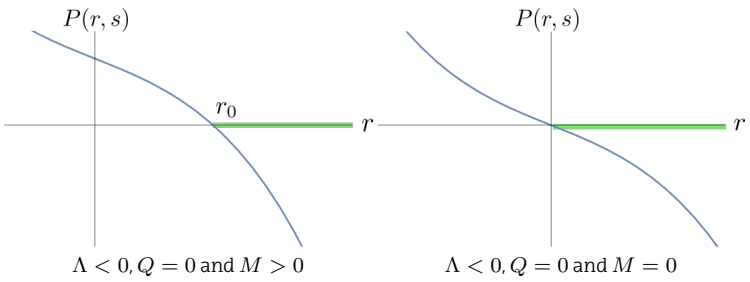

Figure 4.5: Graphical representation of $P(r,s)$ for $\Lambda<0$, $Q=0$, and $M\geq 0$. The allowed intervals are highlighted in green, and r_0 is marked when it exists. For the cases with $M<0$ no r_0 appears because they satisfy $P(r,s)|_{M=-A}=-P(-r,s)|_{M=A}$.

Case 5. Assume $\Lambda<0$ and $Q=0$. For a pictorial representation, see Fig. 4.5.

In this case, $P'(r,s)<0$ for all r and $P(0,s)=2sM$. Therefore there is a positive root if and only if $M>0$. That root is necessarily simple thus satisfying the requirements of r_0 with (a). The interval where $P(r,s)\leq 0$ is $[r_0,\infty)$.

It only remains to study the conditions on Δ for ***Case 1*** and ***Case 4***. With that in mind, let us consider the discriminant a function of Λ and define $f(\Lambda):=\Delta(\Lambda)/\Lambda$, which is a second-order polynomial in Λ with $f''(\Lambda)<0$ for all Λ. Observe that all conditions on Δ are equivalent to $f(\Lambda)\geq 0$. The two solutions for $f(\Lambda)=0$ are $\Lambda_\pm(s)$ as given in (4.65). They exist and are distinct when and only when $\beta:=9sM^2-8Q^2>0$. In such a case, $f(\Lambda)\geq 0$ for $\Lambda\in[\Lambda_-(s),\Lambda_+(s)]$. In the degenerate case $\beta=0$, we find $\Lambda_-(s)=\Lambda_+(s)$ with $f(\Lambda)=0$ only at that point and $f(\Lambda)<0$ elsewhere. Since $f(0)=sM^2-Q^2$, if $f(0)\geq 0$, necessarily $\beta>0$. In addition, $f(0)>0$, $f(0)=0$, and $f(0)<0$ imply $\Lambda_-(s)<0$ and $\Lambda_+(s)>0$, $\Lambda_-(s)=0$ and $\Lambda_+(s)>0$, and (if they exist) $\Lambda_+(s)>0$ and $\Lambda_->0$, respectively. As a result, when $\Lambda>0$, we have $f(\Lambda)>0$ if and only if $\beta>0$. Then, if $f(0)\geq 0$, Λ belongs to the interval $(0,\Lambda_+(s))$, and if $f(0)<0$, then $\Lambda\in(\Lambda_-(s),\Lambda_+(s))$.

Besides, in ***Case 1***, and when $f(\Lambda)=0$ and we have a third double root in $P(r,s)$, we need that (4.67) be satisfied. Since we are sticking to $\Lambda>0$, that relation is just $1-4s^2Q^2\Lambda_\pm(s)>0$. One can check that for $\beta\geq 0$, the following equality holds,

$$1-4s^2Q^2\Lambda_\pm(s)=\frac{\beta}{8Q^4}\left(\beta+4Q^2\mp\sqrt{(\beta+4Q^2)^2-16Q^4}\right). \tag{4.68}$$

Therefore, we have at most one double root if and only if $\beta>0$ in both cases, $\Lambda=\Lambda_-(s)$ and $\Lambda=\Lambda_+(s)$. Recall that a double root r_d must satisfy $P(r_d,s)=0$ and $P'(r_d,s)=0$. First, we consider $4P(r_d,s)-r_dP'(r_d,s)=0$, we solve for $r_d^2=3sMr_d-2sQ^2$, and substitute it (recursively) in $2P(r_d,s)-aP'(r_d,s)=0$. In that way, we obtain an equation linear in both

Λ and r_d. Solving for $1/\Lambda$, and substituting Q^2/r_d by $3M/2 - r_d/(2s)$, we obtain the relation

$$\frac{1}{\Lambda} - 4s^2Q^2 = \frac{2}{3}s^2\beta\left(1 - \frac{sM}{r_d}\right)^{-1}, \tag{4.69}$$

that must hold for $\Lambda = \Lambda_+(s)$ and $\Lambda = \Lambda_-(s)$, thus providing r_{d+} and r_{d-}, respectively. Since $\Lambda_-(s) < \Lambda_+(s)$, we read $r_{d-} < r_{d+}$, and, hence, when $\Lambda = \Lambda_+(s)$ the double root must correspond to r_{1+} (that is, the double root $r_0 = r_\infty$ in Remark 4.1.3). In contrast, $\Lambda = \Lambda_-(s)$ (and as long as $\Lambda_-(s) > 0$, thus making $f(0) < 0$) produces the desired double root that satisfies the conditions of r_0 with (b). As a final remark, let us point out that the extremal case $\Lambda = \Lambda_-(s) = \Lambda_+(s)$ corresponds to a triple root at r_{1+}.

Finally, in ***Case 4*** ($\Lambda < 0$), the only possibility is $f(0) > 0$. Then, $\Lambda \in (\Lambda_-(s), 0)$ for $f(\Lambda) > 0$ and $\Lambda = \Lambda_-(s)$ when $f(\Lambda) = 0$.

We turn our attention to Remark 4.1.5 and Remark 4.1.6.

By construction, the roots R, r_0, and r_∞ of $P(r, s)$, if they exist, are located at $r = 2sm(r)$, so that $m(R) = R/(2s)$, $m(r_0) = r_0/(2s)$, and $m(r_\infty) = r_\infty/(2s)$ are necessarily positive. Then, $P(R, 1) = R^2(1 - s)/s$, $P(r_0, 1) = r_0^\ell(1 - s)/s$, and $P(r_\infty, 1) = r_\infty^\ell(1 - s)/s$ must be non-negative because $s \in (0, 1]$. In particular, they are positive if $s < 1$ and vanish if $s = 1$. Recall that $\ell = 2$ if $Q \neq 0$ and $\ell = 1$ if $Q = 0$.

Now, let us define

$$\mathcal{P}(r) := P(r, 1) + r^\ell = \begin{cases} \dfrac{\Lambda}{3}r^4 + 2Mr - Q^2, & \text{if } Q \neq 0, \\ \dfrac{\Lambda}{3}r^3 + 2M, & \text{if } Q = 0, \end{cases} \tag{4.70}$$

so that $\mathcal{P}(r) = 2r^{\ell-1}m(r)$. Then, the roots of $\mathcal{P}(r)$ coincide with those of $m(r)$, as well as the sign of their first non-vanishing derivatives at those points. Recall that we are restricting the analysis to $\Lambda \geq 0$, and, as shown above, the existence of r_0 is contingent upon $M > 0$. Then, it is clear that $m(r) > 0$ everywhere if $Q = 0$. When $Q \neq 0$, we find that $\mathcal{P}'(r) > 0$ at all points $r > 0$, and also that $\mathcal{P}(0) < 0$. Then, $\mathcal{P}(r)$, and consequently $m(r)$, has one and only one positive root. Since $m(R) > 0$, that root is located in $(0, R)$, with $R \leq r_0$.

□

4.3.2 Existence of a positive infimum

As shown in Lemma 4.1, a positive lower bound $r_0(M, Q, \Lambda, \lambda)$ for the area-radius function exists only when $M > 0, 8Q^2 < 9\lambda M^2$, and $\Lambda \in \big[\Lambda_-(\lambda), \Lambda_+(\lambda)\big)$, with

$$\Lambda_\pm(\lambda) := \frac{3}{32\lambda^4 Q^6}\left[36\lambda^3 M^2 Q^2 - 27\lambda^4 M^4 - 8\lambda^2 Q^4 \pm \sqrt{\lambda^5 M^2\left(9\lambda M^2 - 8Q^2\right)^3}\right]. \quad (4.71)$$

Note that these conditions are valid in the limit $Q = 0$, where

$$\lim_{Q\to 0} \Lambda_-(\lambda) = -\infty \qquad \text{and} \qquad \lim_{Q\to 0} \Lambda_+(\lambda) = \frac{1}{9\lambda^3 M^2}, \quad (4.72)$$

and one should just consider $M > 0$ and $\Lambda \in \big(-\infty, \Lambda_+(\lambda)\big)$.

We can refine these conditions by splitting them in terms of the sign of Λ and the value of Q. The positive lower bound exists in the following cases:

- $C_1 := \Big\{\Lambda > 0, Q \neq 0, M > 0, 8Q^2 < 9\lambda M^2, \text{and } \Lambda \in \big(\Lambda_-(\lambda), \Lambda_+(\lambda)\big) \cap \big(0, \Lambda_+(\lambda)\big)\Big\}$ [2],
- $C_2 := \Big\{\Lambda > 0, Q = 0, M > 0, \text{and } \Lambda \in \big(0, 1/(9\lambda^3 M^2)\big)\Big\}$,
- $C_3 := \Big\{\Lambda = 0, Q \neq 0, M > 0, \text{and } |Q| < \sqrt{\lambda} M\Big\}$,
- $C_4 := \Big\{\Lambda = 0, Q = 0, \text{and } M > 0\Big\}$,
- $C_5 := \Big\{\Lambda < 0, Q \neq 0, M > 0, |Q| < \sqrt{\lambda} M, \text{and } \Lambda \in \big(\Lambda_-(\lambda), 0\big)\Big\}$,
- $C_6 := \Big\{\Lambda < 0, Q = 0, \text{and } M > 0\Big\}$,

where $r_0(M, Q, \Lambda, \lambda)$ is a simple root of $P(r, \lambda)$, and

- $D_1 := \Big\{\Lambda > 0, Q \neq 0, M > 0, \text{with } 8Q^2 < 9\lambda M^2 < 9Q^2 \text{ and } \Lambda = \Lambda_-(\lambda)\Big\}$,
- $D_3 := \Big\{\Lambda = 0, Q \neq 0, \text{and } |Q| = \sqrt{\lambda} M\Big\}$,
- $D_5 := \Big\{\Lambda < 0, Q \neq 0, |Q| < \sqrt{\lambda} M, \text{and } \Lambda = \Lambda_-(\lambda)\Big\}$,

where $r_0(M, Q, \Lambda, \lambda)$ is a double root of $P(r, \lambda)$.

In cases C_1, C_3, and C_5, there are at most three positive bounds, R, r_0, and r_∞, for the allowed regions. By Remark 4.1.4, the degeneracy of R and r_0 into a double root defines the corresponding degenerate cases D_1, D_3, and D_5. For vanishing charge, r_0 is always simple, and C_2, C_4, and C_6 do not have a degenerate counterpart.

In the following, we will just write R, r_0, and r_∞ omitting the dependence on M, Q, Λ, and λ.

[2] By remark 4.1.1, this is either $\{0 < |Q| \leq \sqrt{\lambda} M \text{ and } \Lambda \in (0, \Lambda_+(\lambda))\}$ or $\{0 < 2\sqrt{2}|Q| < 3\sqrt{\lambda} M < 3|Q| \text{ and } \Lambda \in (\Lambda_-(\lambda), \Lambda_+(\lambda)), \text{with } \Lambda_-(\lambda) > 0\}$.

The generic features for the existence of r_0 are a positive mass parameter M, an upper bound for Q^2 proportional to λM^2, and also that Λ must be below a certain maximum threshold. These requirements are qualitatively similar to the conditions for the existence of horizons in GR. Far from being a coincidence, it should be clear that the proof for the existence of horizons is the one just performed in Lemma 4.1 for the specific case $P(r, 1)$.

For the sake of clarity, we have arranged the singularity-free cases correspondingly to well-known black-hole solutions in GR. Cases C_1 and D_1 correspond to Reissner-Nordström-de Sitter, C_2 to Schwarzschild-de Sitter, C_3 and D_3 to Reissner-Nordström, C_4 to Schwarzschild, C_5 and D_5 to Reissner-Nordström-anti-de Sitter, and C_6 to Schwarzschild-anti-de Sitter. The "trivial" (in the sense that they do not possess singularities at $r = 0$) cases of de Sitter, anti-de Sitter, and the flat Minkowski metric are not included in the above list. Regarding the near-horizon geometries, Bertotti-Robinson is not in that list, whereas Nariai is included in C_2. This will become evident when studying the global structure and the horizons of these solutions. However, let us recall that none of the near-horizon geometries are singular.

4.3.3 Existence of a finite supremum

By Remark 4.1.3, the cases in which r_0 exists have a supremum r_∞ if and only if $\Lambda > 0$. In the cases C_1 and C_2, r_0 and r_∞ are simple roots of the polynomial $P(r, \lambda)$ and thus define lower and upper turning points, respectively. In the cases C_3, C_4, C_5, and C_6, r_0 will be the only turning point. In all cases, the solution $r(z)$ has support on the whole real line $z \in \mathbb{R}$, and the ranges for the images are given as follows:

- In C_1 and C_2, the solution $r(z)$ has image on $[r_0, r_\infty]$. The turning points r_0 and r_∞ are reached for finite values of z. Both are symmetry points, and $r(z)$ is thus periodic.

- In C_3, C_4, C_5, and C_6, the solution $r(z)$ has image on $[r_0, \infty)$. The solution is symmetric around the unique turning point r_0. In addition, $r(z) \to \infty$ as $z \to \pm\infty$.

In the degenerate cases where r_0 is a double root, it describes an unstable equilibrium point, which can only be reached at infinite values of z. Therefore:

- In D_1, the solution $r(z)$ has image on $(r_0, r_\infty]$. The solution is symmetric around the turning point r_∞, and $r(z) \to r_0$ as $z \to \pm\infty$.

- In D_3 and D_5, the solution $r(z)$ has image on (r_0, ∞). There are no symmetry points, and this solution goes from $r(z) \to r_0$ as $z \to -\infty$ to $r(z) \to +\infty$ as $z \to +\infty$.

Since curvature invariants diverge for large radii, the cases with a negative cosmological constant (C_5, D_5, and C_6) will not meet our requirements of singularity freedom. Therefore, the present model provides singularity-free domains in the cases C_1, C_2, C_3, and C_4, as well as in the degenerate cases D_1 and D_3.

4.3.4 Non-uniqueness of the spacetime solutions

Whenever $Q \neq 0$, certain values of the parameters define two different spacetimes. One of them is free of singularities and included in the above cases, with r_0 being the infimum of r. The other one contains the origin $r = 0$ and has an upper bound $R \leq r_0$. Note that $P(0, \lambda) < 0$ and $P'(0, \lambda) > 0$ in these cases.

By Remark 4.1.4, we have the following:

- In C_1, C_3, and C_5, the solution $r(z)$, with image on $(0, R]$, has support on an interval $z \in (-z_0, z_0) \subset \mathbb{R}$. This solution is symmetric around $r(0) = R$, where $R < r_0$ is a critical point satisfying $P(R, \lambda) = 0$ and $P'(R, \lambda) > 0$. Besides, $r(\pm z_0) = 0$.
- In D_1, D_3, and D_5, the critical points r_0 and R coincide. In these degenerate cases, the solution $r(z)$, with image on $(0, r_0)$, has support on an interval $z \in (z_0, \infty) \subset \mathbb{R}$. It is a monotonic function, and the constant z_0 can be chosen so that $r(z_0) = 0$ and $r \to r_0$ as $z \to \infty$. The solution has no symmetry points.

This means that different solutions of $r(z)$ provide different spacetimes. Thus, the generalisation of the GR Hamiltonian just presented originates the existence of more than one spacetime solution for the same set of values of the constant parameters M, Q, Λ, and λ whenever $Q \neq 0$. Nevertheless, the singularity-free requirement singles out only one among the two possible solutions.

4.4 Global structure of the new singularity-free spacetimes

We turn our focus to the global structure of the singularity-free spacetime families found above. That is, we restrict the analysis to the sets of values for the parameters M, Q, Λ, and λ included in cases C_1, C_2, C_3, C_4, D_1, and D_3. This means that r_0 exists, and that it is the minimum of the area-radius function r. In addition, we can read the generic conditions $M > 0$ and $\Lambda \geq 0$. By Remark 4.1.6, the mass $m(r)$ will thus be positive in the whole region with infimum r_0, which is completely covered by the coordinates (τ, z) and the line element (4.33). Making contact with the previous study in vacuum, this domain will be named $\mathcal{U} \in \mathcal{M}$, denoting the region with infimum r_0 and, when $\Lambda > 0$, with supremum r_∞.

Note that we are excluding the near-horizon geometries from this analysis. Their qualitative properties (and conformal diagrams) are the same as in GR (see Ref. [97]).

4.4.1 Causal structure

The geometry of the hypersurfaces of constant z is described by the induced metric

$$h_{\mu\nu}dx^\mu dx^\nu = -G(r)d\tau^2 + r^2 d\Omega^2, \tag{4.73}$$

with constant $r = r(z)$. The function G can be intrinsically defined as the norm of the Killing vector field ∂_τ, that is,

$$G := -\tau^\mu \tau_\mu = 1 - \frac{2m(r)}{r}. \tag{4.74}$$

Therefore, the hypersurfaces are timelike or spacelike when $G > 0$ or $G < 0$, respectively (i.e., when ∂_τ is timelike or spacelike), and the set of points $\mathcal{Z}$ where $G|_{\mathcal{Z}} = 0$ is a Killing horizon because ∂_τ is null there.

Next, we compute the mean curvature vector, with components $H^\mu = (2/r)\nabla^\mu r$, of the surfaces of constant τ and z, which corresponds to spheres of constant area $4\pi r^2$:

$$H^\mu \partial_\mu = \frac{2}{r}\frac{dr(z)}{dz}\left(\sqrt{\frac{2m(r)}{r}}\partial_\tau + \left(1 - \frac{2m(r)}{r}\right)\partial_z\right). \tag{4.75}$$

This vector is future-pointing when $dr/dz > 0$ and past-pointing when $dr/dz < 0$. Its norm,

$$H^\mu H_\mu = \frac{4}{r^2}\left(\frac{dr(z)}{dz}\right)^2\left(1 - \frac{2m(r)}{r}\right) = \frac{4}{r^2}\left(1 - \frac{2\lambda m(r)}{r}\right)\left(1 - \frac{2m(r)}{r}\right), \tag{4.76}$$

is manifestly scalar, and thus holds at all points in the manifold. Using that $\lambda \in (0, 1)$, we find that $H^\mu \partial_\mu$ is spacelike when $r > 2m(r)$, null (and non-vanishing) when $r = 2m(r)$, timelike when $r < 2m(r)$ and $r \neq 2\lambda m(r)$, and identically vanishing when $r = 2\lambda m(r)$ (because $dr/dz = 0$ there).

As a result, the spheres of constant τ and z in $\mathcal{U}$ have the following properties:

- They are non-trapped where $r > 2m(r)$.
- They are marginally trapped at the horizons $r = 2m(r)$.
- They are trapped to the future where $r < 2m(r)$ and $dr/dz > 0$.
- They are trapped to the past where $r < 2m(r)$ and $dr/dz < 0$.

In addition, since the hypersurfaces $r = 2\lambda m(r)$ belong necessarily to regions with $G < 0$, they are minimal and spacelike, and they are covered by two-spheres of constant area $4\pi r_0^2$ or $4\pi r_\infty^2$. The non-trapped regions are static, with a timelike ∂_τ, while the homogeneous regions, with a spacelike ∂_τ, are trapped or anti-trapped, depending on the sign of dr/dz.

4.4.2 Horizons

A most relevant fact is that the function G is independent of the parameter λ, and therefore the existence of horizons and their location is determined just as in GR. There are at most three horizons, r_I, r_H, and r_C, each of them related to one of the "classical" parameters of the model, namely, Q, M, and Λ. When $M > 0$, there exists the horizon r_H, the null boundary between a homogeneous ($r < r_H$) and a static ($r > r_H$) region. The inner Cauchy horizon r_I may appear only when $Q \neq 0$, creating an additional (innermost) static region $0 < r < r_I$, with $r_I \leq r_H$. Finally, there is a cosmological horizon $r_C \geq r_H$ whenever $\Lambda > 0$, beyond which G becomes negative. These horizons correspond to the roots of G, and may degenerate into the extremal cases $r_I = r_H, r_H = r_C$, or $r_I = r_H = r_C$, when the multiplicity of the root is higher than one. To analyse the horizon structure of the above solutions, we note that

$$G(r) = -\frac{P(r,1)}{r^\ell}, \tag{4.77}$$

with $\ell = 2$ for $Q \neq 0$ and $\ell = 1$ for $Q = 0$. The existence of the horizons is thus determined by Lemma 4.1. The only difference is that the sign of the first non-vanishing derivative of $G(r)$ and $P(r,1)$ will be the opposite, but, in contrast to what happened with $V(r)$ for the existence of r_0, the sign does not affect the existence of a horizon. Therefore, the sign of the first non-vanishing derivative of $P(r,1)$ is of no relevance. As a side result, the intervals for the existence of r_I, r_H, and r_C will be closed. Restoring the explicit dependence of the critical values R, r_0, and r_∞ on the parameters of the model, they correspond to $r_I := R(M,Q,\Lambda,1)$, $r_H := r_0(M,Q,\Lambda,1)$, and $r_C := r_\infty(M,Q,\Lambda,1)$. Of course, their relative position is the same as in GR, but we need to study whether they are located inside $\mathcal{U}$ or not. Recall that we are restricting to cases C_1, C_2, C_3, C_4, D_1, and D_3. Note also that the roots of $V(r)$ and $G(r)$ cannot coincide.

First, the root r_I of $G(r)$ exists if and only if $Q \neq 0$ because $G(R) < 0$, and $\lim_{r\to 0^+} G(r) > 0$ only when $Q \neq 0$. In that case, $r_I < R \leq r_0$, and the Cauchy horizon is always outside $\mathcal{U}$. As it will be shown later, the conformal diagram does not change when including charge. For $\Lambda = 0$, neither r_∞ nor r_C exists. Since $G(r_0) < 0$ and $\lim_{r\to\infty} G(r) = 1$, the horizon r_H is always located in $\mathcal{U}$. When $\Lambda > 0$, and given $G(r_0) = G(r_\infty) < 0$, there can be no horizons, one degenerate horizon or two horizons.

Lemma 4.2. *Horizons*. Consider $\Lambda_\pm(s)$ defined in (4.65), with $\mu := (8Q^2)/(9M^2) < 1$, as functions of s with support on $(\mu, 1]$. Then both $\Lambda_\pm(s)$ are monotonically decreasing functions attaining their minimum at $s = 1$.

Remark 4.2.1 The function $I(s) := \Lambda_+(1) - \Lambda_-(s)$ has one and only one root $h(M, Q)$.

Remark 4.2.2 The root $r_H = r_0(M, Q, \Lambda, 1)$ of $P(r, 1)$ exists if and only if $s \geq h$, and it is always greater than $r_0(M, Q, \Lambda, s)$. The root is double if $\Lambda = \Lambda_+(1)$ and simple otherwise.

Proof. Let us define $f_\sigma(s) := (32/3)Q^6\Lambda_\sigma(s) + 27M^4$ on $(\mu, 1]$, with $\sigma = \pm 1$. Both $\Lambda_\sigma(s)$ reach their minimum at $s = 1$ if and only if $f_\sigma(s)$ do. Using $8Q^2 = \mu 9M^2$, we find

$$\frac{27M^4}{8} f_\sigma(s) = \left(3\frac{\mu}{s}\left(4 - \frac{\mu}{s}\right) + \varepsilon 8\left(1 - \frac{\mu}{s}\right)^{3/2}\right), \tag{4.78}$$

with $\varepsilon = \sigma\,\mathrm{sgn}(M)$. It is now a straightforward computation to obtain

$$\frac{27M^4}{8} f'_\sigma(s) = \frac{6\mu}{s^3}\left(\mu - 2s + 2\varepsilon(s-\mu)\left(1 - \frac{\mu}{s}\right)^{-1/2}\right) = -\frac{6\mu}{s^3}\left(\sqrt{s-\mu} - \varepsilon\sqrt{s}\right)^2, \tag{4.79}$$

where we needed to consider $s > 0$ and $s - \mu > 0$. As a result, $f'(s) < 0$ in the whole interval $(\mu, 1]$. This proves that both $\Lambda_\pm(s)$ are monotonically decreasing functions of s.

By the above, $I(s) := \Lambda_+(1) - \Lambda_-(s)$ is monotonically increasing for $s > \mu$. In addition, $I(1) > 0$ and $I(\mu) < 0$ for $\mu \in (0, 1)$. Therefore, there can only be one value h such that $I(h) = 0$. We can further constrain that value because $I(9\mu/8) > 0$.

Now, the application of Lemma 4.1 and Remark 4.1.1 for $s = 1$ ensures that $\Lambda_+(1) > 0$ exists. Then, $r_H = r_0(M, Q, \Lambda, 1)$ exists only when (i) $\Lambda \in (\Lambda_-(1), \Lambda_+(1)) \cup (0, \Lambda_+(1))$ (and it is a simple root), (ii) $\Lambda = \Lambda_-(1)$ (and it is a double root), or (iii) $\Lambda = \Lambda_+(1)$ (and it is a double root). We include the third case because we are no longer worried about the sign of $P(r, 1)$ in the surroundings of r_H. The intersections of these intervals with those for the existence of $r_0(M, Q, \Lambda, s)$ yield $\Lambda \in \left[\Lambda_-(s), \Lambda_+(1)\right]$ because we proved above that $\Lambda_\pm(1) \leq \Lambda_\pm(s)$. Note that the interval is empty when $I < 0$. Then, case (ii) does not satisfy the requirements, while cases (i) and (iii) produce a non-empty interval if and only if $I(s) \geq 0$, meaning that $s \geq h$ necessarily because $\Lambda_-(s)$ decreases with s. There are three different possibilities: $s > h$ with either $\Lambda \in \left[\Lambda_-(s), \Lambda_+(1)\right)$, and r_H is simple, or $\Lambda = \Lambda_+(1)$, and r_H is double; and $s = h$ such that $\Lambda = \Lambda_-(s) = \Lambda_+(1)$, and r_H is a double root by Remark 4.1.3.

□

Lemma 4.2 sets the bounds for the existence of r_H and r_C in $\mathcal{U}$. For case C_2, let us recall (4.72), so the limiting condition $\Lambda = \Lambda_+(1)$ becomes $3\sqrt{\Lambda}M = 1$, just as in Schwarzschild-de Sitter.

In summary, each of the families C_1, C_2, and D_1 is subdivided in three disjoint and complementary cases

- $C_1^{\text{BH}} := \Big\{ C_1 \mid \Lambda_+(1) > \Lambda_-(\lambda) \text{ and } \Lambda \in \big(\Lambda_-(\lambda), \Lambda_+(1)\big) \cap \big(0, \Lambda_+(1)\big) \Big\}$,
- $C_1^{\text{EXT}} := \Big\{ C_1 \mid \Lambda_+(1) > \Lambda_-(\lambda) \text{ and } \Lambda = \Lambda_+(1) \Big\}$,
- $C_1^{\text{COS}} := \Big\{ C_1 \mid \Lambda_+(1) \leq \Lambda_-(\lambda) \text{ or } \Lambda \in \big(\Lambda_+(1), \Lambda_+(\lambda)\big) \Big\}$,
- $C_2^{\text{BH}} := \Big\{ C_2 \mid \Lambda \in \big(0, 1/(9M^2)\big) \Big\}$,
- $C_2^{\text{EXT}} := \Big\{ C_2 \mid \Lambda = 1/(9M^2) \Big\}$,
- $C_2^{\text{COS}} := \Big\{ C_2 \mid \Lambda \in \big(1/(9M^2), 1/(9M^2\lambda^3)\big) \Big\}$,
- $D_1^{\text{BH}} := \Big\{ D_1 \mid \Lambda = \Lambda_-(\lambda) < \Lambda_+(1) \Big\}$,
- $D_1^{\text{EXT}} := \Big\{ D_1 \mid \Lambda = \Lambda_-(\lambda) = \Lambda_+(1) \Big\}$,
- $D_1^{\text{COS}} := \Big\{ D_1 \mid \Lambda = \Lambda_-(\lambda) > \Lambda_+(1) \Big\}$,

with

$$\Lambda_\pm(1) := \frac{3}{32Q^6}\left[36M^2Q^2 - 27M^4 - 8Q^4 \pm \sqrt{M^2\left(9M^2 - 8Q^2\right)^3}\right], \tag{4.80}$$

while $C_3^{\text{BH}} := C_3$, $C_4^{\text{BH}} := C_4$, and $D_3^{\text{BH}} := D_3$.

The labels in each subcases are descriptive: We use the superscript "BH" for black hole, so that in C_1^{BH}, C_2^{BH}, and D_1^{BH} both r_H and r_C exist with $r_H < r_C$. In turn, the superscript "COS" stands for Kantowski-Sachs-type solutions where neither r_H nor r_C exists. The cases labelled with the superscript "EXT" correspond to the extremal cases between "BH" and "COS", where the horizons exist and are degenerate, $r_H = r_C$. In cases C_3, C_4, and D_3, the critical hypersurface $r = r_0$ is always hidden inside a horizon r_H, and no further horizons exist.

The deep connection between the horizons r_I, r_H, and r_C, and the critical points R, r_0, and r_∞, as the corresponding roots of $r = 2m(r)$ and $r = 2\lambda m(r)$ allows us to summarise the singularity resolution principle of this model in the following compact form:

"The solution with parameters $(M, Q^2, \Lambda, \lambda)$ avoids the singularity at $r = 0$ if and only if the singularity of a GR black hole with parameters $(\lambda M, \lambda Q^2, \lambda\Lambda)$ is not naked."

This is easy to see because a rescaling $(M, Q^2, \Lambda) \to (\lambda M, \lambda Q^2, \lambda\Lambda)$ maps $G = 0$ to $V = 0$.

4.4.3 Compactification of the covering domain

So far, we already know the character of the horizons $r = 2m(r)$, and also that the hypersurfaces $r = 2\lambda m(r)$ are spacelike [by Remark(4.1.5)] when the critical values of $r(z)$ are simple roots of $V(r)$. However, to eventually complete the form of the Penrose diagrams, we still need to tackle the nature of the double zeros of $V(r)$, which, as seen previously, correspond to $z \to \pm\infty$. We recall that the zeros of $V(r)$ and $G(r)$ cannot coincide.

For that purpose, we study the radial geodesics in the regions around those values of r. Recall that $m(r)$ is necessarily positive there, so all the roots of $G(r)$ and $V(r)$ are covered by or lay at the boundary of the coordinates (τ, z). Considering the affine parameter s (not to be mixed with the constant $s \in (0, 1]$ in Lemma 4.1 and Lemma 4.2), the radial geodesics of (4.33) are determined by

$$\gamma = -\left(1 - \frac{2m(r(z))}{r(z)}\right)\left(\frac{d\tau}{ds}\right)^2 + \left(\frac{dz}{ds}\right)^2 + 2\sqrt{\frac{2m(r(z))}{r(z)}}\frac{d\tau}{ds}\frac{dz}{ds}, \tag{4.81a}$$

$$\mathcal{E} = -\left(1 - \frac{2m(r(z))}{r(z)}\right)\frac{d\tau}{ds} + \sqrt{\frac{2m(r(z))}{r(z)}}\frac{dz}{ds}, \tag{4.81b}$$

with $\tau = \tau(s)$ and $z = z(s)$, $\gamma = 0$, 1, or -1 for null, spacelike or timelike geodesics, respectively, and $\mathcal{E}$ the conserved quantity associated with the timelike Killing vector field ∂_τ, that is, the energy. Combining both equations, we get

$$\left(\frac{dz}{ds}\right)^2 = \mathcal{E}^2 + \gamma\left(1 - \frac{2m(r(z))}{r(z)}\right). \tag{4.82}$$

Note that z is an affine parameter of the radial null geodesics with non-zero energy, because dz/ds is constant. Therefore, the affine distance from any points towards a double root of $V(r)$ goes to infinity. The same holds for all timelike and spacelike geodesics because of the $r'(z)$ term in the denominator of the integral for the proper time or affine parameter. In con-

sequence, geodesics are inextendible at any double roots of $V(r)$, and they must then represent "infinities" in our manifold.

Following the usual procedure (see Ref. [98, 100]), we write the null geodesic vector fields

$$l^\mu \partial_\mu = \left(1 + \sqrt{\frac{2m(r)}{r}}\right)^{-1} \partial_\tau - \partial_z, \tag{4.83a}$$

$$k^\mu \partial_\mu = \left(1 - \sqrt{\frac{2m(r)}{r}}\right)^{-1} \partial_\tau - \partial_z, \tag{4.83b}$$

for $r \neq 2m(r)$. The affine parametrisation means that their metrically associated one-forms are exact, so we can define the functions U and V outside the horizons as

$$dU = -l_\mu dx^\mu = d\tau + \left(1 + \sqrt{\frac{2m(r(z))}{r(z)}}\right)^{-1} dz, \tag{4.84a}$$

$$dV = -k_\mu dx^\mu = d\tau - \left(1 - \sqrt{\frac{2m(r(z))}{r(z)}}\right)^{-1} dz. \tag{4.84b}$$

The additional changes $dU = A(u)du$ and $dV = B(v)dv$ for any arbitrary functions $A(u)$ and $B(v)$, as long as they are smooth and nowhere vanishing, produce Kruskal-type coordinates, with compact ranges for u and v. The metric in terms of these new null coordinates (u, v),

$$ds^2 = -G\big(r(u,v)\big)A(u)B(v)dudv + r(u,v)^2 d\Omega^2, \tag{4.85}$$

is conformally flat at the Lorentzian part. One can check that the determinant of the Jacobian of the change $(\tau, z) \to (U, V)$ is $G(r)/2$, so this coordinate transformation, and thus the one to (u, v), is well defined for all $r \neq 2m(r)$.

To obtain the building blocks for the construction of the Penrose diagrams, we need to obtain the explicit form of $r(u, v)$ near the roots of $G(r)$ and $V(r)$. We define the so-called tortoise function

$$r_*(r) := \mathrm{sgn}(r') \frac{U - V}{2} = \int \frac{1}{\sqrt{-2V(r)}} \frac{1}{G(r)} dr, \tag{4.86}$$

up to a trivial integration constant. The crucial point is that r_* is a function of r only.

A convenient choice of $A(u)$ and $B(v)$ thus yields

$$e^{2r_*(r(u,v))} = e^{\mathrm{sgn}(r')(U(u)-V(v))} = e^{\mathrm{sgn}(r')U(u)}e^{-\mathrm{sgn}(r')V(v)} = (uv)^{2C}, \tag{4.87}$$

for any chosen constant C, and provides the form of the hypersurfaces of constant r in terms of u and v. As we are interested in the zeros of $G(r)$ and $V(r)$ (the location of the horizons and the critical values, respectively) we look for the expansion of (4.86) around them. Recall that the existence of the solution at a certain point $r = a$ requires $a > 0$ and $V(a) \leq 0$.

The first possibility is that $r = a$ is a simple zero of $V(r)$. Then, around $r = a$,

$$r_* = \int \frac{dr}{\sqrt{|r-a|}} \left(\sum_{i=0}^{\infty} C_i (r-a)^i \right) = C_0 \,\mathrm{sgn}(r-a) \sqrt{|r-a|}\, h(r), \tag{4.88}$$

where $C_0 \neq 0$ and $h(r)$ is a function expandable around $r = a$, with $h(a) = 2$. This means that (4.87), with the choice $C = \mathrm{sgn}(r-a)C_0$, reads

$$e^{\sqrt{|r-a|}h(r)} = uv, \tag{4.89}$$

and the hypersuface $r(u,v) = a$ is thus mapped to the curve $uv = 1$. The regions $r > a$ are located where $uv > 1$. Conversely, the points with $r < a$ correspond to $uv < 1$.

The second case corresponds to $r = a$ being either a double zero of $V(r)$ or a single zero of $G(r)$. Then, around $r = a$,

$$r_* = \int \frac{dr}{r-a} \left(\sum_{i=0}^{\infty} C_i (r-a)^i \right) = C_0 \log|r-a| + h(r), \tag{4.90}$$

with $h(r)$ expandable around $r = a$ and $C_0 \neq 0$, so that (4.87) with $C = C_0$ reads

$$|r-a| e^{h(r)/C_0} = uv, \tag{4.91}$$

around $r = a$. In any case, $r = a$ corresponds to the null hypersurface $uv = 0$.

The third and last possibility is that $r = a$ is a double zero of $G(r)$. Then, around $r = a$,

$$r_* = \int \frac{dr}{(r-a)^2} \left(\sum_{i=0}^{\infty} C_i (r-a)^i \right) = -\frac{C_0}{r-a} + C_1 \log|r-a| + h(r), \tag{4.92}$$

where $h(r)$ is expandable around $r = a$. Choosing again $C = \text{sgn}(r-a)C_0$ in (4.87),

$$e^{-1/|r-a|}|r-a|^{\text{sgn}(r-a)C_1/C_0}e^{\text{sgn}(r-a)h(r)/C_0} = uv. \tag{4.93}$$

As a result, $r = a$ corresponds once more to $uv = 0$.

The immediate consequence of the above results, together with the fact that all zeros of $V(r)$ are located at the boundaries of intervals of r in homogeneous regions is that:

- The zeros $r = 2m(r)$ of $G(r)$ show the usual isolated horizon structure when the root is either simple or double. The case of a triple root is prevented by the existence of r_0.
- If $r = 2\lambda m(r)$ is a simple root of $V(r)$, it is a minimal spacelike hypersurface.
- If $r = 2\lambda m(r)$ is a double root of $V(r)$, it represents a null past or future boundary at infinity ($\mathcal{J}^{\pm}$).

4.4.4 Conformal diagrams

With all this information at hand, we present the conformal diagrams for each singularity-free case in Figs. 4.6-4.13. They are supplemented with Fig. 4.14, where we show the plots of the polynomial $P(r, \lambda)$, whose roots indicate the position of the minimal hypersurfaces, and its intersections with the curve $(\lambda - 1)r^\ell$, which denote the values of r where the horizons are located. This descends from the identity

$$P(r, \lambda) = \lambda P(r, 1) + (\lambda - 1)r^\ell, \tag{4.94}$$

so the roots of $P(r, 1)$ — equivalently, the roots of $G(r)$ — clearly correspond to the points where $P(r, \lambda) = (\lambda - 1)r^\ell$. Recall that $\ell = 2$ for $Q \neq 0$ and $\ell = 1$ for $Q = 0$. The above relation holds by construction, showing that $\lambda G(r) + 2V(r) = \lambda - 1$, from where we clearly see that the roots of G and V cannot coincide.

Although we have twelve different cases, the charge Q does not change the global structure of these singularity-free spacetime solutions. Therefore, cases C_1 and C_2, with the corresponding superindex (BH, EXT, COS) have the same diagram. Similarly, C_3 and C_4 have also the same structure, and we only find eight different Penrose diagrams. The shaded regions correspond to the domain $\mathcal{U}$, covered by the coordinates $(\tau, z) \in \mathbb{R}^2$, with metric (4.33). A maximal analytic extension $\mathcal{M}$, following the usual periodic construction, is outlined. The horizons are depicted as red lines, and the critical hypersurfaces as purple lines. Lines are continuous when they lie in $\mathcal{U}$, and dotted when not. Dashed lines correspond to null in-

finities ($\mathcal{J}^{\pm}$); dark grey for asymptotic ends ($r \to \infty$) and purple for "finite" ends ($r \to r_0$). The small rings are holes in the diagram, corresponding to timelike ($i^{\pm}$) and spacelike (i^0) infinities. Thin white curves depict hypersurfaces of constant r, characterising the static (up-down) or homogeneous (left-right) nature of the corresponding regions. Some diagrams cannot be depicted over a simple sheet of paper because they bifurcate at the intersections of horizons and critical hypersurfaces, that is, at the grey rings. Observers coming from diferent directions to such bifurcations have non-intersecting futures. This is depicted in the drawings by a shadowed overlapping of some parts of the diagram over others.

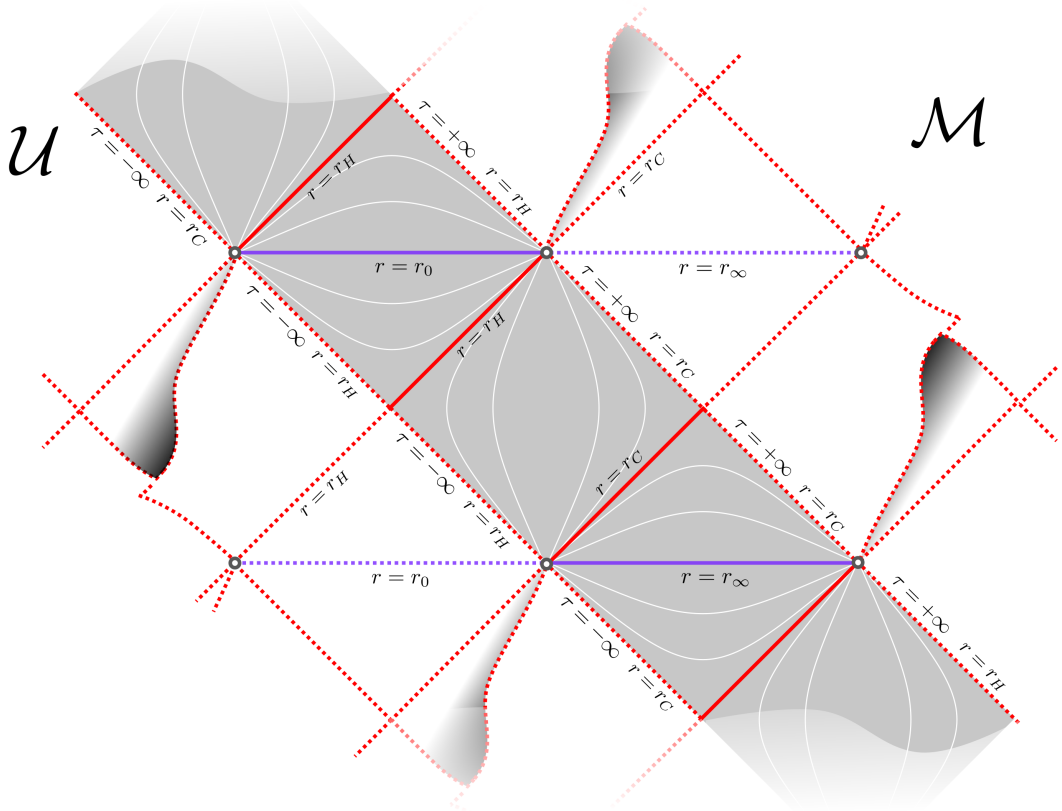

Figure 4.6: Cases C_1^{BH} and C_2^{BH}. The domain $\mathcal{U}$ (shaded in grey) is an infinite and periodic stripe. The maximal extension $\mathcal{M}$ is builded up with infinite copies of $\mathcal{U}$ along all directions, conveniently layering up (in a helical – clockwise – manner) around each grey ring, which is captured by the folding of the sheet atop. Those grey rings denote "holes" in the drawing, and correspond to timelike infinities ($i^{\pm}$). The white curves starting and ending on them are lines of constant r. These geometries modify (and regularise) the singular Reissner-Nordström-de Sitter spacetime. The minimal hypersurface $r = r_0$ replaces the singularity structure of GR, while both $\mathcal{J}^+$ and $\mathcal{J}^-$ are substituted by minimal hypersurfaces $r = r_\infty$. Radially moving observers starting from a static region (those bounded by r_H and r_C) would find and traverse r_H, r_0, r_H, r_C, r_∞, and r_C in finite proper time before reaching a static region isometric to that of their departure. Accelerated observers, on the other hand, may choose to stay at their original static region, never crossing r_H nor r_C, and ending up in the corresponding infinite future i^+.

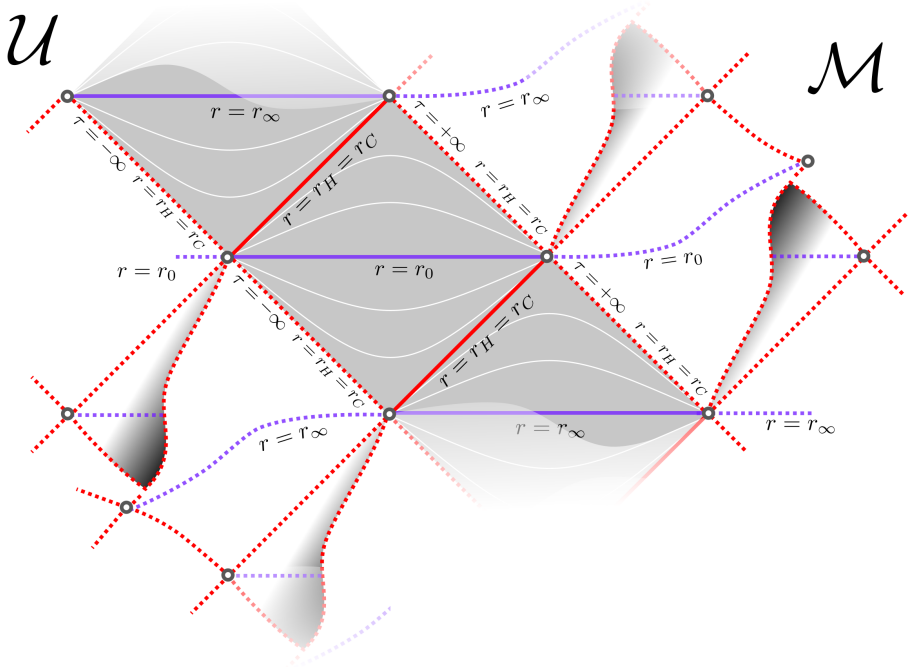

Figure 4.7: Cases C_1^{EXT} and C_2^{EXT}. The horizons r_H and r_C merge, becoming degenerate and bounding homogeneous regions. Therefore, there is no static region in the whole spacetime. The remaining features are the same as explained in Fig. 4.6. The physical interpretation is that of a periodic bouncing cosmology. The existence of horizons, however, allows accelerating observers to decouple from the cosmic evolution, and to end at their corresponding i^+.

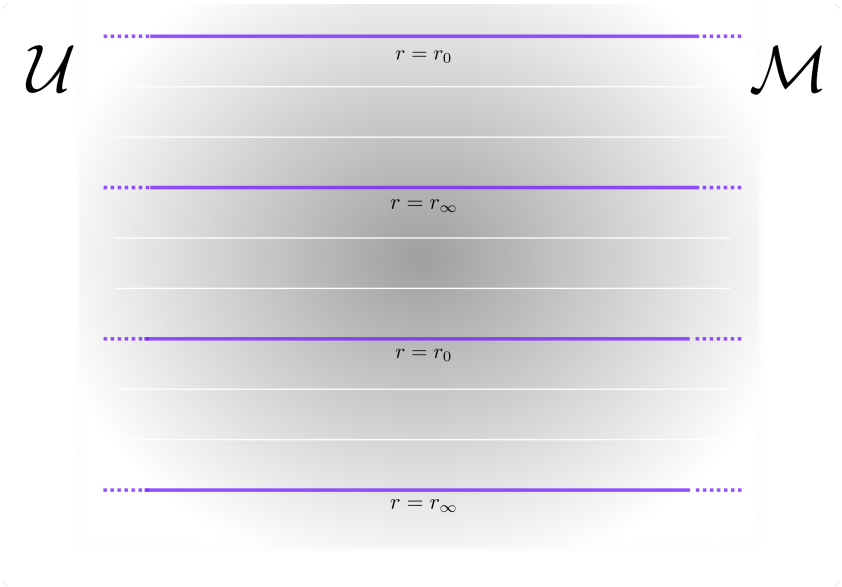

Figure 4.8: Cases C_1^{COS} and C_2^{COS}. There are no horizons, and all hypersurfaces of constant r are spacelike. Note that the diagram is not compactified, to better show the connection with C_1^{EXT} and C_2^{EXT}. As in those cases, this diagram represents a cyclic cosmology. The universe expands and contracts periodically, oscillating between hypersurfaces foliated by spheres of area $4\pi r_0^2$ and $4\pi r_\infty^2$. In this case, the flow of time drags all observers, independently of their acceleration.

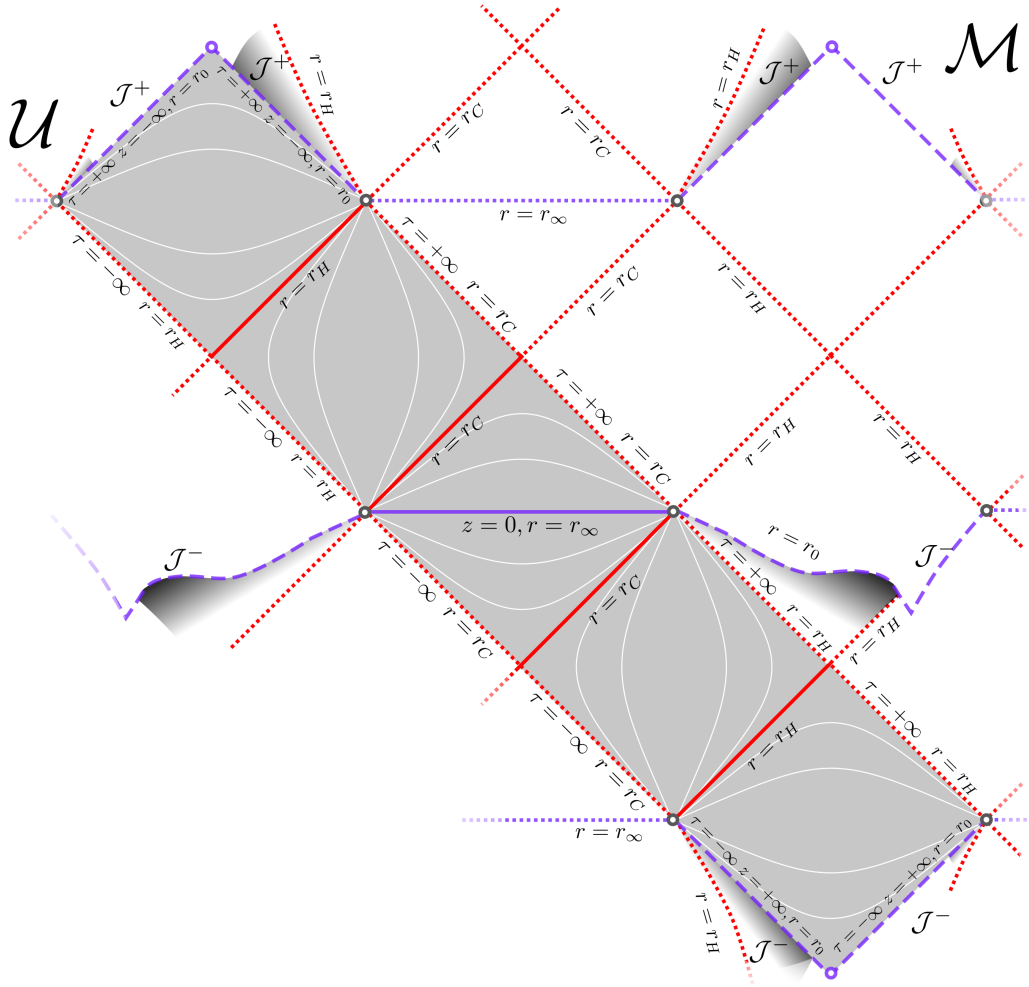

Figure 4.9: Case D_1^{BH}. This corresponds to the case where r_0 is a double root. The diagram for $\mathcal{U}$ is now a finite rectangle. The surfaces $r = r_0$ represent past and future null infinities (dashed purple lines) located at $(\tau, z) \to (-\infty, \infty)$ and $(\tau, z) \to (\infty, -\infty)$, respectively. These infinities are not approached for infinite values of r, but rather as the spacelike homogeneous slices tend to minimal hypersurfaces foliated by spheres of area $4\pi r_0^2$. Indeed, there is a maximum r_∞ for the area radius function that defines a reflection-symmetry point. Radially moving observers starting in a static region (those with vertical thin white lines of constant r) reach that maximum and fall in a different static region after a finite amount of proper time. On the way, they cross a horizon r_C, the critical hypersurface r_∞, and a second horizon r_C. In contrast to Fig. 4.6, the hypersurfaces characterised by $r = r_0$ are no longer traversable. The diagram unfolds at each grey ring.

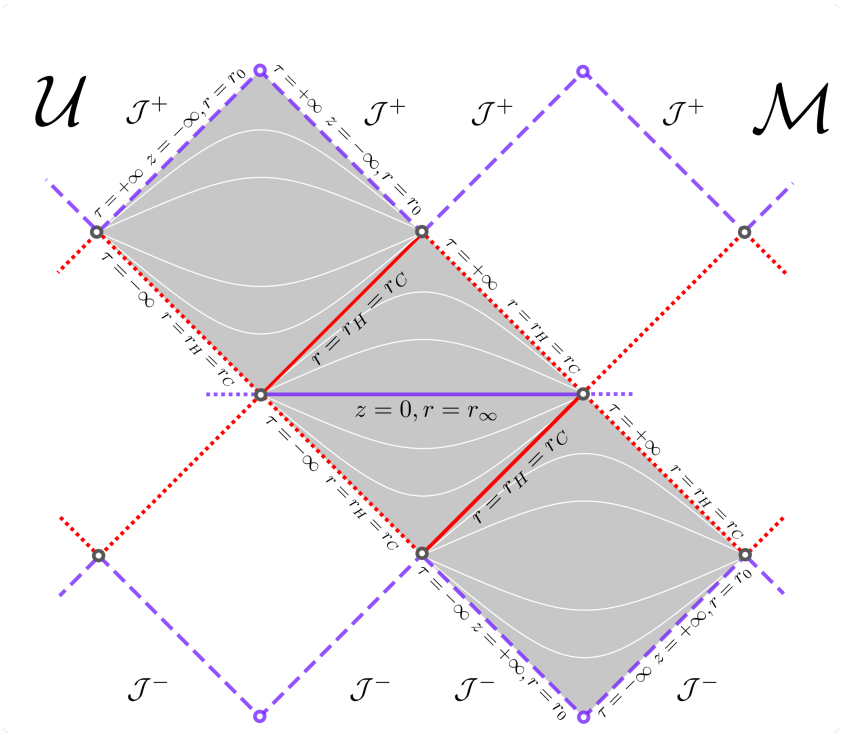

Figure 4.10: Case D_1^{EXT}. The horizons r_H and r_C degenerate, and they always bound homogeneous regions. Similarly to the previous diagram, all surfaces $r = r_0$ are null infinities.

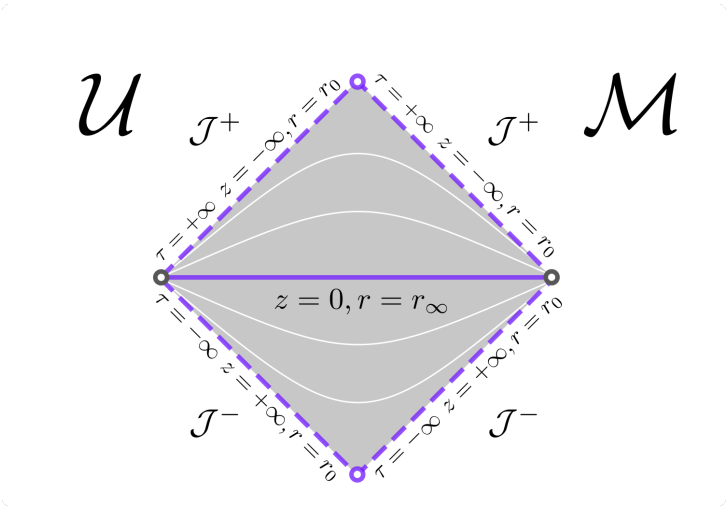

Figure 4.11: Case D_1^{COS}. As in Fig. 4.8, there are no horizons. The main difference with that diagram is that $r = r_0$ are past and future null infinities. The universe asymptotically expands from and contracts to hypersurfaces foliated by spheres of area $4\pi r_0^2$. All observers cross the unique $r = r_\infty$ in finite proper time. It is interesting to point out that this solution represents a closed cosmology and solves both the initial Big-Bang and the final Big-Crunch singularities, while it does not predict a quantum bounce.

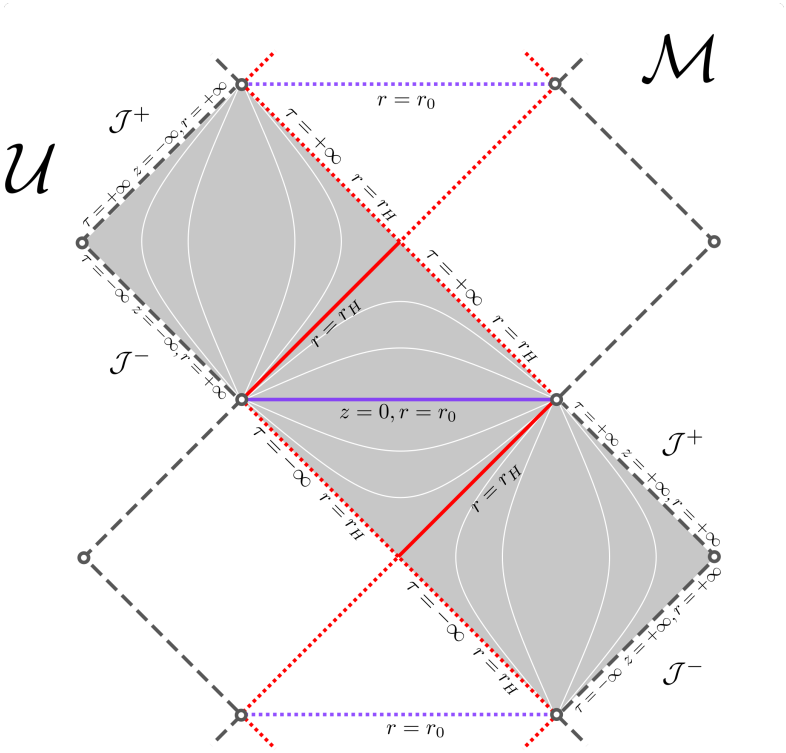

Figure 4.12: Cases C_3^{BH} and C_4^{BH}. It is the same diagram as that in the previous chapter (see Fig. 3.3), but it also stands for the Reissner-Nordström-like solution. We see that small amounts of charge (within the limits of the model) do not affect the causal structure of the spacetime.

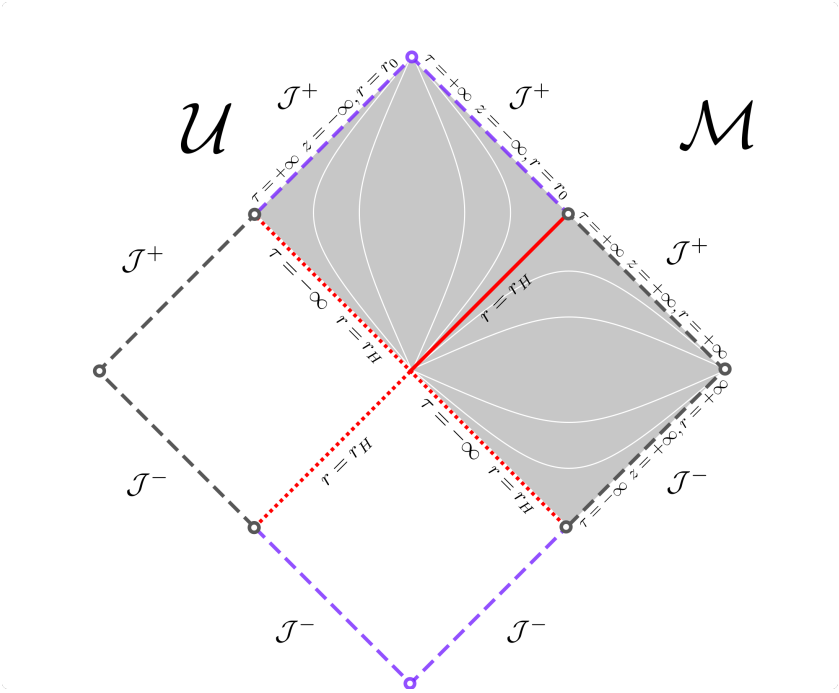

Figure 4.13: Case D_3^{BH}. This stands for the degenerate limit of the above solution. The charge is the maximum allowed by the model, and the surfaces $r = r_0$ become null infinities. Although there is no singularity in this case, observers falling inside the horizon r_H can never leave. In fact, they are doomed to travel forever towards the unreachable minimal hypersurface defined by $r = r_0$.

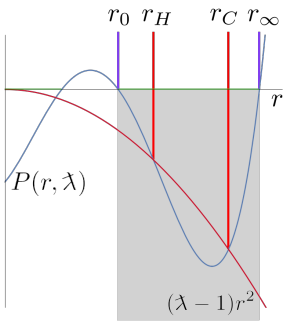

Case C_1^{BH}.

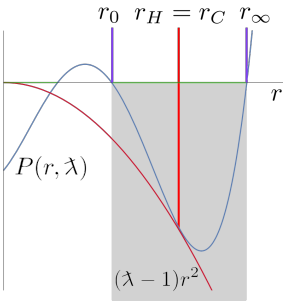

Case C_1^{ext}.

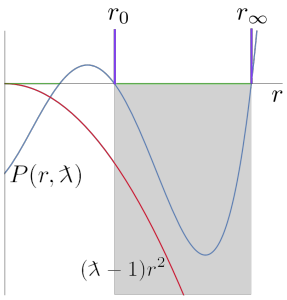

Case C_1^{cos}.

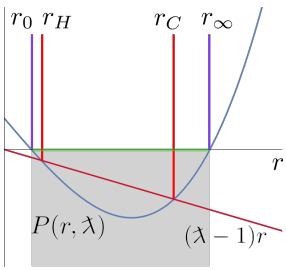

Case C_2^{BH}.

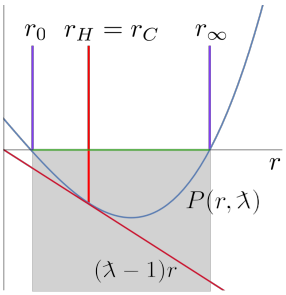

Case C_2^{ext}.

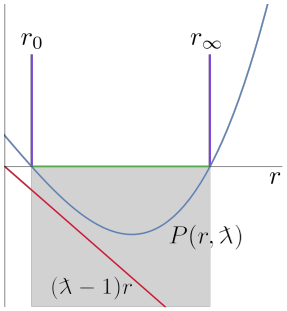

Case C_2^{cos}.

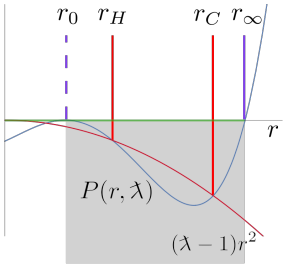

Case D_1^{BH}.

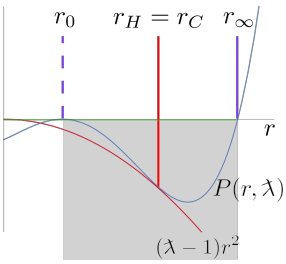

Case D_1^{ext}.

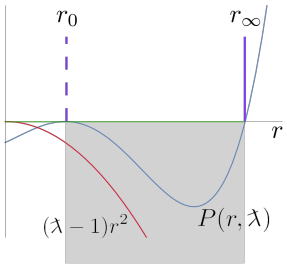

Case D_1^{cos}.

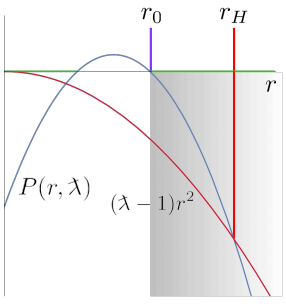

Case C_3^{BH}.

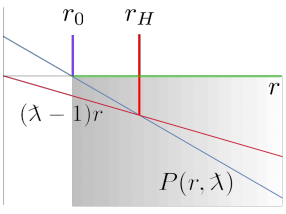

Case C_4^{BH}.

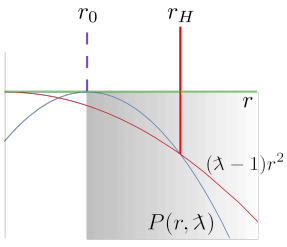

Case D_3^{BH}.

Figure 4.14: The plot in blue is $P(r,\lambda)$, whose roots correspond to the critical points of the area-radius function r. These are marked with a purple line, continuous if the surface is traversable and discontinuous if the surface represents a null boundary of the spacetime. The allowed regions as shown in Lemma 4.1 are highlighted in green. The domain $\mathcal{U}$, i.e., the allowed region with infimum r_0 is always shaded in grey. The red plot is either the half-parabola $(\lambda-1)r^2$ for $Q \neq 0$, or the half-line $(\lambda-1)r$ for $Q = 0$, and its intersections with $P(r,\lambda)$ denote the position of the horizons, marked in red.

Concluding Remarks

The Answer to the Great Question of Life, the Universe and Everything is... Forty-two... So once you do know what the question actually is, you'll know what the answer means.

The Hitchhiker's Guide to the Galaxy
by Douglas Adams.

A complete theory of quantum gravity is still elusive, and the fate of singularities in general relativity remains unravelled. In this thesis, we present an effective approach to polymerise one curvature component in spherical symmetry, as motivated by loop quantum gravity. The strong point of the model is that it is explicitly covariant. The effective corrections are implemented at the Hamiltonian level and endowed with a clear geometric description. This ensures that different gauge choices on phase space correspond to different charts (in the corresponding domains) of the same metric tensor.

To overcome previous no-go results on the covariance of holonomy corrections in non-homogeneous spherically symmetric spacetimes, we perform a systematic analysis of possible deformations of the GR constraints in Chapter 2. More precisely, adhering to the derivative structure of the GR Hamiltonian, we start from a very general Hamiltonian constraint (2.14) and demand that it forms a first-class algebra along with the GR diffeomorphism constraint (2.15). Furthermore, the structure function in that algebra is required to transform adequately for the theory to be embeddable in a four-dimensional manifold. This allows us to construct the corresponding metric tensor (2.61) in terms of phase-space functions in a totally unambiguous way.

We obtain the most general Hamiltonian (2.53) satisfying these conditions in vacuum. Despite starting from a constraint with five generic functions of four variables each, the covariance of the model severely restricts their form, and only seven functions of one same scalar variable remain free. This unique family of constraints generates the canonical form of the algebra along with the diffeomorphism constraint (2.15), and shows that the possible deformations must be sinusoidal functions, which we interpret as the expected covariant holonomy corrections.

Furthermore, following the same procedure as in vacuum, we have found, for the first time in the literature, a Hamiltonian with holonomy corrections consistently coupled to matter degrees of freedom. The addition of local degrees of freedom produces even more anomalies, but we have been able to find a particular solution that describes holonomy modifications in the presence of a scalar field. The effective theory consists of a family of Hamiltonians (2.105), with corresponding metric (2.111), where quantum corrections are parametrised by a single positive and bounded constant λ, which is directly related to the polymerisation scale of the holonomy corrections.

The covariance of this effective theory allows us to study the spacetime solution equipped with the full power of differential-geometry techniques. In particular, in Chapter 3, we analyse in detail the vacuum geometry as the simplest application of the model. In this case, the Schwarzschild singularity is generically replaced by a minimal spacelike transition surface, foliated by spheres of constant radius r_0, inside the horizon. We prove this by explicitly solving the equations of motion for different gauge choices. We also provide the corresponding coordinate transformations between the resulting charts, and we further obtain the maximal analytic extension of the spacetime, which is represented in Fig. 3.4. The computation of geometric invariants shows that the curvature is everywhere finite. Besides, we find global and quasi-local characterisations of the parameter λ, and we check that all energy conditions are satisfied on the horizon and at infinity.

The subsequent study in Chapter 4 generalises the results in vacuum by incorporating a Maxwell field and a cosmological constant. The analysis shows that singularity resolution depends on the parameters of the model, and we perform a systematic classification of the singularity-free solutions, which always show an infimum r_0 for the area-radius function. In contrast to general relativity, their global causal structure is independent of the specific value of the charge, because there is no (inner) Cauchy horizon. In addition, a positive cosmological constant sets a maximum r_∞ for the area-radius function. When located in the manifold, both extremes define minimal spacelike hypersurfaces embedded in homogeneous regions of the spacetime. The GR black hole thus transforms into an endless periodic sequence of non-trapped, trapped, and anti-trapped regions, which are traversable in finite proper time. The theory also gives rise to singularity-free cosmologies (with and without horizons) that describe bouncing universes. They show alternate periods of expansion and contraction, connecting hypersurfaces foliated by spheres of finite minimum and maximum area. These generic properties are depicted in Figs. 4.6-4.13. Furthermore, we find a convenient gauge to solve the effective equations of motion, which provides a chart (4.33) that completely covers the whole singularity-free spacetimes.

Most remarkably, the Minkowski spacetime is always a solution of this effective theory for any value of the positive constant λ. In turn, the indeterminate but well-defined limit of vanishing λ corresponds to general relativity. In that case, the hypersurfaces $r = r_0$ become unavailable, thus emerging as the central singularity.

The conditions for singularity resolution are wide enough to include any spherical astrophysical black hole. The effective theory provides an entirely regular description, with everywhere finite curvature invariants, for nearly neutral black holes of large mass embedded in a universe with a small positive cosmological constant.

Bibliography

Deep in the human unconscious is a pervasive need for a logical universe that makes sense.

Dune
by Frank Herbert

Published Works

[1] A. Alonso-Bardaji and D. Brizuela. Holonomy and inverse-triad corrections in spherical models coupled to matter. Eur. Phys. J. C **81**, 283 (2021). arXiv:2010.14437.

[2] A. Alonso-Bardaji and D. Brizuela. Anomaly-free deformations of spherical general relativity coupled to matter. Phys. Rev. D **104**, 084064 (2021). arXiv:2106.07595.

[3] A. Alonso-Bardaji and D. Brizuela. Holonomy corrections in effective midisuperspace models. Contribution to: 16th Marcel Grossmann Meeting, 4239-4246 (2023).

[4] A. Alonso-Bardaji, D. Brizuela, and R. Vera. An effective model for the quantum Schwarzschild black hole. Phys. Lett. B **829**, 137075 (2022). arXiv:2112.12110.

[5] A. Alonso-Bardaji, D. Brizuela, and R. Vera. Nonsingular spherically symmetric black-hole model with holonomy corrections. Phys. Rev. D **106**, 024035 (2022). arXiv:2205.02098.

[6] A. Alonso-Bardaji, D. Brizuela, and R. Vera. Singularity resolution by holonomy corrections: Spherical charged black holes in cosmological backgrounds. Accepted in Phys. Rev. D (2023). arXiv:2302.10619.

Basic References

[7] A. Einstein. Die Feldgleichungen der Gravitation (The Field Equations of Gravitation). Sitzungsberichte der Preussischen Akademie der Wissenschaften zu Berlin, 844–847 (1915). A. Einstein. Die Grundlage der allgemeinen Relativitätstheorie (The Foundation of the General Theory of Relativity). Ann. Phys. **49**, 769-822 (1916).

[8] C. W. Misner, K. S. Thorne, and J. A. Wheeler. Gravitation. W. H. Freeman (1973).

[9] K. Schwarzschild. Über das Gravitationsfeld eines Massenpunktes nach der Einsteinschen Theorie (On the Gravitational Field of a Mass Point according to Einstein's Theory). Sitzungsber. Preuss. Akad. Wiss., 189–196 (1916).

[10] J. Droste. The field of a single centre in Einstein's theory of gravitation, and the motion of a particle in that field. KNAW Proceedings **19**, 197–215 (1917).

[11] J. T. Jebsen. Über die allgemeinen kugelsymmetrischen Lösungen der Einsteinschen Gravitationsgleichungen im Vakuum (On the general spherically symmetric solutions of Einstein's gravitational equations in vacuo). Ark. Mat. Ast. Fys. **15**, 1–9 (1921).

[12] G. D. Birkhoff and R. E. Langer. Relativity and Modern Physics. Harvard University Press (1923).

[13] P. Painlevé. La Mécanique classique et la théorie de la relativité (Classical mechanics and the theory of relativity). C. R. Acad. Sci. **173**, 677–680 (1921).

[14] A. Gullstrand. Allgemeine Lösung des statischen Einkörperproblems in der Einsteinschen Gravitationstheorie (General solution to the static one-body problem in Einstein's theory of gravitation). Ark. Mat. Astron. Fys. **16**, 1-15 (1922).

[15] A. S. Eddington. The Mathematical Theory of Relativity. Cambridge University Press (1923).

[16] J. L. Synge. The Gravitational Field of a Particle. Math. Proc. R. Ir. Acad. **53**, 83–114 (1950).

[17] G. Szekeres. On the Singularities of a Riemannian Manifold. Publ. Math. Debr. **7**, 285–301 (1960).

[18] M. D. Kruskal. Maximal Extension of Schwarzschild Metric. Phys. Rev. **119**, 1743–1745 (1960).

[19] H. Reissner. Über die Eigengravitation des elektrischen Feldes nach der Einsteinschen Theorie (On the self-gravity of the electric field according to Einstein's theory). Ann. Phys. **355**, 106–120 (1916).

[20] G. Nordström. Een en ander over de energie van het zwaartekrachtsveld volgens de theorie van Einstein (On the Energy of the Gravitation field in Einstein's Theory). Proc. Kon. Ned. Akad. Wet. **20**, 1238-1245 (1918).

[21] F. Kottler. Über die physikalischen Grundlagen der Einsteinschen Gravitationstheorie (On the physical foundations of Einstein's theory of gravitation). Ann. Phys. **56**, 401–461 (1918).

[22] A. Friedmann. Über die Krümmung des Raumes (On the Curvature of Space). Z. Phys. **10**, 377–386 (1922). A. Friedmann. Über die Möglichkeit einer Welt mit konstanter negativer Krümmung des Raumes (On the Possibility of a World with Constant Negative Curvature of Space). Z. Phys., **21**, 326–332 (1924).

[23] A. G. Lemaître. Un Univers homogène de masse constante et de rayon croissant rendant compte de la vitesse radiale des nébuleuses extragalactiques (A Homogeneous Universe of Constant Mass and Increasing Radius accounting for the Radial Velocity of Extra-galactic Nebulæ). Ann. Soc. Sci Bruxelles **47A**, 49–59 (1927).

[24] H. P. Robertson. Kinematics and World-Structure. Astrophys. J. **82**, 284 (1935). H. P. Robertson. Kinematics and World-Structure II. Astrophys. J. **83**, 187 (1936). H. P. Robertson. Kinematics and World-Structure III. Astrophys. J., **83**, 257 (1936).

[25] A. G. Walker. On Milne's Theory of World-Structure. Proc. London Math. Soc. **42**, 90–127 (1937).

[26] G. Lemaître. L'Univers en expansion (The Expanding Universe). Ann. Soc. Sci Bruxelles, **53**, 51 (1933).

[27] R. C. Tolman. Effect of Inhomogeneity on Cosmological Models. Proc. Natl. Acad. Sci. USA **20**, 169–76 (1934).

[28] H. Bondi. Spherically Symmetrical Models in General Relativity. Monthly Notices of the Royal Astronomical Society **107**, 410–425 (1947).

[29] J. R. Oppenheimer and H. Snyder. On Continued Gravitational Contraction. Phys. Rev. **56**, 455–459 (1939).

[30] R. Penrose. Gravitational Collapse and Space-Time Singularities. Phys. Rev. Lett. **14**, 57–59 (1965).

[31] S. W. Hawking and G. F. R. Ellis. The Large Scale Structure of Space-Time. Cambridge University Press (1973).

[32] J. M. M. Senovilla. Singularity Theorems and Their Consequences Gen. Rel. Grav. **30**, 701–848 (1998). A critical appraisal of the singularity theorems. Phil. Trans. R. Soc. A. **380**, 20210174 (2022).

[33] C. Rovelli. Quantum Gravity. Cambridge University Press (2004).

[34] A. Ashtekar and J. Lewandowski. Background independent quantum gravity: a status report. Class. Quant. Grav. **21**, R53 (2004)

[35] T. Thiemann. Modern Canonical Quantum General Relativity. Cambridge University Press (2007).

[36] C. Rovelli. Zakopane lectures on loop gravity. PoS, QGQGS2011 (2011).

[37] A. Ashtekar and E. Bianchi. A short review of loop quantum gravity. Rept. Prog. Phys. **84**, 042001 (2021).

[38] C. Rovelli and L. Smolin. Discreteness of area and volume in quantum gravity. Nucl. Phys. B **442**, 593–622 (1995). [Erratum. Nucl.Phys.B **456**, 753–754 (1995)].

[39] A. Ashtekar and J. Lewandowski. Quantum theory of geometry. I: Area operators. Class. Quant. Grav. **14**, A55–A82 (1997).

[40] A. Ashtekar, A. Corichi, and P. Singh. Robustness of key features of loop quantum cosmology. Phys. Rev. D **77**, 024046 (2008).

[41] M. Bojowald. Loop Quantum Cosmology. Living Reviews in Relativity **11**, 4 (2008).

[42] I. Agulló and P. Singh. Loop Quantum Cosmology in Loop Quantum Gravity: The First 30 Years, 183–240. WSP (2017).

[43] E. Fermi. Tentativo di una Teoria Dei Raggi β (Attempt at a theory of β rays). Nuovo Cim. **11**, 1–19 (1934).

[44] A. Ashtekar, T. Pawlowski and P. Singh. Quantum nature of the big bang: Improved dynamics. Phys. Rev. D **74**, 084003 (2006).

[45] A. Ashtekar and P. Singh. Loop quantum cosmology: a status report. Class. Quant. Grav. **28**, 213001 (2011).

[46] A. Ashtekar. Symmetry reduced loop quantum gravity: A bird's eye view. Int. J. Mod. Phys. D **25**, 1642010 (2016).

[47] V. Taveras. Corrections to the Friedmann equations from loop quantum gravity for a universe with a free scalar field. Phys. Rev. D **78**, 064072 (2008).

[48] I. Agulló, A. Ashtekar, and W. Nelson. Extension of the quantum theory of cosmological perturbations to the Planck era. Phys. Rev. D **87**, 043507 (2013). I. Agulló, A. Ashtekar, and W. Nelson. The pre-inflationary dynamics of loop quantum cosmology: confronting quantum gravity with observations. Class. Quant. Grav. **30**, 085014 (2013).

[49] A. Ashtekar, J. C. Baez and K. Krasnov. Quantum geometry of isolated horizons and black hole entropy. Adv. Theor. Math. Phys. **4**, 1-94 (2000).

[50] A. Ashtekar and M. Bojowald. Quantum geometry and the Schwarzschild singularity. Class. Quant. Grav. **23**, 391–411 (2006).

[51] A. Perez. Black holes in loop quantum gravity. Rept. Prog. Phys. **80**, 126901 (2017).

[52] M. Bojowald. Black-Hole Models in Loop Quantum Gravity. Universe **6**, 125 (2020).

[53] M. Bojowald. No-go result for covariance in models of loop quantum gravity. Phys. Rev. D **102**, 046006 (2020).

[54] C. G. Boehmer and K. Vandersloot. Loop quantum dynamics of the Schwarzschild interior. Phys. Rev. D **76**, 104030 (2007).

[55] L. Modesto. Semiclassical Loop Quantum Black Hole. Int. J. Theor. Phys. **49**, 1649–1683 (2010).

[56] A. Joe and P. Singh. Kantowski-Sachs spacetime in loop quantum cosmology: bounds on expansion and shear scalars and the viability of quantization prescriptions. Class. Quant. Grav. **32**, 015009 (2015).

[57] A. Corichi and P. Singh. Loop quantization of the Schwarzschild interior revisited. Class. Quant. Grav. **33**, 055006 (2016).

[58] J. Olmedo, S. Saini, and P. Singh. From black holes to white holes: a quantum gravitational, symmetric bounce. Class. Quant. Grav. **34**, 225011 (2017).

[59] J. Ben Achour, F. Lamy, H. Liu, and K. Noui. Polymer Schwarzschild black hole: An effective metric. EPL **123**, 20006 (2018).

[60] J. G. Kelly, R. Santacruz, and E. Wilson-Ewing. Effective loop quantum gravity framework for vacuum spherically symmetric spacetimes. Phys. Rev. D **102**, 106024 (2020).

[61] A. Ashtekar, J. Olmedo, and P. Singh. Quantum extension of the Kruskal spacetime. Phys. Rev. D **98**, 126003 (2018).

[62] A. Ashtekar, J. Olmedo, and P. Singh. Quantum Transfiguration of Kruskal Black Holes. Phys. Rev. Lett., 121(24):241301, 2018.

[63] N. Bodendorfer, F. M. Mele, and J. Münch. Effective quantum extended spacetime of polymer Schwarzschild black hole. Class. Quant. Grav., **36**, 195015 (2019).

[64] N. Bodendorfer, F. M. Mele, and J. Münch. (b,v)-type variables for black to white hole transitions in effective loop quantum gravity. Phys. Lett. B **819**, 136390 (2021).

[65] A. Ashtekar and J. Olmedo. Properties of a recent quantum extension of the Kruskal geometry. Int. J. Mod. Phys. D **29**, 2050076 (2020).

[66] M. Bojowald, S. Brahma, and D.-h. Yeom. Effective line elements and black-hole models in canonical loop quantum gravity. Phys. Rev. D **98**, 046015 (2018).

[67] M. Bojowald, G. M. Paily and J. D. Reyes. Discreteness corrections and higher spatial derivatives in effective canonical quantum gravity. Phys. Rev. D **90**, 025025 (2014).

[68] R. Gambini and J. Pullin. Black Holes in Loop Quantum Gravity: The Complete Space-Time. Phys. Rev. Lett. **101**, 161301 (2008).

[69] R. Gambini and J. Pullin. Loop Quantization of the Schwarzschild Black Hole. Phys. Rev. Lett. **110**, 211301 (2013).

[70] R. Gambini, J. Olmedo and J. Pullin. Quantum black holes in loop quantum gravity. Class. Quant. Grav. **31**, 095009 (2014).

[71] R. Gambini, J. Olmedo, and J. Pullin. Spherically symmetric loop quantum gravity: analysis of improved dynamics. Class. Quant. Grav. **37**, 205012 (2020).

[72] R. Tibrewala. Inhomogeneities, loop quantum gravity corrections, constraint algebra and general covariance. Class. Quant. Grav. **31**, 055010 (2014).

[73] M. Bojowald, S. Brahma, and J. D. Reyes. Covariance in models of loop quantum gravity: Spherical symmetry. Phys. Rev. D **92**, 045043 (2015).

[74] D. Arruga, J. Ben Achour and K. Noui. Deformed General Relativity and Quantum Black Holes Interior. Universe **6**, 39 (2020).

[75] R. Tibrewala. Spherically symmetric Einstein-Maxwell theory and loop quantum gravity corrections. Class. Quant. Grav. **29**, 235012 (2012).

[76] R. Gambini, E. M. Capurro, and J. Pullin. Quantum spacetime of a charged black hole. Phys. Rev. D **91**, 084006 (2015).

[77] J. G. Kelly, R. Santacruz, and E. Wilson-Ewing. Black hole collapse and bounce in effective loop quantum gravity. Class. Quant. Grav. **38**, 04LT01 (2021).

[78] R. Gambini, F. Benítez, and J. Pullin, A Covariant Polymerized Scalar Field in Semi-Classical Loop Quantum Gravity. Universe **8**, 526 (2022).

[79] V. Husain, J. G. Kelly, R. Santacruz, and E. Wilson-Ewing, Quantum Gravity of Dust Collapse: Shock Waves from Black Holes. Phys. Rev. Lett. **128**, 121301 (2022). V. Husain, J. G. Kelly, R. Santacruz, and E. Wilson-Ewing, Fate of quantum black holes. Phys. Rev. D **106**, 024014 (2022).

[80] M. Bojowald. Hamiltonian formulation of general relativity, in Canonical Gravity and Applications: Cosmology, Black Holes, and Quantum Gravity, 17–112. Cambridge University Press (2010).

[81] R. M. Wald. General Relativity. University of Chicago Press (2010).

[82] R. Arnowitt, S. Deser, and C. W. Misner. Dynamical Structure and Definition of Energy in General Relativity. Phys. Rev. **116**, 1322–1330 (1959).

[83] C. Teitelboim. How commutators of constraints reflect the spacetime structure. Ann. Phys. **79**, 542–557 (1973).

[84] C. J. Isham and K. V. Kuchar. Representations of spacetime diffeomorphisms. I. Canonical parametrized field theories. Ann. Phys. **164**, 288–315 (1985). C. J. Isham and K. V. Kuchar. Representations of spacetime diffeomorphisms. II. Canonical geometrodynamics. Ann. Phys. **164**, 316–333 (1985).

[85] V. Varo. The Covariant Phase Space of Gravity with Boundaries Ph.D. thesis, UC3M (2022).

[86] J. F. Barbero G. Real Ashtekar variables for Lorentzian signature space-times. Phys. Rev. D **51**, 5507–5510 (1995).

[87] J. M. Pons, D. C. Salisbury, and L. C. Shepley. Gauge transformations in the Lagrangian and Hamiltonian formalisms of generally covariant theories. Phys. Rev. D **55**, 658–668 (1997).

[88] M. Bojowald. Spherically symmetric quantum geometry: states and basic operators. Class. Quant. Grav. **21**, 3733–3753 (2004).

[89] M. Bojowald and R. Swiderski. Spherically symmetric quantum geometry: Hamiltonian constraint. Class. Quant. Grav. **23**, 2129–2154 (2006).

[90] J. B. Griffiths and J. Podolský. Exact Space-Times in Einstein's General Relativity. Cambridge University Press (2009).

[91] R. Beig. Arnowitt-Deser-Misner energy and g_{00}. Phys. Lett. A **69**, 153–155 (1978).

[92] L. B. Szabados. Quasi-Local Energy-Momentum and Angular Momentum in General Relativity. Living Rev. Rel. **12**, 4 (2009).

[93] R. Bartnik. The mass of an asymptotically flat manifold. Commun. Pure Appl. Math. **39**, 661–693 (1986).

[94] A. Herrero and J. A. Morales-Lladosa. Painlevé–Gullstrand synchronizations in spherical symmetry. Class. Quantum Grav. **27**, 175007 (2010).

[95] M. Mars, M. M. Martín-Prats, and J. M. M. Senovilla. Models of regular Schwarzschild black holes satisfying weak energy conditions. Class. Quantum Grav. **13**, L51–L58 (1996).

[96] H. Maeda. Quest for realistic non-singular black-hole geometries: regular-center type. JHEP **11**, 108 (2022).

[97] I. Bengtsson, S. Holst, and E. Jakobsson. Classics illustrated: limits of spacetimes. Class. Quant. Grav. **31**, 205008 (2014).

[98] D. R. Brill and S. A. Hayward. Global structure of a black hole cosmos and its extremes. Class. Quantum Grav. **11**, 359 (1994).

[99] B. O'Neill. Semi-Riemannian Geometry With Applications to Relativity. Academic Press (1983).

[100] J. M. M. Senovilla. Lecture notes on conformal diagrams. UPV/EHU.